



HAL
open science

Molecular and nanostructured catalysts for lignin and N-heterocycle transformation

Julien Hervocho

► **To cite this version:**

Julien Hervocho. Molecular and nanostructured catalysts for lignin and N-heterocycle transformation. Catalysis. Université Rennes 1; Universität Rostock (1419-..), 2021. English. NNT : 2021REN1S046 . tel-03508479

HAL Id: tel-03508479

<https://theses.hal.science/tel-03508479>

Submitted on 3 Jan 2022

HAL is a multi-disciplinary open access archive for the deposit and dissemination of scientific research documents, whether they are published or not. The documents may come from teaching and research institutions in France or abroad, or from public or private research centers.

L'archive ouverte pluridisciplinaire **HAL**, est destinée au dépôt et à la diffusion de documents scientifiques de niveau recherche, publiés ou non, émanant des établissements d'enseignement et de recherche français ou étrangers, des laboratoires publics ou privés.

THESE DE DOCTORAT DE

L'UNIVERSITE DE RENNES 1

ECOLE DOCTORALE N° 596

Matière, Molécules, Matériaux

Spécialité : Chimie Moléculaire et Macromoléculaire

Par

Julien HERVOCHON

Molecular and Nanostructured Catalysts for Lignin and *N*-heterocycle Transformation

Thèse présentée et soutenue à Rennes, le 26 Janvier 2021

Unité de recherche : ISC Rennes UMR 6226

Rapporteurs avant soutenance :

Karine Philippot, Directrice de Recherche, Laboratoire de Chimie de Coordination, Toulouse (France)

Axel Jacobi Von Wangelin, Professeur, Université de Hambourg (Allemagne)

Composition du Jury :

Examineurs : Karine Philippot

Axel Jacobi Von Wangelin

Alain Roucoux

Christophe Darcel

Dir. de thèse : Cedric Fischmeister

Dir. de thèse : Matthias Beller

Directrice de Recherche, LCC, Toulouse (France)

Professeur, Université de Hambourg (Allemagne)

Professeur, Ecole Nationale Supérieure de Chimie de Rennes

Professeur, Université Rennes 1

Ingénieur de Recherche, Université Rennes 1

Professeur, Leibniz-Institute für Katalysis, Rostock (Allemagne)

Acknowledgements

The following work has been carried out in the team of "Organometallics: Materials & Catalysis (OMC)", CNRS, ISCR (Institut des Sciences Chimiques de Rennes)-UMR 6226, Univ Rennes, between Janvier 2018 and april 2019 and in Leibniz-Institute für Katalys (Likat) in Rostock between April 2019 and November 2020. I have spent unforgettable 3 years since my first step into both laboratories.

First and foremost, I would like to express my sincere acknowledgements to my supervisors: Dr. Kathrin Junge, Prof. Matthias Beller and Dr. Cédric Fischmeister, who gave me the opportunity to study thier laboratories. From them I learned a lot both in scientific research and in life. Their patient guidance, enthusiastic encouragement and critical comments guiding me how to properly think about the science and pursue revolutionary research. I am grateful for their encouragements to me to work on multiple topics to learn more about chemistry. I deeply appreciate their patience in helping me to solve the problems in chemistry and in my life.

I would like to extend my appreciation to the jury members: Dr. Karine Philippot, Prof. Axel Jacobi von Wangelin, Christophe Darcel, Alain Roucoux, and I thank them for spending their valuable time in reading my thesis.

I am indebted to Prof. Christophe Darcel, Dr. Mathieu Achard, Dr. Rafael Gramage-Doria, Dr. Jean-François Soulé, Dr. Henri Doucet, Dr. Sylvie Dérien, who offered their time for useful suggestions and discussions in my research during the past three years.

It is also my pleasure to thank Dr. Thierry Roisnel and Dr. Vincent Dorcet (X-Ray diffraction Center and TEM EDS Analysis Univ Rennes) for their help in X-Ray diffraction analysis.

Additionally, I feel very happy to work with these lab mates: Shengdong Wang, Changsheng Wang, Apurba Ranjan Sahoo, Antoine Bruneau-Voisine, Duo Wei, Luciana Sarmento Fernandes, Paolo Zardi, Haoran Li, Arpan Sasmal, Zhuan Zhang, Haiyun Huang, Shuxin Mao, Yixuan Cao, Harikrishnan Jayaprakash, Chakkrit Netkaew, Peter McNeice, Ruiyang Qu, Veronica Papa, Wu Li, Thomas Leischner, Helen Hornke, Svenja Budweg, Johannes Fessler, Niklas Heinrich, David Leonard, Leandro Duarte, Dario Formenti, Pavel Ryabchuk, Florian Bourriquen and I would like to thank all of them for their help in the lab.

. Last but not least, I would like to attribute my immense gratefulness to my mother and especially my girlfriend, who are always standing beside me and giving me support whenever I need and to have accepted my departure to a foreign country.

This work was co-financed by the Bretagne region as a part of an ARED project and by Leibniz-Institut für Katalysis (LIKAT, Germany).



Table of contents

General introduction	6
Chapter 1	8
Lignin valorisation by catalysis	8
I/Introduction	9
1/ Lignocellulosique biomass	9
a/ Cellulose	9
b/ Hemicellulose	11
c/ Lignin.....	12
2/ Lignin extraction	15
a/ The Kraft Process.....	15
b/ Sulfite lignin.....	16
c/ Organosolv Process	17
3/ Biomass valorisation	18
a / Oxidative cleavage.....	18
b/ Hydrogenolysis	22
c/ Redox-neutral	26
II/ Results and discussions	29
1/ Introduction	29
2/ Ligand and Catalyst synthesis	33
a/ PNP Ligand synthesis	34
b/ Synthesis of Cobalt PNP complexes.	34
c/ Phosphine free Ligands.....	39
d/ Synthesis of phosphine-free complexes.	40
3/ Catalytic tests	41
III/ Conclusion	45
IV/ Experimental Part	46
Chapter 2	58
Convenient synthesis of cobalt nanoparticles for the hydrogenation of quinolines in water.	58
I/ Introduction	59
II/ Results and discussions	68
III/ Conclusion	75
IV/ Experimental Data	76

1. General information	76
2. General procedure for the catalytic hydrogenation of quinoline	76
3. Recycling test	76
4. Scale-up reaction	76
5. TEM/EDS Analyses	77
6. Product characterization	78
Chapter 3: Stereoselective hydrogenation of <i>N</i>-Heterocycles over heterogeneous ruthenium	86
I/ Switchable diastereoselective quinoline hydrogenation to decahydroquinoline over Ru/C	87
I/Introduction	87
II/Results and discussions	90
III/ Conclusion	99
IV/Experimental Data	99
Part II: Mild, selective and practical diastereoselective hydrogenation of pyridines and arenes	109
I/Introduction	109
II/Results and discussion	111
III/ Conclusion	120
IV/Experimental Data	120
General Conclusion	142

General introduction

Nowadays, chemistry needs to be environmentally friendly and sustainable to meet the objectives of a sustainable development. For that, many ways are being implemented to reduce pollution, toxicity and save energy in chemical processes. It is in this perspective that "green chemistry" was born in the late 90's. Green chemistry concepts are essential to enable the development of cleaner and more environmentally friendly chemical processes. With this in mind, Anastas and Warner¹ proposed the 12 principles of green chemistry, which can be broken down as follows: use of catalysts that are as selective as possible; avoid waste; maximize the incorporation of all materials in the final product (atom saving); efficient production; products that are little or non-toxic for humans and the environment; reduce accidents; reduce energy expenditure (ordinary Temperature and ordinary Pressure); use renewable raw materials rather than depleting ones; real-time analysis; avoidance of species modifications; making auxiliary substances unnecessary or harmless to degradation; producing compounds that degrade after operation into derivatives that are harmless to the environment. Currently, catalysis using transition metals is frequently used either in the industrial environment or in research laboratories as a tool to increase efficiency and selectivity and reduce by-product and waste formation. Another pillar of sustainable and green chemistry concerns the shift from a fossil-based chemistry to a biosourced chemistry. Here again, catalysis either heterogeneous or homogeneous are ubiquitous for the development of biorefineries and efficient transformations of platform chemicals.²

The objective of this thesis is part of this general effort, through the design of new efficient and selective catalytic system more respectful of the environment.

The work carried out during this thesis is divided into three distinct parts. The first part aims at valorizing lignin, an underexploited biopolymer derived from lignocellulosic biomass.³ Lignin is a biopolymer based on phenol structural units, it is therefore the most important renewable material to produce aromatic compound. Unfortunately, the complex and multiple structures of this natural polymer, as well as the diversity of the processes used for its extraction limit its valorisation as a raw material. Consequently, 98% of industrial lignin is used as firewood for heat and energy production.⁴ The second chapter of this thesis will concern the design of a new

¹ a) P. T. Anastas, J. C. Warner, *Green Chemistry, Theory and Practice*, Oxford University Press, **1998**; b) P. Anastas, N. Eghbali, *Chem. Soc. Rev.*, **2010**, *39*, 301-312.

² Selected reviews: a) A. Corma, S. Iborra, A. Velty, *Chem. Rev.*, **2007**, *107*, 6, 2411–2502; b) J. N. Chheda, G. W. Huber, J. A. Dumesic, *Angew. Chem. Int. Ed.*, **2007**, *46*, 7164 – 7183; c) C. H. Christensen, J. Rass-Hansen, C. C. Marsden, E. Taarning, K. Egeblad, *ChemSusChem*, **2008**, *1*, 283 – 289; d) G. R. Petersen, J. J. Bozell, *Green Chem.*, **2010**, *12*, 539–554; e) J. C. Serrano-Ruiz, R. Luque, A. Sepúlveda Escribano, *Chem. Soc. Rev.*, **2011**, *40*, 5266–5281; f) P. Gallezot, *Chem. Soc. Rev.*, **2012**, *41*, 1538–1558; g) P. J. Deuss, K. Barta, J. G. de Vries, *Catal. Sci. Technol.*, **2014**, *4*, 1174–1196. h) U. Omoruyi, S. Page, J. Hallett, P. W. Miller, *ChemSusChem*, **2016**, *9*, 2037 – 2047; i) F. Liguori, C. Moreno-Marrodan, and P. Barbaro, *ACS Catal.*, **2015**, *5*, 1882–1894; j) L. T. Mika, E. Cséfalvay, Á. Németh, *Chem. Rev.*, **2018**, *118*, 505–613; k) U. Biermann, U. Bornscheuer, M. A. R. Meier, J. O. Metzger, H. J. Schäfer, *Angew. Chem. Int. Ed.*, **2011**, *50*, 3854–3871.

³ a) J. Zakzeski, P. C. A. Bruijninx, A. L. Jongerijs, B. M. Weckhuysen, *Chem. Rev.*, **2010**, *110*, 3552–3599; b) R. Rinaldi, R. Jastrzebski, Dr. M. T. Clough, J. Ralph, M. Kennema, P. C. A. Bruijninx, B. M. Weckhuysen, *Angew. Chem. Int. Ed.*, **2016**, *55*, 8164–8215; c) M. Zaheer, R. Kempe, *ACS Catal.*, **2015**, *5*, 1675–1684.

⁴ Berlin, et al., *Bioenergy Research: Advances and Applications*, **2014**.

catalytic system for the hydrogenation of *N*-heterocyclic compounds. *N*-Heterocycles are important building blocks in natural and synthetic bioactive molecules among which 1,2,3,4-tetrahydroquinoline is specifically valuable with numerous applications in drugs and agrochemicals.⁵ Recently, such molecules have found interest as hydrogen reservoirs in the hot topic of future energy carriers.⁶ In the continuity of the second chapter, we will focus on the diastereoselective hydrogenation of *N*-heterocycles compounds, in particular quinoline and pyridine derivatives. Stereocontrol in these reductions is important because substituted saturated rings with defined configuration are common structural features of biologically or pharmacologically active molecules.

⁵ I. Muthukrishnan, V. Sridharan, J. Carlos Menendez, *Chem. Rev.*, **2019**, *119*, 5057-5191.

⁶T. Shimbayashi, K. Fujita, *Tetrahedron*, **2020**, *76*, 11, 130946.

Chapter 1

Lignin valorisation by catalysis

1/Introduction

1/ Lignocellulosique biomass

Lignocellulosic biomass is the most abundant natural source of carbon on earth⁷. It comes from agricultural and forestry residues or from wood processing. No crops needed for food production are therefore necessary to produce lignocellulosic biomass.

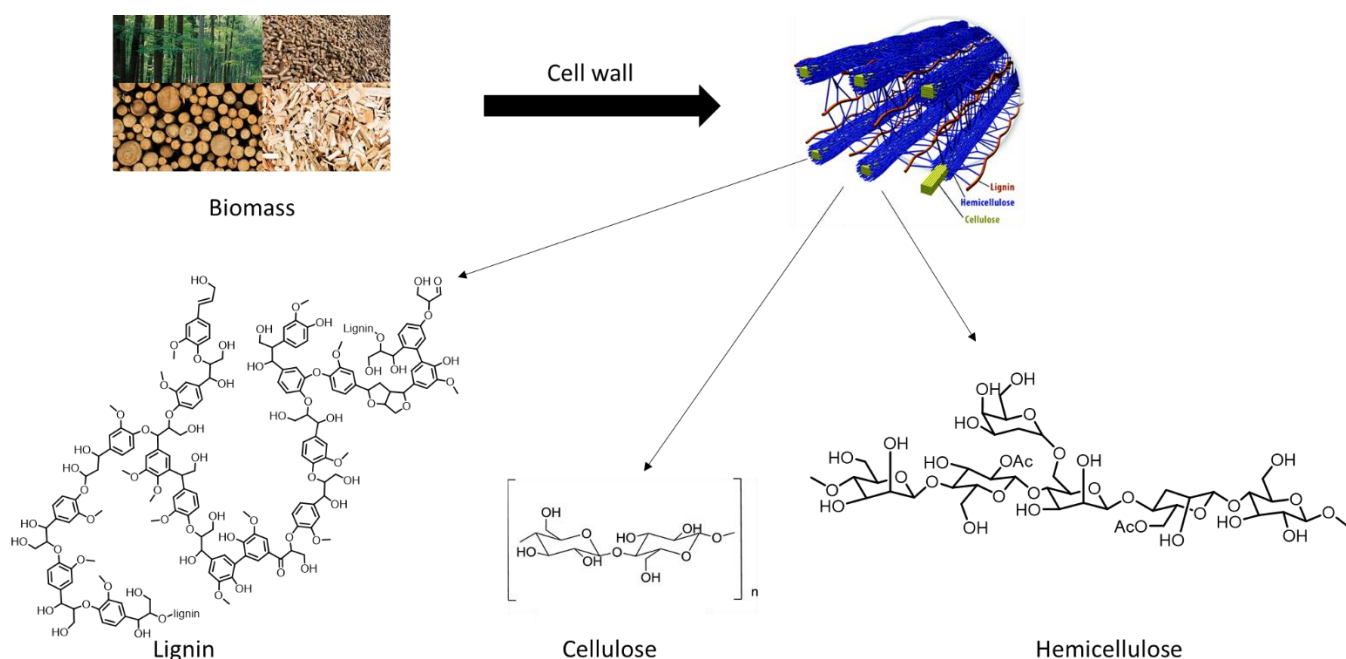


Figure 1 : Constitution of the lignocellulosic biomass.

Lignocellulosic biomass is composed of three major fractions: cellulose (35-50%), hemicellulose (25-30%) and lignin (15-30%) (Figure 1). These three components derived from lignocellulose are extracted by different treatments which are presented in the following sections.

a/ Cellulose

Cellulose is the most abundant biopolymer on earth. It mainly forms the cell wall of plants. Cellulose is a homopolymer composed of numerous D-anhydroglucopyranose units linked by glycosidic bonds, the repeating unit is called cellobiose (Figure 2).

⁷ S. Laurichesse, L. Avérous, *Progress in Polymer Science*, **2014**, 39, 1266-1290.

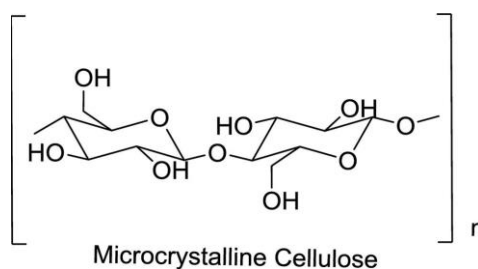


Figure 2: Cellulose structure

Cellulose is currently the element derived from lignocellulosic biomass with the most important industrial value. By hydrolysis, it is possible to obtain glucose which is a chemical platform for the synthesis of numerous products of industrial interest.⁸

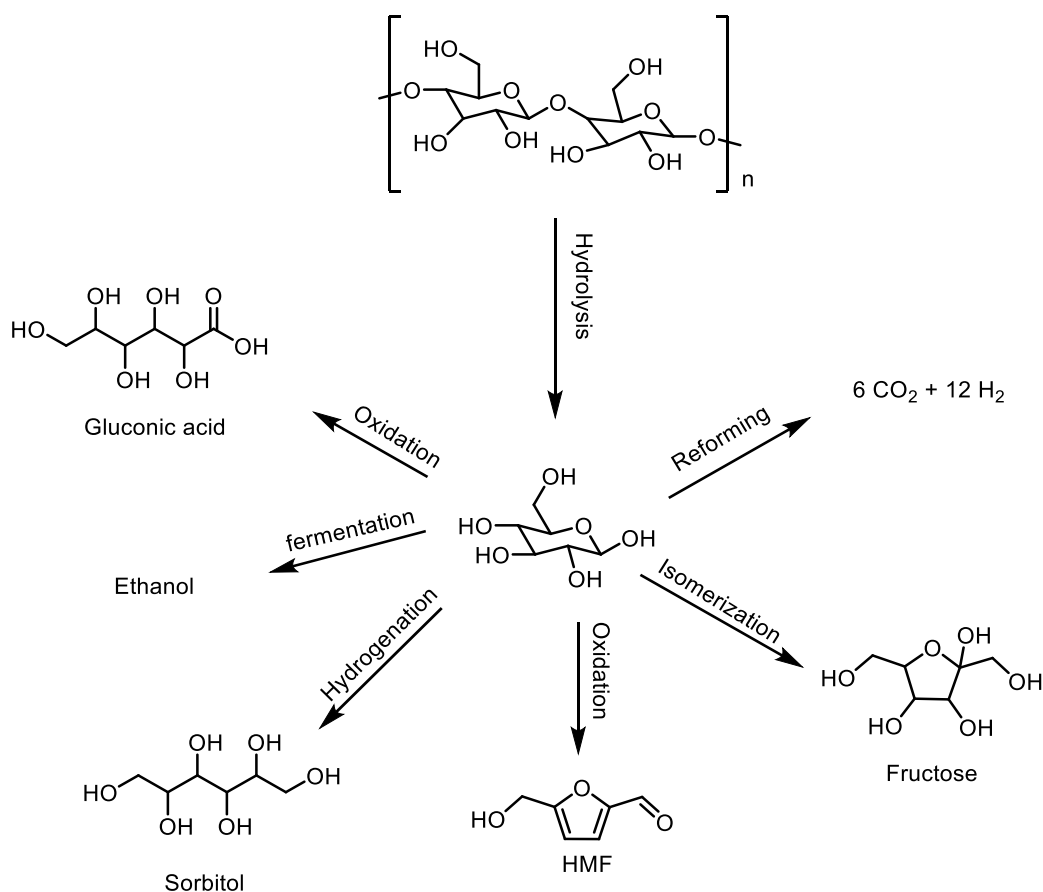


Figure 3: Cellulose platform chemicals

Glucose can be converted into sorbitol (hydrogenation), 5-hydroxymethylfurfural (HMF)(oxidation), hydrogen (reforming), gluconic acid (oxidation) (Figure 3). Of all glucose

⁸ M. Besson, P. Gallezot, C. Pinel, *Chem. Rev.*, **2014**, *114*, 1827–1870.

derivatives, gluconic acid is the most important for the chemical industry. In 2007, the world annual production was 100,000 tons,⁹ used in pharmaceutical and food applications and as water-soluble cleaner for removing calcareous and rust deposits. The fermentation of glucose can also lead to the formation of bioethanol, which can then be used as biofuel or blended with conventional fuel.¹⁰

b/ Hemicellulose

Hemicellulose is an amorphous branched polymer consisting of different monomers such as glucose, xylose, mannose, galactose (Figure 4).

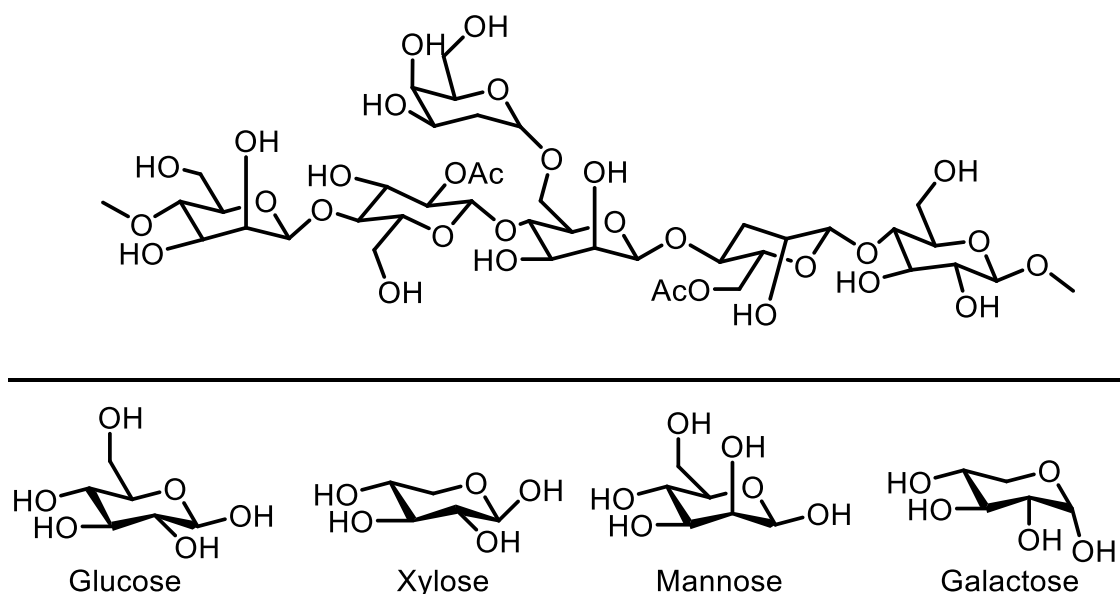


Figure 4: Hemicellulose structure

The main research concerning the valorisation of hemicelluloses has focused on their conversion to ethanol as a fuel source (second generation) or to platform chemical.¹¹ This conversion involves three steps: *i*) pre-treatment of the biomass to isolate hemicellulose, *ii*) depolymerization of hemicellulose into simple sugars by hydrolysis (acidic or enzymatic), *iii*) fermentation of the sugars into ethanol. For the moment, the difficulty for obtaining pure hemicellulose and their great diversity are slowing down the implementation of this kind of process on an industrial scale.

⁹ S. Anastassiadis, I. G. Morgunov. *Recent Pat. Biotechnol.*, **2007**, *1*,167-180

¹⁰ Okafor, N. *Modern Industrial Microbiology and Biotechnology*, (Science Publishers, Enfield, New Hampshire, 2007).

¹¹ F. M. Gírio, C. Fonseca, F. Carneiro, L.C. Duarte, S. Marques, R. Bogel-Lukasik. *Bioresour. Technol.*, **2010**, *101*, 4775–4800.

c/ Lignin.

Lignin is a three-dimensional amorphous polymer composed of methoxylated phenylpropane structures.¹² It represents a very complex structure that can change according to the plant and its environment (Figure 5). This feature is responsible for the slow development of lignin-based biorefineries.

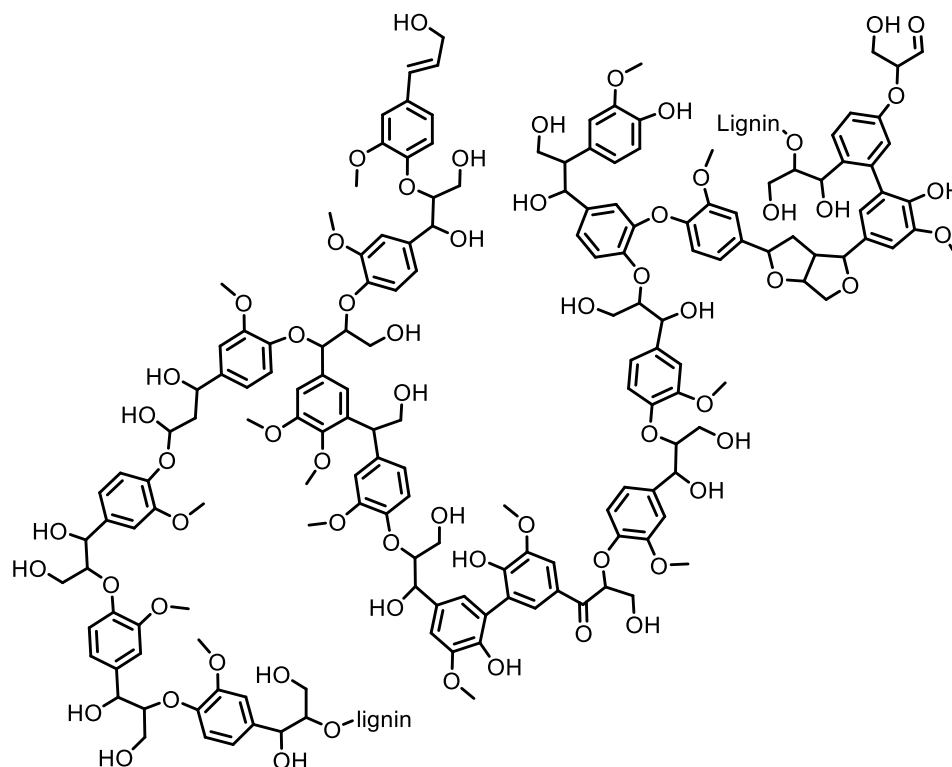


Figure 5: General Structure of lignin.

Lignins are present in the secondary walls of plant cells. They contribute greatly to the structural support of the plant by providing rigidity to the cell walls.¹³ It is important noting that lignin represents the second most abundant biopolymer on earth and the biopolymer with the highest content in aromatic groups.¹⁴

Currently, the paper industry alone generates 70 million tons of lignin per year. Indeed, lignin is a by-product of the Kraft paper synthesis¹⁵ and owing to the difficulties encountered for lignin valorisation, it is mainly used as a combustible.¹⁶

Lignin is a polymer composed of three phenolic monomers: coumaryl alcohol, coniferyl alcohol and synapil alcohol (Figure 6). The difference between these compounds is the presence of a methoxy group in position 3 or 5 of the phenyl group. The proportion of these precursors

¹² F. S.Chakar, A. J. Ragauskas. *Ind. Crops Prod.*, **2004**, *20*, 131-141.

¹³ C.-J. Liu, *Molecular Plant.*, **2012**, *5*, 304-317.

¹⁴ M.D. Kärkäs, B. S. Matsuura, T.M. Monos, G. Magallanes, C. R. J. Stephenson, *Org. Biomol. Chem.*, **2016**, *14*, 1853–1914.

¹⁵ D. Areskog, J. Li, G. Gellerstedt, G. Henriksson, *Biomacromolecules*, **2010**, *11*, 904–910.

¹⁶ E. Novaes, M. Kirst, V. Chiang, H. Winter-Sederoff, R. Sederoff, *Plant. Physiology*, **2010**, *154*, 555-561.

depends on the nature and the physico-chemical environment (soil, climate...) of the plant which directly influences the composition of lignin. Therefore, there is not one lignin but numerous types of lignin.

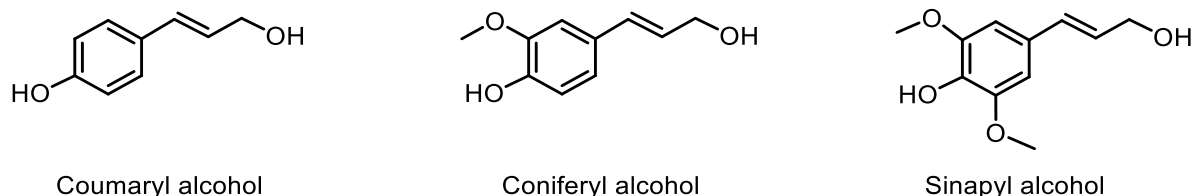
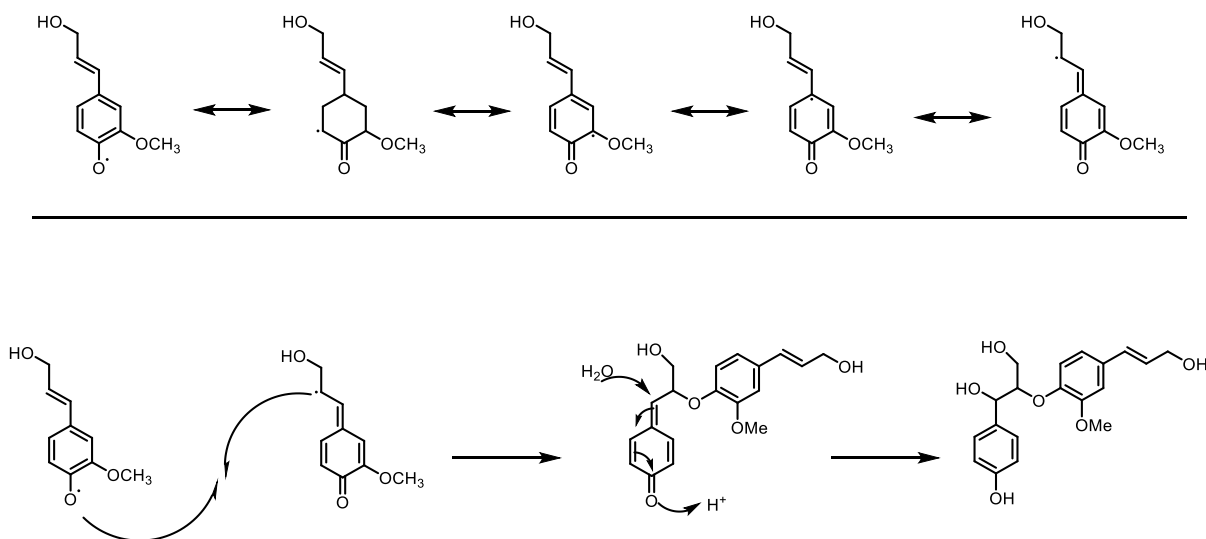


Figure 6: Lignin monomer

Lignin biosynthesis is a polymerization reaction of the different monolignoles.¹⁷ The first step is the radical oxidation of the monolignoles by enzymatic approaches such as peroxidase or lactase. The radical species formed are stabilized by the delocalization of the radical to its conjugated system (Scheme 1). Due to the radical delocalization, there are multiple possibilities of bond formation between two radical moieties. The process is repeated until a lignin polymer is obtained. The most stable radical intermediates are those where the radical is carried by phenolic oxygen and carbon in the β position. Thus, the bond between these two intermediates (β -O-4) is preponderant in lignin.



Scheme 1: Radical Form of lignin.

A convention has been set up to classify the different types of bonds that can be found in lignin. The carbons on the aromatic ring are numbered from 1 to 6, and the carbons present on the aliphatic chain are named α , β and γ (Figure 7). Thus, a β -O-4 bond refers to a bond between

¹⁷ T. Higushi. *Wood Sci. Technol.*, **1990**, 24, 23–63.

the aliphatic carbon at the β position of a monolignol and an oxygen bonded to a carbon at position 4 on the aromatic ring of another unit.

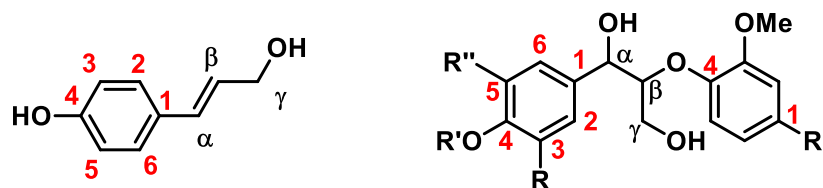


Figure 7: β -O-4 bond

Two types of bonds are commonly considered: on the one hand, ether bonds, potentially hydrolysable, composed of the β -O-4, α -O-4, and 4-O-5 bonds are the bonds mainly targeted in industrial delignification processes (Figure 8). β -O-4 (aryl ether) bonds are the most common bonds (about 45-60%).¹⁸ On the other hand, carbon-carbon bonds (β - β) known as "condensed" bonds are much more resistant to degradation. Finding methods to selectively cleave these bonds while preserving the aromatic nature of the lignin fragments represents one of the major issues for lignin valorisation.

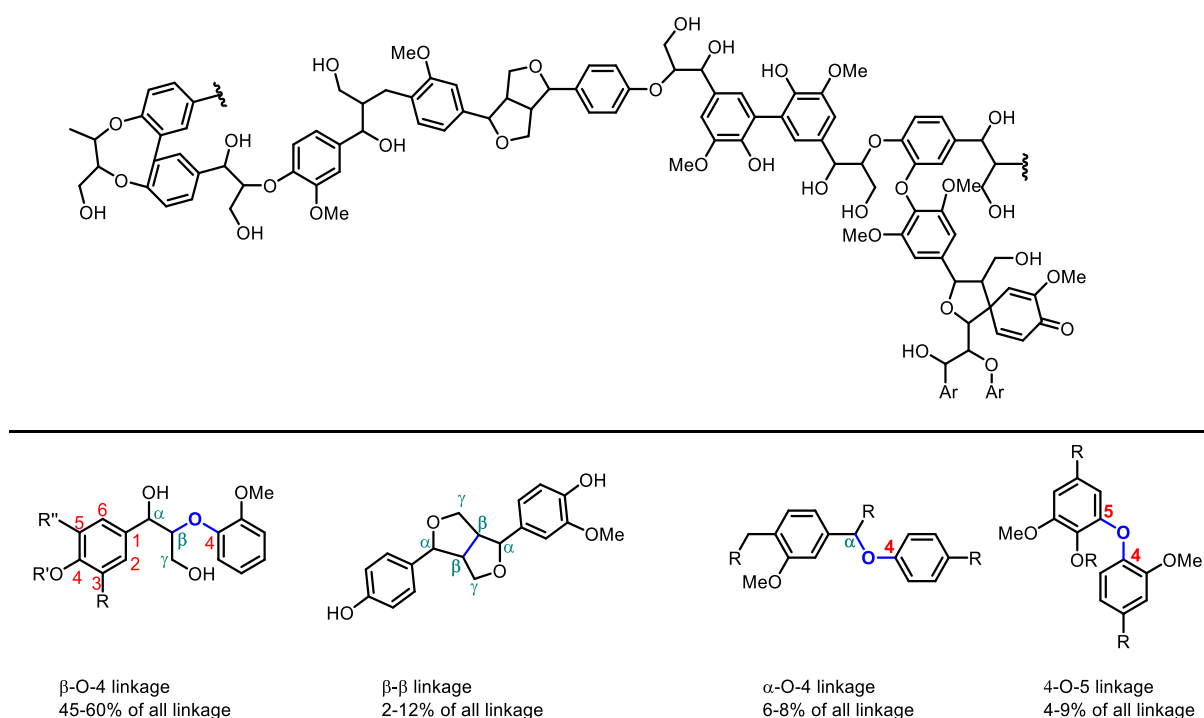


Figure 8: Main linkage motifs present in lignin^{19,20,21}

¹⁸ J. Zakzeski, P. C. A. Bruijninx, A.L. Jongerius, B.M. Weckhuysen. *Chem Rev.*, **2010**, *110*, 3552-3599.

¹⁹ P. Azadi, O. R. Inderwildi, R. Farnood, D. A. King, *Renewable and Sustainable Energy Reviews.*, **2013**, *21*, 506-523.

²⁰ F. S. Chakar, A. J. Ragauskas, *Ind. Crops Prod.*, **2004**, *20*, 131-141.

²¹ J. Ralph, K. Lundquist, G. Brunow, F. Lu, H. Kim, P. F. Schatz, J. M. Marita, R. D. Hatfield, S. A. Ralph, J. H. Christensen, W. Boerjan, *Phytochem. Rev.*, **2004**, *3*, 29-60.

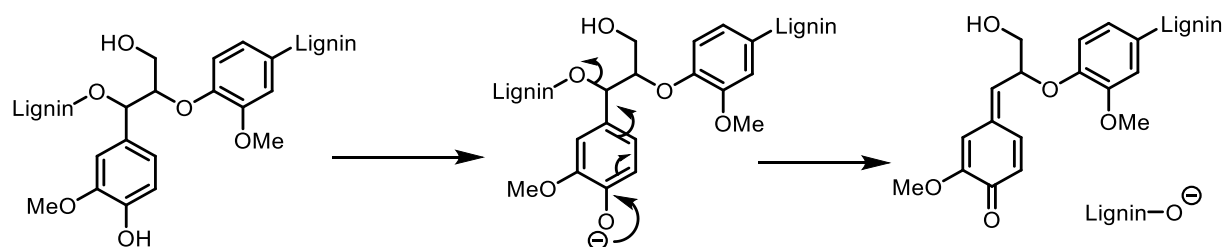
In addition, the composition of the patterns and the distribution of the bonds are highly dependent on the lignin nature. It is therefore essential to target a specific type of lignin according to the targeted applications.

2/ Lignin extraction

As lignin is bound to hemicellulose and cellulose, it is necessary to separate those three components but the high molar mass and three-dimensional network of lignin makes it insoluble in most common solvents. There are several extraction methods; chemical, mechanical²² and enzymatic.²³ In the following paragraphs we will be particularly interested in the three main methods of chemical isolation which are the Kraft, sulphite and Organosolv methods.

a/ The Kraft Process

The Kraft process is the most common process around the world,²⁴ representing 85% of the lignin world production which is estimated between 30 and 75 tons per day.²⁵ Kraft lignins represent the largest volume of lignin generated but only a tiny part is available. Indeed, most of the lignin is reused as an energy source for the paper industry.²⁶ During the process, wood chips are treated at high temperature (150-180°C) with sodium hydroxide and sodium sulphide for 2 to 5 hours.²⁷ Under these conditions, lignins will mainly fragment by labile bonds of the α - and β -ether-type.



Scheme 2: Kraft lignin process

Under the alkaline reaction conditions, the phenolic units will be deprotonated and the resulting phenolate groups will lead to the formation of methyl quinone units by releasing an alcoholate group (Scheme 2).²⁸ The reaction continues with the addition at the α -position of sulfide or

²² T. Hanninen, A. Thygesen, S. Mehmood, B. Madsen, M. Hughes, *Industrial Crops and Products*, **2012**, *39*, 7-11.

²³ D. Fu, G. Mazza, Y. Tamaki, *J. Agric. Food Chem.*, **2010**, *58*, 5, 2915-2922.

²⁴ C. Wang, S. S. Kelley, R. Venditti, *ChemSusChem.*, **2016**, *9*, 770-783.

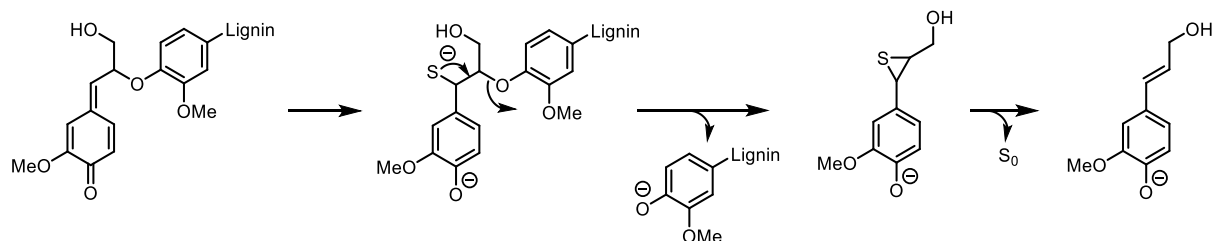
²⁵ A. Berlin, M. Balakshin, *Chapter 18 - Industrial Lignins: Analysis, Properties, and Applications*, in *Bioenergy Research: Advances and Applications*, V.K. Gupta, M.G.T.P. Kubicek, and J.S. Xu, Editors., **2014**, Elsevier: Amsterdam. p. 315-336.

²⁶ B. M. Upton, A. M. Kasko, *Chem. Rev.*, **2016**, *116*, 2275-2306.

²⁷ P.J Kleppe, *Kraft pulping*. Tappi, **1970**, *53*, 1, 35-47.

²⁸ J. Gierer, *Wood Science and Technology.*, **1980**, *14*, 241-266.

bisulfite ions arising from the decomposition of sodium sulphide,²⁹ followed by an intramolecular nucleophilic substitution which will induce the cleavage of the aryl-ether bond and finally the elimination of elemental sulfur (Scheme 3).²⁰

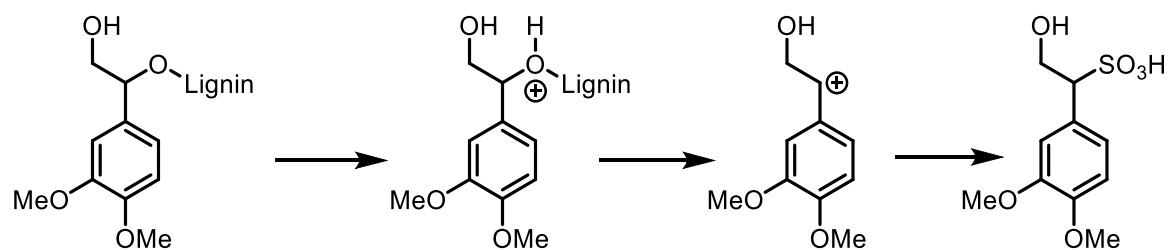


Scheme 3: Kraft lignin process

After several hours of treatment, two phases are obtained: a first solid phase composed of cellulose and a second liquid phase, called "black liquor" containing lignin. Finally, the black liquor is acidified to precipitate the lignin.

b/ Sulfite lignin

Like the kraft process, the sulfite process comes from the paper industry but it is carried out under acidic conditions. The biomass is treated with sulfurous acid and sodium bisulfate at a temperature ranging between 120 and 140°C.³⁰ This delignification method will mainly induce the cleavage of the aryl-ether bond.³¹ The first step consists in the sulfonation of the lignin, mainly at carbon α (Scheme 4). This step explains the high sulfur content of the lignins resulting from the sulfite process.



Scheme 4: Sulfite Process

Lignosulphates are the only lignin derivatives currently valued in large quantities. The presence of sulfonic acid groups gives it amphiphilic properties and good solubility in water, which

²⁹ G. Koch., *Handbook of pulp*. Vol. 1. **2006**.

³⁰ J. F. Kadla, Q. Dai, *Pulp*, in *Kirk-Othmer Encyclopedia of Chemical Technology*., **2000**, John Wiley & Sons, Inc.

³¹ W. O. S. Doherty, P. Mousavioun, C.M. Fellows. *Industrial Crops and Products*., **2011**, 33, 259-276.

allows it to be used as a surfactant, emulsifier or ion exchange resins.³² On an industrial scale, the main application is the production of vaniline.³³

c/ Organosolv Process

The principle of the organosolv process is to extract lignin from the biomass by a solution composed of an organic solvent and an aqueous phase (Acidic or basic).³⁴ Hemicelluloses are then precipitated in ethanol and a high purity lignin is obtained after distillation of the solvents.³⁵ A wide variety of processes has been developed depending on the extraction solvents used (Table 1).³⁶ The main organic solvents used are methanol and ethanol but solvent systems based on formic acid and acetic acid are also known. An acid catalyst can also be used to increase the yield of the reaction but too high catalytic charge can induce the formation of unwanted by-products.

Table 1: different organosolv processes

Process	Solvent
Alcell	Ethanol/water
Alcetocell	Acetic acid/water
Acetosolv	Acetic acid/HCl
ASAM	Sulfite alcalin/Anthraquinone/Methanol
Batelle	Phenol/HCl/water
Formacell	Acetic acid/Formic acid/water
Milox	Formic acid/ Hydrogen peroxide
Organocell	Methanol/NaOH/Anthraquinone

Depending on the experimental conditions, acidic or basic, the reaction proceeds by the cleavage of the ether bonds in α or β position, respectively. The most commonly used organosolv process is called Alcell¹⁹ (Figure 9) which uses water and ethanol as solvent. The wood chips are first loaded into the extractors operating at a temperature of 190°C and a pressure of 28 bars. After one hour, the primary liquor containing dissolved lignin, hemicellulose and furfural is sent from the extractor to the product recovery section. The resulting liquor is sent to a liquid/vapour separator (flash drum) where some of the ethanol is reused on the extraction line. The lignins are finally recovered by settling in the clarifier and then centrifuged. The remaining liquid phase is then distilled to recycle the solvent and extract the recoverable by-products such as sugars and furfural. then centrifuged. The Organosolv process is for the moment not enough cost-effective to replace existing paper processes and this technique is hardly used in the paper industry. Indeed, the pulp with the paper obtained is of lower quality and solvent recycling is expensive. However, the organosolv process being mild, the lignin is slightly altered and therefore obtained with a very high purity and many chemical functions available. These characteristics make organosolv lignins a prime candidate for further raw material synthesis.

³² L. Zoumpoulakis, J. Simitzis. *Polymer International*, **2001**, 50, 3, 277-283.

³³ H. Priefert, J. Rabenhorst, A. Steinbüchel. *Microbiol. Biotechnol.*, **2001**, 56, 296–314.

³⁴ E. Muurinen, Organosolv pulping: a review and distillation study related to peroxyacid pulping. (Oulun yliopisto, **2000**).

³⁵ R. Katahira, A. Mittal, K. McKinney, P. N. Ciesielski, B. S. Donohoe, S. K. Black, D. K. Johnson, M. J. Bidy, G. T. Beckham. *ACS Sustain. Chem. Eng.*, **2014**, 2, 1364–1376.

³⁶ F. J. Calvo-Flores, J. A. Dobado, *ChemSusChem.*, **2010**, 3, 1227-1235

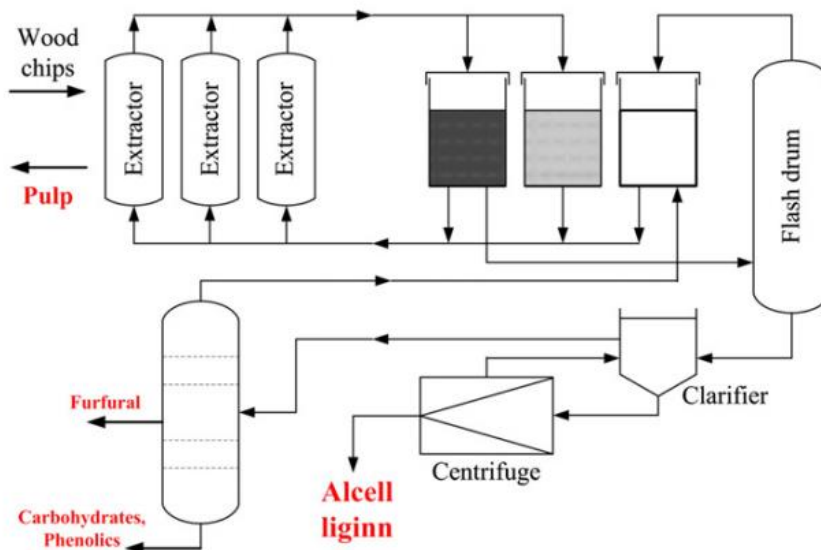


Figure 9: Industrial organosolv process (Reproduced from ¹⁹)

3/ Biomass valorisation

As stated previously, lignin is the most abundant aromatic group-containing biopolymer on earth. It is therefore highly studied in the research field as a renewable alternative to fossil-based aromatics since the depolymerization of lignin, through ether bond cleavage is likely to lead to the formation of synthon currently derived from petroleum.³⁷ By catalytic way, there are mainly three methods implemented for ether-bond cleavage: oxidative cleavage, hydrogenolysis and redox-neutral.

In all three cases, lignin depolymerization presents a number of challenges. First of all, many synthons are obtained, hence leading to purification issues. Secondly, experimental conditions that are too harsh may be responsible for condensation and degradation reactions leading to the formation of unusable residue. Finally, depending on the origin of the lignin and its mode of extraction, the synthons obtained will be different. It is for these reasons that research work has focused on lignin models.³⁸ The use of simple models is essential as they overcome the problems of solubility, heterogeneity and analysis difficulties related to the complexity of lignin.³⁹

a / Oxidative cleavage

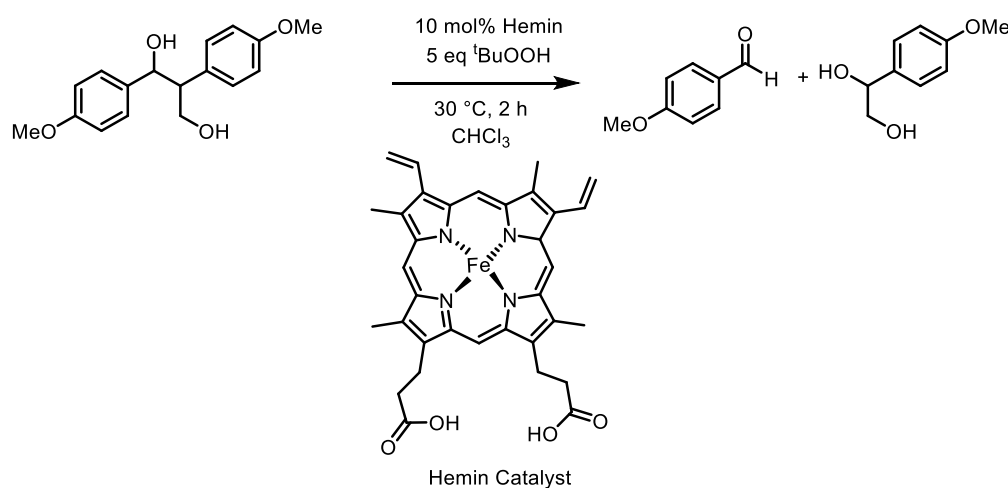
Oxidative cleavage is one of the techniques used for the isolation of aromatic products from lignin. This method increases complexity and functionalization of the products formed.

³⁷ R. T. Mathers, *J. Polym. Sci. Part Polym. Chem.*, **2012**, *50*, 1–15.

³⁸ a) C. Canevali, M. Orlandi, L. Pardi, B. Rindone, R. Scotti, J. Sipilä, F. Morazzoni, *J. Chem. Soc., Dalton Trans.*, **2002**, 3007–3014. b) V. Sippola, O. Krause, T. Vuorinen, *J. Wood Chem. Technol.*, **2004**, *24*, 323–340. c) K. Kervinen, H. Korpi, M. Leskelä, T. Repo, *J. Mol. Catal. A: Chem.*, **2003**, *203*, 9–19.

³⁹ Zakzeski, J., Bruijninx, P. C. A., Jongerius, A. L. & Weckhuysen, B. M. *Chem. Rev.*, **2010**, *110*, 3552–3599.

Industrially, lignin is oxidized by nitrobenzene, hydrogen peroxide or metal oxides.⁴⁰ Early reports on the oxidative degradation of lignin models were centered on the use of biomimetic catalysts, such as metal porphyrins.⁴¹ This kind of catalyst are analogous to the hemo-protein ligninase, isolated from the white-rot fungus, which are enzymes that catalyze the oxygenated C–C bond cleavage of lignin model systems.^{42,43} In 1985, T. Higuchi and co-workers studied the cleavage of the C-C bond by the hemin catalyst, a Fe-porphyrin complex.⁴⁴ It was shown that the hemin catalyst was effective for lignin model degradation at 30 °C in the presence of 5 equiv. of *t*BuOOH to obtain an aldehyde as the major product, together with an hydroxylated product (Scheme 5).



Scheme 5: Oxidative cleavage with hemin catalyst.

An electron transfer mechanism has been proposed in this oxidative cleavage reaction. The catalytically active intermediate would be a Fe(V)-Oxo species. It was proposed that a one-electron abstraction by Fe(V)-oxo from the substrate generates a radical cation which will initiate the oxidative cleavage of the C-C bond and induced the formation of an aldehyde and a radical product. An oxidation induced by water or hydroperoxide allows the final product to be obtained and regeneration of Fe(V) species. (Scheme 6). Co-Schiff based complexes are known to catalyze the aerobic oxidation of phenol under mild conditions via the formation of a Co-Superoxo complex intermediate which allows the formation of a reactive phenoxy radical.⁴⁵ They are also known for the activation of oxygen^{46, 47} and have been used to catalyse a plethora of transformation.⁴⁸

⁴⁰ Pandey, M. P.; Kim, C. S. *Chem. Eng. Technol.*, **2011**, *34*, 29-41.

⁴¹ B. Meunier, *Chem. Rev.*, **1992**, *92*, 1411–1456.

⁴² M. Tien, T. K. Kirk, *Proc. Natl. Acad. Sci. U. S. A.*, **1984**, *81*, 2280–2284.

⁴³ M. Kuwahara, J. K. Glenn, M. A. Morgan, M. H. Gold, *FEBS Lett.*, **1984**, *169*, 247–250.

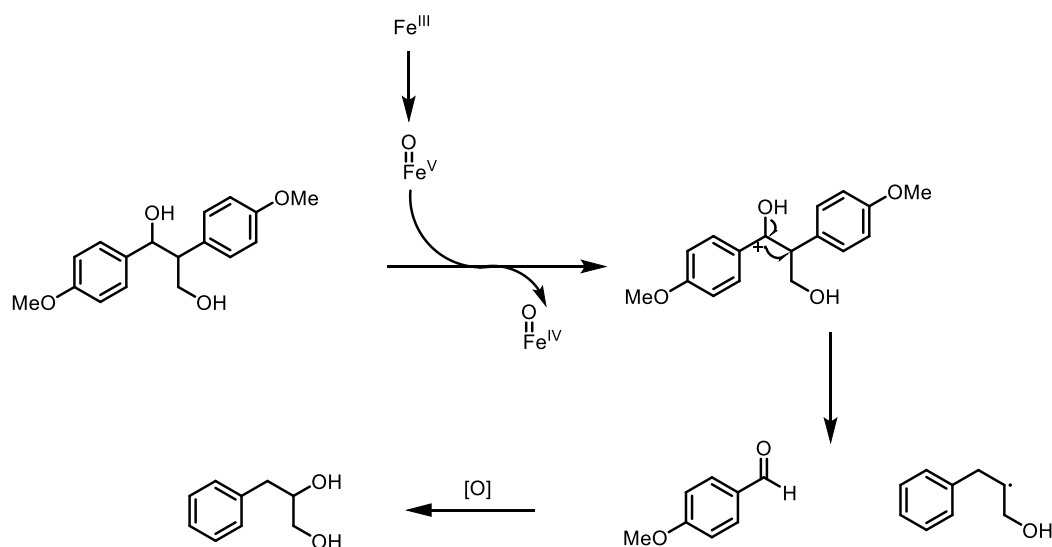
⁴⁴ T. Habe, M. Shimada, T. Okamoto, B. Panijpan, T. Higuchi, *J. Chem. Soc., Chem. Commun.*, **1985**, 1323–1324.

⁴⁵ Zombeck, A. Drago, R. S. Corden, B. B. Gaul, J. H., *J. Am. Chem. Soc.*, **1981**, *103*, 7580-7585.

⁴⁶ R. D. Jones, D. A. Summerville, F. Basolo, *Chem. Rev.*, **1979**, *79*, 139–179.

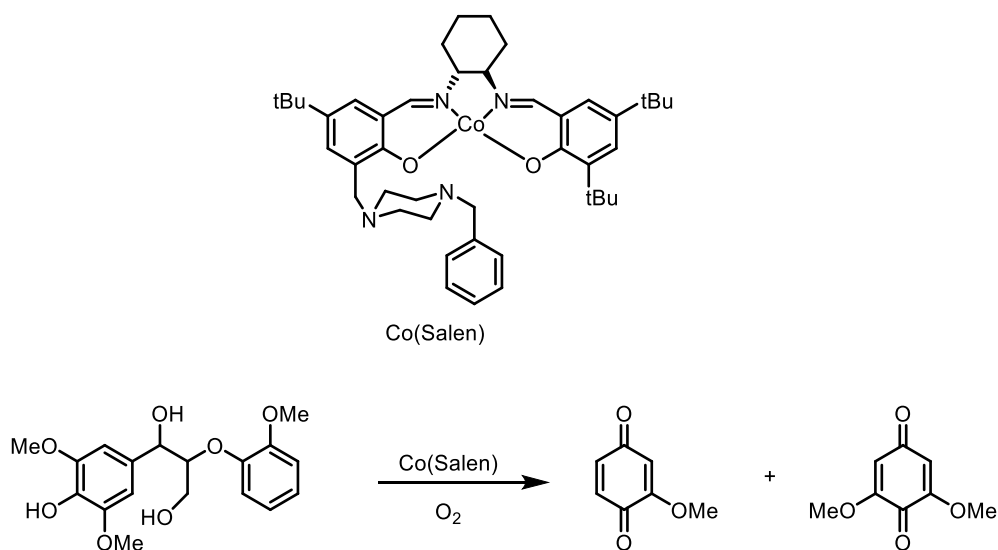
⁴⁷ J. Piera and J.-E. Bäckvall, *Angew. Chem., Int. Ed.*, **2008**, *47*, 3506–3523.

⁴⁸ P. G. Cozzi, *Chem. Soc. Rev.*, **2004**, *33*, 410–421.



Scheme 6: Oxidative cleavage mechanism

In 2013, Bozell and co-workers demonstrated one of the first examples of selective oxidation of lignin by a Co(Salen) complex (Scheme 7).⁴⁹



Scheme 7: Oxidative cleavage of a lignin model with Co(Salen).

Under optimized conditions, the reaction was possible with a catalyst loading of 5 mol% at room temperature under 4 bars of oxygen for 16 hours. The reaction was further extended to a number of lignin models (Table 2).

⁴⁹ B. Biannic, J. J. Bozell, *Org. Lett.*, **2013**, *15*, 2730–2733.

Table 2: Scope of reaction ^a

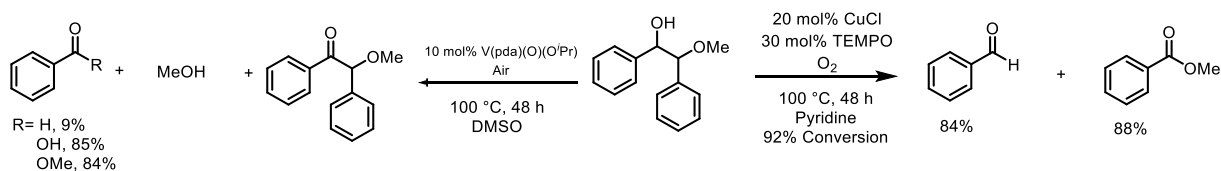
Entry	Substrate	t (h)	1 (%)	2 (%)	3 (%)
1		16	-	72	11
2		16	83	-	-
3 ^b		24	51	-	22
4		16	-	81	traces
5		16	17	86	traces
6 ^b		48	21	64	traces
7		48	0 ^d	10	0 ^e

^a Yields are given for isolated material. ^b 10 mol% of catalyst used. ^c Yields relative to 2 equiv. of product formed. ^d 14% 2,5DMBQ isolated, ^e 30% aldehydes.

Oxidation of substituted benzyl alcohol proceeded smoothly, and 2,6-dimethoxybenzoquinone was obtained in high yield although increasing substitution at the benzylic position slowed the reaction (Table 2, Entry 1). Vanillyl alcohol was oxidised to methoxybenzoquinone in high yield and selectivity (Entry 2). However, adding a methine in alpha of the alcohol offered the methoxybenzoquinone in moderate yield (Entry 3). Several phenolic lignin dimers with a β -aryl ether bond were also converted to the corresponding benzoquinone. Compound present in entry 4 was converted to 2 equiv of **2** in excellent yield. Gratifyingly, compound presenting residual β -O-4 linkage remaining after lignin isolation were also oxidized to high yield of **2** (Table 2, Entries 5-7). More moderate yields of **1** were observed for these dimers as a result of possible rapid dimerization of the intermediate phenoxy radical to biphenols or diphenoquinones.

Another oxidation route for lignin fragmentation makes use of radicals. Inspired by nature, much research work has focused on the development of oxidative single electron transfer methods using a radical initiator. The most common oxidants are the derivatives of (2,2,6,6-Tétraméthylpipéridin-1-yl)oxy (TEMPO) and 9-azabicyclo[3.3.1]nonane N-oxyl (ABNO)⁵⁰

In 2011, Hanson and co-workers compared aerobic oxidation of lignin models using homogeneous copper and vanadium catalysts.⁵¹ They began their investigations of a lignin model containing a β -1 bond with a catalyst composed of CuCl (20 mol%), TEMPO (30 mol%) in pyridine at 100°C for 48 hours in an oxygen atmosphere. This system allows the formation of benzaldehyde and methyl benzoate in 92% conversion (Scheme 8).



Scheme 8: Vanadium et copper oxidative cleavage.

In contrast to the CuCl / TEMPO system, the vanadium-catalyzed aerobic oxidation produced benzoin methyl ether, which can also undergo C-C bond cleavage and over-oxidation to benzoic acid. With this catalyst, benzaldehyde, methanol, benzyl and benzoin can also be observed as minor products.

[b/ Hydrogenolysis](#)

Hydrogenolysis takes place between hydrogen or a hydrogen donor reactant and a target compound and is a reductive process. The reaction generally takes place with supported metal catalysts (Pt, Ru, Rh, Pd, Ni, etc.). It is a popular and efficient method for cracking the C–O linkages, especially β -O-4 linkages in lignin and for producing aromatic platform chemicals from lignin.⁵² While the ultimate goal of lignin depolymerization has yet to be realized due to

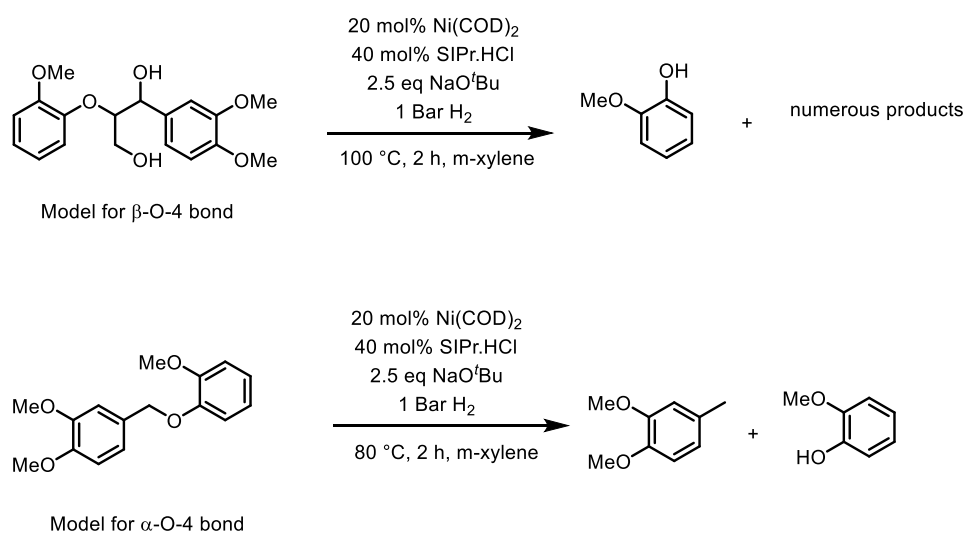
⁵⁰ M. Tien, T. K. Kirk, *Science*, **1983**, 221, 661–663.

⁵¹ B. Sedai, C. Díaz-Urrutia, R. T. Baker, R. Wu, L. A. Silks, S. K. Hanson, *ACS Catal.*, **2011**, 1, 794–804.

⁵² M. Zaheer, R. Kempe, *ACS Catal.*, **2015**, 5, 1675–1684.

catalyst inefficiencies and the complexity of lignin, a variety of metal complexes and hydride sources have been demonstrated for the reductive cleavage of C–O bond frameworks in lignin models. One of the first example of C–O cleavage by hydrogenolysis have been developed by Martins and co-workers in 2010.⁵³ They screened several hydride reagents including silanes, borohydride salts, alkyl zinc and alkyl aluminum reductants. Optimally, they found the combination of Ni(COD)₂ with 1,1,3,3-tetramethyldisiloxane (TMSDO) was an efficient method for reductive demethoxylation of arenes. One year later, Chatani developed a nickel-catalyzed method for removing oxygenated functionalities, such as alkoxy and pivaloxy groups, on aromatic rings using hydrosilane as a mild reducing agent.⁵⁴

In 2011, Hartwig and Sergeev reported the first exemple of C–O bond cleavage of lignin models incorporating a variety of alkyl aryl ether compounds.⁵⁵ They accomplished this reduction via a Ni-NHC complex (Scheme 9). The Ni catalyst formed in situ was compatible with different hydride sources but ultimately, 1 bar of dihydrogen was used as the reducing source. They demonstrated efficiency for Ar–OAr, Ar–OMe and ArCH₂–OMe substrates, its ability to reduce Csp²–O and Csp³–O bonds. It is important to note that this catalyst is selective for aryl-aryl bonds in the presence of aryl-alkyl ether bonds, showing promise for the selective depolymerization of 4–O–5 bonds.



Scheme 9: Lignin Hydrogenolysis with Nickel catalyst

Despite the high selectivity and mild reaction conditions in comparison to classic lignin hydrogenolysis reactions, this system employs high loadings of sodium *tert*-butoxide as an additive and an expensive NHC ligand.

The reaction conditions necessary for the hydrogenation of lignin are very harsh. That is why a lot of work uses heterogeneous catalysts. As an example, Anastas et al. described in 2014 the depolymerisation by hydrogenation of an organosolv lignin catalysed by Cu-Porous Metal

⁵³ P. Álvarez-Bercedo, R. Martin, *J. Am. Chem. Soc.*, **2010**, *132*, 17352–17353.

⁵⁴ M. Tobisu, K. Yamakawa, T. Shimasakia, N. Chatani, *Chem. Commun.*, **2011**, *47*, 2946–2948.

⁵⁵ A. G. Sergeev and J. F. Hartwig, *Science*, **2011**, *332*, 439–443.

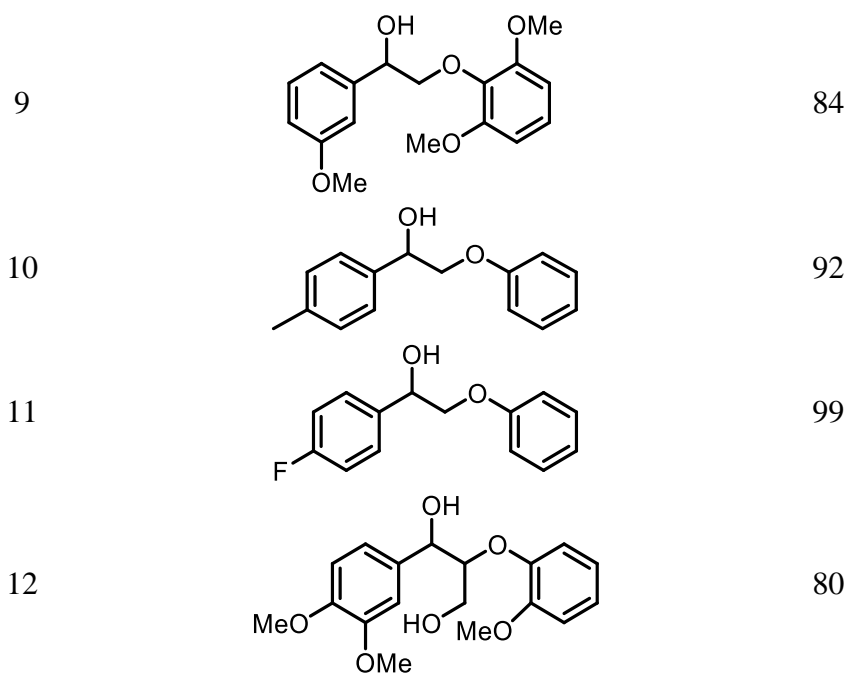
Oxyde at 180°C for 14 hours with a hydrogen pressure of 4 bar.⁵⁶ More recently, in 2016, Cai and co-workers, reported a highly dispersed Pd-Ni BMNPs immobilized on ZrO₂ (Table 3).⁵⁷

Table 3: Lignin hydrogenolysis with bimetallic Pd-Ni Catalyst.

Entry ^a	Substrate	Yield ^b (%)
1		100
2		97
3		86
4		83
5		81
6		94
7		92
8		81

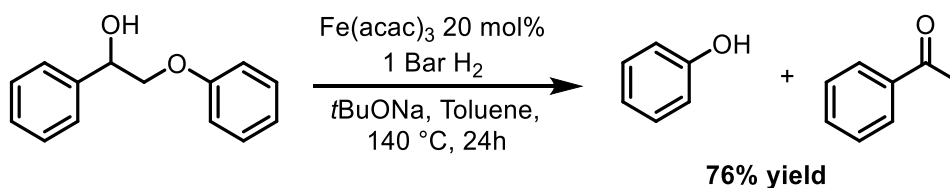
⁵⁶ K. Barta, G. R. Warner, E. S. Beach, P. T. Anastas, *Green Chem.*, **2014**, *16*, 191.

⁵⁷ J. W. Zhang, Y. Cai, G. P. Lu, C. Cai, *Green Chem.*, **2016**, *18*, 6229-6235.



Reaction conditions: 0.5 mmol of substrate, 2.5% catalyst (catalyst amount was based on palladium), 0.25 mmol NaBH₄, 80 °C, 6 h. ^bYields were determined by GC.

After optimizing the reaction, they investigated the β -O-4 bond cleavage in detail by including different substituents. Gratifyingly, introducing one methoxy group at R₃ or R₄ positions had no negative influence on the yield (Table 3, entry 2). A slight decrease of yields was observed when R₁ or R₂ were methoxy-group (Table3, entries 3 and 4), which can be explained by the increased Bond Dissociation of Energie (BDE) of the β -O-4 linkage. For the substrates bearing two or more methoxy groups, promising yields were afforded (Table 3, entries 5–9). A less bulky substrate with a methyl at the R₁ position also underwent efficient fragmentation (Table3, entry 10). Moreover, a substrate with an electron-withdrawing group at the R₁ position can also be efficiently fragmented (Table3, entry 11). Besides, to exactly mimic lignin, a β -O-4 model compound with γ -CH₂OH was also tested for the reaction, and a satisfactory yield was obtained (Table3, entry 12). In 2013, An iron based catalytic system for the selective reductive cleavage of aryl C-O bonds was reported by Yao and all.⁵⁸ Using an Iron(III) acetylacetonate as a catalyst precursor, *t*BuONa as a base, 1 bar of hydrogen pressure at 140 °C for 24 h. A dimeric lignin model compound that contained a b-O-4 linkage was smoothly converted into the desired products with high selectivity (Scheme 10).



Scheme 10: C-O cleavage by Fe(acac)₃.

⁵⁸ Y. Ren, M. Yan, J. Wang, C. Zhang, K. Yao, *Angew. Chem. Int. Ed.*, **2013**, 52, 12674–12678.

c/ Redox-neutral

A third route for lignin valorisation consists in the redox neutral fragmentation of lignin. In this approach, the reductant is removed from the feedstock to be later reused. In a first step, oxidation of the alcohol function present in the molecule by dehydrogenation generates a carbonyl group formally releasing dihydrogen. In a second step, this borrowed hydrogen is reused for the cleavage of the C-O bond. The ideal redox-neutral transformation would require a catalyst capable of carrying out the oxidation and reduction reaction at the same time by a so-called hydrogen-borrowing process. One of the first report on redox-neutral process was published by Ellman, Bergman and co-workers in 2010 (Table 4).⁵⁹

Table 4: Redox neutral depolymerization with $Ru(H)_2(CO)(PPh_3)_3$

Entry ^a	Ligand	Conv ^d (%)	PhCOMe Yield (%)	PhOH Yield(%)
1	None	45	5	6
2	PPh_3 ^b	39	<1	5
3	PCy_3 ^b	27	4	5
4		11	0	0
5		32	0	<1
6		32	0	0
7		37	5	6
8		>99	>99	>99

^a Reactions were run in sealed tubes under nitrogen. ^b 2 equiv relative to Ru. ^c Yields and conversions were determined by GC/MS relative to an internal standard. ^d Average of two duplicate experiments.

Their approach uses a ruthenium catalyst formed in-situ from $Ru(H)_2(CO)(PPh_3)_3$ in combination with a ligand. They started their investigations using 2-phenoxy-1-phenylethan-1-ol as a model substrate to screen different varieties of monodentate and bidentate ligands. As depicted in Table 4, in the absence of ligand, $Ru(H)_2(CO)(PPh_3)_3$ delivered only a small amount

⁵⁹ M. Nichols, L. M. Bishop, R. G. Bergman, J. A. Ellman, *J. Am. Chem. Soc.*, **2010**, *132*, 12554–12555.

of product and low conversions were obtained with monodentate phosphine ligand (Table 4, entries 2-3). Bidentate ligands performed well for the dehydrogenation step to form phenoxyacetophenone but did not allow the C-O bond cleavage (Table 4, entry 4-7). Finally, Ph-xantphos was identified as the best ligand enable almost full conversion and quantitative yields (Table 4, entry 8).

Table 5 : Scope of the reaction.

$\text{Ar}-\text{CH}(\text{OH})-\text{CH}_2-\text{OAr}' \xrightarrow[\text{Toluene, 135 }^\circ\text{C, 4 h}]{\text{RuH}_2\text{CO}(\text{PPh})_3 \text{ 1 mol\%}, \text{Ph-xantphos 1 mol\%}} \text{Ar}-\text{C}(=\text{O})-\text{CH}_3 + \text{Ar}'\text{OH}$		
Entry	Substrate	Yield (%) ^a
1		99
2		88
3		62
4		98
5		89

^a Average isolated yield of the corresponding ketone based on two duplicate experiments.

A few other lignin models were tested delivering the products from the cleavage reaction in good yield (Table 5). A slight decrease in yield was observed when using a substituted 2,6-dimethoxy phenol (Table 5, entry 3).

In 2013, Leitner, Klankermayer and co-workers reported an even more active ruthenium complex combining the ruthenium precursor $[\text{Ru}(\text{cod})(\text{methallyl})_2]$ (cod = 1,5 cyclooctadiene; methallyl = $\eta^3\text{-C}_4\text{H}_7$) with a tripodal phosphine.⁶⁰ First tests showed that monodentate and bidentate ligands such as PPh_3 and dppp (dppp = 1,3-bis(diphenylphosphino)propane) resulted in low conversions (Table 6, entries 1-2). However, by using a tripodal phosphine, a very active system was obtained, offering 65% and 67% of acetophenone and phenol, respectively (Table 6, entry 3). An increased activity was observed with (diphenylphosphinoethyl)phenylphosphine (**C**) where the lignin pattern was fragmented with yields of 83% and 84% (Table 6, entry 4).

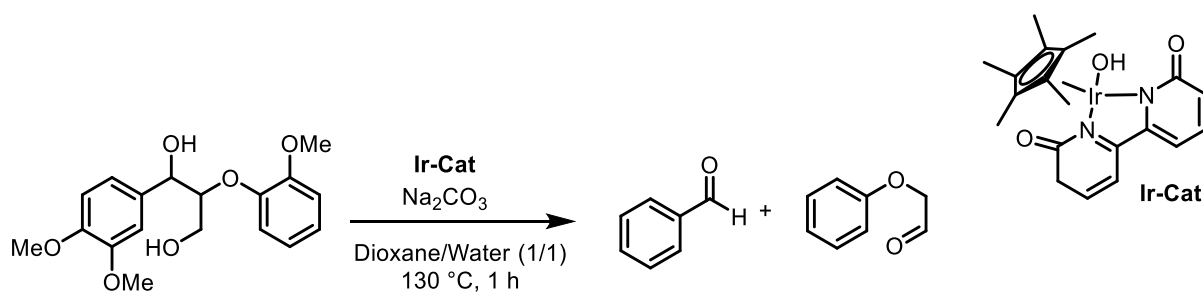
⁶⁰ T. vom Stein, T. Weigand, C. Merckens, J. Klankermayer, W. Leitner, *ChemCatChem*, **2013**, 5, 439–441.

Table 6: Redox neutral lignin deolmerization with $Ru(COD)(methallyl)_2$

Entry	Ligand	Phenol Yield(%)	Acetophenone Yield(%)
1	PPh_3 ^b	5	5
2	DPPE	1	2
3	B	65	67
4	C	84	83

a) Reaction conditions: 0.2 mmol substrate, 5 mol % precursor, 5 mol % ligand, 0.5 mL toluene, 135 °C, 2 h. Yields were determined by GC with dodecane as internal standard. [b] 3 equivalents of PPh_3 with respect to precursor.

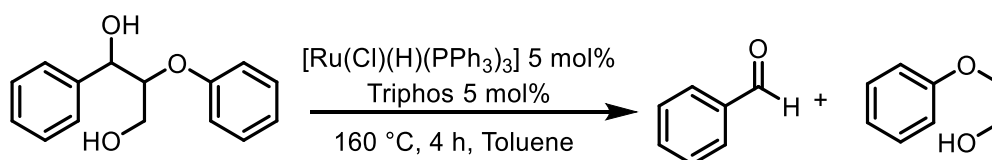
In 2018, Bruijninx and co-workers⁶¹, developed a new catalytic cleavage of the β -O-4 linkage using a anionic Cp^*Ir -bipyridionate complex. In this work, primary alcohol was oxidized as an activation strategy. thus opening lignin depolymerisation pathways via cleavage of the $C\alpha$ - $C\beta$ bond in the β -O-4 linkages, rather than the more common β -aryl ether ($C-O$) pathway (Scheme 11).

**Scheme 11 :** lignin model cleavage by Ir.

An alternative cleavage pathway was reported by Klankermayer⁶² and co-workers yet using these Ru -triphos system. Indeed, the authors were able to carry out redox-neutral $C-C$ bond cleavage on γ -OH containing lignin model substrates using $[Ru(Cl)(H)(PPh_3)_3]$ as a catalyst precursor, Triphos as a ligand at 160 °C for 4 h (Scheme 12).

⁶¹ C. S. Lancefield, L. W. Teunissen, B. M. Weckhuysen, P. C. A. Bruijninx, *Green Chem.*, **2018**, *20*, 3214-3221.

⁶² T. Stein, T. Hartog, J. Buendia, S. Stoychev, J. Mottweiler, C. Bolm, J. Klankermayer, W. Leitner *Angew. Chem. Int. Ed.*, **2015**, *54*, 1 – 6.



Scheme 12: C-C bond cleavage by Ru-triphos.

As depicted in this description of the state of the art, different methods for lignin depolymerisation can be envisioned. From our point of view, the redox-neutral method seems to be the most interesting in the context of green and sustainable chemistry since it does not require the use of external oxidants or reducing agent. Thus far, the reported research on this topic make use of noble metals such as ruthenium (described hereabove) or iridium. The use of non-noble and abundant metals would be of great interest for the valorisation of lignin. The first chapter of this manuscript will present the results obtained with cobalt complexes supported by bifunctional ligands for the redox-neutral depolymerisation of lignin.

II/ Results and discussions

1/ Introduction

Owing to their topological and electronic versatility, pincer ligands have arisen as a useful motif of supporting ligands for transition-metal compounds. Since their introduction by Shaw in 1976⁶³ and the pioneering work of Van Koten in 1978,⁶⁴ many catalysts have been developed for hydrogenation/dehydrogenation reactions, including catalysts supported by tridentate pincer ligands. Pincer type catalysts have the particularity of possessing a non-innocent ligand. More specifically, the ligand plays an indispensable role in the catalytic cycle and interacts directly with other reagents during various elementary steps.

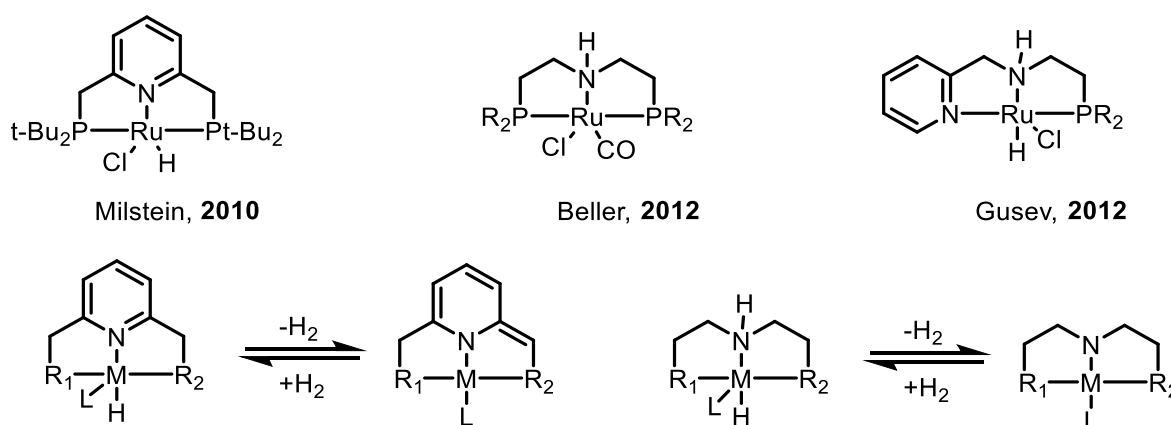


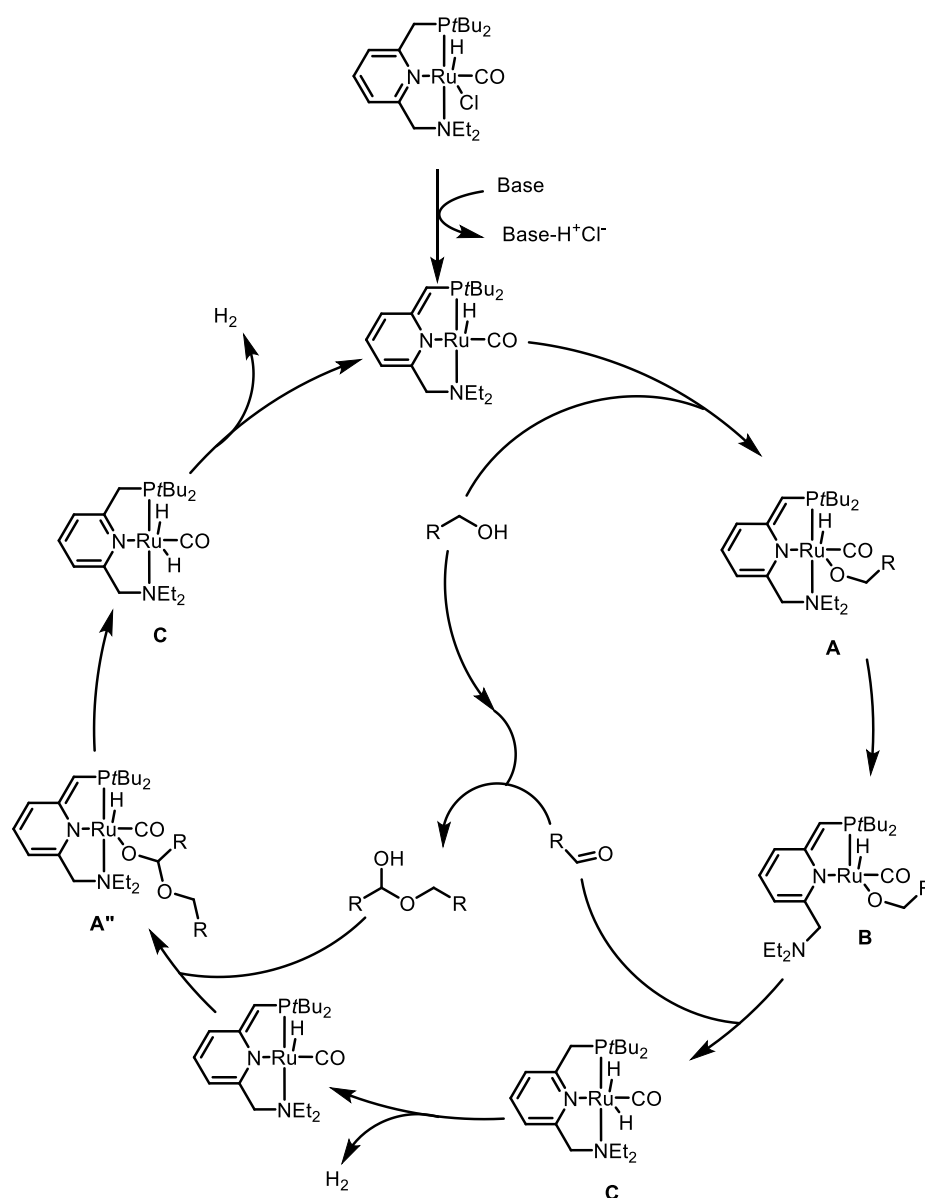
Figure 10: ruthenium PNP

⁶³ C. J. Moulton, B. L. Shaw, *J. Chem. Soc. Dalton Trans.*, **1976**, 1020–1024.

⁶⁴ G. van Koten, K. Timmer, J. G. Noltes, A. L. Spek, *J. Chem. Soc. Chem. Commun.*, **1978**, 250–252.

Such catalyst architectures incorporating non-innocent ligands operates via a so-called cooperative mechanism. Tridentate non-innocent pincer ligands generally PNP and PNN-type display mainly two types of cooperativity: aromatisation/dearomatisation and reversible transition from the amino to the amido form (Figure 10).

The Milstein group is one of the pioneers in the area of aromatic pincer ligands for cooperative metal-ligand catalysis.⁶⁵ The reactivity of these complexes is based on the cooperation between the metal and the aromatic ligand through reversible chemical bond activation. In this system, there is no change in the oxidation state of the metal because the nitrogen atom corresponding to the pyridine changes from an L (amino) group to an X (amido) group by the rupture of the aromaticity of the pyridine heterocycle. This operating mechanism is illustrated in Scheme 13 with the esterification of alcohols.

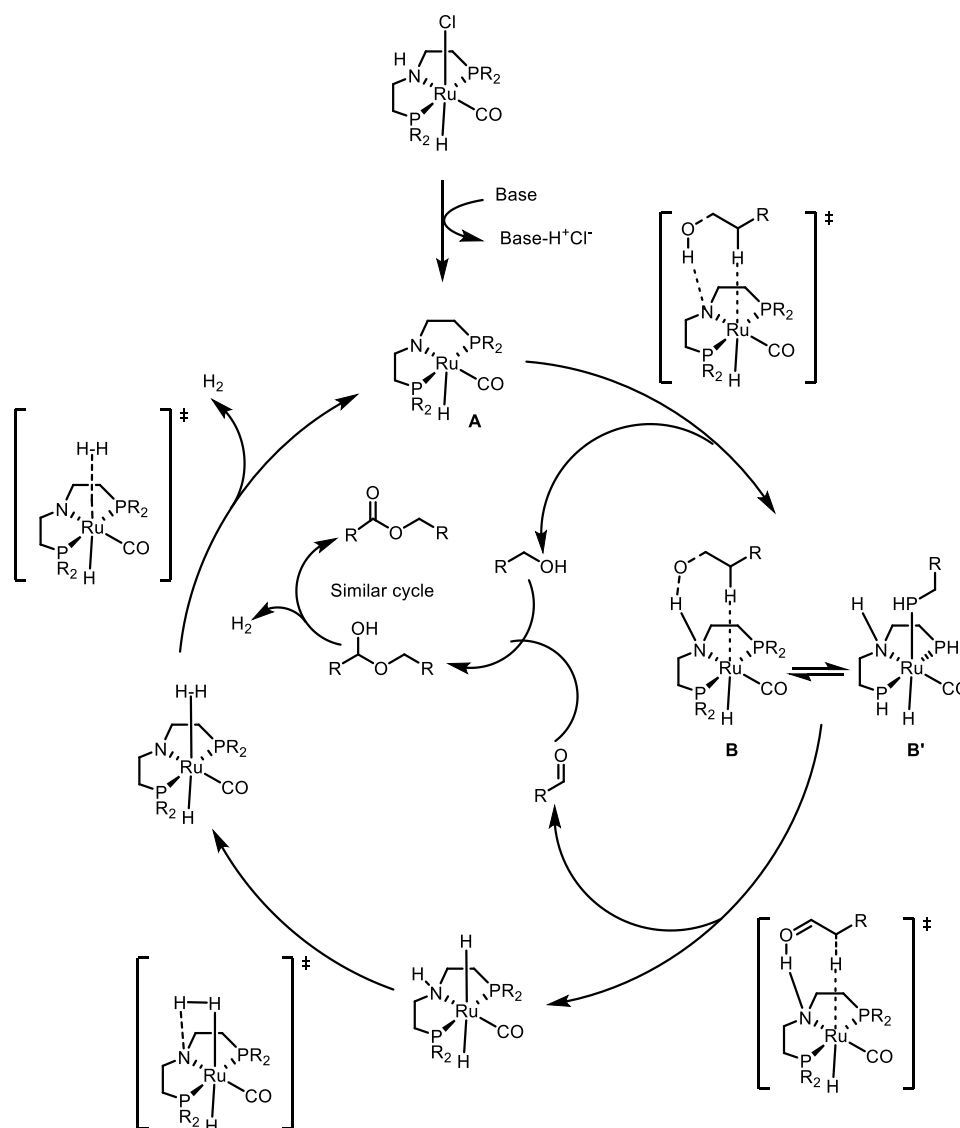


Scheme 13: Aromatic PNP catalytic mechanism

⁶⁵ Zhang, G. Leitus, Y. Ben-David, D. Milstein, *Angew. Chem. Int. Ed.*, **2006**, *45*, 1113-1115.

Pre-catalyst activation by a base releases the catalyst in its dearomatized and basic amido form. This catalyst subsequently activates the alcohol involving deprotonation by the ligand thus regenerating the pyridine ligand. The decooordination of one of the ligands is necessary to create a vacant site and allow the β -elimination and formation of an aldehyde and hemiacetal upon reaction with the alcohol. This step is facilitated with PNN ligands because the nitrogen ligand is more labile than the phosphorus ligand. The release of dihydrogen will allow the regeneration of the catalyst. Finally, the hydroxy function of the hemiacetal reacts in the same manner than the alcohol to deliver the symmetrical ester.

More recently, the Beller group has been studying the use of ruthenium complexes with PNP aliphatic pincer ligands for the dehydrogenation of alcohols.⁶⁶ Like aromatic ligands, aliphatic pincer complexes permit the activation of chemical bonds through metal-ligand cooperation (Scheme 14). In the process, the oxidation state of the metal does not change, but the nitrogen which was initially a two electrons donor amino-ligand is converted into an amido-ligand.



Scheme 14: Aliphatic PNP catalyst mechanism

⁶⁶ M. Nielsen, A. Kammer, D. Cozzula, H. Junge, S. Gladiali, M. Beller, *Angew. Chem. Int. Ed.*, **2011**, *50*, 9593-9597.

Here too, the catalyst can be generated in-situ from the chlorinated metal complex. In the presence of a base the catalyst releases HCl to give the amido catalytic species (A). This basic amido ligand then deprotonates the alcohol molecule through a transition state involving the coordination of the hydrogen present at the α -position in the alcohol. The alcohol is therefore dehydrogenated via a concerted mechanism to give an aldehyde. This aldehyde will further react with another alcohol molecule to form a hemiacetal. This hemiacetal will react in the same way as described earlier to form a symmetrical ester (Scheme 14).

The evolution of chemistry and green chemistry has pushed the search for new complexes containing, more abundant and therefore less expensive transition metals. Pincer complexes of manganese or cobalt were thus recently reported (Figure 11).⁶⁷

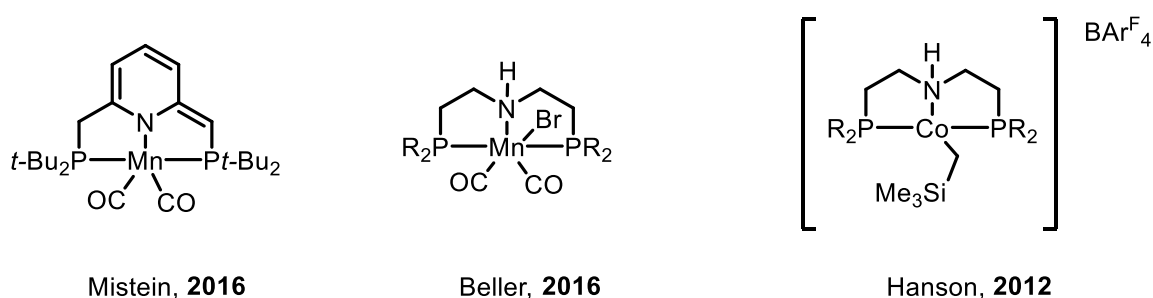


Figure 11: Catalyst based on abundant transitions metals

Catalysts supported by bifunctional pincer ligands have been widely used for hydrogenation in particular for ketone,⁶⁸ nitrile⁶⁹ and ester⁷⁰ hydrogenation reactions as well as for alcohol dehydrogenation reactions.⁷¹

For this project, we wish to use cobalt complexes supported by pincer ligands for the β -O-4 bond cleavage of lignin model by redox-neutral method. Cobalt catalysts have been described for the reductive alcohol amination reaction. In 2016, Mistein and co-workers developed a catalyst capable of forming pyrroles from diols and amine.⁷² Under optimized reaction conditions, 2,5-dihydroxyhexane derivatives and various amines allowed the formation of 1.2.5 substituted pyrroles with only water and dihydrogen as by-products (Table 7).

⁶⁷ A. Mukherjee, D. Milstein. *ACS Catal.*, **2018**, 8, 11435–11469.

⁶⁸ N. Gorga, B. Stöger, L. F. Veiros, E. Pittenauer, G. Allmaier, K. Kirchner. *Organometallics.*, **2014**, 33, 6905–6914.

⁶⁹ A. Mukherjee, D. Srimani, S. Chakraborty, Y. Ben-David, D. Milstein. *J. Am. Chem. Soc.*, **2015**, 137, 28, 8888–8891.

⁷⁰ E. Balaraman, B. Gnanaprakasam, L. J. W. Shimon, D. Milstein. *J. Am. Chem. Soc.* **2010**, 132, 47, 16756–16758.

⁷¹ C. Gunanathan, D. Milstein, *Science*, **2013**, 341, 1229712.

⁷² P. Daw, S. Chakraborty, J.A. Garg, Y. Ben-David, D. Milstein, *Angew. Chem. Int. Ed.*, **2016**, 128, 14585 – 14589.

Table 7: Reductive amination of alcohol with a cobalt-PNN catalyst

Entry	Diol	Amine	t (h)	Yield ^b (%)
1			24	88
2			24	93
3			24	90
4			24	70
5			24	87
6			36	25 ^c
7			36	22 ^c
8			36	56 ^c
9			24	58 ^c

[a] Conditions: diol (0.5 mmol), amine (0.5 mmol), 5 mol%, toluene (2 mL), and 4 Å molecular sieves heated in a closed Schlenk tube for 24–36 h. [b] Yield of isolated product. [c] Yield determined by GC.

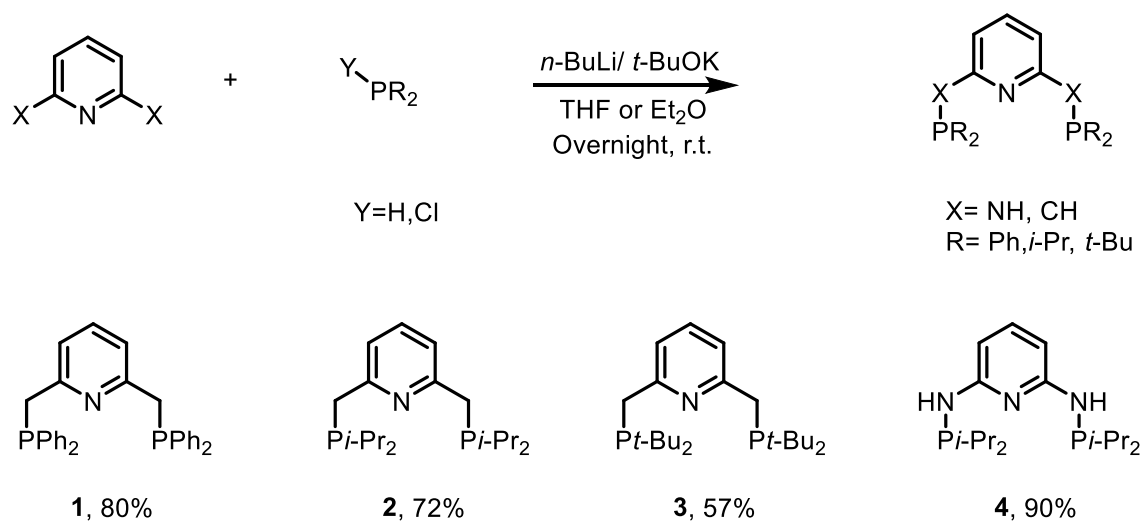
While linear primary alkyl and benzyl amines provided the products in good to excellent yields (Table 7, entries 1–5, 8 and 9), the reaction of less nucleophilic anilines with 2,5-hexanediol led only to poor yields (Table 7, entries 6 and 7). Attempts to isolate the active Co^I catalyst or an in situ generated intermediate from the reaction mixture failed. Nevertheless, metal–ligand cooperation (MCL) by amine/amide and aromatisation/dearomatisation ligand transformation was discussed.

2/ Ligand and Catalyst synthesis

We initiated our work with the synthesis of cobalt (II) catalysts supported by aromatic PNP ligands. The ligands were synthesized using reported procedure and characterized by

NMR^{73,74,75,76}. However, since cobalt (II) complexes are paramagnetic and therefore not easily analyzed by NMR, most complexes were characterized by X-ray analyses.

a/ PNP Ligand synthesis



Scheme 15: PNP ligand synthesis

PNP ligands were synthesized from lutidine or in the case of **4** from 2,6-diaminopyridine and the corresponding phosphines or chlorophosphines. The yields obtained range between 57% and 90% (Scheme 15).

b/ Synthesis of Cobalt PNP complexes.

The cobalt complexes have been synthesized from the previously presented ligand and anhydrous cobalt chloride (II) (CoCl₂) stored in a glove box. As described in the literature.^{73, 77, 78, 79} CoCl₂ and ligands **1-4** were stirred in THF at room temperature for 17 h. During this reaction, a precipitate formed and was separated and washed with ethanol and diethyl ether. The product was dried and recrystallized in a biphasic DCM/heptane solvent system to furnish the desired complexes in good to excellent yields (65-93%) (Scheme 16).

⁷³ G. Müller, M. Klinga, M. Leskelä, B. Rieger. *Z. anorg. allg. chem.*, **2002**, 628, 2839-2846

⁷⁴ J. Neumann, S. Elangovan, A. Spannenberg, K. Junge, M. Beller. *Chem. Eur. J.*, **2017**, 23, 5410 – 5413.

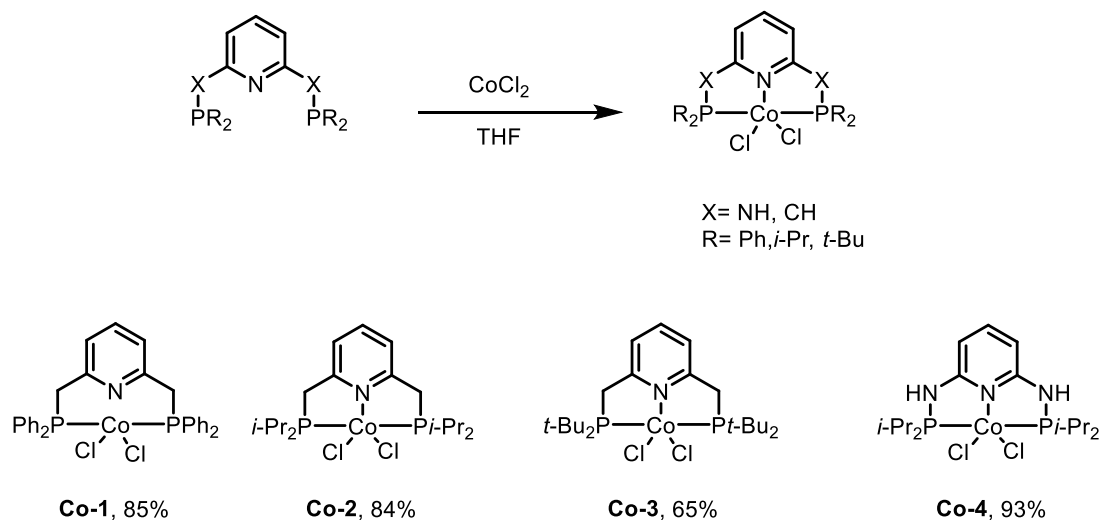
⁷⁵ M. Kawatsura, J. F. Hartwig, *Organometallics*, **2001**, 20, 1960-1964.

⁷⁶ T. Hille, T. Irrgang, R. Kempe, *Chem. Eur. J.*, **2014**, 20, 1–5.

⁷⁷ E. Khaskin, Y. Diskin-Posner, L. Weiner, G. Leitun, D. Milstein. *Chem. Commun.*, **2013**, 49, 2771--2773 2771.

⁷⁸ S. Rösler, J. Obenauf, and R. Kempe. *J. Am. Chem. Soc.*, **2015**, 137, 7998–8001.

⁷⁹ Z. Shao, S. Fu, M. Wei, S. Zhou, Q. Liu. *Angew. Chem. Int. Ed.*, **2016**, 55, 14653 –14657



Scheme 16: Cobalt complexes

The molecular structures of **Co-1**, **Co-2** and **Co-3** are presented below (Figure 11-13) and then characteristic bond lengths and angles are reported in Table 8. **Co-4** could not be crystallised

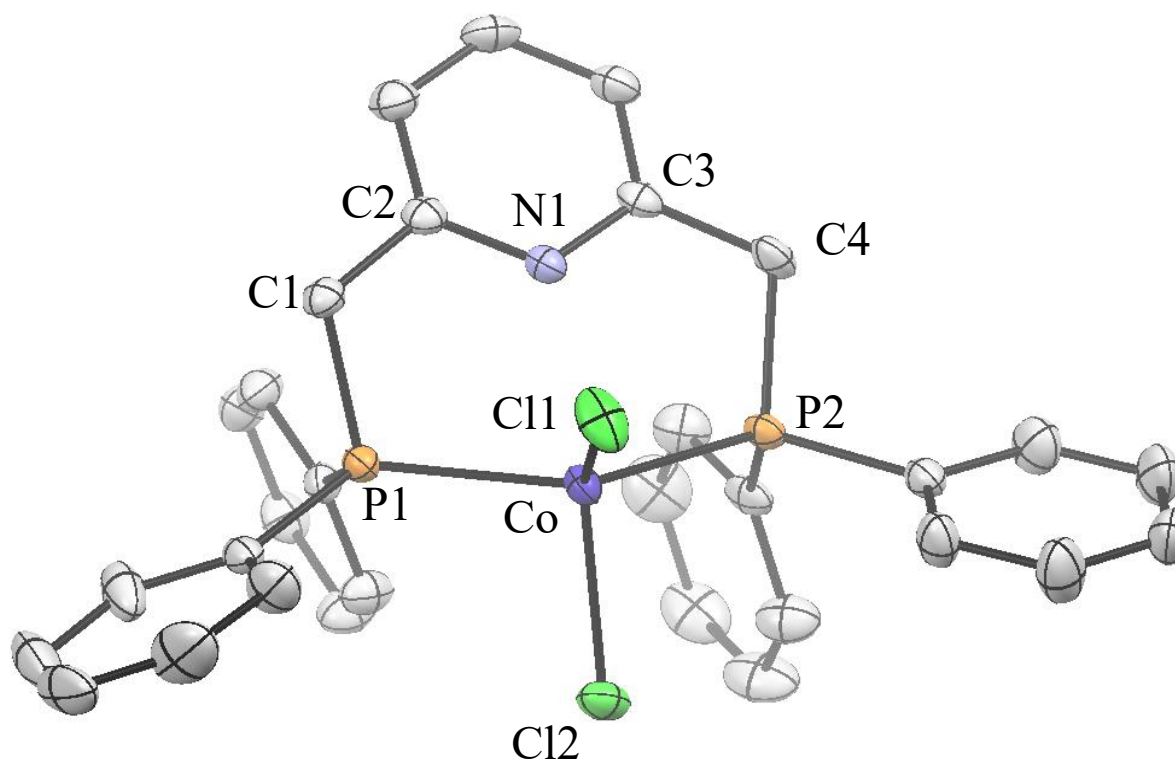


Figure 11: Molecular structure of Co-1 represented as 50% probability ellipsoid. H atoms are omitted for clarity

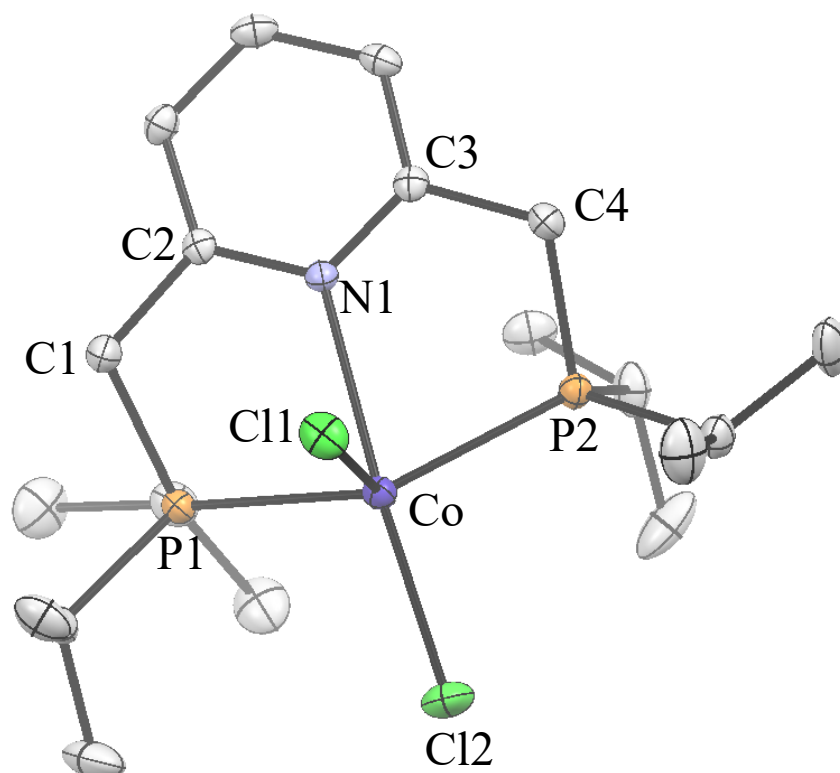


Figure 12: Molecular structure of Co-2 represented as 50% probability ellipsoid. H atoms are omitted for clarity

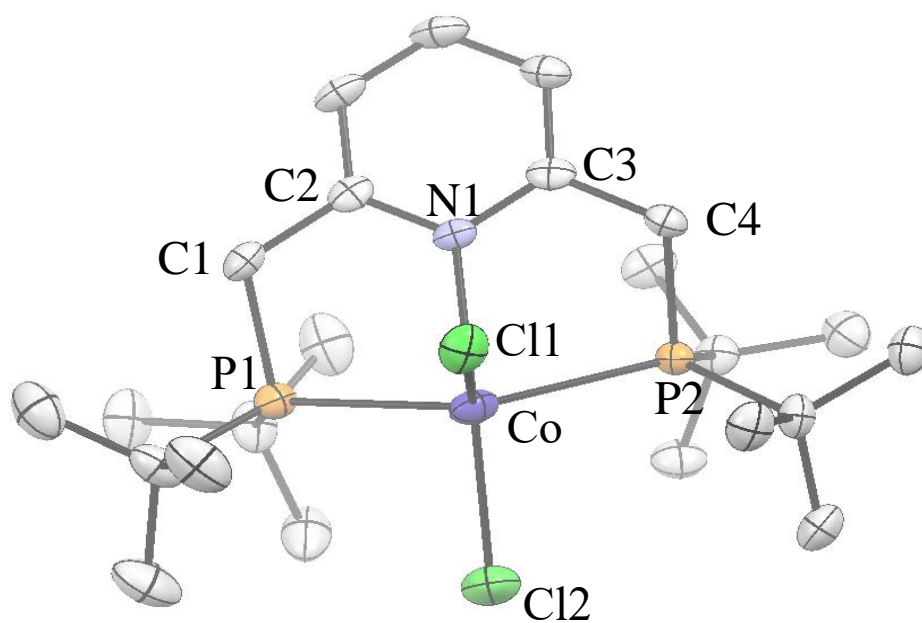
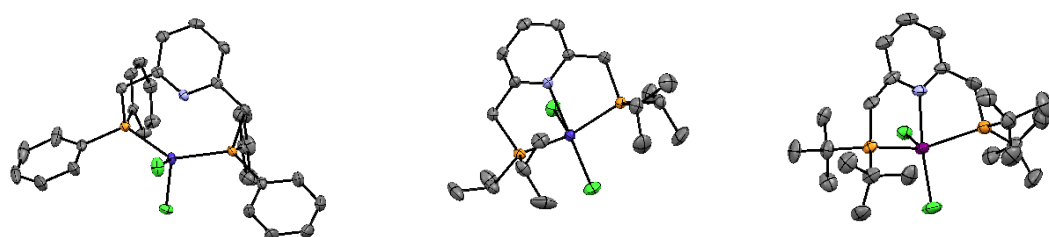


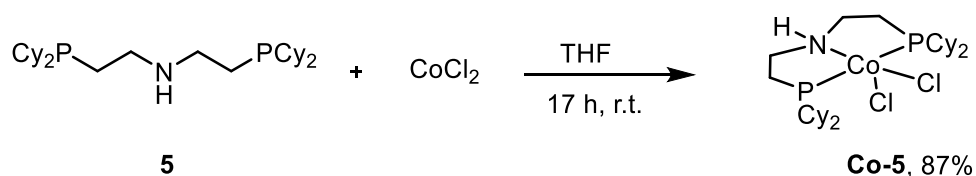
Figure 13: Molecular structure of Co-3 represented as 50% probability ellipsoid. H atoms are omitted for clarit

Table 8: Selected bond length (Å) and angles (°) in metallacycle


	Co-1	Co-2	Co-3
d(Co-N1)	2,497	2,415	2,289
d(Co-P1)	2,363	2,401	2,466
d(Co-P2)	2,359	2,401	2,499
d(Co-Cl1)	2,249	2,300	2,332
d(Co-Cl2)	2,285	2,285	2,295
P1-C1-C2	107,33	110,0	112,56
P2-C4-C3	111,02	111,14	110,14
Co-P1-C1	103,63	101,47	99,5
Co-P2-C4	108,78	103,45	95,71
P1-Co-P2	127,42	129,73	135,72
Cl1-Co-Cl2	111,75	106,36	111,85

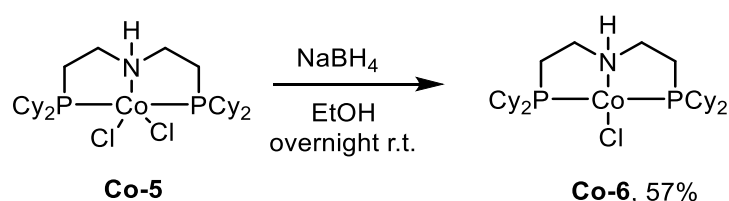
It is interesting to note that in complex **Co-1**, usually reported with a Co-N bond,⁸⁰ the distance cobalt-nitrogen is very long and not considered as a bond by X-Ray analysis software (Ortep and Mercury). Indeed, this molecular structure evidenced a Co-N distance of 2.497 Å whereas for the complexes **Co-2** and **Co-3** they are 2.415 and 2.289 Å, respectively. It must be noted that an overview of reported structures of LnCoCl₂(pyridine) complexes revealed an average of bond lengths ranging from 2.0 Å to 2.15 Å. The Co-N bond length in the pincer complexes **Co-1** to **Co-3** are therefore among the longest reported. The other distances and angles are relatively identical.

Cobalt complexes supported by aliphatic PNP ligand were also prepared from the commercial ligand **5** using similar experimental procedures (Scheme 17).

*Scheme 17:* Aliphatic PNP complex

⁸⁰ Lin Chen, Pengfei Ai, Jianming Gu, Suyun Jie, Bo-Geng Li, *Journal of Organometallic Chemistry*, 716, **2012**, 55-61,

The PNP ligand **5** and cobalt (II) chloride were stirred in THF for 17 h at room temperature to give the cobalt complex **Co-5** which was characterized by ^1H NMR as described in the literature.⁸¹ As reported by Beller and Junge,⁸² a Co(I) species is likely generated and involved in reduction reactions. Given the use of a reducing agent and a base in the catalytic tests, the aim was also to reduce the number of additives by isolating an activated form of the catalyst. In order to skip an activation step during catalysis, we have prepared the Cobalt (I) **Co-6** complex upon reduction of cobalt (II) **Co-5** with sodium borohydride (1 equiv.) in ethanol (Scheme 18). The reaction mixture was then filtered and the solvent evaporated. The product was set to crystallize in a biphasic toluene/heptane solvent system leading to nice blue crystals and a yield of 57%. This strategy was applied to all the complexes previously described but without success.



Scheme 18: Cobalt(I) synthesis

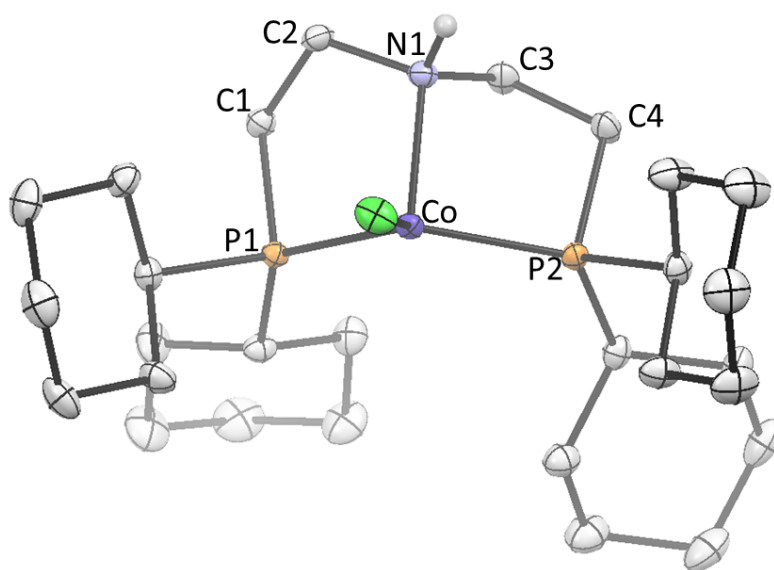


Figure 14: Molecular structure of Co-3 represented as 50% probability ellipsoid. H atoms are omitted for clarity

⁸¹ Z. Shao, S. Fu, M. Wei, S. Zhou, Q. Liu. *Angew. Chem. Int. Ed.*, **2016**, *55*, 1 – 6

⁸² K. Junge, B. Wendt, A. Cingolani, A. Spannenberg, Z. Wei, H. Jiao, M. Beller. *Chem. Eur. J.*, **2018**, *24*, 1046–1052.

The molecular structure of **Co-7** is presented above (Figure 14) and its characteristic bond lengths and angles are reported in Table 9.

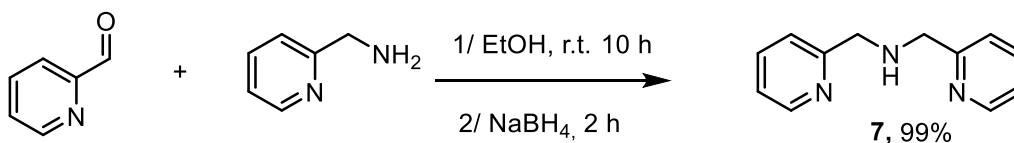
To the best of our knowledge, the complex **Co-6** has not been isolated and characterised. The presence of the amino-ligand (N-H) was unambiguously evidenced by X-Ray crystallography. Of note, the Co-N bond distance in the Co(I) complex **Co-6** was much shorter than in the Co(II) complex **Co-5**, 2.14 vs 2.38 Å, respectively.

Table 9: Selected bond length (Å) and angles (°) in metallacycle

Co-6	
Co-N1	2,142
Co-Cl1	2,258
Co-P1	2,260
Co-P2	2,232
Co-P1-C1	102,03
Co-P2-C4	100,88
P1-C1-C2	110,17
P2-C4-C3	108,92
P1-Co-P2	118,17
C1-C2-N1	112,05
C4-C3-N1	110,25
N1-Co-Cl1	113,38

c/ Phosphine free Ligands.

The complexes supported by PNP ligands display in general very high efficiencies, but they are not easily synthesized and they are expensive due to the cost of the ligands. For this reason, we have also prepared and used N,N,N and C,N,C ligands that are generally more easily accessible. The ligand **7** was easily synthesized in high yield from methylaminopyridine and picolinaldehyde. These two reagents stirred overnight at room temperature furnished the corresponding imine which was reduced in a second step with sodium borohydride to yield the ligand **7** in quasi-quantitative yield (Scheme 19).⁸³

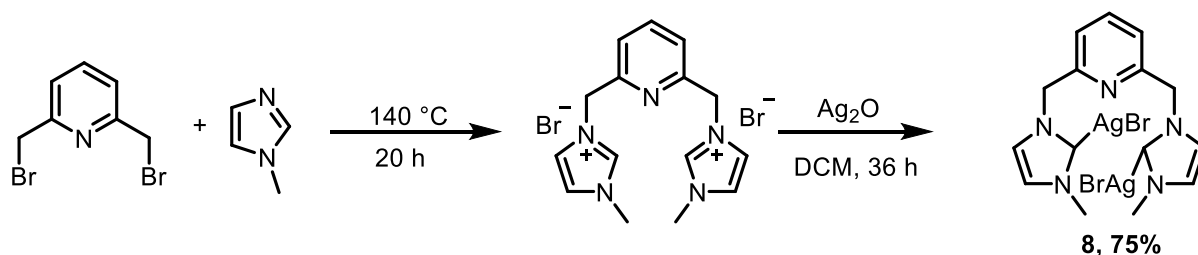


Scheme 19: Synthesis of N,N,N ligand

A bis-*N*-Heterocyclic carbene(NHC)-containing ligand was also prepared. Introduction of this ligand was envisioned through the synthesis of a silver transmetalation agent **8**. The silver complex **8** was obtained in two steps and isolated in 75% yield (Scheme 20).⁸⁴

⁸³ Y. Liu, R. Xiang, X. Du, Y. Ding, B. Ma. *Chem. Commun.*, **2014**, 50, 12779-12782.

⁸⁴ H. Ibrahim, M. D. Bala. *J. Organomet Chem.*, **2015**, 794, 301-310.

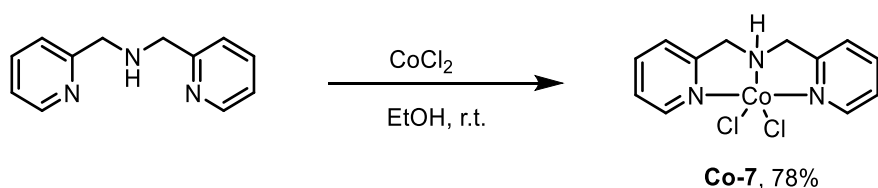


Scheme 20: Synthesis of a bis-NHC ligand precursor

d/ Synthesis of phosphine-free complexes.

As in the case of the synthesis of cobalt complexes supported by PNP ligands, the precursor used was anhydrous cobalt chloride (II). Complex **Co-7** was obtained by mixing the ligand and cobalt chloride (II) in ethanol for 17 h at room temperature.⁸⁵ **Co-7** was obtained as a violet powder in 78% yield. Complex **Co-7** was crystallised in a biphasic DCM/heptane solvent and a molecular structure obtained by X-Ray.

The molecular structure of **Co-7** is presented below (Figure 15 and its characteristic bond lengths and angles are reported in table 10. Here again, this molecular structure was not previously described in the literature (Scheme 21). The structure shows that the Co-N2 (*NH*) distance is shorter than in Co-5 (2.21 Å vs 2.38 Å). This also the case for Co-N1 (*pyr*) distance which are shorter than in Co1-Co3. 2.



Scheme 21: Synthesis of N,N,N-cobalt complex Co-7

Table 10: Selected bond length (Å) and angles (°) in metallacycle

Co-7	
Co-N1	2,071
Co-N2	2,239
Co-N3	2,088
Co-Cl1	2,304
Co-Cl2	2,345
Cl1-Co-Cl2	100,76
N1-Co-N3	125,32
Co-N2-C4	118,44
Co-N1-C1	120,06
N1-C1-C2	116,00
N2-C4-C3	115,13

⁸⁵ H.F. Abd El-Halim, G.G. Mohamed. *J. Mol. Struct.*, **2016**, 1104, 91-95.

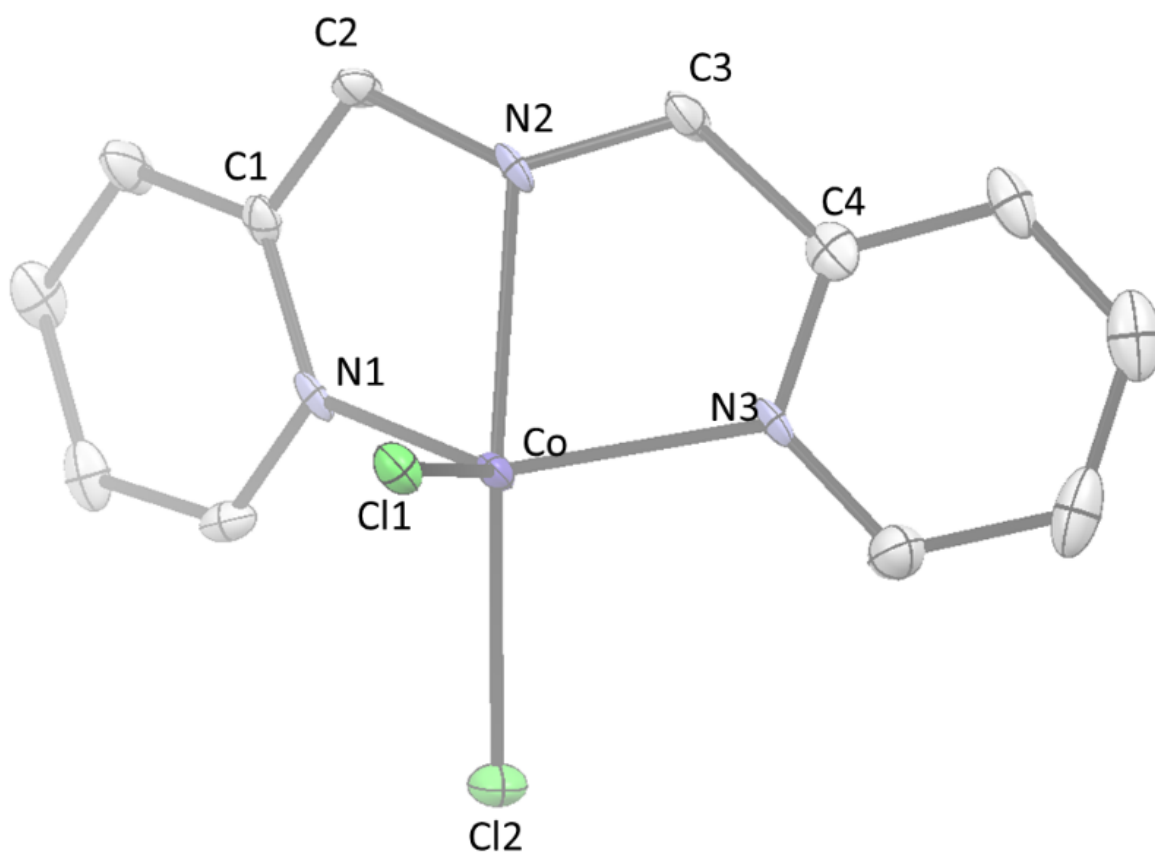
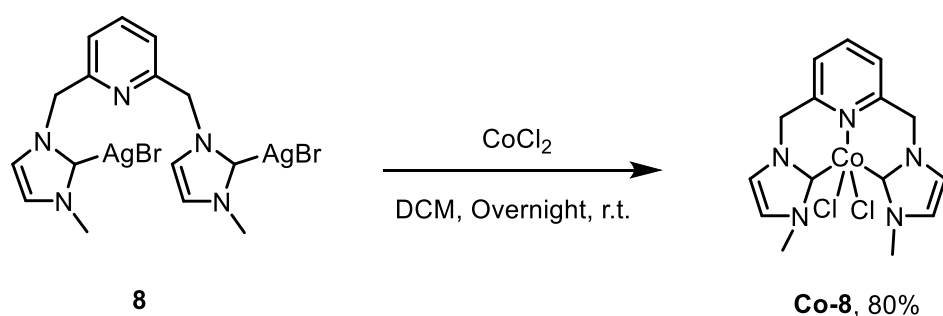


Figure 15: Molecular structure of Co-3 represented as 50% probability ellipsoid. H atoms are omitted for clarity

Similarly, complex **Co-8** was synthesized by transmetalation between silver and cobalt. A new complex was obtained but it has not been possible to get suitable crystals for molecular structure determination. (Scheme 22).⁸⁴

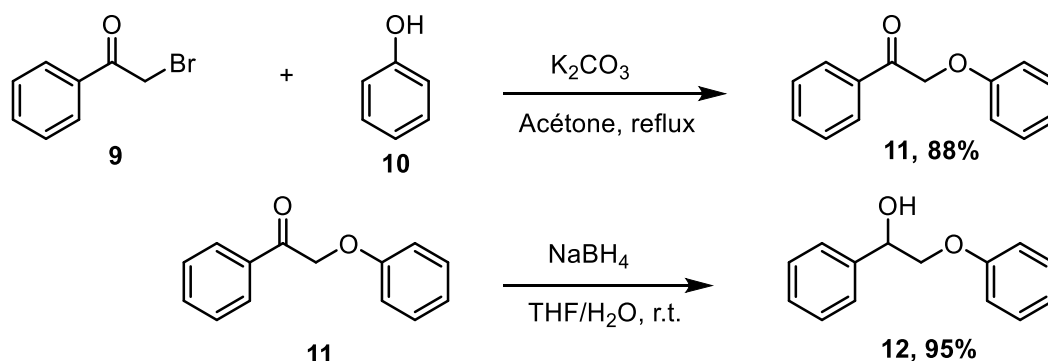


Scheme 22: Bis NHC complex Co-8

3/ Catalytic tests

As presented in the introduction, our aim was to perform the cleavage of the β -O-4 bond in a redox neutral manner by a hydrogen auto-transfer also-called hydrogen borrowing transformation. For this reason, the previously synthesized catalysts were investigated with a

lignin model containing a β -O-4 linkage. This lignin-model was synthesized in the laboratory in two steps.⁶⁴



The first step consists in the nucleophilic substitution of bromine by the phenolate group. In a second step, the ketone **11** was reduced to alcohol by adding a stoichiometric quantity of sodium borohydride (Scheme 23).

All the catalysts prepared and described here above have been evaluated under the conditions described by Milstein for the reductive amination of alcohol. The lignin model was thus submitted to 5 mol% of catalyst in the presence of potassium *t*-butoxide and sodium triethyl borohydride at 135 °C in toluene⁷² (Table 11).

Table 11: Catalysts screening.

Entry	Catalyst	Ratio 13/14/15/16 ^b	Conversion (%) ^a
1	Co-1	1/2/18/5	<20
2	Co-2	0/1/6/1	<20
3	Co-3	0/0/1/2	<20
4	Co-4	0/1/2/18	<20
5	Co-5	1/1/1/0	<20
6	Co-6	0/0/1/6	<20
7	Co-7	4/8/22/1	<20
8	Co-8	1/2/2/2	<20
9	Co-9	0/1/2/2	<20

Conditions: [Co] (0.023 mmol ; 5 mol%) ; lignin-model (0,100 g ; 0,47 mmol) 135 °C, toluene (2 mL) a) Determined by gas chromatography with calibration using dodecan as ISTD. b) determined by GC with comparison of area.

As described in Table 11, all the catalysts displayed poor but similar performances. All of them showed conversion below 20% and surprisingly, 4 products were formed and identified by GC-MS. The formation of the expected products **13** and **15** is a clear evidence that the hydrogenolysis took place. However, this reaction was not complete and selective as supported

by the presence of **16**, i.e. the dehydrogenated starting material but also by the presence of **14** resulting from the reduction of **13** thus evidencing a competitive reaction between the reduction of **13** and the hydrogenolysis of **16**.

Considering the similar results obtained whatever the catalyst, attempts to improve these preliminary results were conducted with the cobalt complex **Co-7** as it contains the easiest and cheapest ligand to synthesize. Several parameters such as the base and hydride source were investigated. As shown in Table 12, a striking result was evidenced as it was first shown that the hydride source was not mandatory but most of all it was demonstrated that the reaction could be conducted in the absence of cobalt catalyst. Indeed, 53% conversion was obtained with 50 mol% of *t*BuOK and, 83% conversion with 1.1 equiv. of the same base (Table 12, entries 3 and 5). This type of alkaline cleavage was in fact known and reported by Jameel and co-workers in 2014⁸⁶ and earlier by Kunze.⁸⁷

Table 12: Optimisation reactions

Entry	Catalyst	Base (X mol%)	NaHBt ₃ (Y mol%)	Ratio (13/14/15/16) ^b	Conversion (%) ^a
1	Co-7	<i>t</i> -BuOK (10)	-	2/1/4/1	20
2	Co-7	<i>t</i> -BuOK (10)	5	4/8/22/1	27§
3	Co-7	<i>t</i> -BuOK (50)	-	2/1/1/3	49
4	-	<i>t</i> -BuOK (50)	-	2/1/1/3	53
5	Co-7	<i>t</i> -BuOK (110)	-	1/1/6/0	81
6	-	<i>t</i> -BuOK (110)	-	1/1/4/0	82

Conditions : [**Co-7**] (0.023 mmol ; 5 mol%) ; **12** (0,100 g ; 0,47 mmol) 135 °C, toluene (2 mL). ^a Determined by gas chromatography with calibration using dodecan as ISTD. ^b determined by GC with comparison of area.

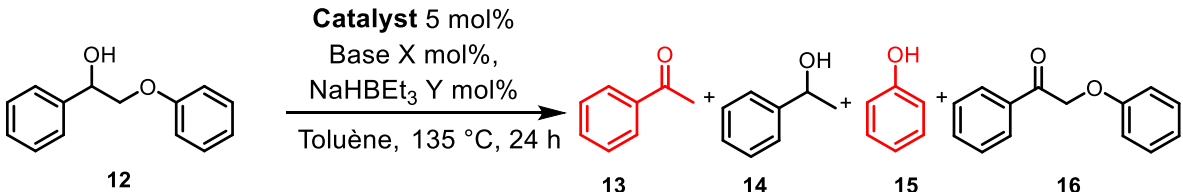
These results demonstrate that the reaction can be conducted in the absence of catalyst. However, the utilization of stoichio- or sub-stoichiometric amount of base is not conceivable with regards to green and sustainable chemistry. Other bases were thus screened in order to restore a catalytic process (Table 13). Interestingly, cesium carbonate did not promote the alkaline cleavage of **12** but addition of **Co-7** only barely promoted the cleavage of the precursor (Table 13, entries 1-4). With KHMDS, the situation was somehow similar to *t*BuOK since

⁸⁶ W. Huo, W. Li, M. Zhang, W. Fan, H. Chang, H. Jameel, *Catal Lett.*, **2014**, *144*, 1159–1163.

⁸⁷ J. Gierer, I. Kunze, *Acta Chem Scand*, **1961**, *15*, 803-807.

KHMDS on its own performed the cleavage of **12** (Table 13, entries 5-7). Sodium ethoxide was also inadequate to promote a catalytic transformation (Table 13, entries 8,9)

Table 13 : Base screening

					
Entry	Catalyst	Base (X mol%)	NaHBET ₃ (Y mol%)	Ratio (13/14/15/16) ^b	Conversion (%) ^a
1	-	Cs ₂ CO ₃ (110)	-	-	0
2	Co-7	Cs ₂ CO ₃ (110)	-	-	7
3	Co-7	Cs ₂ CO ₃ (10)	-	-	3
4	Co-7	Cs ₂ CO ₃ (110)	10	5/1/7/1	14
5	-	KHMDS (110)	-	2/1/1/0	89
6	Co-7	KHMDS (110)	-	4/3/3/1	100
7	Co-7	KHMDS (50)	-	5/1/10/1	43
8	Co-7	NaOEt (10)	10	1/1/3/1	13
9	Co-7	NaOEt (110)	-	1/1/1/1	13

Conditions: [Co-7] (0.023 mmol ; 5 mol%) ; **12** (0,100 g ; 0,47 mmol), toluene (2 mL). ^a Determined by gas chromatography with calibration using dodecan as ISTD. ^b determined by GC with comparison of area.

Due to the inconclusive results obtained with cobalt complexes, we have evaluated iron and manganese complexes supported by a PNP ligands. Previous work from the Beller group demonstrated that iron⁸⁸ and manganese⁸⁹ complexes supported by pincer ligands were able to perform dehydrogenation reactions. The first transfer hydrogenation of ketones using an earth abundant Mn-based complex was also achieved. Notably, no phosphine ligands were required to stabilize this catalyst. In 2014, Schneider and Jones⁹⁰ used iron pincer complexes for the acceptorless dehydrogenation of alcohols and diols and for the reverse hydrogenation of challenging ketone substrates. The yields and chemoselectivities under mild and base free conditions.

Fe-1 and **Mn-1** catalysts were tested under the reaction conditions described by Beller for Mn and Schneider for Fe (Table 14, entries 1 and 5) and led to conversions of 12% and 14%, respectively. As the manganese complex was known to be light-sensitive, the reaction was carried out in the dark, but there was no difference with the reaction carried out under natural day light (Table 14, entries 2 and 3), where 20% conversion was obtained. Finally, the iron

⁸⁸ E. Alberico, P. Sponholz, C. Cordes, M. Nielsen, H. J. Drexler, W. Baumann, H. Junge, M. Beller, *Angew. Chem. Int. Ed.* **2013**, *52*, 14162–1416

⁸⁹ M. Perez, S. Elangovan, A. Spannenberg, K. Junge, M. Beller, *ChemSusChem*, **2017**, *10*, 83-86.

⁹⁰ S. Chakraborty, P. O. Lagadis, M. Förster; E. A. Bielinski, N. Hazari, M. C. Holthausen, W. D Jones, S. Schneider, *ACS Catal.* **2014**, *4*, 3994-4003

complex **Fe-1** was tested under higher temperature condition but the conversion barely increased to 23%.

Table 14: Fe and Mn Catalyst.

Mn-1 **Fe-1**

12 **13** **14** **15** **16**

Entry	Catalyst	Base (X mol%)	Temperature (°C)	Ratio (13/14/15/16) ^d	Conversion (%) ^a
1 ^b	Mn-1	10	135	1/3/2/0	20
2 ^c	Mn-1	10	135	1/3/2/0	21
3	Mn-1	20	135	2/1/5/3	20
4	Fe-1	-	100	1/1/4/2	14
5	Fe-1	-	135	1/1/0/0	22
6	Fe-1	-	120	1/3/2/0	23
7	Fe-1	<i>t</i> -BuOK (10)	135	3/1/3/1	16

Conditions: Catalyst (0.023 mmol ; 5 mol%) ; **12** (0,100 g ; 0,47 mmol), toluene (2 mL). ^a determined by gas chromatography using dodecane as internal standard. ^b24 h in natural day light, ^c24 h in the dark. ^d determined by GC with comparison of area.

III/ Conclusion

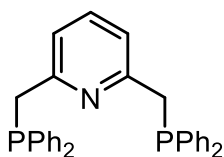
We have prepared and characterized a series of cobalt (II) pincer complexes based on PNP, NNN and CNC ligand architectures. We have obtained several so far not reported X-Ray molecular structures. These complexes have been evaluated in the hydrogenolysis cleavage of a model of lignin. So far, we have been able to observe the cleavage of the model substrate but this reactivity was essentially promoted by the base present in the reaction media without noticeable implication of the cobalt catalysts. However, with these complexes in hands we looked for another application in the domain of sustainable chemistry and moved to the hydrogenation of *N*-heterocycles as a route for the chemical storage of hydrogen which is a current hot topic of interest.

IV/ Experimental Part.

All the experiments were carried out under an argon atmosphere either inside the argon-filled glove box or using standard Schlenk line techniques. All the commercial reagents and metal precursor were purchased from Sigma Aldrich, Alfa-Aesar, Strem and used as received. Toluene, THF, DCM were dried on a MBraun Solvent purification system and degassed by “freeze pump thaw” and stored under 3 Å molecular sieves. Ethanol was stored under 3 Å molecular sieves. DL-1-phenylethanol was dried over CaH₂, distilled and stored under 3 Å molecular sieves in the glove box. The reactions were monitored using a Shimadzu 2014 gas chromatograph equipped with an Equity TM– 1 Fused Silica capillary column (30 m × 0.25 mm × 0.25 μm) and a FID detector. Conversions were determined by internal calibration using dodecane as standard. Proton nuclear magnetic resonance (¹H NMR) spectra were recorded on a Bruker Avance III 400 MHz spectrometer. ¹H and ¹³C chemical shifts (δ) are reported in ppm vs tetramethylsilane (δ = 0.00 ppm) and determined by reference to the residual non-deuterated solvents (δ = 7.26 for CHCl₃ and 77.0 CHCl₃). Coupling constants (J) are given in Hertz.

1/ Ligand synthesis

Synthesis of (Ph₂)₂PNP **1**

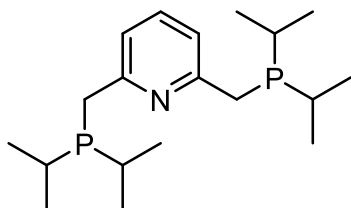


In a dried Schlenk tube, *t*-BuOK (0.673 g, 6 mmol, 6 equiv.) was added to a solution of diphenylphosphine (0.52 mL, 3 mmol, 2 equiv.) in 15 mL of THF. The solution turned red. The Schlenk tube was cooled to 0 °C and 2,6-bis-(chloromethyl)pyridine (0.26 g, 1.5 mmol, 1 equiv.) was added dropwise. The solution turned yellow. The reaction mixture was stirred at r.t. for 24 h. The solvent was evaporated under vacuum and the recovered solid was dissolved in 20 mL of dichloromethane. 20 mL of water was added and the organic phase was separated. The aqueous phase was washed with 10 ml of dichloromethane. The organic phases were grouped and dried over Na₂SO₄. After filtration and solvent evaporation, the product was obtained as a white solid of sufficient purity in 80% yield. NMR data were consistent with reported data⁹¹

³¹P NMR (Tol, ⁸d), δ ppm: -10,72

¹H NMR (400 MHz ; Tol ⁸d), δ ppm : 7,46 (m, 8H, Ar); 7,03-7,16 (m, 12H, Ar) ; 6,85 (t, 1H, J=8,0 Hz, Ar) ; 6,59 (d, 2H, J= 8,0 Hz, Ar) ; 3,53 (s, 4H, -CH₂-).

⁹¹ G. Müller, M. Klinga, M. Leskelä, B. Rieger. *Z. anorg. allg. chem.*, **2002**, 628, 2839-2846

Synthesis of (*i*-Pr₂)₂PNP **2**

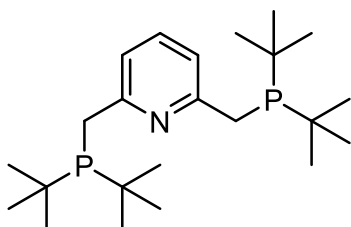
At 0 °C, *n*-BuLi (1,6 M in hexanes) (5.4 mL; 8.64 mmol, 2 equiv.) was added to a solution of 2,6 lutidine (0.5 mL; 4.29 mmol, 1 equiv.) and TMEDA (1.3 mL; 8.62 mmol, 2 equiv.) in 10 mL of diethylether. The solution was stirred for 4 h at r.t. The solution was cooled at -90 °C and chlorodiphenylphosphine (1.4 mL, 8.61 mmol, 2 equiv.) in 10 mL of diethylether was added dropwise.

The solution was stirred at -90 °C for 30 minutes and then 15 h at r.t. The reaction mixture was filtered, and the solvent was evaporated under vacuum furnishing a yellow oil. This oil was purified by distillation at 120 °C under vacuum. Yield 72%.

NMR data were consistent with reported data.⁹²

³¹P NMR (Tol ⁸d), δ ppm: 11,17

¹H NMR (400 MHz ; Tol ⁸d), δ ppm : 7,16-6,93 (m, 3H, ArPyr) ; 3,08 (d, 4H, J=8,0 Hz, CH₂) ; 1,77-1,64 (m, 4H,-CH) ; 1,12-0,98 (m, 24H, -CH₃).

Synthesis of (*t*-Bu₂)₂PNP **3**

At 0 °C, *n*-BuLi (1,6M) (5,9 mL; 9.57 mmol, 2 equiv.) was added dropwise to a solution of 2-6 lutidine (0.5 g; 4.67 mmol, 1 equiv.) in 5 mL of diethyl ether. The reaction mixture was heated at 40 °C for 15 h and then cooled at -78 °C. Di-terbutylphosphine (1.85 mL; 9.33 mmol, 1 equiv.) was added dropwise and the solution was stirred at r.t for 10 minutes. The reaction was quenched with

degassed water and extracted with diethyl ether. The extracted solution was dried with Na₂SO₄. The product was recrystallized in diethyl ether at -35 °C. Yield 57%.

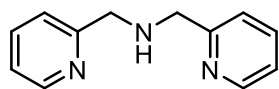
NMR data were consistent with reported data⁹³

³¹P NMR (Tol ⁸d), δ ppm: 36,8

¹H NMR (400 MHz ; Tol ⁸d), δ ppm : 7,30 (d, J= 8,0 Hz, 2H); 7,22 (t, 1H, J= 8,0 Hz) ; 3,14 (d, J= 3,0 Hz, 4H) ; 1,18 (d, J=10,0 Hz, 36H).

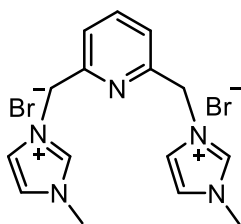
⁹² J. Neumann, S. Elangovan, A. Spannenberg, K. Junge, M. Beller. *Chem. Eur. J.*, **2017**, 23, 5410 – 5413

⁹³ M. Kawatsura, J. F. Hartwig. *Organometallics*, **2001**, 20, 1960-1964

Synthesis of NNN ligand **7**

Methylaminopyridine (0.26 mL; 2.52 mmol, 1 equiv.) was added to picolinaldehyde (0.24 mL; 2.52 mmol, 1 equiv.) in 10 mL of ethanol. The solution was stirred overnight at r.t. NaBH₄ (0.19 g; 5.05 mmol, 2 equiv.) was added and the solution was stirred 2 h at r.t. The solvent was evaporated under vacuum and 5 mL of water was added. The solution was at pH= 10 and a few mL of a NH₄Cl solution was added until pH=8. The product was extracted with dichloromethane (3x10 mL). The solution was dried with Na₂SO₄. After filtration and solvent evaporation, the product was obtained as a yellow oil of sufficient purity in 99% yield. NMR data were consistent with reported data⁹⁴

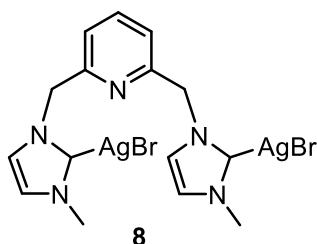
¹H NMR (400 MHz ; DMSO, ⁶d), δ ppm: 8,50 (d, J=5,6 Hz, 2H) ; 7,76 (t, J=8,0 Hz, 2H) ; 7,47 (d, J=8,0 Hz, 2H) ; 7,25 (t, J=6,0 Hz, 2H), 3,84 (s, 4H) ; 3,35 (s, 1H).

Synthesis of Bis (NHC) ligand **8**

In a dried Schlenk tube, 2,6-bis (bromomethylpyridine) (0.150 g; 0.566 mmol, 1 equiv.) and 1-methylimidazole (0.093g; 1.132 mmol, 2 equiv.) were stirred neat at 140 °C for 20 h. After cooling to r.t the reaction crude was triturated in THF. The solvent was evaporated under vacuum, the product was obtained as a brown solid of sufficient purity in 95% yield.

NMR data were consistent with reported data⁹⁵

¹H NMR (400 MHz ; DMSO ⁶d), δ ppm : 9,20 (s, 2H) ; 7,97 (t, J=8,0 Hz, 1H); 7,75 (bs, 2H); 7,73 (bs, 2H) 7,48 (d, J=8,0 Hz, 2H), 5,56 (s, 4H) ; 3,92 (s,6H).



In a dried Schlenk tube, 2,6-bis[3-methylimidazolium-1-ylmethyl]pyridine dichloride(0,100 g, 0,28 mmol, 1 equiv.) and silver oxide (0,133 g, 0,57 mmol, 2 equiv.) in 15 mL of 1,2-dichlorethane stirred for 36 h at 45 °C. The Schlenk tube was protected from light with aluminium foil. The product was filtered over celite and extracted with dichloromethane. The solvent was evaporated and the solid washed with heptane and dried under vacuum leading to a yellow/white solid and yield 75%.

NMR data were consistent with reported data.⁹⁶

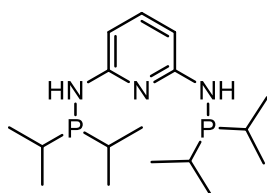
¹H NMR (400 MHz ; DMSO, ⁶d), δ ppm: 7,84 (t, J=8,0 Hz, 1H) ; 7,56 (d, J=2,0 Hz, 2H) ; 7,43 (d, J=2Hz, 2H) ; 7,34 (d, J=8,0 Hz, 2H), 5,40 (s, 4H) ; 3,76 (s,6H).

⁹⁴ Y. Liu, R. Xiang, X. Du, Y. Ding, B. Ma, *Chem. Commun.*, **2014**, 50, 12779-12782.

⁹⁵ . Naya, D. Vázquez-García, A. Fernández, M. López-Torres, V. Ojea, I. Marcos, J. M. Vila and J. Fernández. *Eur. J. Inorg. Chem.* **2016**, 422–431

⁹⁶ H. Ibrahim, M. D. Bala. *J Organomet Chem.* **2015**,794, 301–310.

Synthesis of (*i*-Pr₂)₂PNNNP **4**



To pyridine-2,6-diamine (0.218 g; 2 mmol, 1 equiv.) dissolved in 25 mL of THF was added triethylamine (0.62 ml) and the solution was cooled at 0 °C. Chlorodiisopropylphosphine (0.67 mL; 4.20 mmol, 2.1 equiv.) was added and the reaction mixture was stirred at 50 °C overnight. The solution was filtered and washed with THF. The solvent was evaporated to obtain a colorless oil in 90% yield.

NMR data were consistent with reported data⁹⁷

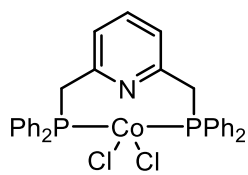
³¹P NMR (Tol ⁸d) δ ppm: 48,23;

¹H NMR (400 MHz; Tol ⁸d), δ ppm: 7,23(t, J= 8 Hz, 1H,); 6,39 (dd, J= 8,0 Hz, 2,1 Hz, 2H); 4,34 (d, J= 11,1 Hz, 2H); 1,69-1,82 (m, 4H); 1,11-0,98 (m, 24H).

⁹⁷ T. Hille, T. Irrgang, R. Kempe. *Chem. Eur. J.* **2014**, *20*, 1–5

2/ Cobalt complexes

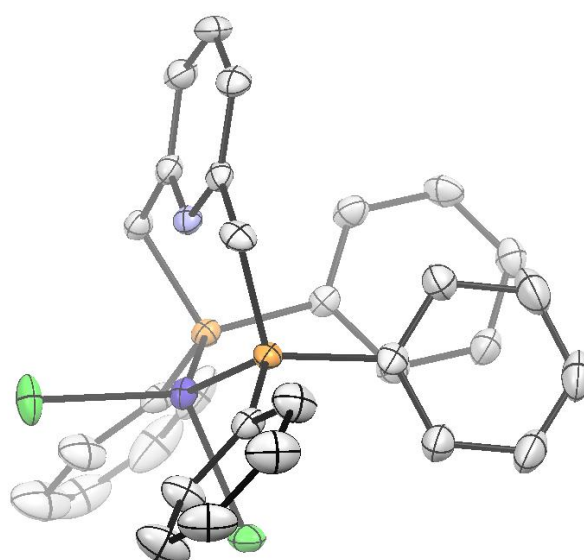
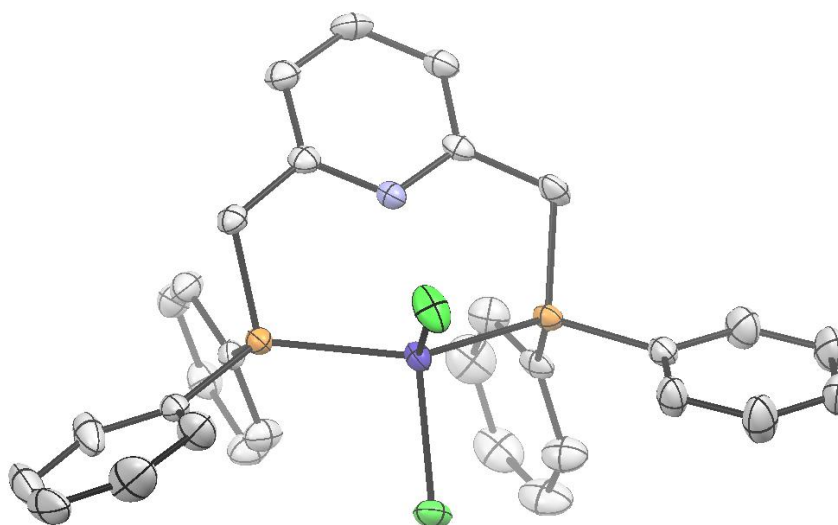
Synthesis of $(\text{Ph}_2)_2\text{PNPCoCl}_2$ **Co-1**



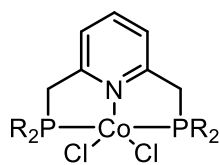
Co-1

In the glove box, a dried Schlenk tube was loaded with anhydrous CoCl_2 (0.025 mg, 0,19 mmol, 1equiv.) which was dissolved in 5 ml of ethanol. 2,6-bis((diphenylphosphaneyl)methyl)pyridine **1** (0,090 mg, 0,19 mmol, 1 equiv.) was dissolved in 3 mL of dichloromethane and rapidly added dropwise to the mixture. The reaction mixture was stirred overnight at room temperature and the precipitated product was separated and washed with ethanol and diethyl ether. The product was dried and recrystallized in a

biphasic DCM/heptane system. The product was obtained as a blue powder in 85% yield.

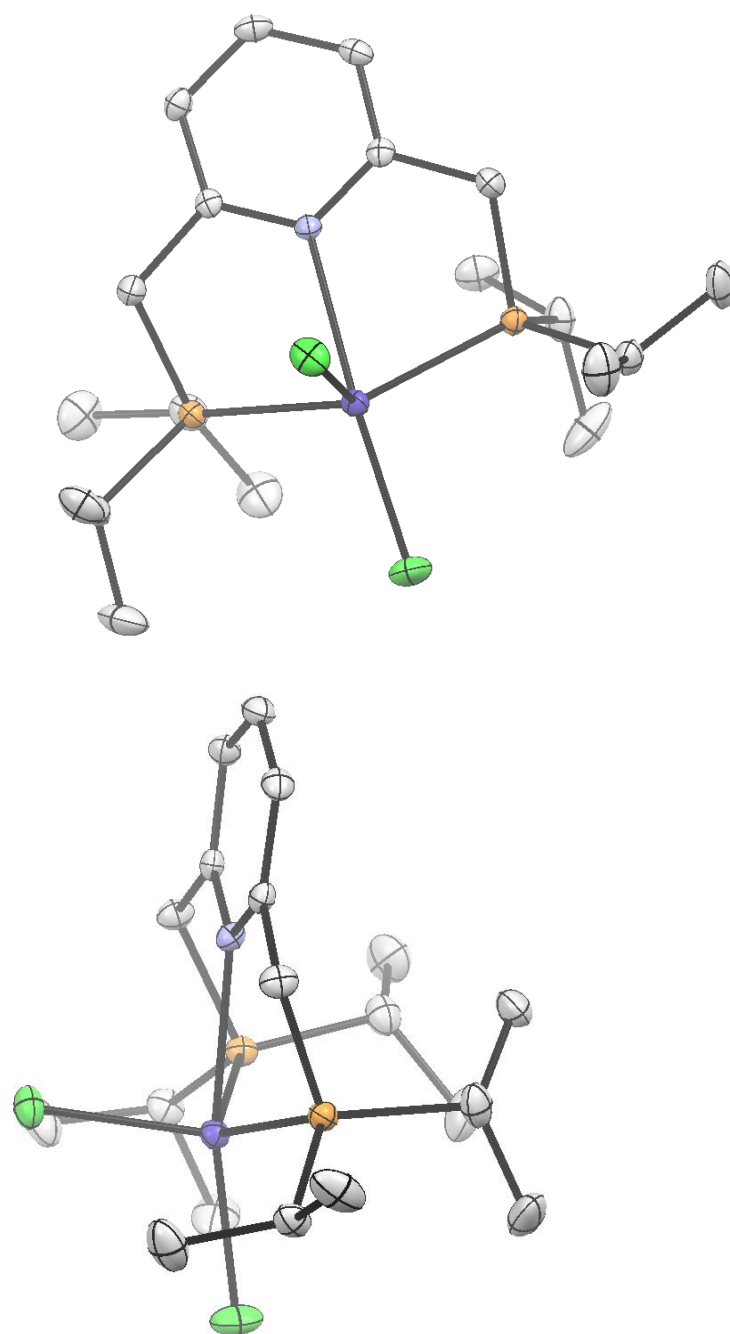


X-ray molecular structure of **Co-1**

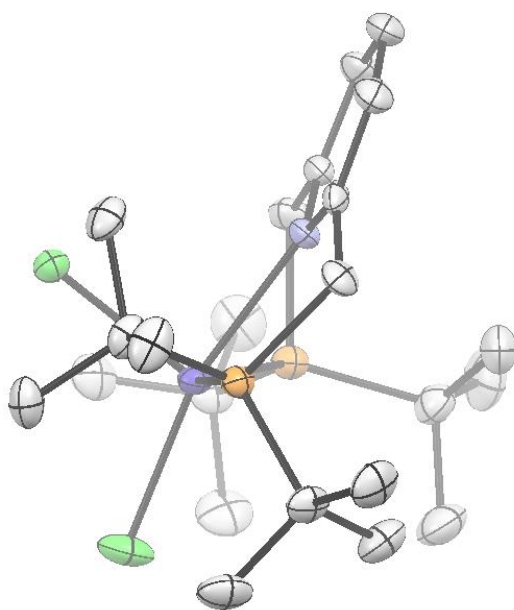
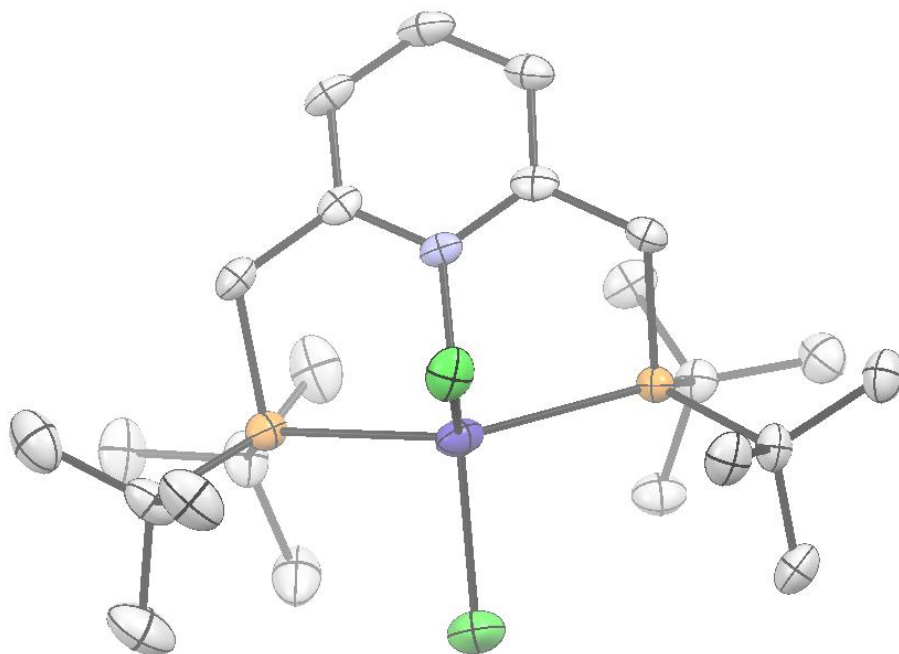
Synthesis of $(i\text{-Pr}_2)_2\text{PNPCoCl}_2$ and $(t\text{-Bu}_2)_2\text{PNPCoCl}_2$ **Co-2-3**

R = $i\text{-Pr}_2$, **Co-2**
 $t\text{-Bu}_2$, **Co-3**

In the glove box, in a dried Schlenk tube, CoCl_2 (0,295 mmol, 1equiv.) was dissolved in 4 ml of THF. The corresponding ligand **2-3** (0,295 mmol, 1 equiv.) was dissolved in 4 mL THF and rapidly added dropwise. The reaction mixture was stirred overnight at r.t. during which period a precipitate appeared. This precipitate was separated by filtration and washed with THF (3x2 mL). The product was dried under vacuum and recrystallized in a biphasic DCM/heptane solvent mixture. The product was obtained as a blue powder in 84% yield.

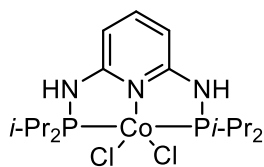


X-ray molecular structure of **Co-2**



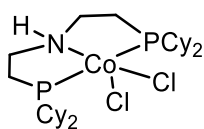
X-ray molecular structure of **Co-3**

Synthesis of (*i*-Pr₂)₂PNNNPCoCl₂ **Co-4**

**Co-4**

In a dried Schlenk tube, CoCl₂ (2.0 mmol; 0,260 g) was dissolved in 20 mL of THF and added to a solution of Py(NHP(*i*Pr)₂)₂ **4** (2.0 mmol; 0.683 g). The solution was stirred overnight at 50 °C. The solution was filtered and the filtrate dried under vacuum yielding a red powder in 93% yield.

Synthesis of (Cy₂)₂PNPCoCl₂ **Co-5**

**Co-5**

In a glove box, in a dried Schlenk tube, CoCl₂ (0.025 g, 0,19 mmol, 1 equiv.) was dissolved in THF. bis(2-(dicyclohexylphosphaneyl)ethyl)amine (0,093g, 0,19 mmol, 1 equiv.) was dissolved on THF and added on the cobalt. The solution changes from blue to pink/violet after addition. The reaction mixture was stirred overnight at r.t. The solution was concentrated to leave a few mL of solvent. Heptane 7,5 mL was added and the mixture was stirred 1 h. The

solution was filtered and the recovered solid was dried under vacuum. The product was obtained a pink powder in 87% yield.

NMR data were consistent with reported data⁹⁸

¹H NMR (400 MHz, CD₂Cl₂); δ ppm: 3,33 (br), 1,89 (br), -1,57 (br), -3,19 (br), -9,89 (br).

Synthesis of (Cy₂)₂PNPCoCl **Co-6**

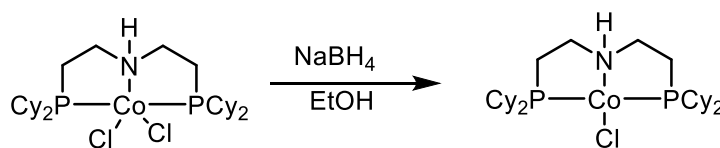
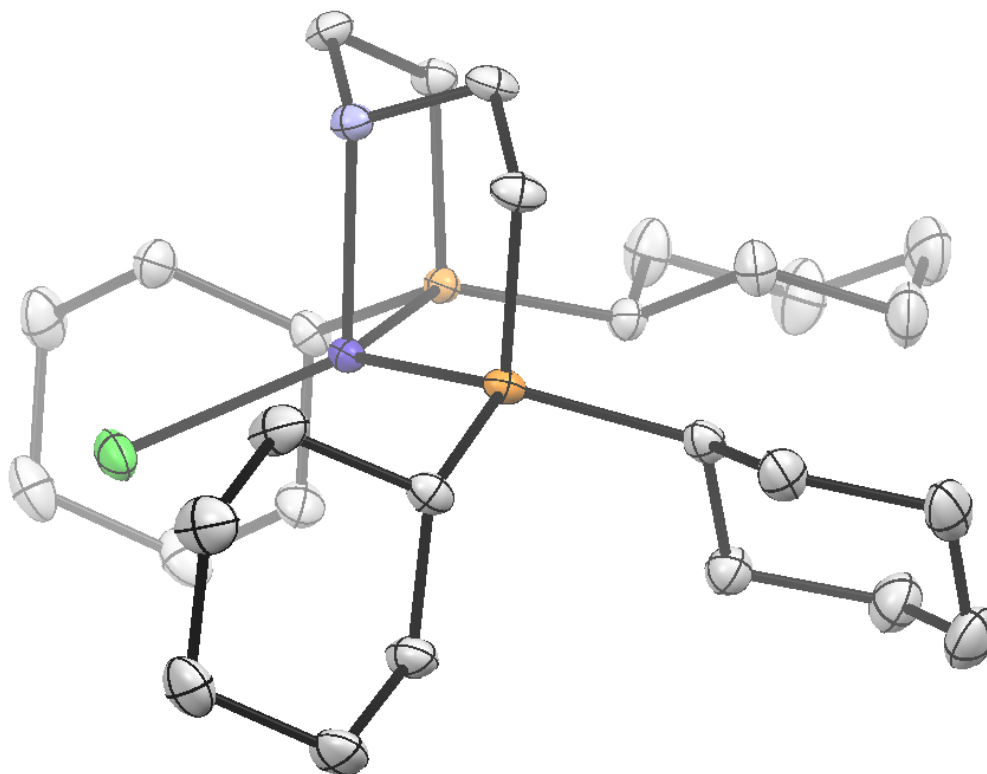
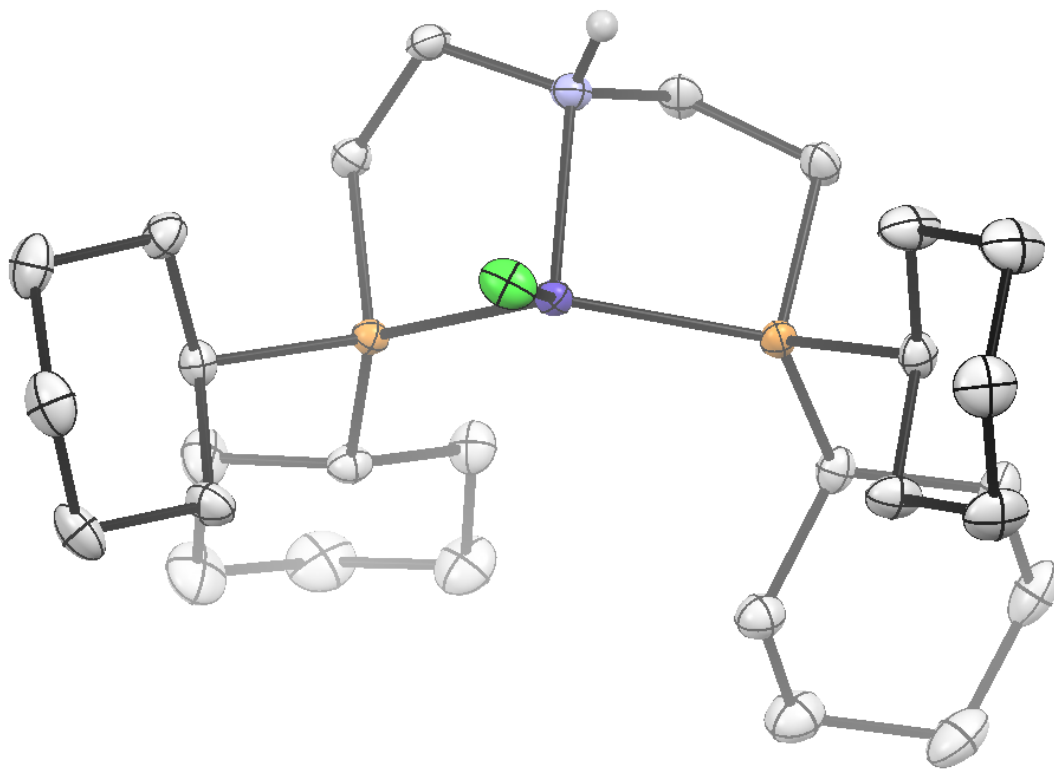


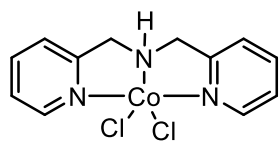
Figure 4 : Synthesis (Cy₂)₂PNPCoCl₂

In dried Schlenk tube, Cy₂PNPCoCl₂ **5** (0.129 g; 0.2974 mmol, 1 equiv.) was dissolved in 10 mL of dry ethanol. NaBH₄ (0.0112 g; 0.2974 mmol, 1 equiv.) was added in small portions at 0 °C. The solution turned brown after a few minutes. The reaction mixture was stirred overnight at r.t. The resulting blue/green solution was concentrated to dryness and toluene was added. The solution was filtered, and the solvent evaporated. The product was set to crystallize in a biphasic toluene/heptane solvent. The product was obtained as blue crystals in 55% yield.

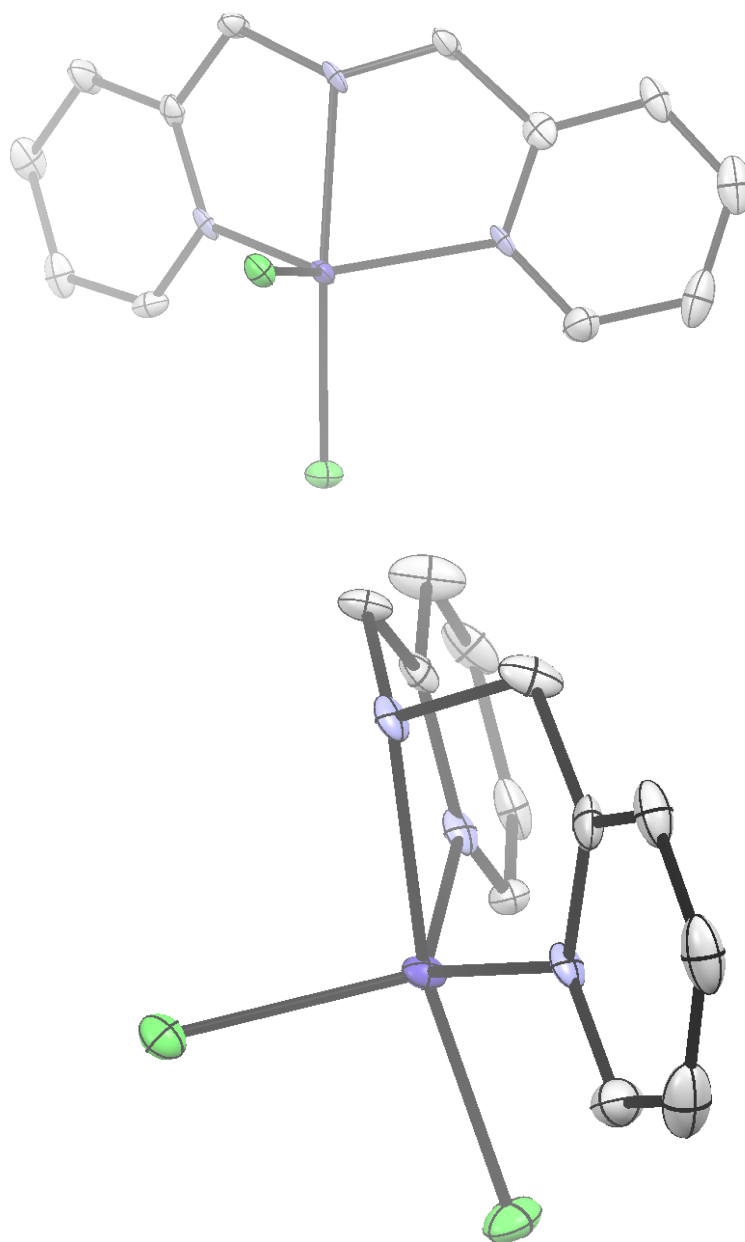
⁹⁸ Lin Chen, Pengfei Ai, Jianming Gu, Suyun Jie, Bo-Geng Li, *J. Organomet. Chem.*, 716, **2012**, 55-61,



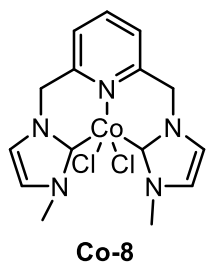
X-ray molecular structure of **Co-6**

Synthesis of NNNCoCl_2 **Co-7****Co-7**

In a dried Schlenk tube, CoCl_2 (0.319 g; 2.07 mmol, 1 equiv.) was dissolved in 10 mL of dry EtOH and bis(pyridin-2-ylmethyl)amine **7** (0.413 mg; 2.07 mmol, 1 equiv.) was added. The solution rapidly turned to violet and was stirred overnight. The solution was filtered and washed with ethanol. The product was dried under vacuum and crystallized in a biphasic DCM/Heptane solvent yielding the product as purple crystals in 78% yield.

X-ray molecular structure of **Co-7**

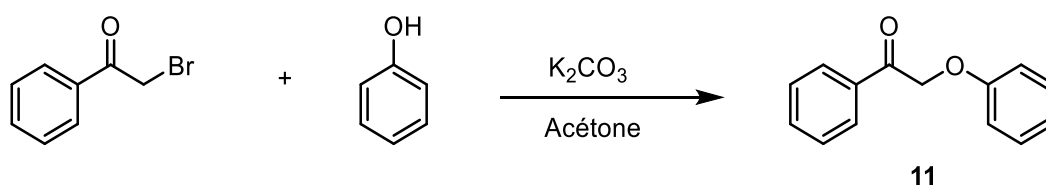
Synthesis of (Bis NHC)CoCl₂ **Co-8**



In a dried Schlenk tube, Bis-(NHC) **8** (0.100 g; 0.16 mmol, 1 equiv.) in 10 mL of dichloromethane was added to CoCl₂ (0,021 g, 1,16 mmol, 1 equiv.) in 10 mL of dichloromethane. The solution was stirred overnight at r.t. The solution was filtered and washed with dichloromethane. The solvent was evaporated and methanol added. The resulting suspension was filtered on celite. The product was dried under vacuum and obtained as a green solid in 80% yield.

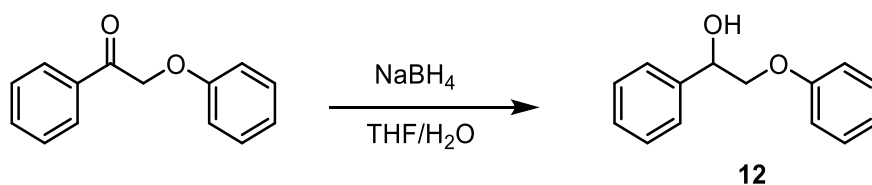
3/ Synthesis of the lignin model

The lignin-model **12** was synthesized in two steps.



In a 250 ml flask, phenol (0.520 g; 5.68 mmol) and potassium carbonate (1.040 g; 6.80 mmol) were dissolved in 50 mL of acetone. To this solution was added bromo-acetophenone (1.00 g; 5.02 mmol). The reaction mixture was refluxed for 4 h. The solution was cooled and filtered. The solvent was evaporated under vacuum leading to a white/yellow solid. The solid was recrystallized in ethanol. The product **11** was obtained as a white solid in 88% yield. NMR data were consistent with reported data⁹⁹

¹H NMR (CDCl₃): 8,04 (d, J=8,0 Hz, 2H, Har); 7,65 (t, J=8,0 Hz, 1H, Har); 7,53 (dd, J=8,0, 5,1Hz, 2H, Har); 7,32 (t, J=8,0 Hz, 2H, Har); 7,01 (t, J=8,0 Hz, 1H, Har); 6,98 (d, J=8,0 Hz, 2H, Har); 5,30 (s, 2H, -CH₂).



2-phenoxy-1-Phenylethanone **11** (0.4618 g; 2.17 mmol) and THF/water mixture (4:1) was introduced in a Schlenk tube. NaBH₄ (0.16 g; 4.351 mmol) was added in small portions. The reaction mixture was stirred for 1 h at r.t. The solution was quenched by a saturated solution of

⁹⁹ N. Luo, M. Wang, H. Li, J. Zhang, H. Liu, F. Wang. *ACS Catal.* **2017**, 7, 4571–4580

NH₄Cl. The crude product was washed with ethyl acetate (3x20ml) and the recovered phase was washed with brine and dried over Na₂SO₄. The product was dried under vacuum yielding a white solid in 95% yield.

NMR data were consistent with reported data⁹⁰

¹H NMR (CDCl₃): δ ppm: 7,49-7,23 (m, 7H, Har); 7,01-6,90 (m, 3H, Har); 5,13 (dd, J=8,0-3,2 Hz, 1H, Ar); 4,12 (dd, J=9,2; 3,2 Hz, 1H, CH); 4,02 (t, J=9,2 Hz, 1H, HO-CH).

4) Catalytic tests

General procedure.

In a glove box, a Schlenk tube was charged sequentially with lignin model **12** (0,100g ; 0,46 mmol), t-BuOK (0,0052 g ; 0,046mmol), Cobalt catalyst (0,00109 g ; 0,023 mmol), 2 mL of toluene and NaHBET₃ (0,025 mL, 0,025 mmol). The reaction mixture was stirred at 135 °C for 24 h. After the reaction, the Schlenk tube was cooled at r.t and the reaction mixture was analyzed by gas chromatography.

Chapter 2

Convenient synthesis of cobalt nanoparticles for the hydrogenation of quinolines in water

I/ Introduction

Heterocycles are important skeleton with many utilities in various domain of chemistry. Among heterocyclic structures, *N*-heterocycles, present in many natural compounds or produced synthetically have shown great utility and efficiency in the pharmaceutical chemistry¹⁰⁰ and more recently in the field of energy storage.¹⁰¹ For instance, quinoline derivatives constitute a class of compounds of proven therapeutic importance. Quinoline is an aromatic organic compound of the chemical formula C₉H₇N. It can be described by the assembly of a benzene molecule and a pyridine molecule. Quinoline was first extracted from tar by F. Runge in 1834 (Figure 1).¹⁰² Quinoline structure appears in many molecules found in nature, among which quinine is certainly the most well-known (Figure 1). Quinine is a natural alkaloid extracted from cinchona tree bark. For many years it was the only efficient treatment for malaria.¹⁰³ Currently, it is only used for the severe treatment of malaria, due in part to its undesirable side effects. Quinidine is a stereoisomer of quinine is also used in the treatment of malaria.¹⁰⁴ This molecule also has antiarrhythmic properties (heart rhythm disorder).

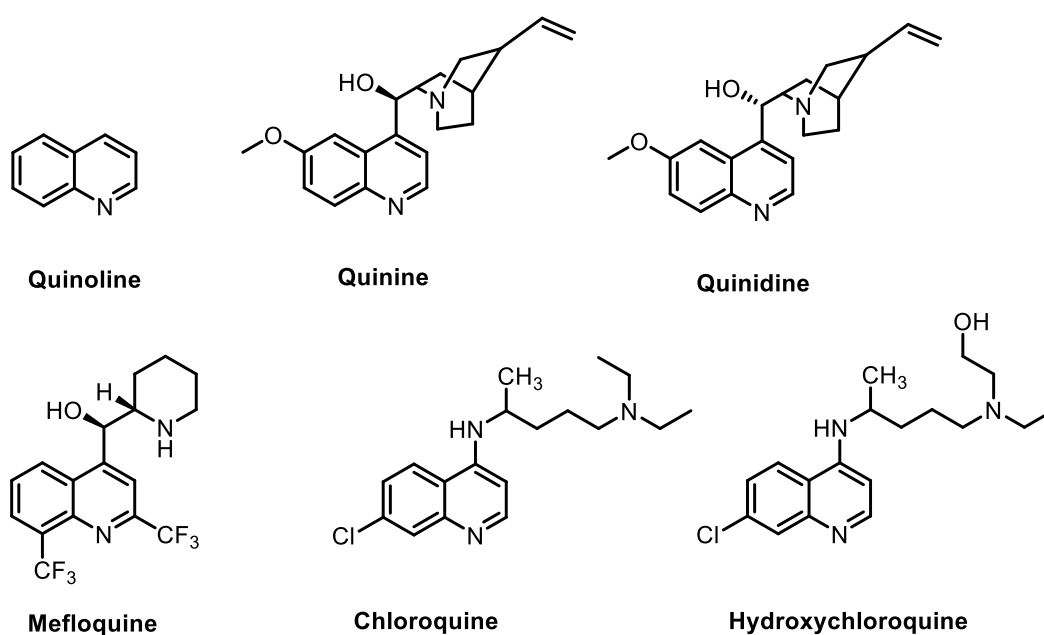


Figure 1: Natural quinoline and quinoline derivatives

Chloroquine,¹⁰⁵ discovered in 1940, was the first synthetic antimalarial drug. It has, like quinine, an anti-malarial action but also an anti-amibiasis activity, particularly at the hepatic

¹⁰⁰ R. Rahi, M. Fang, A. Ahmed, R. A. Sanchez-Delgado, *Dalton Trans.*, **2012**, 41, 14490-14497.

¹⁰¹ R. H. Crabtree, *Energy Environ. Sci.*, **2008**, 1, 134-138

¹⁰² R. Heusch, B. Leverkusen, Ullmann's *Encyclopedia of Industrial Chemistry*, **2000**.

¹⁰³ A. Korolhovas, J. H. Burcklaltre, Ed. *Wiley Interscience Pub.*, **1983**, 404.

¹⁰⁴ N. L. Allinger, M. P. Cava, D. Jong, C. Don, C. R. Johnson, N. A. Lebel, C. A. Stevens, Ed. *Science/Mc Graw-Hill*, **1975**, 774.

¹⁰⁵ C. V. Plow, *Current topic in Microbiology and Immunology*, **2005**, 295, 55-79.

locations of the amoeba where it concentrates in the liver. Its derivative hydroxychloroquine¹⁰⁶ is also an anti-malarial drug with also an anti-rheumatic activity, in particular rheumatoid arthritis and lupus erythematosus. Chloroquine and hydroxychloroquine are currently being debated for their use as COVID-19 treatment. Mefloquine,¹⁰⁷ introduced in 1971, belongs to the quinoline methanol family and is chemically related to quinine. It has long been a drug for malaria prophylaxis, but the development of widespread resistance, in addition to undesirable side effects, has considerably reduced its use (Figure 1).

Tetrahydroquinoline (THQ) is a relevant heterocyclic structure found in many natural and unnatural compounds with biological properties. For instance, 2-Methyl-1,2,3,4-tetrahydroquinoline is present in human brain. Discorhadin C, a polycyclic system based on tetrahydroquinoline, is a marine alkaloid.¹⁰⁸ Dynemycin, a natural antitumor antihistone, has a complex structure built on the tetrahydroquinoline system.¹⁰⁹ The 2,4,6 trisubstituted tetrahydroquinoline, isolated from *Martinella iquitosensis*, exhibits activity as a bradykinin antagonist and with α -adrenergic, histaminergic, and muscarinic receptors.¹¹⁰ Agusterein, galipeine, galipinine and cuspareine are the four 2-substituted 1-Methyltetrahydroquinoline alkaloids isolated from the bark of *Galipea officinal* Hancock by professor Ingrid Jacquemond-Collet et al. in 1999.¹¹¹ *Galipea officinal* Hancock is a shrub indigenous to the mountains of Venezuela that has marked influence on the spinal motor nerves, thus, serves a cure for paralytic affections (Figure 2).¹¹²

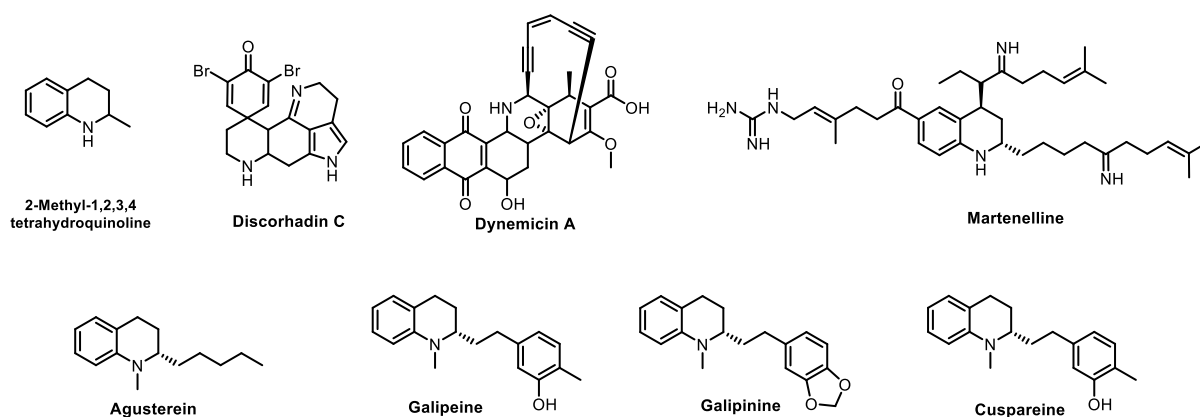


Figure 2: Bioactive tetrahydroquinoline derivatives

Quinoline hydrogenation is a challenging reaction because of the possible catalyst deactivation due to coordination of quinoline or 1,2,3,4-THQ. Many homogeneous catalysts¹¹³ have been

¹⁰⁶ J. E. Nord, P. K. Shah, R. Z. Rinaldi, M. H. Weisman, *Seminars in Arthritis and Rheumatism*, **2004**, *33*, 336-355.

¹⁰⁷ L. Schmidt, R. Crosby, J. Rasco, D. Vaughan, *Antimicrobial Agent and Chemotherapy*, **1978**, *13*, 1011-1030.

¹⁰⁸ J. D. White, K. M. Yager, T. Yakura, *J. Am. Chem. Soc.*, **1994**, *116*, 1831-1838.

¹⁰⁹ M. Konishi, H. Ohkuma, T. Tsuno, T. Oki, *J. Am. Chem. Soc.*, **1990**, *112*, 3715-3716.

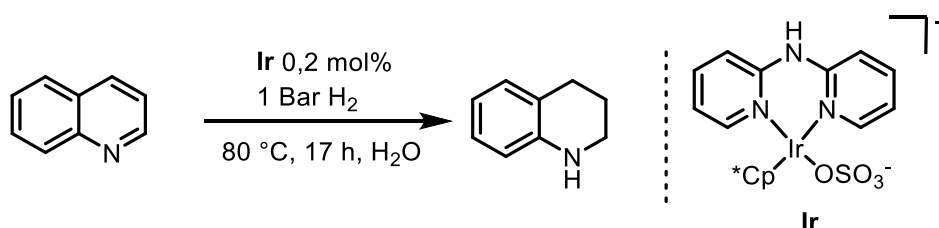
¹¹⁰ K. M. Witherup, R. W. Ransom, S. L. Varga, S. M. Pitzenberger, V. J. Lotti, J. Lumma, *J. U.S. Pat. US.*, **1994**, *5*, 288-725.

¹¹¹ I. Jacquemond-Collet, S. Hannedouche, N. Fabre, I. Fouraste, C. Moulis, *C. Phytochemistry*, **1999**, *51*, 1167-1169.

¹¹² I. Jacquemond-Collet, F. Benoit-Vical, M. A. Valentin, E. Stanislas, M. Mallie, I. Fouraste, *Planta. Med.*, **2002**, *68*, 68-69.

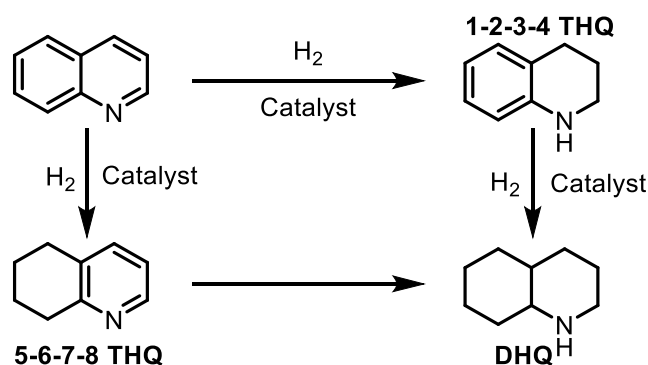
¹¹³ (a) R. A. Sanchez-Delgado, E. Gonzalez, *Polyhedron*, **1989**, *8*, 1431-1436; (b) W. B. Wang, S. M. Lu, P. Y. Yang, X. W. Han, Y. G. Zhou, *J. Am. Chem. Soc.*, **2003**, *125*, 10536-10537; (c) H. Zhou, Z. Li, Z. Wang, T. Wang, L. Xu, Y. He, Q.-H. Fan, J. Pan, L. Gu, A. S. C. Chan, *Angew. Chem., Int. Ed.*, **2008**, *47*, 8464-8467; (d) H. Li, J.

reported for the hydrogenation of quinolines while iridium-based catalysts exhibited best performances and chemoselectivities. In 2019, Wang and al.¹¹⁴ developed an iridium-based catalyst bearing an electron-enriched dipyridylamine ligand for the reversible hydrogenation of quinoline derivatives. The catalyst can be operated under mild reaction conditions in water without any additive, hence meeting the requirements for clean and sustainable processes (Scheme 1). Homogeneous catalysts based on non-noble metals such as Fe,¹¹⁵ Mn,¹¹⁶ Co¹¹⁷ have also been reported.



Scheme 1: Quinoline hydrogenation by homogeneous Ir catalyst.

In the past decade, numerous heterogeneous catalysts based on noble metals such as Rh,¹¹⁸ Au¹¹⁹ and Ru¹²⁰ have been reported



Scheme 2: quinoline hydrogenation pathways.

Jiang, G. Lu, F. Huang, Z.-X. Wang, *Organometallics*, **2011**, *30*, 3131-3141; (e) G. E. Dobereiner, A. Nova, N. D. Schley, N. Hazari, S. J. Miller, O. Eisenstein, R. H. Crabtree, *J. Am. Chem. Soc.*, **2011**, *133*, 7547-7562; (f) J. Wu, J. H. Barnard, Y. Zhang, D. Talwar, C. M. Robertson, J. Xiao, *Chem. Commun.*, **2013**, *49*, 7052-7054; (g) X.-F. Cai, W.-X. Huang, Z.-P. Chen, Y.-G. Zhou, *Chem. Commun.*, **2014**, *50*, 9588-9590; (h) Y. Wang, Z. Huang, X. Leng, H. Zhu, G. Liu, Z. Huang, *J. Am. Chem. Soc.*, **2018**, *140*, 4417-4429; (i) A. Vivancos, M. Beller, M. Albrecht, *ACS Catal.*, **2018**, *8*, 17-21.

¹¹⁴ S. Wang, H. Huang, T. Roisnel, C. Bruneau, C. Fischmeister, *ChemSusChem.*, **2019**, *12*, 179-184.

¹¹⁵ S. Chakraborty, W. B. Brennessel, W. D. Jones, *J. Am. Chem. Soc.*, **2014**, *136*, 8564-8567.

¹¹⁶ V. Papa, Y. Cao, A. Spannenberg, K. Junge, M. Beller, *Nat. Catal.*, **2020**, *3*, 135-142; (b) Y. Wang, Z. Shao, G. Li, Y. lan, Q. Liu, *J. Am. Chem. Soc.* **2019**, *141*, 17337- 17349.

¹¹⁷ (a) R. Xu, S. Chakraborty, H. Yuan, W. D. Jones, *ACS Catal.*, **2015**, *5*, 6350-6354; (b) R. Adam, J. R. Cabrero-Antonino, A. Spannenberg, K. Junge, R. Jackstell, M. Beller, *Angew. Chem., Int. Ed.*, **2017**, *56*, 3264-3268; (c) J. R. Cabrero-Antonino, R. Adam, K. Junge, R. Jackstell, M. Beller, *Catal. Sci. Technol.*, **2017**, *7*, 1981-1985.

¹¹⁸ A. Karakulina, A. Gopakumar, I. Akçok, B. L. Roulier, T. LaGrange, S. Katsyuba, S. Das, P. J. Dyson, *Angew. Chem. Int. Ed.*, **2016**, *55*, 292-296.

¹¹⁹ D. Ren, L. He, L. Yu, R. S. Ding, Y. M. Liu, Y. Cao, H. Y. He, K. N. Fan, *J. Am. Chem. Soc.*, **2012**, *134*, 17592-17598.

¹²⁰ B. Sun, D. Carnevale, G. Süß-Fink, *J. Organomet. Chem.*, **2016**, *821*, 197-205.

. However, with heterogeneous catalysts the selective hydrogenation of quinoline is more difficult. Indeed, there are different hydrogenable sites on quinoline. The most well-known pathway is the hydrogenation of the pyridil group to form the 1,2,3,4-THQ. A second and less known pathway is the hydrogenation of the phenyl group to form the 5,6,7,8-THQ. Finally, in some cases, both groups are hydrogenated to form decahydroquinoline (DHQ) (Scheme 2).

As for homogeneous catalysis, the development of less expensive heterogeneous catalysts is a highly important topic in catalysis. In 2015, the group of Beller developed the selective hydrogenation of heteroarenes using cobalt oxide/cobalt nanoparticles modified by nitrogen doped graphene layers on alumina.¹²¹ Various catalysts were synthesized varying the source of metals, ligands and supports. All these materials were tested for their catalytic activity for the benchmark hydrogenation of quinoline to 1,2,3,4-THQ at 120 °C and 20 bar of hydrogen. The best catalyst was prepared using Co(OAc)₂·4H₂O as a metal precursor, 1, 10-phenantroline (**L1**) as nitrogen ligand and α-Al₂O₃ as a support. Using the Co₃O₄-Co/NGr@α-Al₂O₃ NPs (**L1**) the desired product 1,2,3,4-tetrahydroquinoline was obtained in 90% yield under 10 bar H₂ at 120 °C for 48 h in toluene (Table 1, entry 1). Decreasing the catalyst loading to 3 and 2 mol% showed similar reactivity than 4 mol% (Table 1, entry 2 and 3). Catalysts prepared with different ligands (2,2'-bipyridine (**L2**) and 2,2':6',2''-terpyridine (**L3**)) have been tested under similar conditions and showed significantly lower activity for this transformation (Table 1, entries 4 and 5).

Table 1: Catalytic Hydrogenation of Quinoline: Variation of Catalysts and Reaction Conditions^a

L1

L2

L3

Entry	Catalyst (mol%)	Yield ^b (%)
1	Co/ L1 /α-Al ₂ O ₃ (4)	90 (88 ^c)
2	Co/ L1 /α-Al ₂ O ₃ (3)	94
3	Co/ L1 /α-Al ₂ O ₃ (2)	92
4	Co/ L2 /α-Al ₂ O ₃ (4)	37
5	Co/ L3 /α-Al ₂ O ₃ (4)	52

^aReaction conditions: 0.5 mmol of quinoline, 4 mol % Co₃O₄-Co/NGr@α-Al₂O₃, in 2 mL toluene under 10 bar of H₂. ^bGC yield using dodecane as an internal standard.

The substrate scope was explored with 4 mol% catalyst, under 20 bar hydrogen at 120 °C for 48 h. Generally, quinolines with various functional groups were converted to the corresponding 1,2,3,4-THQ in high yields. Interestingly substrates containing halogen (Cl) in position 6 or 8 were smoothly hydrogenated without any dehalogenated compound detected (Table 2, entry 2, 6). 2,2'-biquinoline reacted in a selective manner to give 1,2,3,4-tetrahydro-2,2'-biquinoline

¹²¹ F. Chen, A.-E. Surkus, L. He, M.-M. Pohl, J. Radnik, C. Topf, K. Junge, M. Beller, *J. Am. Chem. Soc.*, **2015**, *137*, 11718-11724.

(Table 2, entry 5) with only one pyridyl ring hydrogenated. In the case of 2-(4-methylpent-3-en-1-yl)quinoline (Table 2, entry 8) bearing a reducible carbon-carbon double bond, no hydrogenation of the olefin was observed, the desired product is obtained in 49% yield, and 39% starting material was recovered. Interestingly, 4-methylquinoline (Table 2, entry 9) was hydrogenated to give two products: 4-methyl-1,2,3,4-tetrahydroquinoline and 4-methyl-5,6,7,8-tetrahydroquinoline, respectively. Similarly, 2,4-dimethylquinoline (Table 2, entry 10) led to 2,4-dimethyl-1,2,3,4-tetrahydroquinoline and 2,4-dimethyl-5,6,7,8-tetrahydroquinoline. Other *N*-heterocycle such as acridine, benzo-*h*-quinoline and indole were hydrogenated in good to excellent yield (Table 2, entries 11-13)

Table 2: *Co*3O4-*Co*/N*Gr*@ α -Al2O3 NPs Catalyzed Hydrogenation of Various Quinolines

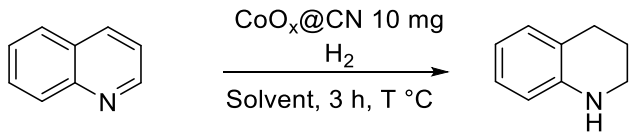
Entry	Substrate	Product	Yield ^b
1			95
2			81
3			92
4			81
5			79
6			94
7			80
8			49
9			51/36
10			16/67
11			86
12			92
13			83

^a Reaction conditions: 0.5 mmol of substrate, 4 mol % *Co*3O4-*Co*/N*Gr*@ α -Al2O3, in 2 mL of toluene under H₂. ^b Isolated yield.

One year later, Wang disclosed cobalt encapsulated in *N*-doped graphene layers for the hydrogenation of quinolines in 3-15 h, in methanol at 120 °C under 30 bar of hydrogen pressure.

¹²² The hybrids (denoted as CoOx@CN) were obtained in one step through pyrolysis of *D*-glucosamine hydrochloride (GAH), cobalt acetate, and melamine at 800 °C. In a first time, the condition reactions were optimized using quinoline as a model-substrate. Solvent, temperature and pressure have been varied.

Table 3: Influence of Solvent, Temperature and Hydrogen Pressure on the Hydrogenation of Quinoline Catalyzed by CoOx@CN^a



Entry	T °C	P (Bar)	Solvent	Conv (%)
1	120	30	Cyclohexane	63
2	120	30	Toluene	92
3	120	30	H ₂ O	98
4	120	30	EtOH	92
5	120	30	MeOH	100
6	100	30	MeOH	81
7	120	20	MeOH	70

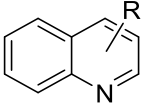
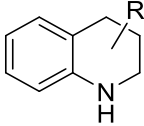
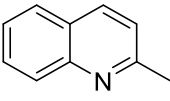
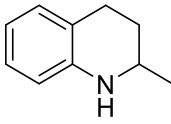
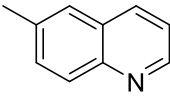
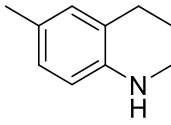
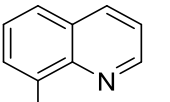
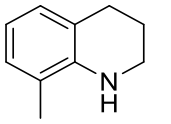
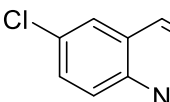
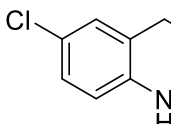
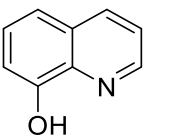
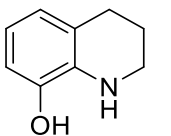
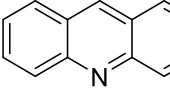
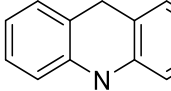
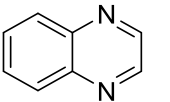
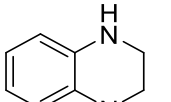
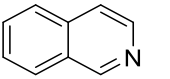
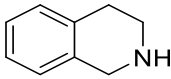
^aReaction conditions: quinoline (0.5 mmol), CoOx@CN (10 mg), solvent (5 mL), 3 h.

As shown in Table 3, polar solvent such as H₂O, MeOH or EtOH gave high conversions (92-100%) in 1,2,3,4-THQ (Table 3, entry 3-5). However, using non-polar solvent such as cyclohexane and toluene gave two different results. Indeed, cyclohexane offered only 63% conversion and toluene 92% conversion. It seems that CoOx@CN performs generally better in protic solvents. The catalytic activity of CoOx@CN was sensitive to the reaction temperature. Reducing the reaction temperature to 100 °C with 30 bar of H₂ (Table 3, entry 6) produced a marked drop in conversion (81%). Finally, reducing the pressure to 20 bar, decreased the conversion to 70% (Table 3, entry 7). Further studies were conducted at 30 bar and 120 °C.

With the optimized reaction parameters in hand, the general scope of CoOx@CN in the hydrogenation of quinoline compounds was investigated. Quinoline compounds substituted with a methyl group in position 2, 6 and 8 were converted into the corresponding 1,2,3,4-THQ with full conversion (Table 4, entries 2-4). Notably quinoline substituted with halogen in position 7 offered the corresponding halo-THQ without any dehalogenation (Table 4, entry 5). What should be noted is the facile reduction of 8-hydroxyquinolines to biologically active 1,2,3,4-tetrahydro-8-hydroxyquinoline, a compound that can inhibit leukotriene formation in macrophages (Table 4, entry 6). Also noteworthy is the fact that other biologically important *N*-heteroarenes such as acridine, quinoxaline, and isoquinoline were also converted into the target products in high yields (Table 4, entries 7-9).

¹²² Z. Wei, Y. Chen, J. Wang, D. Su, M. Tang, S. Mao, Y. Wang, *ACS Catal.*, **2016**, 6, 5816-5822.

Table 4: Chemoselective Hydrogenation of Various Substituted Quinolones and N-Heterocycles^a

Entry	Substrate	Product	Time (h)	Conv. (%) ^b	Yield (%) ^b
1			3	100	95
2			10	100	94
3			10	100	95
4			6	99	95
5 ^c			3	99	94
6 ^d			12	100	89
7			4	96	88
8			10	87	77
9			15	100	92

^aReaction conditions: substrate (0.5 mmol), CoOx@CN (10 mg), CH₃OH (5 mL), 3 MPa of H₂, 120 °C. ^bDetermined by GC (internal standard, n-dodecan), isolated yields. ^cAt 110 °C. ^dCoOx@CN (20 mg) at 140 °C.

More recently, Corma and co-workers,¹²³ described the hydrothermal preparation of nanolayered mixed cobalt-molybdenum sulfide. The hydrogenation of quinoline to the corresponding 1,2,3,4-THQ was investigated as a benchmark system to compare the catalytic activity of the prepared cobalt-molybdenum sulfide materials. Initial experiments were performed using toluene as a solvent, under 12 bar of hydrogen, at 150 °C. Further optimization experiments were carried out with the most active catalyst (Co-Mo-S-0.83) (Table 5).

¹²³ I. Sorribes, L. Liu, A. Doménech-Carbó, A. Corma, *ACS Catal.*, **2018**, *8*, 4545-4557.

Table 5: Regioselective Hydrogenation of Quinoline Catalyzed by Co-Mo-S-0.83

Entry	Solvent	Conversion (%) ^b	Yield (%) ^b
1	EtOH	94	91
2	MeOH	84	83
3	1,4 dioxane	60	50
4	CH ₃ CN	20	14
5	THF	21	11
6	<i>n</i> -Bu ₂ O	67	58
7	Toluene	>99	98
8 ^c	-	99	98 ^d
9 ^e	Toluene	99	99(92)
10 ^f	Toluene	87	87
11 ^g	Toluene	92	90

^aReaction conditions: quinoline (0.25 mmol), catalyst (6.5 mg), solvent (1.6 mL). ^bDetermined by GC using dodecane as an internal standard; yield of isolated product on a 10 mmol scale given in parentheses. ^c2 h. ^dAverage value for six catalytic reactions: 97.8 ± 1.1. ^e120 °C, 12 h. ^f100 °C, 18 h. ^g120 °C, 12 h, 6 bar of H₂.

First, the influence of the solvent was investigated (Table 5, entries 1-8). In general, the use of solvents other than toluene led to lower reactivity. At a longer reaction time (10h), excellent conversion of quinoline was also achieved by using protic solvents, such as ethanol and methanol (Table 5, entries 1 and 2). Interestingly, in the absence of any solvent 1,2,3,4-THQ was obtained in excellent yield in 2 h (Table 5, entry 8). The catalytic hydrogenation of quinoline could also be achieved at lower temperature, affording 1,2,3,4-THQ in a quantitative yield at 120 °C or 87% yield at 100 °C after a longer reaction time (Table 5, entries 9 and 10). When the hydrogen pressure was halved, quinoline was almost fully converted, affording 1,2,3,4-THQ in 90% yield (Table 5, entry 11). The scope of the chemo- and regioselective hydrogenation protocol in the presence of catalyst Co-Mo-S-0.83 was broadly investigated for the hydrogenation of many quinolines substituted with different functional groups.

Quinolines bearing a methyl group on either the benzene or the heteroarene ring reacted smoothly, affording the corresponding products in excellent yields. Halogen-substituted quinolines were also readily transformed, leading to the corresponding halogenated 1,2,3,4-tetrahydroquinolines in high isolated yields. The most interesting part was the functional groups tolerance that was studied by exploring other reducible substituents. High chemoselectivity to the N-heteroarene ring hydrogenation was achieved in the presence of sensitive alkene groups that were well-retained in the final hydrogenated products (Table 6, entries 1 and 2). It should be noted that this selectivity was reached even at high conversions of substrates. Interestingly, the ketone sensitive group was also well tolerated in the hydrogenative reaction environment (Table 6, entry 4). Furthermore, 1,2,3,4-tetrahydroquinolines substituted with carboxylic acid derivative groups, including esters and amides and also cyanides were selectively hydrogenated in good to excellent yields (Table 6, Entries 3-5-6-7).

Table 6: Chemo- and Regioselective Hydrogenation of Substituted Quinolines Catalyzed by Co-Mo-S-0.83^a

Entry	Substrate	Product	Conv (%) ^b	Yield (%) ^c
1			95	74
2			96	82
3			99	87
4			97	77
5			>99	74
6			99	97
7			98	78

Reaction conditions unless specified otherwise: substrate (0.25 mmol), catalyst (6.5 mg), toluene (1.6 mL). ^bDetermined by GC using dodecane as an internal standard. ^cYield of isolated product

As depicted in this non-exhaustive but representative state of the art, many heterogeneous cobalt catalysts have been prepared in the past decade. However, most of them were prepared by multi-step reactions and pyrolysis. Initially interested by the reduction of quinoline promoted by the cobalt complexes described in chapter I and sodium borohydride, it became obvious that cobalt particles were likely generated and involved in the observed catalytic activity. Metal-nanoparticles represent an alternative to these heterogeneous catalysts in particular those elaborated in an easy and straightforward manner. Reports from Jacobi von Wangelin demonstrated the suitability of stabilised or quasi-naked cobalt nanoparticles in hydrogenation reactions.¹²⁴ In this context, the reduction of cobalt salts with sodium borohydride caught our

¹²⁴ (a) S. Sandl, F. Schwarzhuber, S. Pöllath, J. Zweck, A. Jacobi von Wangelin, *Chem. Eur. J.*, **2018**, *24*, 3403-3407; (b) P. Büschelberger, E. Reyes-Rodríguez, C. Schöttle, J. Treptow, C. Feldmann, A. Jacobi von Wangelin, R. Wolf, *Catal. Sci. Technol.*, **2018**, *8*, 2648-2654.

attention considering that the hydrolysis of NaBH₄ in the presence of Co(II) salt leading to various cobalt species¹²⁵ including nanoparticles is well established.¹²⁶ Inspired by these results, we developed a novel cobalt-catalysed hydrogenation of quinoline and quinoline derivatives in aqueous media.

II/ Results and discussions

We started our investigations with the reduction of quinoline **1** with the cobalt complex **Co-7** synthesised and used for the redox-neutral lignin reaction in the previous chapter. More specifically, a high-pressure reactor was successively loaded with **Co-7** (5 mol%), NaBH₄ (10 mol%), *i*-PrOH (1 mL) and quinoline **1**, charged with dihydrogen and heated to 115 °C.

As shown in table 1, only a low conversion of **1** was observed using 20 bar of hydrogen (Table 7, entry 1). However, increasing the pressure to 30 bar offered a quantitative conversion of **1** (Table 7, entry 2). Nevertheless, a magnetic black powder was observed in the reaction media, leaving thought for the formation of cobalt (0) particles. To clarify this issue, we conducted control experiments first using CoCl₂ as a catalyst precursor having in mind that such cobalt salt is known to generate Co(0) particles in the presence of sodium borohydride. Surprisingly, the same reactivity as **Co-7** was observed (Table 7, entry 3) suggesting the formation of Co(0) particles from **Co-7**. This matter of fact is corroborated by the detection of compound **3** sometimes generated by heterogeneous catalysis but never observed under homogeneous catalysis conditions. Finally, without any cobalt source, no reactivity was observed (Table 7, Entry 4).

Table 7: Optimization of the reaction.

Entry	Catalyst	H ₂	Conv. (%) ^b	2 (%) ^b	3 (%) ^b
1	Co-7	20	10	10	0
2	Co-7	30	100	90	10
3	CoCl ₂	30	100	90	10
4	-	30	0	0	0

^a Conditions: Quinoline (0.100 g; 0.78 mmol), Co (5 mol%), NaBH₄ (2.95 mg, 10 mol%), isopropanol (1 mL), 17 h, 115 °C (oil bath temperature). ^bConversion determined by ¹H NMR.

A screening of solvent was then carried out. As depicted in Table 1, no conversion was observed using a non-polar solvent such as toluene (Table 8, entry 1). Decreasing the solution concentration with 3 mL in isopropanol lead to a lower conversion (Table 8, entry 3). Using

¹²⁵ U. B. Demerci, P. Miele, *Phys. Chem. Chem. Phys.*, **2010**, *12*, 14651-14665; (b) U. B. Demerci, O. Akdim, J. Andrieux, J. Hannaeur, R. Chamoun, P. Miele, *Fuel Cells*, **2010**, *10*, 335-350.

¹²⁶ G. N. Glavee, K. J. Klabunde, C. M. Sorensen, G. C. Hadjipanayis, *Langmuir*, **1993**, *9*, 162-169; (b) X. Liang, L. Zhao, *RSC Advances*, **2012**, *2*, 5485-5487; (c) P. Brack, S. E. Dann, K. G. Upul Wijayantha, *Energy Sci. Eng.*, **2015**, *3*, 174-188; (d) C. Che, H. Huang, Z. Zhang, X.-Q. Dong, X. Zhang, *Chem. Commun.*, **2017**, *53*, 4612-4615.

different polar solvents such as water or THF offered different results. Indeed, using THF only 14% conversion was observed when 99% conversion was achieved in water (Table 8, entry 4-5). Finally, mixtures of solvents such as THF/H₂O and *i*-PrOH/ H₂O did not allow for better results (Table 8, entry 6-7). In conclusion, water does not only provide the highest conversion it does also ensure a chemoselective transformation.

Table 8: Solvent Screening^a

Entry	Solvent	Conv. (%) ^b	2 (%) ^b	3 (%) ^b
1	Toluene	0	0	0
2	<i>i</i> -PrOH (1 mL)	100	90	10
3	<i>i</i> -PrOH (3 mL)	75	73	2
4	H ₂ O	99	99	-
5	THF	14	14	-
6	THF/H ₂ O	44	44	-
7	<i>i</i> -PrOH/ H ₂ O	96	96	-

^a Conditions: Quinoline (0.100 g; 0.78 mmol), CoCl₂ (0.038 mmol; 5 mol%), NaBH₄ (2.95 mg, 10 mol%), H₂O (1 mL), 17 h, T = 115 °C, oil bath temperature. ^b Conversion and product ratio were determined by ¹H NMR.

Further optimizations were carried out varying the amount of sodium borohydride, the hydrogen pressure and the temperature. As depicted in Table 9, only minor amounts of catalytic hydrogenation of **1** to **2** occurred at 20 bar of hydrogen (Table 9, entry 1). Increasing the temperature to 130 °C resulted in better performances but with moderate repeatability (Table 8, entry 2). However, repeatable and quantitative reactions were achieved at 130 °C and 30 bar of hydrogen pressure (Table 9, entry 3). Applying a reduced catalyst loading (2.5 mol%) still resulted in 72% conversion and excellent selectivity (Table 9, entry 4). Following these preliminary results, several other experimental parameters were varied. Literature reports on the hydrolysis of NaBH₄ catalysed by Co(II) salts clearly established that the Co(II)/NaBH₄ ratio is a key parameter determining the nature of the generated cobalt species.¹²⁴ Hence, the hydrogenation of quinoline was studied in the presence of different amounts of NaBH₄ showing an interesting influence on the reaction selectivity. The reaction could be performed with only 5% of NaBH₄ but again the repeatability of the reaction was not fully satisfactory leading to 80% to full conversions (Table 9, entry 6). Notably, increasing the amount of sodium borohydride to 20 mol% and to 50 mol%, respectively resulted in a different reduction pathway leading to product **3** arising from the hydrogenation of the carbon-ring (Table 9, entries 7-8). Apparently, different kinds of active cobalt nanoparticles are formed depending on the amount of sodium borohydride. This selectivity issue has already been mentioned with several heterogeneous catalysts with sometimes trace amounts of fully hydrogenated product.¹²⁷

¹²⁷ (a) S. Zhang, Z. Xia, T. Ni, Z. Zhang, Y. Ma, Y. Qu, *J. Catal.*, **2018**, 359, 101-111; (b) H-y Jiang, J. Xu, B. Sun, *App. Organometal. Chem.*, **2018**, 32, 4260-4268; (c) X. Wang, W. Chen, L. Zhang, T. Yao, W. Liu, Y. Lin, H. Ju, J. Dong, L. Zheng, W. Yan, X. Zheng, Z. Li, X. Wang, J. Tang, D. He, Y. Wang, Z. Deng, Y. Wu, Y. Li, *J. Am. Chem. Soc.*, **2017**, 139, 9419-9422.

Notably, the reaction was successfully scaled-up to 2 g of quinoline using the best experimental conditions (Table 9, entry 9).

Table 9: Catalytic hydrogenation of quinoline^a

Entry	NaBH ₄ (mol%)	P (H ₂) (bar)	T (°C) ^b	Conv. (%) ^c	2 (%) ^c	3 (%) ^c
1	10	20	115	10	10	0
2	10	20	130	84-99	84-99	0
3	10	30	130	≥ 99 ^f	≥ 99	0
4 ^d	10	30	130	72	72	0
5	2.5	30	130	36	36	0
6	5	30	130	79-≥ 99	79-≥ 99	0
7	20	30	130	≥ 99 ^f	82	8
8	50	30	130	>99 ^f	78	22
9 ^e	10	30	130	≥ 99 ^f	≥ 99	0

^a Conditions: Quinoline (0.100 g; 0.78 mmol), CoCl₂ (0.038 mmol; 5 mol%), NaBH₄ (2.95 mg, 10 mol%), H₂O (1 mL), 17 h. ^b Oil bath temperature. ^c Conversion and product ratio were determined by ¹H NMR. ^d CoCl₂ (2.5 mol%). All experiments were done twice. ^e 2 g scale of quinoline, ^f 1 not detected by NMR.

The activation period corresponding to the amount of time between the addition of water to CoCl₂/NaBH₄ and quinoline was also considered and studied as a key parameter. As the reduction of cobalt salts by NaBH₄ is a fast reaction, a study was conducted with short activation periods and low catalyst loading. The initial assumption was verified as an increase in conversion was observed upon increasing the activation period to 6 minutes. Further extension of this activation period led to lower performances indicating the evolution of the catalytic species into non- or less reactive species (Table 10).

Table 10: Co-nanoparticles catalyzed hydrogenations of quinoline: Influence of the activation period^a

Entry	t (min)	Conv. (%) ^b	2 (%) ^b
1	0	15	15
2	3	19	19
3	6	23	23
4	8	16	16

^a Conditions: Quinoline (0.100 g; 0.78 mmol), CoCl₂ (0.038 mmol; 1 mol%); NaBH₄ (2 mol%), H₂O (1 mL), H₂ (30 bar), 130 °C, 17 h. ^b Conversion and yield determined by ¹H NMR

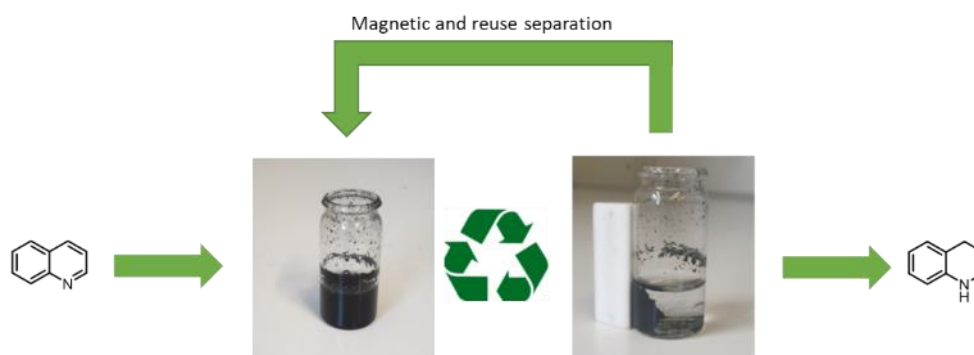
Next, we examined the influence of various cobalt(II) precursors. Apart from cobalt(II) acetylacetonate which was less suitable for this reaction, it is worth noting that the less toxic (NH₄)₂Co(SO₄)₂·6H₂O was found as effective as CoCl₂ (Table 11, entry 3) and was used in some examples of the substrate scope study (*vide infra*).

Table 11: Catalytic hydrogenations of quinoline: Evaluation of Co(II) precursors^a

Entry	Catalyst	Toxicity	Conv. (%) ^b	2 (%)
1	CoCl ₂ (5 mol%)		≥ 99 ^d	≥ 99 ^d
2	Co(acac) ₂ (5 mol%)		84 ^c	84
3	(NH ₄) ₂ Co(SO ₄) ₂ ·6H ₂ O (5 mol%)		≥ 99 ^d	≥ 99 ^d
4	CoCl ₂ ·6H ₂ O (5 mol%)		≥ 99 ^d	≥ 99 ^d

^a Conditions: Quinoline (0.100 g, 0.78 mmol), NaBH₄ (10 mol%), H₂O (1 mL), H₂ (30 bar), 130 °C, 17 h. ^b Conversion determined by ¹H NMR. ^c Average of 3 reactions (79%, 85%, 89%). All reactions were done two or three times. ^d **1** not detected by NMR

As mentioned in the early observations of the reaction, the presence of black magnetic particles in the reaction media was clearly evidenced. The recycling of the Co-Nps was thus evaluated by means of consecutive quinoline hydrogenation runs taking advantage of this magnetic property of the in situ formed cobalt particles allowing for a facile separation of the heterogeneous catalyst (Figure 3).

**Figure 3:** Separation of magnetic cobalt particles

After a first run performed under the previously optimised conditions, the reaction mixture was extracted with ethyl acetate and the aqueous phase containing the cobalt catalyst was reloaded with sodium borohydride, quinoline and stirred at 130 °C for 17 h under 30 bar of dihydrogen. Following this procedure, it was possible to perform three runs with excellent conversion and selectivity after which a quick drop in conversion was observed without deterioration of selectivity (Figure 4). This result is attributed to the deactivation of the catalyst as a black layer accumulated with time over the vial walls. This assumption was confirmed by analysing the reaction mixture arising from a recycling test in which the vial walls were coated by a black solid. Indeed, cobalt could not be detected by EDS analyses of this reaction mixture indicating that all the cobalt was coated onto the vial walls and was catalytically inactive. Another recycling experiment was performed in which the aqueous reaction mixture was separated from

the insoluble material after the first run. The generated black solid was washed with water and a second run was started under standard conditions giving a lower conversion of only 50%. This observation is most likely explained by the removal of soluble catalytic cobalt species and sodium and boron compounds.

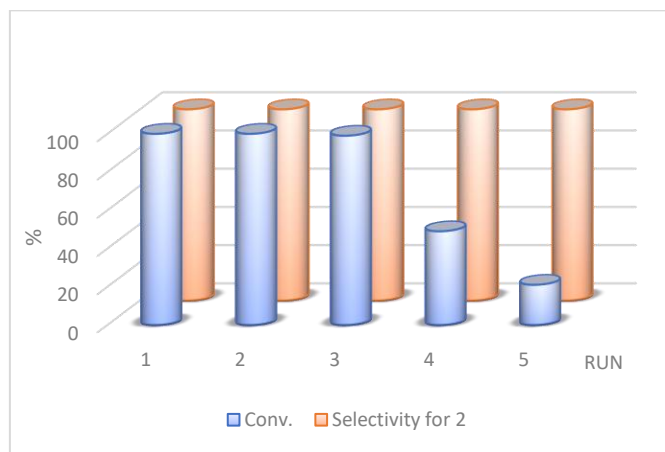


Figure 4: Catalytic hydrogenation of quinoline: Recycling of cobalt catalyst

With these results in hands, we turned our attention to the nature of the catalyst. As mentioned in the introduction, the hydrolysis of NaBH_4 in the presence of CoCl_2 is a very complex process likely to generate several cobalt species. Several parameters such as the ratio $\text{CoCl}_2/\text{NaBH}_4$ or the rate of hydrolysis influence this process. In general, we applied for the catalytic experiments a catalyst prepared by hydrolysis of NaBH_4 in the presence of CoCl_2 in a 2/1 ratio. The resulting dark suspension in water was analysed by Transmission Electron Microscopy and Energy Dispersive Spectrometry. As shown in Figure 5, the analysed material consisted essentially of nano-sheet structures containing cobalt, as demonstrated by EDS analyses.

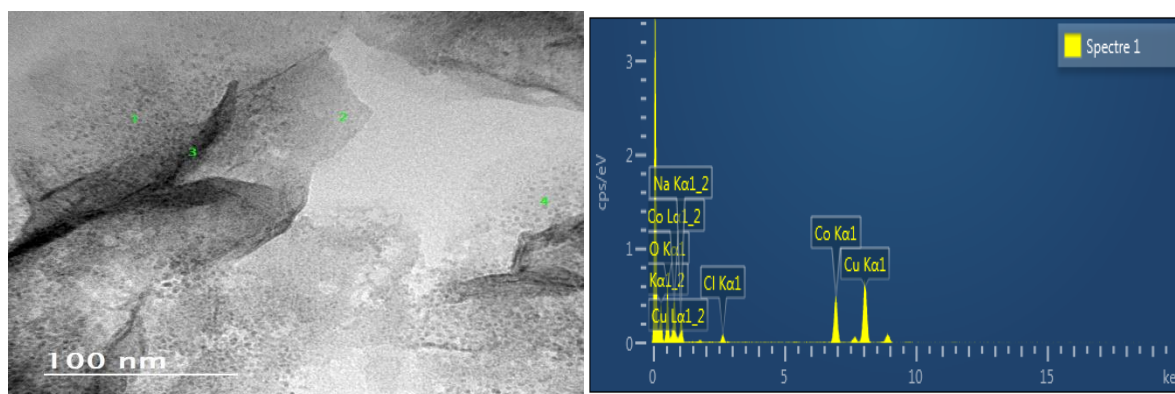


Figure 5: TEM image and EDS analysis.

Interestingly and despite the absence of any stabilizers, it was also possible to identify cobalt nanoparticles by HRTEM (Figure 6, d). We were also interested in the stability of the formed nano-sheet structures during catalysis. For this reason, a reaction mixture arising from the

hydrogenation of quinoline under standard conditions was also analysed by TEM. As displayed in Figure 7, this reaction mixture yet consisted in amorphous particles but of bigger size and it was no longer possible to identify crystalline particles. Consequently, the contribution of cobalt nanoparticles to the overall catalytic activity cannot be discarded in the first run, but other “true” heterogeneous cobalt species are also involved as evidenced by the recycling test. However, it is worth noting that cobalt nanoparticles prepared from organometallic cobalt complexes and sodium borohydride in isopropanol were inactive for the hydrogenation of quinoline.¹²⁸

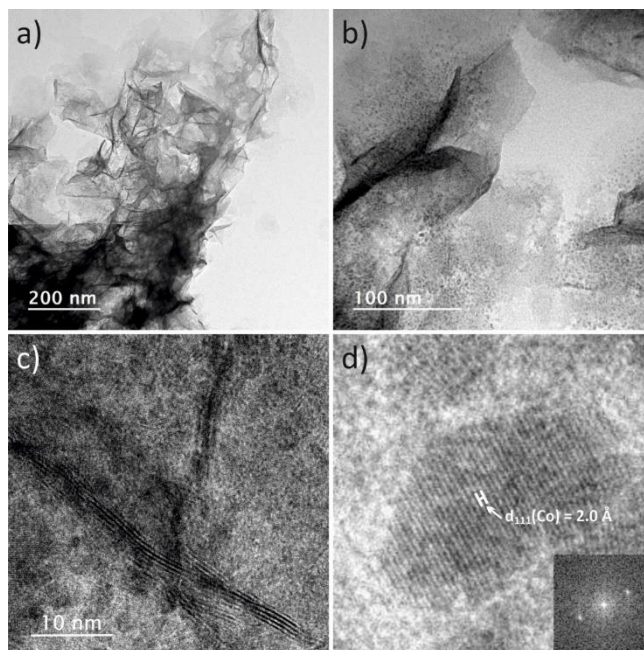


Figure 6: a, b, c: TEM images of catalytic material; d: HRTEM image of crystalline particle with corresponding Fast Fourier Transform.

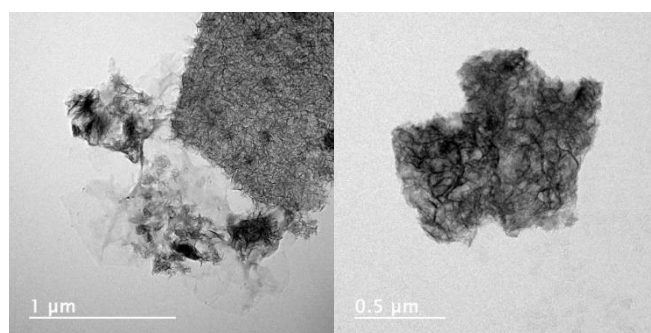
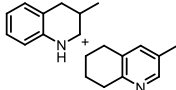
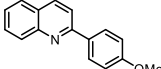
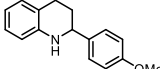
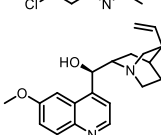
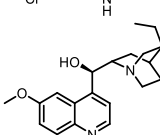
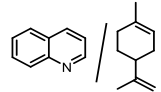
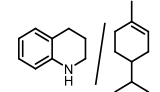
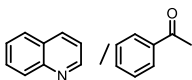
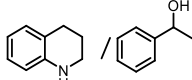
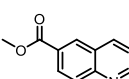
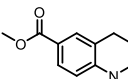


Figure 7: TEM images of particles suspended in a reaction mixture

¹²⁸ P. Puylaert, A. Dell’Acqua, F. El Ouahabi, A. Spannenberg, T. Roisnel, L. Lefort, S. Hinze, S. Tin, J. G. de Vries, *Catal. Sci. Technol.*, **2019**, *9*, 61-64.

Table 12: Scope and limitations^d

Entry	Substrate	T (°C)	Product	Conv ^b /Yield ^c (%)
	$ \begin{array}{c} \text{5 mol\% Co} \\ \text{10 mol\% NaBH}_4 \\ \xrightarrow{\hspace{1cm}} \\ \text{30 bar H}_2, \text{H}_2\text{O,} \\ \text{17 h, 130-150 }^\circ\text{C} \end{array} $			
1		130		>99 (83)
2		130		77/39 (23/4)
3 ^d		130		85 (57)
4		150		0
5		150		0
6		130		>99 (70)
7		130		>99 (81)
8		150		90 (87)
9		150		>99 (99)
10		130		>99 (97)
11		150		>99 (75)
12 ^e		150		>99 (67)
13		150		>99 (95)
14 ^d		130		>99/>99
15 ^e		150		>99 (80)
16		150		>99/98
17 ^e		150		>99 (73)
18		150		>99 (73)
19		130		>99 (62)
20		150		>99 (95)

21 ^d		130		74 (46)
22		150		>99 (84)
23		150		0
24		150		0

^a Substrate (0.5 mmol), NaBH₄ (1.90 g, 0.005 mmol), CoCl₂ (5 mol%), H₂O (1 mL), H₂, 30 bar, t = 17 h, T = oil bath temperature.
^b Conversion determined by ¹H NMR. ^c (Isolated yields). ^d (NH₄)₂Co(SO₄)₂·6H₂O (5 mol%); °40 bar H₂.

The scope and limitations of the catalyst was investigated by the hydrogenation of a broad range of substrates diversely substituted on the phenyl- or pyridyl-ring (Table 12). The substitution of the pyridyl-ring by alkyl or aryl groups led to the desired products in good yields with the exception of 3-methylquinoline where a mixture of the corresponding tetrahydroquinoline along with 3-methyl-5,6,7,8-tetrahydroquinoline was formed (Table 12, entry 2). On the contrary, quinolines substituted at the pyridyl-ring by bromine and chlorine atoms were unreactive even at a temperature of 150 °C (Table 12, entries 4-5). This disappointing result must nevertheless be modulated as such reactions have not been reported in the literature. It should also be mentioned that no dehalogenation was observed with the brominated reagents as it was reported with Pd-nanoparticules.¹²⁹ In the case of the chloro-substituted derivative dechlorination occurred to a small extent (~5 %). Nevertheless, these failures provide some hints on the reaction mechanism indicating that *N*-coordination of quinolone to the catalyst is likely necessary. Interestingly, the catalyst was found much less sensitive to the substitution pattern on the phenyl ring. Indeed, alkyl-, alkoxy- and halo-substituted products were obtained in good to high yields (Table 12, entries 6-12). The chemoselectivity of the catalyst was then investigated using either functionalized reagents or mixtures of reagents. Thus, the selective hydrogenation of quinoline derivatives in the presence of an ester group or internal carbon-carbon double bonds was demonstrated (Table 12, entries 14 and 17). However, as exemplified in entry 14, the catalyst also selectively hydrogenated a terminal carbon-carbon double bond. The selective reduction of quinolines bearing carbonyl-functionalities was investigated, as only very few catalysts for such transformations have been reported. As evidenced in entries 15-17, the formyl- and keto- group were readily hydrogenated while the ester group was not reduced *vide supra*. The scope of the reaction was further extended to other *N*-heterocyclic compounds that were all converted with high conversion leading to the desired products in good to excellent yields except for isoquinoline and 1H-benzimidazole (Table 12, entries 18-24). As explained earlier, the less toxic (NH₄)₂Co(SO₄)₂·6H₂O precursor was employed in some examples and found to be a suitable cobalt precursor, too (Table 12, entries 3, 14, 21).

III/ Conclusion

In conclusion, we have prepared catalytically active cobalt particles by hydrolysis of NaBH₄ in the presence of Co(II) salts. The catalyst consists initially of a mixture of cobalt nanoparticles

¹²⁹ Y. Zhang, J. Zhu, Y.-T. Xia, X.-T. Sun, L. Wu, *Adv. Synth. Catal.*, **2016**, 358, 3039-3045.

and cobalt-containing nanosheets and evolves to bigger cobalt particles upon reuse. The activity and chemoselectivity of this catalyst are comparable to other well-defined heterogeneous catalyst made of cobalt only. Notably, this catalyst is easily prepared from inexpensive cobalt precursors and readily accessible to synthetic chemists. Furthermore, the catalyst preparation does not need any additives and to the contrary of many heterogeneous catalysts, it is prepared and used in water hence making the overall process convenient and more environmentally friendly.

IV/ Experimental Data.

1. General information

All reagents were obtained from commercial sources and used as received. Were used as received. Toluene was dried on a MBraun Solvent Purification System apparatus and degassed prior to use. NaBH₄, 98% was purchased from Sigma-Aldrich, CoCl₂ 99% was purchased from Strem, (NH₄)₂Co(SO₄)₂·6H₂O 98% was purchased from Alfa. Distilled-deionised water was used. NMR spectra were recorded on Bruker Avance I 300 MHz or Avance III 400 MHz spectrometers. Chemical shifts are given in ppm and referenced vs TMS using the residual solvent signal.

2. General procedure for the catalytic hydrogenation of quinoline

A high-pressure reactor was charged sequentially with CoCl₂ (5 mol%), Sodium borohydride (10 mol%), 1 mL of H₂O and quinoline (100 mg, 0.78 mmol). The reactor was then charged with H₂ (30 bar) and stirred at the appropriate temperature (oil bath) for 17 h. The reactor was cooled down to r.t. and carefully depressurized. The reaction mixture was extracted three times with ethyl-acetate and the grouped organic fraction dried with sodium sulfate and the solvent evaporated under vacuum. The crude product was analyzed by ¹H NMR. This crude product was then purified by flash column chromatography on silica gel using a mixture of heptane and ethyl acetate as the eluent.

3. Recycling test

After 17h, the reactor was slowly depressurized. The reaction medium was washed 3 times with ethyl acetate and the organic phase was analyzed by ¹H NMR. The reaction medium was loaded with quinoline, NaBH₄ and 30 bar of hydrogen. After 17 h at 130 °C, the reaction media was analyzed by ¹H NMR showing complete disappearance of quinoline.

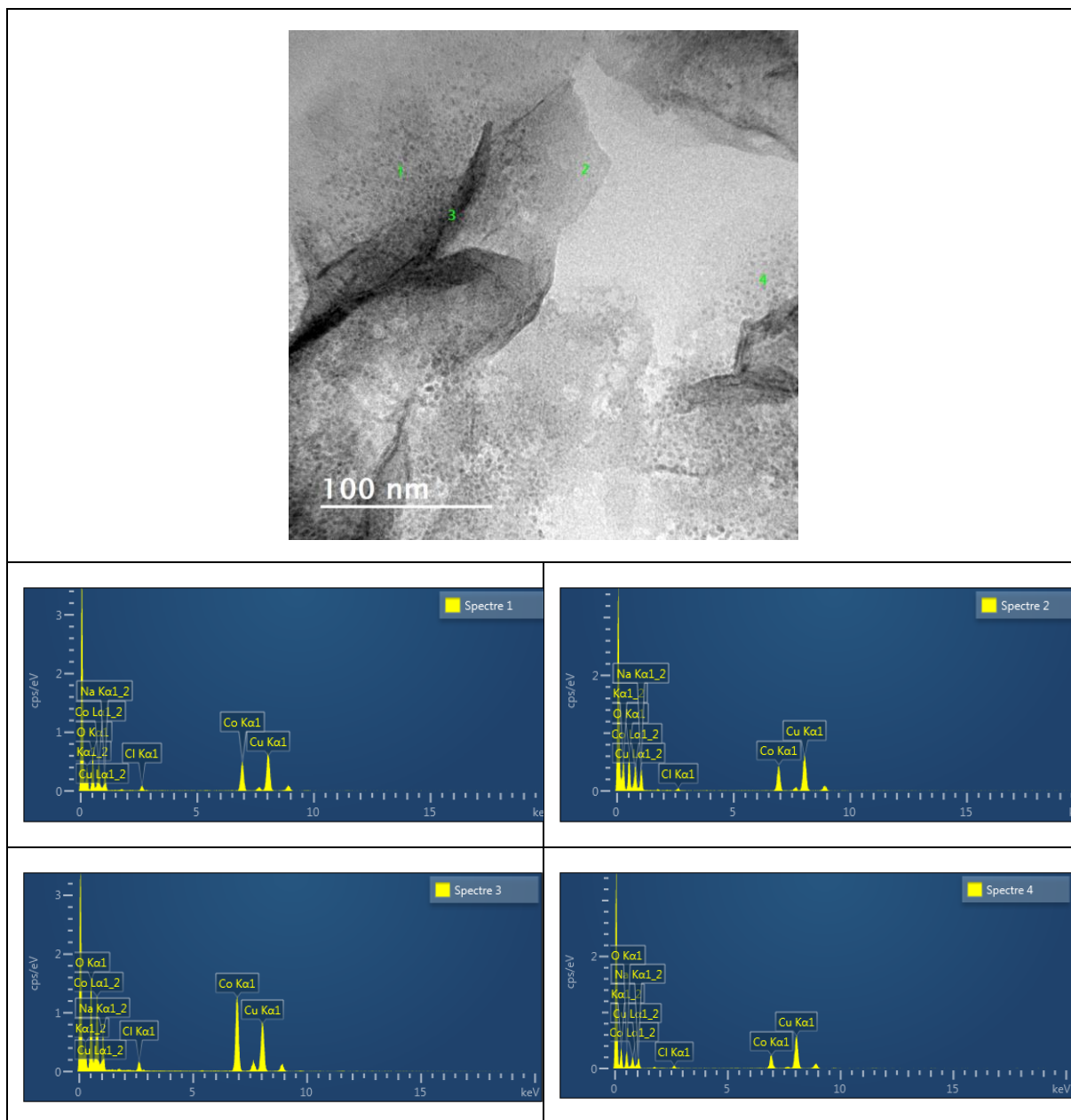
4. Scale-up reaction.

The reaction was conducted in a Hastelloy-C 100 mL Parr autoclave using 2 g (15.5 mmol) of quinoline, 100.4 mg (5 mol%) of CoCl₂ and 58.2 mg (10 mol%) of NaBH₄ and 20 mL of water. The analysis protocol was the one adopted for 0.5 mmol scale reactions. ¹H NMR showed full conversion of quinolone with selective formation of 1,2,3,4,-tetrahydroquinoline

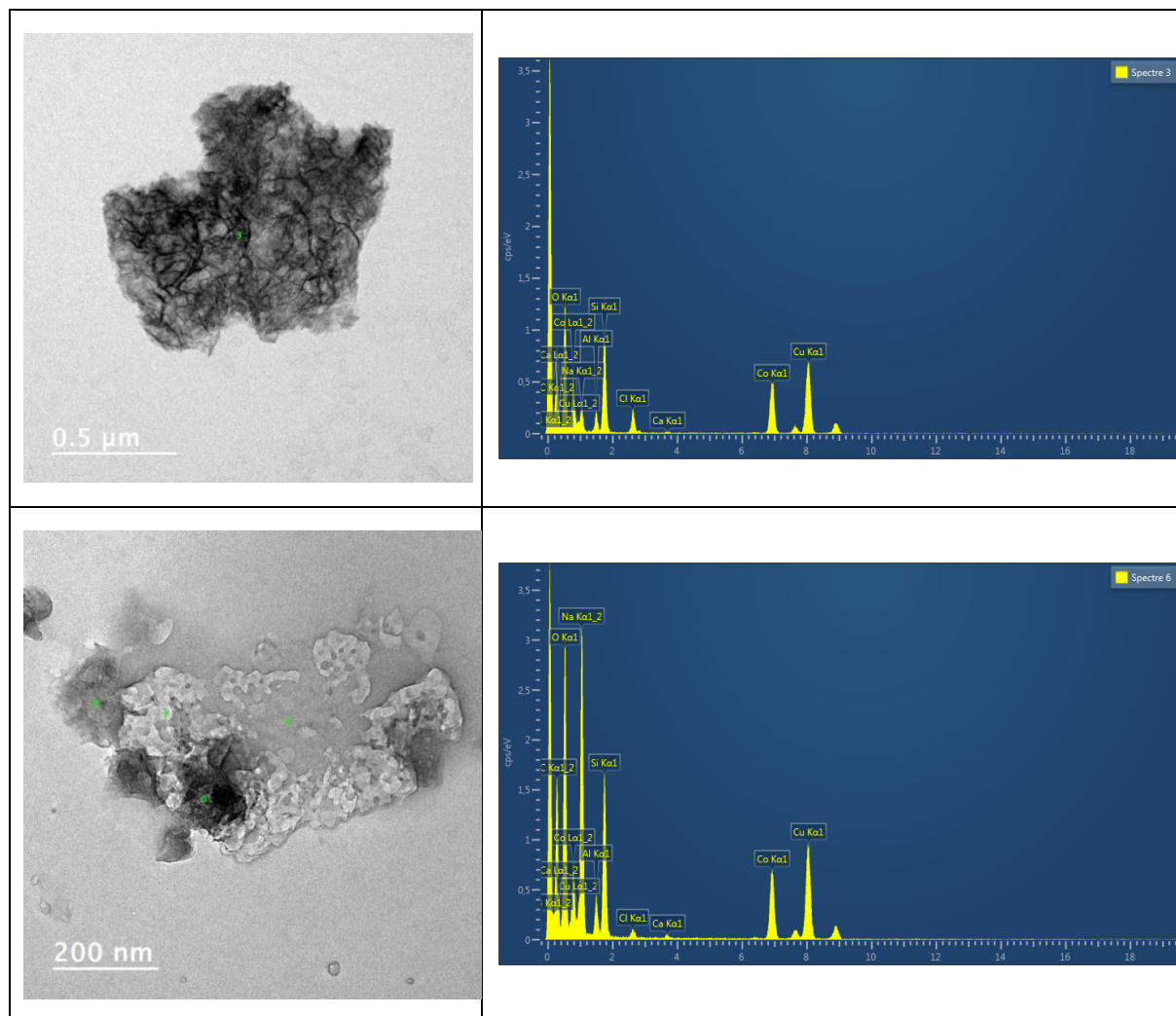
5. TEM/EDS Analyses

2 samples were analyzed by TEM/EDS (JEOL 2100 LAB6 operating at 200 kV coupled with an energy-dispersive X-ray spectroscopy detector SDD X-Oxford 80 mm²).

A first sample was prepared by hydrolysis of NaBH₄ in the presence of CoCl₂ in a 2/1 ratio. After decantation of the reaction media, drops of the supernatant were deposited onto holey carbon grids. Representative TEM pictures and EDS analyses are presented hereafter.

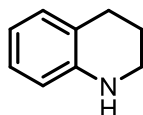


A second sample was analyzed after a catalytic run as described in the general method. Representative TEM pictures and EDS analyses are presented hereafter.



6. Product characterization

1,2,3,4-tetrahydroquinoline



Colorless oil, 100% conversion, 99% yield.

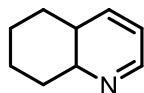
NMR data were consistent with reported data¹³⁰

¹³⁰ Y. Zhang, J. Zhu, Y.-T. Xia, X.-T. Sun, L. Wu, *Adv. Synth. Catal.* **2016**, *358*, 3039-3045.

^1H NMR (400 MHz, CDCl_3): δ = 6.97 (t, J = 8.5 Hz, 2H), 6.62 (t, J = 7.2 Hz, 1H), 6.48 (d, J = 7.8 Hz, 1H), 3.69 (bs, 1H), 3.31 (t, J = 6.4 Hz, 2H), 2.78 (t, J = 6.4 Hz, 2H), 1.96 (m, 2H).

^{13}C NMR (101 MHz, CDCl_3): δ = 144.8, 129.5, 126.7, 121.5, 117.0, 114.2, 42.0, 27.0, 22.2.

5,6,7,8-tetrahydroquinoline



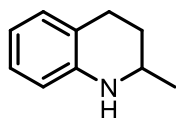
Colorless oil

NMR data were consistent with reported data¹³¹

^1H NMR (400 MHz, CDCl_3): δ = 8.32 (dd, J = 5.0, 1.0 Hz, 1H), 7.32 (d, J = 8.0 Hz, 1H), 6.99 (m, 1H), 2.91 (t, J = 8.0 Hz, 2H), 2.75 (t, J = 8.0 Hz, 2H), 1.85-1.78 (m, 2H), 1.76-1.69 (m, 2H);

^{13}C NMR (CDCl_3 , 101 MHz) δ 158.6, 147.4, 138.9, 132.8, 122.1, 33.5, 30.03, 23.2, 22.7.

2-methyl-1,2,3,4-tetrahydroquinoline

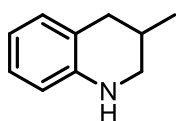


Colorless oil, 100% conversion, 83% yield.

NMR data were consistent with reported data¹³⁰

^1H NMR (400 MHz, CDCl_3): δ = 6.97 (m, 2H), 6.62 (t, J = 7.3 Hz, 1H), 6.48 (d, J = 8.3 Hz, 1H), 3.70 (bs, 1H), 3.45 – 3.38 (m, 1H), 2.91-2.81 (m, 1H), 2.77 – 2.71 (m, 1H), 1.99-1.91 (m, 1H), 1.67-1.56 (m, 1H), 1.23 (d, J = 6.8 Hz, 3H). ^{13}C NMR (101 MHz, CDCl_3): δ = 144.9, 129.4, 126.8, 121.2, 117.1, 114.1, 47.3, 30.3, 26.7, 22.8.

3-methyl-1,2,3,4-tetrahydroquinoline



Colorless oil, 77% conversion, 23% yield.

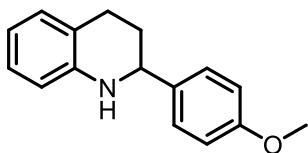
NMR data were consistent with reported data¹³⁰

^1H NMR (400 MHz, CDCl_3): δ = 6.95 (m, 2H), 6.61 (t, J = 8.1 Hz, 1H), 6.49 (d, J = 7.3 Hz, 1H), 3.84 (bs, 1H), 3.28 (ddd, J = 9.3, 3.7, 1.9 Hz, 1H), 2.90 (t, J = 9.8 Hz, 1H), 2.78 (m, 1H), 2.44 (m, 1H), 2.11 – 2.03 (m, 1H), 1.05 (d, J = 6.7 Hz, 3H).

¹³¹ D. Forberg, T. Schwob, R. Kempe, *Nature Commun.*, **2018**, 9, 1751-1758.

^{13}C NMR (101 MHz, CDCl_3): $\delta = 144.3, 129.5, 126.7, 121.1, 116.9, 113.9, 48.9, 35.5, 27.3, 19.0$.

2-(4-methoxyphenyl)-1,2,3,4-tetrahydroquinoline



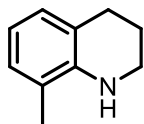
yellow solid, 85% conversion, 57% yield.

NMR data were consistent with reported data¹³²

^1H NMR (400 MHz, CDCl_3) δ 7.31 (d, $J = 8.6$ Hz, 2H), 7.01 (m, 2H), 6.89 (d, $J = 8.6$ Hz, 2H), 6.64 (t, $J = 8.6$ Hz, 1H), 6.53 (d, $J = 8.6$ Hz, 1H), 4.38 (dd, $J = 9.5, 3.2$ Hz, 1H), 3.97 (bs, 1H), 3.81 (s, 3H), 2.93 (ddd, $J = 16.4, 10.9, 5.5$ Hz, 1H), 2.74 (dt, $J = 16.3, 4.7$ Hz, 1H), 2.12-2.05 (m, 1H), 2.01-1.91 (m, 1H).

^{13}C NMR (101 MHz, CDCl_3) δ 150.3, 144.6, 136.2, 129.7, 128.1, 127.3, 117.6, 114.5, 114.4, 56.20, 55.8, 37.8, 31.6, 27.0.

8-methyl-1,2,3,4-tetrahydroquinoline



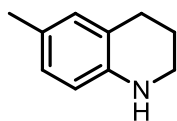
yellow oil, 100% conversion, 70% yield,

NMR data were consistent with reported data¹³⁰

^1H NMR (400 MHz, CDCl_3): $\delta = 6.89 - 6.84$ (m, 2H), 6.55 (t, $J = 7.4$ Hz, 1H), 3.65 (br, 1H), 3.38 (t, $J = 5.3$ Hz, 2H), 2.79 (t, $J = 6.6$ Hz, 2H), 2.08 (s, 3H), 1.97 - 1.91 (m, 2H). ^{13}C NMR (101 MHz, CDCl_3): $\delta = 142.8, 128.0, 127.5, 121.3, 120.1, 116.5, 42.5, 27.4, 22.3, 17.3$.

NMR data were consistent with reported data²⁷

6-methyl-1,2,3,4-tetrahydroquinoline



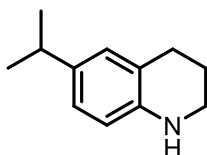
yellow oil, 100% conversion, 81% yield,

¹³² D. Pi, H. Zhou, P. Cui, R. He, Y. Sui, *ChemistrySelect*. **2017**, 2, 3976-3979.

NMR data were consistent with reported data¹³³

¹H NMR (400 MHz, CDCl₃) δ 6.82 (m, 2H), 6.44 (m, 1H), 3.55 (bs, 1H), 3.30 (m, 2H), 2.77 (t, J=6,3 Hz, 2H), 2.25 (s, 3H), 1.97 (m, 2H); ¹³C NMR (101 MHz, CDCl₃) δ 142.5, 130.2, 127.3, 126.3, 121.7, 114.0, 42.3, 27.0, 25.5, 20.5.

6-Isopropyl-1,2,3,4-tetrahydroquinoline

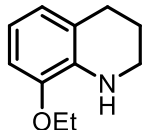


yellow oil, 90% conversion, 87% yield

NMR data were consistent with reported data¹³⁴

¹H NMR (300 MHz, CDCl₃): δ (ppm): 6.91 (m, 2H), 6.49 (d, J = 8.2 Hz, 1H), 3.68 (br, 1H), 3.32 (t, J = 5,5 Hz, 2H), 2.78-2.87z (m, 3H), 1.96-2.03 (m, 2H), 1.27 (d, J = 6.9 Hz, 6H); ¹³C NMR (75 MHz, CDCl₃): δ (ppm): 144.1, 139.0, 127.9, 125.8, 121.8, 114.9, 44.9, 36.2, 27.5, 24.8, 22.9.

8-Ethoxy-1,2,3,4-tetrahydroquinoline

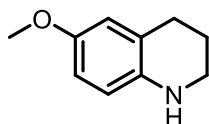


yellow oil, 100% conversion, 99% yield,

NMR data were consistent with reported data¹³⁵

¹H NMR (300 MHz, CDCl₃): δ (ppm): 6.59 – 6.63 (m, 3H), 4.05 (q, J = 7.0 Hz, 2H), 3.36 (m, 2H), 2.80 (t, J = 6.4 Hz, 2H), 1.99 (m, 2H), 1.44 (t, J = 7.0 Hz, 3H); ¹³C NMR (75 MHz, CDCl₃): δ (ppm): 145.7, 134.7, 121.7, 121.5, 115.8, 108.4, 63.7, 41.6, 26.9, 22.3, 15.2.

6-methoxy-1,2,3,4-tetrahydroquinoline



¹³³ J. Zhang, Z. An, Y. Zhu, X. Shu, H. Song, Y. Jiang, W. Wang, X. Xiang, L. Xu, J. He, *ACS Catal.*, **2019**, 9, 12, 11438-11446

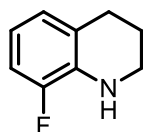
¹³⁴ B. Sahoo, C. Kreyenschulte, G. Agostini, H. Lund, S. Bachmann, M. Scalone, K. Junge, M. Beller, *Chem. Sci.*, **2018**, 9, 8134-8141.

yellow oil, 100% conversion, 97% yield,

NMR data were consistent with reported data¹³⁴

¹H NMR (400.13 MHz, CDCl₃): δ 6.61 (m, 2H), 6.47 (d, J= 8.4 Hz, 1H), 3.74 (s, 1H), 3.58 (bs, 1H), 3.26 (m, 2H), 2.77 (t, J= 6,6 Hz, 2H), 1.99 (m, 2H); ¹³C NMR (125.77 MHz, CDCl₃): δ 151.9, 138.8, 123.0, 115.7, 114.9, 113.0, 53.9, 42.4, 27.2, 22.5.

8-fluoro-1,2,3,4-tetrahydroquinoline

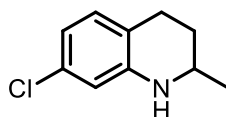


yellow oil, 100% conversion, 75% yield,

NMR data were consistent with reported data¹³⁵

¹H NMR (400.13 MHz, CDCl₃): δ 6.84-6.77 (m, 2H), 6.55 (m, 2H), 3.97 (br, 1H), 3.37 (t, J= 6,4 Hz, 2H), 2.82 (t, J= 6,4 Hz, 2H), 1.99 (m, 2H); ¹³C NMR (101 MHz, CDCl₃): δ 151.0 (d, J= 238 Hz), 133.3 (d, J= 11.9 Hz), 124.6 (d, J= 2.6 Hz), 123.7 (d, J= 3.9 Hz), 115.6 (d, J= 7,2 Hz), 112.20 (d, J= 18.4 Hz), 41.3, 26.6, 21.9.

7-Chloro-2-methyl-1,2,3,4-tetrahydroquinoline

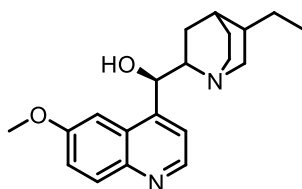


Colorless liquid, 100% conversion, 68% yield,

NMR data were consistent with reported data¹³⁵

¹H NMR (300 MHz, CDCl₃): δ (ppm) 6.86 (d, J = 8.0 Hz, 1H), 6.56 (dd, J = 8.0, 2.1 Hz, 1H), 6.44 (d, J = 2.1 Hz, 1H), 3.38 (dtd, J = 12.6, 6.3, 3.0 Hz, 1H), 2.88–2.52 (m, 2H), 1.93 (dddd, J = 12.9, 5.4, 3.9, 3.0 Hz, 1H), 1.56 (dddd, J = 12.9, 11.0, 9.7, 5.7 Hz, 1H), 1.21 (d, J = 6.3 Hz, 3H). ¹³C NMR (75 MHz, CDCl₃): δ (ppm) 145.7, 131.9, 130.2, 119.3, 116.6, 113.3, 47.0, 29.8, 26.1, 22.5.

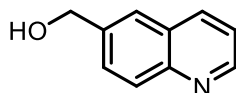
¹³⁵ B. Vilhanova, J. A. Van Bokoven, M. Ranocchiari, *Adv. Synth. Catal.* **2017**, 359, 677–686.

Hydroquinine

White solid, 100% conversion 95% yield

NMR data were consistent with reported data¹³⁶

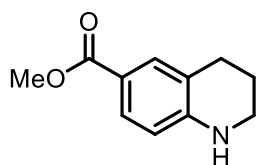
¹H NMR (400 MHz, CDCl₃) δ: 8.57(1H, d, J = 4.5 Hz), 7.95 (1H, d, J = 9.2 Hz), 7.48 (1H, d, 4.6 Hz), 7.29(m, 2H), 5.49 (1H, d, J = 4.0 Hz), 4.32(br, 1H), 3.92 (3H, s), 3.47-3.39 (1H, m), 3.13-3.00 (2H, m), 2.70-2.57 (1H, m), 2.40-2.33 (1H, m), 1.78-1.68 (3H, m), 1.52-1.37 (3H, m), 1.30-1.19 (2H, m), 0.81 (3H, t, J = 7.3 Hz); ¹³C NMR (101 MHz, CDCl₃) δ: 157.7, 148.0, 147.5, 144.2, 131.5, 126.7, 121.4, 118.5, 101.5, 72.18, 59.8, 58.7, 55.7, 43.3, 37.6, 28.4, 27.7, 25.5, 21.6, 12.10.

6-(Hydroxymethyl)quinoline

Yellow oil, 100% conversion 80% yield

NMR data were consistent with reported data¹³⁷

¹H NMR (400 MHz, CDCl₃) δ 8.89-8.87(dd, J= 4.5, 2.0 Hz, 1H), 8.16-8.07 (m, 2H), 7.81 (s, 1H), 7.70 (dd, J= 8.6, 2.0 Hz, 1H), 7.42-7.38 (dd, J= 8.2, 4.5 Hz, 1H); 4.91 (s, 2H), ¹³C NMR (101 MHz, CDCl₃) δ 150.3, 147.8, 138.4, 136.1, 129.7, 128.7, 128.0, 125.0, 121.4, 64.9.

methyl 1,2,3,4-tetrahydroquinoline-6-carboxylate

¹³⁶ C. Palacio, S. Connon, *Org. Lett.*, **2011**, *13*, 6, 1298-1301.

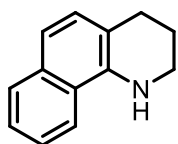
¹³⁷ N.Muria, M. Yonaga, K. Tanaka, *Org. Lett.* **2012**, *14*, 5, 1278-1281.

Colorless liquid, 100% conversion, 92% yield

NMR data were consistent with reported data¹³⁵

¹H NMR (300 MHz, CDCl₃) δ 7.66 – 7.62 (m, 2H), 6.40 – 6.37 (m, 1H), 3.08 (s, 3H), 3.35 (m, 2H), 2.76 (t, *J* = 6.0 Hz, 2H), 1.97 – 1.83 (m, 2H). ¹³C NMR (75 MHz, CDCl₃) δ 167.5, 149.8, 131.3, 129.1, 119.9, 117.5, 112.6, 51.5, 41.7, 26.9, 24.4.

1,2,3,4-tetrahydrobenzo[h]quinoline



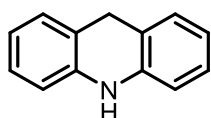
Yellow oil, 100% conversion, 73% yield.

NMR data were consistent with reported data¹³⁸

¹H NMR (400 MHz, CDCl₃) δ 7.80-7.69 (m, 2H), 7.46-7.40 (m, 2H), 7.24-7.15 (m, 2H), 4.27 (br, 1H), 3.50 (t, *J* = 5.6 Hz, 2H), 2.95 (t, *J* = 5.6 Hz, 2H), 2.11-2.03 (m, 2H).

¹³C NMR (101 MHz, CDCl₃) δ 139.1, 133.1, 129.9, 128.6, 125.0, 124.8, 123.3, 119.9, 117.0, 115.9, 43.4, 26.1, 22.2.

9,10-Dihydroacridine



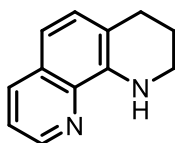
White solid, 100% conversion, 62% yield.

NMR data were consistent with reported data¹³⁷

¹H NMR (400 MHz, CDCl₃) δ 7.11-7.06 (m, 4H), 6.85 (m, 2H), 6.67 (dd, *J* = 7.9, 0.8 Hz, 2H), 5.95 (br, 1H), 4.06 (s, 2H).

¹³C NMR (101 MHz, CDCl₃) δ 140.3, 128.7, 127.1, 120.8, 120.2, 113.6, 31.5.

1-2,3,4-Tetrahydro-1,10-phenanthroline



¹³⁸ F. Ding, Y. Zhang, R. Zhao, Y. Jiang, R. L.-Y. Bao, K. Lin, L. Shi, *Chem. Commun.* **2017**, 53, 9262-9264.

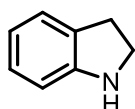
Yellow oil, 100% conversion, 95% yield.

NMR data were consistent with reported data¹³⁷

¹H NMR (400 MHz, CDCl₃) δ 8.68 (dd, J = 4.12, 1.53 Hz, 1H), 8.00 (dd, J = 8.30, 1.74 Hz, 1H), 7.30-7.27 (m, 1H), 7.16 (d, J = 8.3 Hz, 1H), 6.97 (d, J = 8.24 Hz, 1H), 5.97 (br, 1H), 3.53 (t, J = 5.36 Hz, 2H), 2.92 (t, J = 6.32 Hz, 2H), 2.10-2.04 (m, 2H);

¹³C NMR (101 MHz, CDCl₃) δ 147.1, 140.8, 137.6, 136.0, 129.2, 127.5, 120.7, 116.7, 113.2, 41.4, 27.2, 22.0.

Indolin

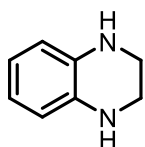


yellow oil, 100% conversion, 81% yield,

NMR data were consistent with reported data¹³⁷

¹H NMR (400 MHz, CDCl₃) δ 7.12 (d, J= 7.2 Hz, 1H), 7.02 (t, J=7.5, 1H), 6.71 (t, J= 7.5, 1H), 6.78-6.76 (d, J=7.5 Hz, 1H), 3.75 (br, 1H), 3.55 (t, J= 8.4 Hz, 2H), 3.04 (t, J= 8.4 Hz, 2H); ¹³C NMR (101 MHz, CDCl₃) δ 151.7, 129.4, 127.3, 124.7, 118.7, 109.5, 47.5, 15.72.

1,2,3,4-Tetrahydroquinoxaline



yellow liquid, 100% conversion, 84% yield,

NMR data were consistent with reported data¹³⁷

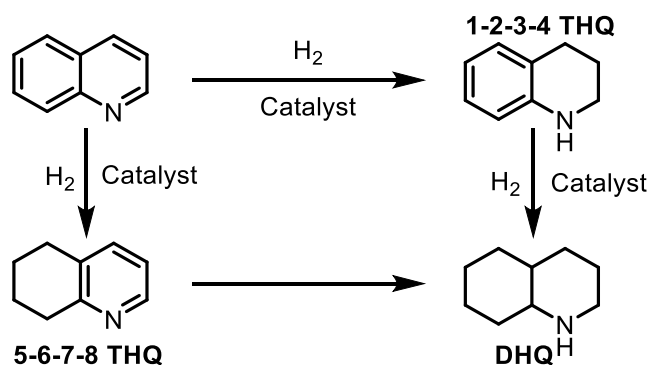
¹H NMR (400 MHz, CDCl₃): δ(ppm): 6.60-6.56 (m, 2H), 6.52-6.48 (m, 2H), 3.42 (s, 4H); ¹³C NMR (101 MHz, CDCl₃) δ (ppm): 133.8, 118.9, 114.9, 41.5.

Chapter 3: Stereoselective hydrogenation of *N*- Heterocycles over heterogeneous ruthenium

I/ Switchable diastereoselective quinoline hydrogenation to decahydroquinoline over Ru/C

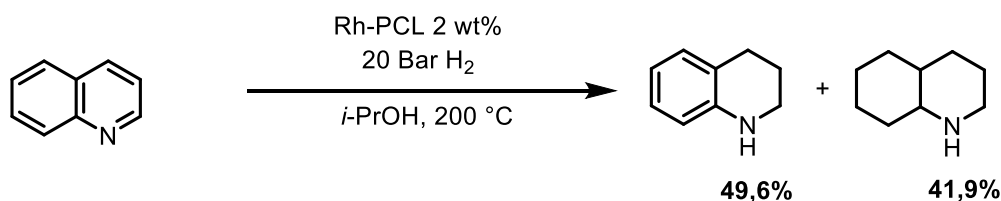
I/Introduction.

In the previous chapter, we described studies for the hydrogenation of quinoline. As shown above many works have been done on this topic applying homogeneous or heterogeneous catalysts based on noble and non-noble metals. Compared to the partial hydrogenation, the complete hydrogenation of quinoline to decahydroquinoline (DHQ) is a more challenging reaction. The decahydroskeleton is widely used in the synthesis of chemicals¹³⁹ and pharmaceuticals.¹⁴⁰ In general, this hydrogenation is performed in two steps¹⁴¹ (Scheme 1). For one possible pathway first the hydrogenation of quinoline to 1,2,3,4-THQ is discussed, followed by the reduction to DHQ. In a second pathway, 5,6,7,8-THQ is preferably generated, which is then hydrogenated to DHQ.



Scheme 1: Possible pathways for the hydrogenation of quinoline.

In 2002, Campanati and *al.*¹⁴², reported for this transformation a highly dispersed Rh catalyst by ion-exchange of PLCs. It was possible to obtain a good yield for the fully hydrogenated quinoline DHQ at 200 °C, 20 bar of hydrogen and with 2 wt% of catalyst (Scheme 2).



Scheme 2: Quinoline hydrogenation over Rh-PLC.

In 2010, Li and co-workers,¹⁴³ completed the hydrogenation of quinoline to DHQ using a Ru/HAP catalyst system. The reaction was carried out at 150 °C, 50 bar hydrogen, with

¹³⁹ G. Perot, *Catalysis Today*, **1991**, 10, 4, 447-472.

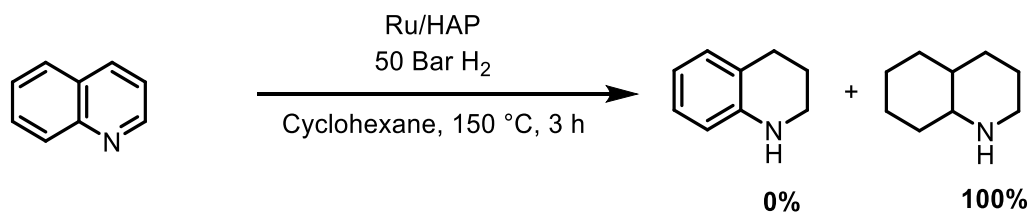
¹⁴⁰ P. Bouyssou, C. Le Goff, J. Chenault, *Journal of Heterocyclic Chemistry*, **1992**, 29, 4, 895-898.

¹⁴¹ M. Campanati, S. Franceschini, O. Piccolo, A. Vaccari, *Catalysis of Organic Reactions*, **2005**, 101-110.

¹⁴² M. Campanati, M. Casagrande, I. Fagiolino, M. Lenarda, L. Storaro, M. Battagliarin, A. Vaccari, *Journal of Molecular Catalysis A: Chemical*, **2002**, 184, 1-2, 267-272.

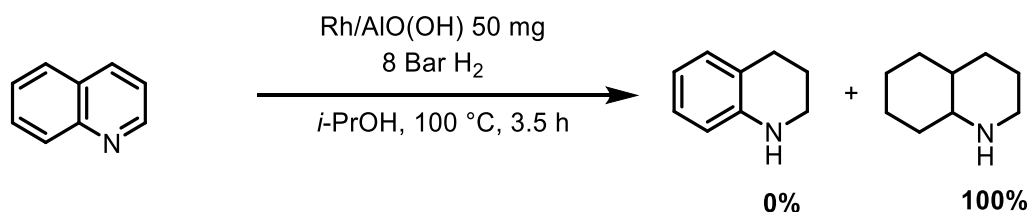
¹⁴³ Y. P. Sun, H. Y. Fu, D. L. Zhang, R. X. Li, H. Chen, X. J. Li, *Catal. Commun.*, **2010**, 12, 188-192

cyclohexane as a solvent in 3 h. The hydrogenation result was attributed to the existence of hydroxyl groups on the surface (Scheme 3).



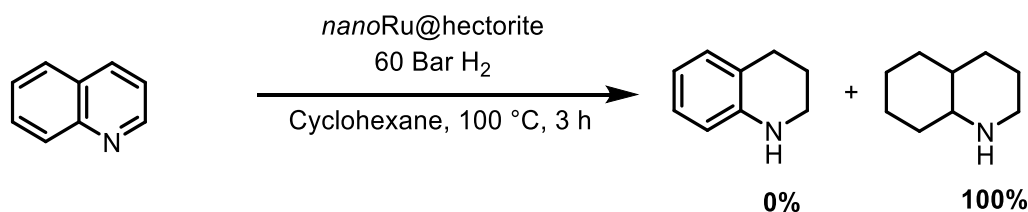
Scheme 3: Quinoline hydrogenation over Ru/HAP.

Later Fan and *al.*¹⁴⁴ developed the complete hydrogenation of quinoline over a Rh/AIO(OH) catalyst at 100 °C, 8 bar of hydrogen, *i*-PrOH as a solvent during 3.5 hours. The catalyst showed excellent catalytic properties for the hydrogenation of quinoline to DHQ, which was ascribed to the formation of a hydrogen bond between the surface hydroxyl group on AIO(OH) and the aromatic compound. (Scheme 4)



Scheme 4: Quinoline hydrogenation over Rh/AIO(OH).

The same year, Süß-Fink,¹⁴⁵ reported a nano-Ru@hectorite catalyst providing a mild and effective method for the catalytic hydrogenation of quinoline with switchable selectivity between py-THQ (>99%) in water and DHQ (>99%) in cyclohexane. The more challenging product DHQ was obtained at 100 °C, 60 bar of hydrogen and 3 h (Scheme 5).



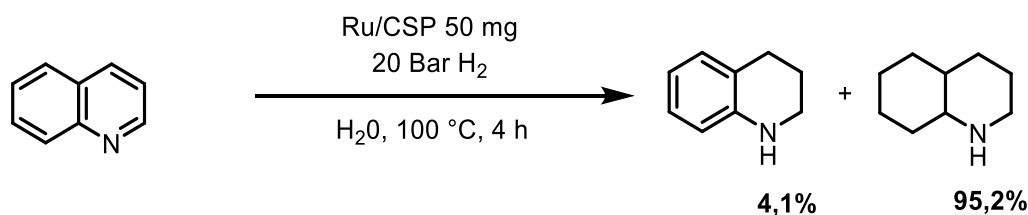
Scheme 5: Quinoline hydrogenation over nanoRu@hectorite.

A year later, Li¹⁴⁶ proposed a highly active and selective hydrogenation of quinoline to decahydroquinoline in water under mild conditions by using ruthenium nanoparticles supported on glucose-derived carbon spheres (Scheme 6). These results are attributed to hydrogen bonding between quinoline and hydroxyl groups of the support as well as to the π - π stacking interaction between quinoline and the aromatic system of the carbon support.

¹⁴⁴ G. Y. Fan, J. Wu, *Catal. Commun.*, **2013**, *13*, 81-85.

¹⁴⁵ B. Sun, F. A. Khan, A. Vallat, G. Süß-Fink, *Appl. Catal. A*, **2013**, *467*, 310-314.

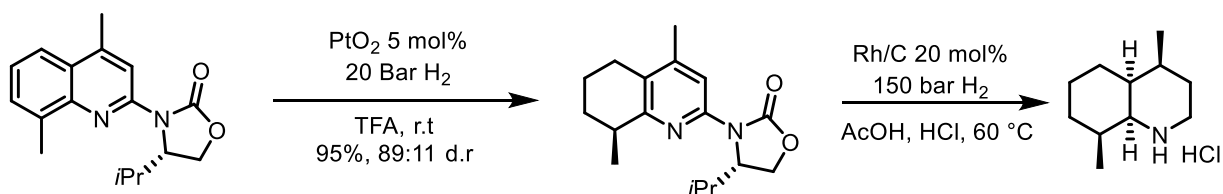
¹⁴⁶ D. Zhu, H. Jiang, L. Zhang, X. Zheng, H. Fu, M. Yuan, H. Chen, R. Li. *ChemCatChem.*, **2014**, *6*, 2954-2960.



Scheme 6: Quinoline hydrogenation over Ru/CSP.

Enantiomerically pure saturated heterocycles are important building blocks and fragments of many biologically active compounds.¹⁴⁷ The asymmetric hydrogenation of heteroaromatic substrates presents an attractive strategy for their preparation and the last years have seen many significant contributions to this field.¹⁴⁸ However, despite these advances in asymmetric hydrogenation of (hetero)aromatics, many challenges remain. Thus, the stereoselective hydrogenation of quinolines to decahydroquinolines with high diastereoselectivity has not been described to the best of our knowledge.

In 2010, Glorius¹⁴⁹ described the stereoselective hydrogenation of auxiliary-substituted quinolines. They elegantly disclosed the first strategy for the stereoselective formation of chiral 5,6,7,8-tetrahydro- and decahydroquinolines with newly formed stereocenters in the cyclohexane ring (Scheme 7).



Scheme 7: Diastereoselective dearomative hydrogenation using oxazolidinone as a chiral auxiliary.

To this end, exposure of 2-oxazolidinone-substituted quinoline to Adam's catalyst in trifluoroacetic acid delivered the reduced product with 95% yield and 89: 11 d.r. Further hydrogenation of 5,6,7,8-THQ with Rh/C and increased hydrogen pressure of 150 bar, resulted in complete reduction as well as removal of the oxazolidinone, furnishing decahydroquinoline in 99% yield and 97: 3 d.r.

Complementary to that work, here we describe the direct diastereoselective hydrogenation of quinoline to DHQ derivatives under mild conditions. Interestingly, the selectivity can be switched by the temperature with a commercially available Ru/C.

¹⁴⁷ T. Shigeyama, K. Katakawa, N. Kogure, M. Kitajima, H. Takayama, *Org. Lett.*, **2007**, 9, 20, 4069-4072.

¹⁴⁸ a) P. Kukula, R. Prins, *Top. Catal.*, **2003**, 25, 29-42; b) M. Besson, C. Pinel, *Top. Catal.*, **2003**, 25, 43-61 c) D. S. Wang, Q. A. Chen, S. M. Lu, and Y. G. Zhou, *Chem. Rev.*, **2012**, 112, 2557-2590.

¹⁴⁹ M. Heitbaum, R. Fröchlich, F. Glorius, *Adv. Synth.*, **2010**, 352, 357-362

II/Results and discussions.

The catalytic materials were prepared adapting a protocol from us reported for other catalysts of this class.¹⁵⁰ Initially, a chelate between RuCl₃·xH₂O and 1,10-phenanthroline, chitin or chitosan was *in-situ* generated. In some cases, carbon was added as support and the heterogeneous mixture stirred in ethanol for 24 h. Afterwards, the solvent was removed and the obtained solids were pyrolyzed at 800 °C (temperature ramp 25 °C·min⁻¹) under an Ar atmosphere for 2 h. The resulting materials possess a ruthenium content of around 2,5 %wt. Applying this protocol, 5 different materials were prepared. Their catalytic activity was evaluated using quinoline **1** as model substrate and 20 mg of catalyst loading, 30 bars of hydrogen at 130 °C and a mixture (1/1) *t*-amylalcohol/water as a solvent.

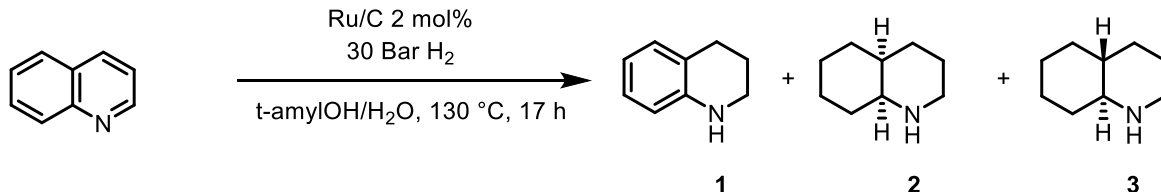
Table 1: Catalyst Screening^a

Entry	Catalyst	Conversion ^b (%)	Yield THQ ^b (1)	Yield DHQ ^b (2 and 3)	Selectivity ^c (2:3)
1	Ru/C 5wt%	100	0	100%	37:63 d.r
2	Ru/Phen(1/10)@C	87	67%	0	0
3	Ru/Phen(1/2)@C	100	100%	0	0
4	Ru/Chitin	100	72%	0	0
5	Ru/Chitosan	0	0	0	0

Reaction conditions: ^aQuinoline (64,8 mg, 0.5 mmol), catalyst (20 mg), *t*-amylOH/H₂O (1/1 mL), H₂ (30 bar), 130 °C, 17 h. ^bConversion and yield determined by GC using hexadecane as internal standard. ^cd.r. determined by GC.

As shown in Table 1, the ruthenium/chitosan system was not able to perform the desired reaction (Table 1, entry 5). The three other catalysts are capable to hydrogenate quinoline but give 1,2,3,4-THQ as the main product (Table 1, entries 2-4). Surprisingly, only the commercially available Ru/C formed the fully hydrogenated product DHQ. Indeed, in the presence of this system we obtained quantitative conversion of quinoline to DHQ with a diastereoselectivity for the *trans* isomer of 37:63. With this results in hand, we decided to perform the reaction with Ru/C from different suppliers.

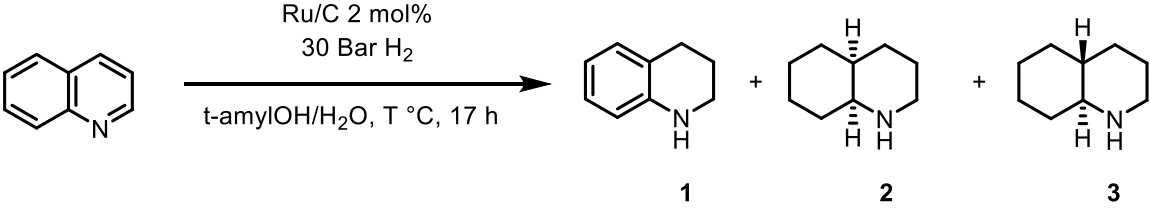
¹⁵⁰ R. V. Jagadeesh, T. Stemmler, A.-E. Surkus, M. Bauer, M.-M. Pohl, J. Radnik, K. Junge, H. Junge, A. Brückner, M. Beller, *Nat. Protocols*, **2015**, *10*, 916-926.

Table 2: Hydrogenation of quinoline: Screening of different Ru/C catalysts^a


Entry	Catalyst	Conversion (%)	Yield THQ ^b (1)	Yield DHQ ^b (2 and 3)	Selectivity ^c (2:3)
1	Ru/C 5% Alfa	100	0	100	37:63 d.r
2	Ru/C 5% Strem (Evonik P3060)	100	0	100	84:16 d.r
3	Ru/C 5% Strem Escat 44101	100	0	100	86:14 d.r
4	Ru/C 5% Strem	100	0	100	38:62 d.r
5	Ru/Al ₂ O ₃ 5% Alfa	100	0	100	84:16 d.r
6	Ru/C 5% Evonik P3059 Sigma	100	0	100	60:40 d.r
7	Ru/C 5% TCI	100	0	100	83:17 d.r
8	Ru/C 5% Sigma	100	0	100	38:62 d.r

Reaction conditions: ^aQuinoline (64.8 mg, 0.5 mmol), Ru/C (20 mg), t-amylOH/H₂O (1/1 mL), H₂ (30 bar), 130 °C, 17h. ^bConversion and yield determined by GC using hexadecane as internal standard. ^cd.r. determined by GC.

As summarized in Table 2, different Ru/C samples were purchased from Sigma, Strem, TCI and Alfa Aesar. For the first screening, we tested a catalyst from Alfa Aesar (Table 2, entry 1). Surprisingly, we obtained different results depending on the source of the catalyst purchased. At 130 °C, all catalysts allowed for complete conversion to DHQ, but the reaction performed with different selectivity. Two catalysts from Strem (Table 2, entries 2-3) and a catalyst from TCI (Table 2, entry 7) gave a preferential selectivity for cis isomer with around 80:20 d.r. We also ordered a ruthenium catalyst supported on aluminum oxide (Table 2, entry 5), which produced a selectivity for cis isomers in 84:16 d.r. One catalyst from Sigma synthesized by Evonik (Entry 6) was less selective than the others with 60:40 d.r. Finally, two Ru/C catalysts from Sigma and Strem (Table 2, entries 4 and 8) provided a trans selectivity with 38:62 d.r. In the next step, the reaction parameters were further optimized continuing with the three Ru/C catalysts as they provided a higher selectivity for the trans isomers, (Ru/C from Alfa Aesar, Sigma and Strem; Table 2, entries 1-4-8).

Table 3: Hydrogenation of quinoline: Temperature screening^a


Entry	Temperature (°C)	Catalyst	Conversion (%)	Yield THQ ^b (1)	Yield DHQ ^b (2 and 3)	Selectivity ^c (2:3)
1	150	Ru/C 5% Strem	100	0	100	4:96 d.r
2	60	Ru/C 5% Alfa	100	40	60	92:8 d.r
3		Ru/C 5% Strem	100	0	100	91:9 d.r
4		Ru/C 5% Sigma	100	27	83	91:9 d.r
5		Ru/C 5% Alfa	100	50	50	92:8 d.r
6	40	Ru/C 5% Strem	100	37	63	93:7 d.r
7		Ru/C 5% Sigma	100	33	67	93:7 d.r

Reaction conditions: ^aQuinoline (64,8 mg, 0.5 mmol), Ru/C (20 mg), t-amylOH:H₂O (1:1 mL), H₂ (30 bar), T °C, 17h. ^bConversion and yield determined by GC using hexadecane as internal standard. ^cd.r. determined by GC.

First, the temperature was varied (Table 3). It was noted that by increasing the temperature to 150 °C (Table 3, entry 1), the selectivity increased for the trans isomer leading to 4:96 d.r. Interestingly, decreasing the temperature allows to change the diastereoselectivity of the process. In fact, at 60 °C (Table 3, entries 2-4), the three catalysts offered a selectivity of more than 90% for the cis-isomer DHQ **2**. However, the chemoselectivity changed depending on the catalyst. The catalysts from Alfa Aesar and Sigma allowed a complete conversion of quinoline and provided DHQ in 60% and 83% yield, respectively (Table 3, entries 2 and 4). In contrast, the Strem catalyst allowed a quantitative and selective conversion towards cis-DHQ at 60 °C (Table 3, entry 3). Further decrease of the temperature to 40 °C (Table 3, entries 5-7) gave a mixture of 1,2,3,4-THQ **1** and DHQ **2** in the presence of all catalysts. In the next steps, the reaction was further optimized with the Ru/C catalyst coming from Strem.

Table 4: Hydrogenation of quinoline: Hydrogen pressure screening^a

Entry	T (°C)	PH ₂ (Bar)	Conversion (%)	Yield THQ ^b (1)	Yield DHQ ^b (2 and 3)	Selectivity ^c (2:3)
1	60	10	100	20	80	93:7 d.r
2	150	10	100	0	100	18:82 d.r
3	60	20	100	0	100	95:5 d.r
4	150	20	100	0	100	5:95 d.r
5	60	30	100	0	100	91:9 d.r
6	150	30	100	0	100	4:96 d.r

Reaction conditions: ^aQuinoline (64.8 mg, 0.5 mmol), catalyst (20 mg), *t*-amylOH/H₂O (1/1 mL), H₂ (P bar), T °C, 17h. ^bConversion and yield determined by GC using hexadecane as internal standard. ^cd.r. determined by GC.

In Table 4, the optimization of the hydrogen pressure at a temperature of 150 °C and 60 °C is shown. Previous reactions were done at a pressure of 30 bars (Table 4, entries 5-6). Decreasing the pressure to 20 bars of hydrogen offered a full conversion to DHQ and a very high selectivity. Indeed, at 60 °C selectively the *cis*-DHQ **2** (95:5 d.r.) was formed (Table 4, entry 3), while at 150 °C the *trans*-DHQ **3** (5:95 d.r.) was preferentially obtained (Table 4, entry 4). However, using 10 bars of hydrogen a lower stereoselectivity was observed at 150 °C (Table 4, entry 2). At 60 °C (Table 4, entry 1), the catalyst was less reactive forming two products, 1,2,3,4-THQ **1** and *cis*-DHQ **2**, respectively in 20% and 80 % yield.

Table 5: Hydrogenation of quinoline: Solvent Screening at 60 °C^a

Entry	Solvent	Conversion (%)	Yield THQ ^b (1)	Yield DHQ ^b (2 and 3)	Selectivity ^c (2:3)
1	<i>t</i> -amylOH/H ₂ O	100%	0	100	95:5 d.r
2	H ₂ O	100%	69	31	93:7 d.r
3	<i>t</i> -amylOH	100%	79	21	100:0 d.r
4	EtOH	100%	69	31	95:5 d.r
5	<i>i</i> -PrOH	100%	44	56	93% d.r
6	THF	100%	75	25	100:0 d.r
7	EtOH/ H ₂ O	100%	58	42	92:8 d.r
8	<i>i</i> -PrOH/H ₂ O	100%	0	100	90:10 d.r
9	THF/H ₂ O	100%	35	65	92:8 d.r

Reaction conditions: ^aQuinoline (64.8 mg, 0.5 mmol), catalyst (20 mg), *t*-amylOH/H₂O (1/1 mL), H₂ (20 bar), 60 °C, 17h. ^bConversion and yield determined by GC using hexadecane as internal standard. ^cd.r. determined by GC.

Finally, the influence of the solvent was evaluated at a temperature of 60 °C (Table 5). In the previous tests a mixture 1/1 *t*-amylOH/H₂O was used. When we used one of these solvents alone, the chemoselectivity was significantly reduced (Table 5, entries 2-6). In general, the combination of organic solvents with water increased the chemoselectivity of the reaction. For example, ethanol alone offered a DHQ yield of 31% (Table 5, entry 4), but with water as a co-solvent, an increased yield of 42% was found. The same effect was observed with THF, 25% alone (Table 5, entry 6) and 65% with water (Table 5, entry 9). Using a mixture of *i*-PrOH/H₂O and *t*-amylOH/H₂O allowed for a total conversion to DHQ with very good diastereoselectivity, respectively 90:10 and 95:5 (Table 5, entries 1 and 8).

Selected solvents have also been tested at 150 °C (Table 6). Using only water offered full conversion to DHQ but a lower stereoselectivity 35:65 d.r. (Table 6, entry 2). Applying a mixture isopropanol/water 1-isopropyldecahydroquinoline is formed as side-product. As a consequence, the mixture *t*-amylOH/H₂O was chosen as a solvent for the following catalytic reactions (Table 6, entry 1).

Table 6: Hydrogenation of quinoline: Solvent Screening at 150 °C^a

Entry	Solvent	Conversion (%)	Yield THQ ^b (1)	Yield DHQ ^b (2 and 3)	Selectivity ^c (2:3)
1	<i>t</i> -amylOH/H ₂ O	100	0	100	4:96 d.r
2	H ₂ O	100	0	100	35:65 d.r
3	<i>i</i> -PrOH/H ₂ O	100	0	35	6:94 d.r
4	THF/H ₂ O	100	0	100	6:94 d.r

Reaction conditions: ^aQuinoline (64,8 mg, 0.5 mmol), catalyst (20 mg), *t*-amylOH/H₂O (1/1 mL), H₂ (20 bar), 150 °C, 17h. ^bConversion and yield determined by GC using hexadecane as internal standard. ^cd.r. determined by GC.

To determine the mechanism of the catalytic reaction, the kinetic profiles of quinoline hydrogenation were recorded at 60 °C and 150 °C.

At 60 °C (Figure 1), quinoline is rapidly converted to 1,2,3,4-THQ **1** and in a second step **1** is smoothly hydrogenated to the *cis*-DHQ. After 10 hours reaction time, THQ is completely converted to *cis*-DHQ. No 5,6,7,8-THQ was observed in this reaction.

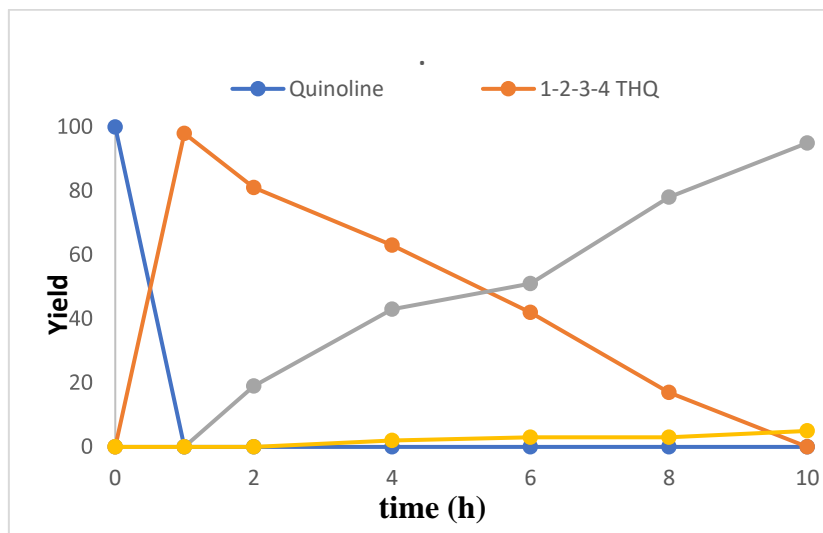
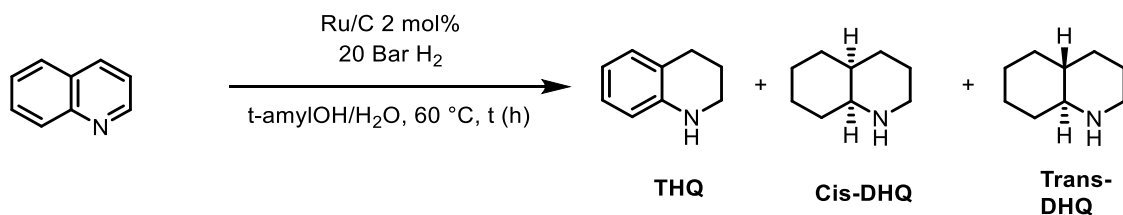


Figure 1: Kinetic profile quinoline hydrogenation at 60°C.

At 150 °C, the formation of 1,2,3,4-THQ was not observed. After 30 minutes, quinoline was directly converted to cis-DHQ and in a second step cis-DHQ was smoothly converted to the trans isomer. Hence, we can conclude that the cis compound is the kinetically favored product, while the trans component is the thermodynamically preferred product (Figure 3). A likely explanation for this epimerization is the dehydrogenation of the initial product cis-DHQ to form 2,3,4,4a,5,6,7,8-octahydroquinoline (Figure 2). Then, re-hydrogenation of the imine intermediate will give the more stable trans product.

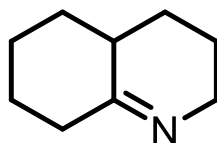
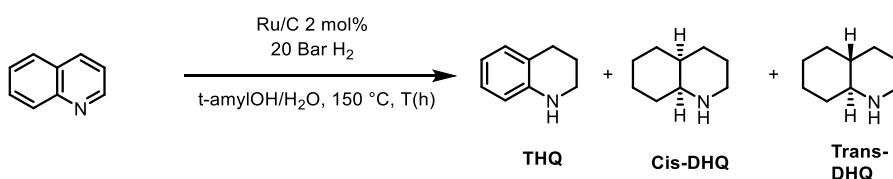


Figure 2: 2,3,4,4a,5,6,7,8-octahydroquinoline



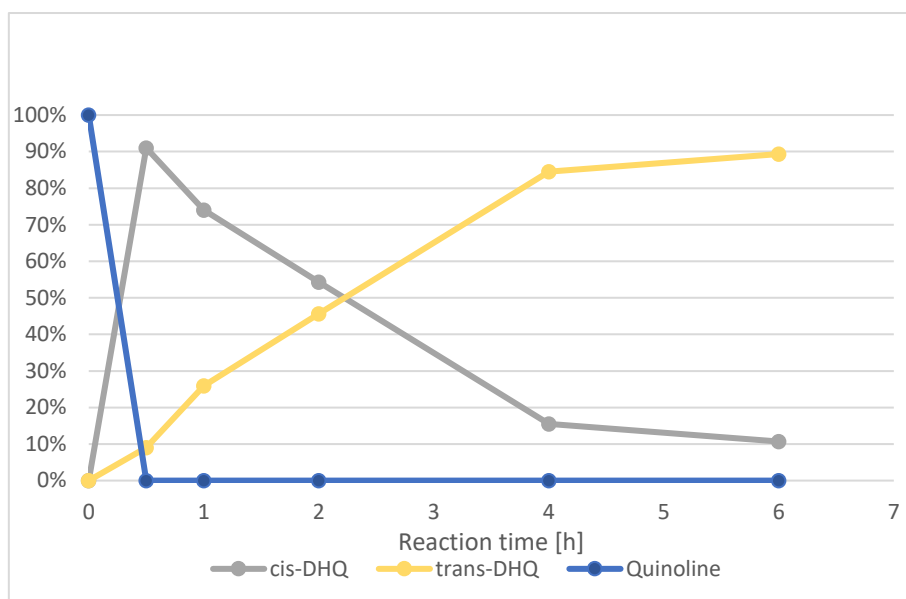


Figure 3: Kinetic profile quinoline hydrogenation at 150 °C.

Eventually, the hydrogenation of quinoline was chosen to assess the recycling of Ru/C from Strem with 1 mol% catalyst. After each cycle, the catalyst was filtered, washed several times with ethanol, dried under vacuum, and was reused directly without any further reactivation. The recycled catalyst has been used for 2 times, and a significant loss in activity and selectivity was observed after the first run. Indeed, in the second run we did not observe the formation of DHQ (Figure 4).

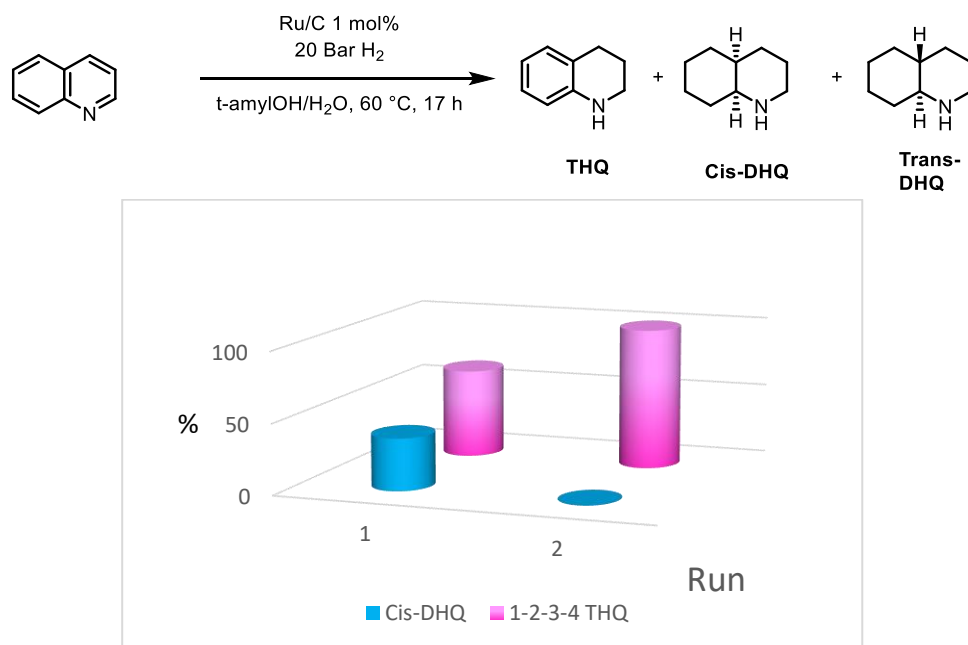
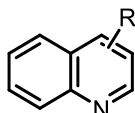
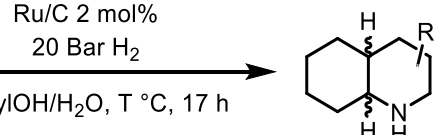
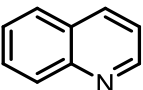
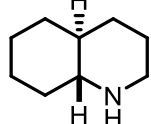
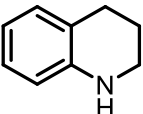
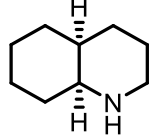
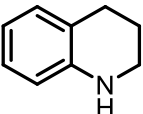
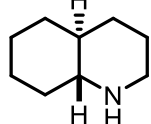


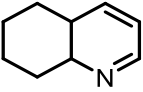
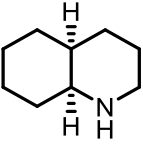
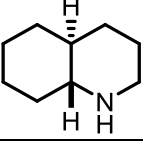
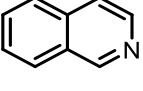
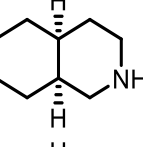
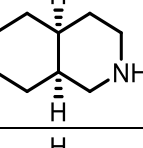
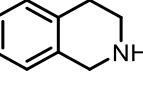
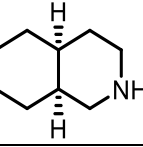
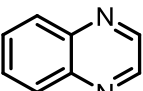
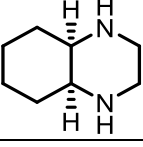
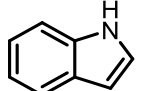
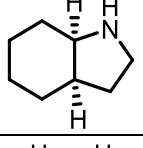
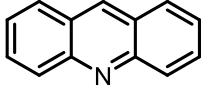
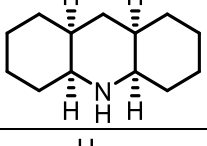
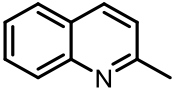
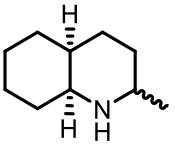
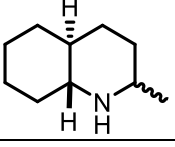
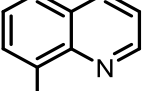
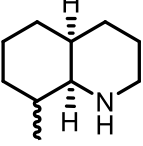
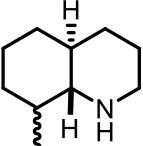
Figure 4: Quinoline hydrogenation: Recycling Ru/C.

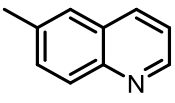
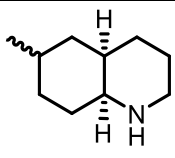
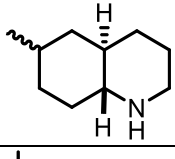
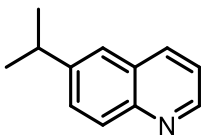
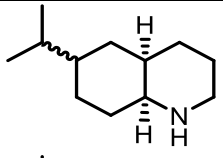
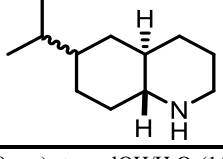
With the optimized conditions in hand, we investigated the scope of the reaction (Table 7). At 60 °C, the hydrogenation of 1,2,3,4-THQ (Table 7, Entry 3) and 5,6,7,8-THQ (Table 7, entry 5) provided cis-DHQ in 79% and 71% yield and a high selectivity with 92% and 93% d.r, respectively. Increasing the temperature to 150 °C, a reverse diastereoselectivity was detected to trans-DHQ with 94% d.r in both cases (Table 7, entries 4-6). Interestingly, isoquinoline was

more difficult to be hydrogenated. Indeed, 100 °C was necessary to reach full conversion to the cis-decahydroisoquinoline (Table 7, entry 7, 96% yield, 87% d.r). Isoquinoline was also tested at 150 °C (Table 7, entry 8) and the major product formed was the same than at 100 °C. Here, no epimerization was observed, which can be explained by the more difficult dehydrogenation to form the respective imine product. A comparable result was observed using 1,2,3,4-tetraisoquinoline (Table 7, entry 9, 93% yield, 85% d.r). Next, derivatives with alkyl substitution on the pyridyl and phenyl rings have been tried. Clearly, adding a third pro-chiral group, e.g. 2-methyl-quinoline, increases the complexity of the possible products. To assign the selectivity correctly the main products has been crystallised by the formation of a corresponding hydrochloride salt and we are waiting for crystal structure. Moreover, at 60 °C, 2-methylquinoline (Table 7, entry 13) was converted to the corresponding decahydroquinoline with 80% yield. In this case, two isomers were formed with 91% d.r. Increasing the temperature to 150 °C (Table 7, entry 14), offered four isomers and a different major product with 89% d.r. A methyl group in position 6 or 8 was converted, at 60 °C, to the corresponding DHQ with 97% and 75% yield (Table 7, entries 15 and 17), respectively, four isomers were observed with one major compound, 84% and 78% d.r. At 150°C, the reaction selectivity changed and 6 isomers can be observed for both substrates. Here, one major product was obtained with 84% and 65% d.r, respectively (Table 7, entries 16-18). Finally, a bulkier quinoline has been applied in the catalytic reaction. At 80 °C, 6-isopropylquinoline (Table 7, entry 19) was converted to the corresponding DHQ in 78% yield. Two isomers were observed with a diastereomeric ratio of 87:13. Increasing the temperature to 150°C (Entry 20) offered six different isomers and 90% d.r. The different major products were formed at 60 °C and 150 °C.

Table 7: Hydrogenation of quinolines: Scope of the reaction^a

Entry	Substrate	T (°C)	Product	Conv/Yield ^b (%)	d.r. ^c (%)	Isomers
1		60		100/98	95	2
2		150		100/98	95	2
3		60		100/79	92	2
4		150		100/82	94	2

5		60		100/71	93	2
6		150		100/75	94	2
7		100		100/96	87	2
8		150		100/96	88	2
9		100		100/93	85	2
10		150		100/88	82	2
11		60		100/96	87	2
12		150		100/90	97	2
13		60		100/80	91	2
14		150		100/82	89	4
15		60		100/75	78	4
16		150		100/99	65	6

17		60		100/97	84	4
18		150		100/99	84	6
19		80		100/78	87	2
20		150		100/78	90	6

Reaction conditions: Substrate (0.5 mmol), Ru/C (20 mg), *t*-amylOH/H₂O (1/1 mL), H₂ (20 bar), T °C, 17h. Isolated yield %d.r. determined by GC.

The scope of the reaction was further extended to other *N*-heterocyclic compounds that were all converted to the desired product in good to excellent yields. Quinoxaline (Table 7, entry 10) was hydrogenated to *cis*-decahydroquinoxaline with 88% yield and 82:18 d.r. The switch of the diastereoselectivity seems to be impossible for this compound. The same result was observed with acridine (Table 7, entry 12) with the formation of *cis*-tetradecahydroacridine with 90% yield and 97:3 d.r. Finally, indole (Table 7, entry 11) was transferred to *cis*-octahydroindoline, at 60°C, with 96% yield an 87:13 d.r. Unfortunately, at 150 °C, too many products are formed and a main product cannot be isolated.

III/ Conclusion

To conclude, we performed the switchable diastereoselective hydrogenation of quinoline to the decahydroquinoline with a commercially available Ru/C catalyst. The formation of *cis*-decahydroquinoline was possible under relatively mild conditions (60°C), while under harsher condition the selectivity changed leading to the *trans*-decahydroquinoline. At the time this manuscript is written, catalyst characterization is undergoing.

IV/Experimental Data.

All the manipulations were conducted under air using standard glassware. Ru/C was purchased from Sigma Aldrich, Strem, Alfa Aesar, TCI. Chitin from shrimp shells was purchased from Sigma Aldrich. Chitosan from shrimp shells with low viscosity was purchased from Sigma Aldrich. Other chemicals and solvents were purchased from Sigma Aldrich, Alfa Aesar, Tokyo Chemical Industry, Acros Organics and used without any further purifications.

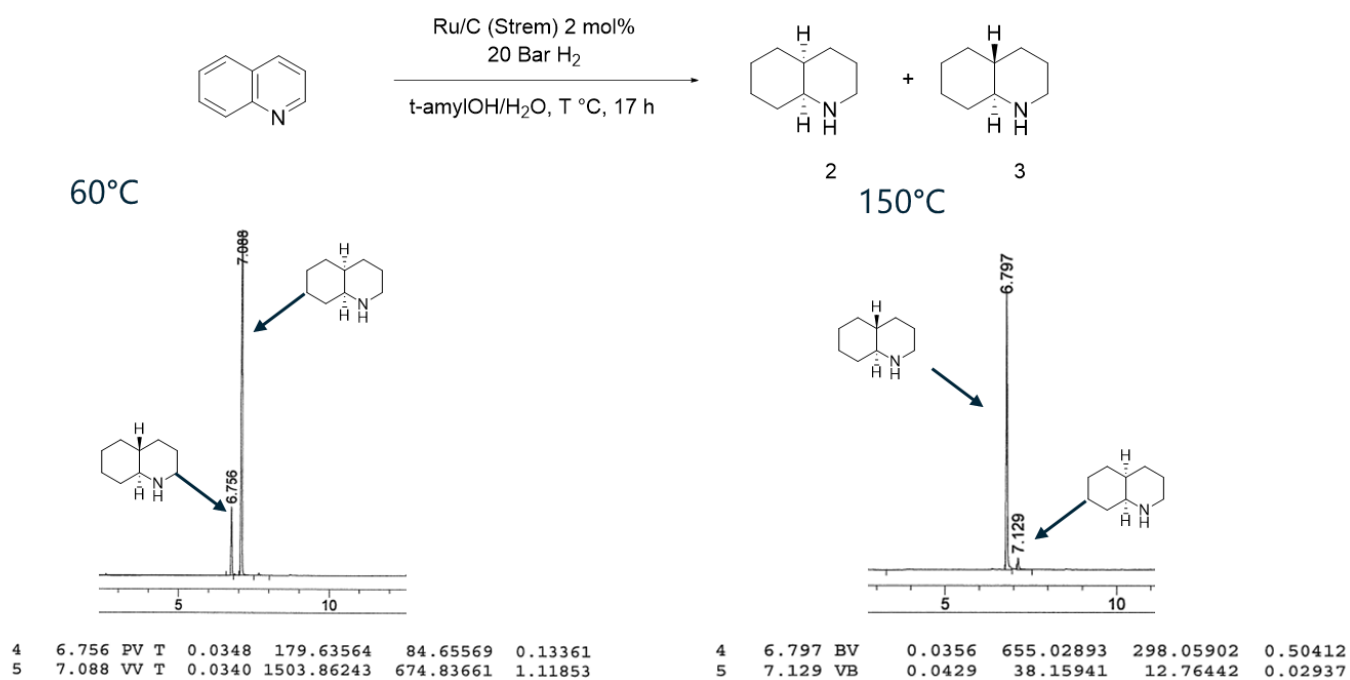
All hydrogenation experiments were carried out in 300 mL autoclave (PARR Instrument Company) in 4-mL glass vials.

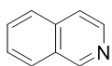
GC Conversion and yields were determined by GC-FID, HP6890 with FID detector, column HP530 m x 250 mm x 0.25 μm . Analysis of the gas sample in the dehydrogenation process was performed using GC HP Plot Q (FID – hydrocarbons, Carboxen / TCD - permanent gases), Ar - carrier gas. The GC was externally calibrated using certified gas mixtures from commercial suppliers (Linde and Air Liquide).

General procedure for hydrogenations

A 4 mL glass vial equipped with a Teflon coated oval magnetic stirring bar and a plastic screwcap was charged with a substrate (0.5 mmol, 1.0 equiv.), the Ru/C catalyst, and 2 mL of the appropriate solvent (or solvent mixture). The silicone septum was punctured with a syringe needle and the vial was placed in an aluminium plate, which was then transferred into the 300 mL autoclave. Once sealed, the autoclave was placed into an aluminium block and purged two times with hydrogen (at around 20 bar). Then, it was pressurised with H₂ and heated up to the required temperature under thorough stirring (700 rpm). After 16 hours, the autoclave was removed from the aluminium block and cooled to room temperature in a water bath. The remaining hydrogen was discharged, and the vials containing reaction products were removed from the autoclave. An internal standard (30 mg of *n*-hexadecane) was added to the crude reaction mixture, followed by the addition ethyl acetate to fill the 4 mL vial. The resulting mixture was intensively stirred for 30 s, and then, the solid catalyst was separated by filtration over a celite pad (~2 cm) and the liquid phase was subjected to GC analysis.

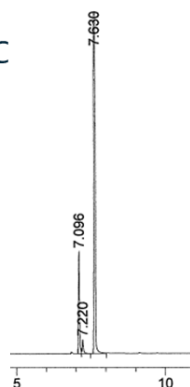
GC Data





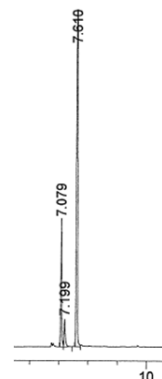
Ru/C (Strem) 2 mol%
20 Bar H₂
t-amylOH/H₂O, T °C, 17 h

100 °C

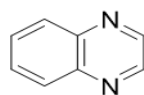


4	7.096 BV	0.0362	288.50610	128.51306	0.21706
5	7.220 VB	0.0419	50.79415	17.46873	0.03821
6	7.630 BV	0.0371	2067.40796	889.84656	1.55540

150°C



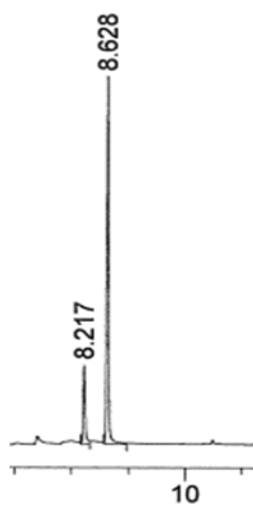
5	7.079 BV	0.0341	359.85275	161.11475	0.26277
6	7.199 VV	0.0420	94.93756	34.62149	0.06933
7	7.610 VV	0.0360	1504.96777	674.95221	1.09895



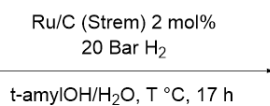
Ru/C (Strem) 2 mol%
20 Bar H₂

t-amylOH/H₂O, T °C, 17 h

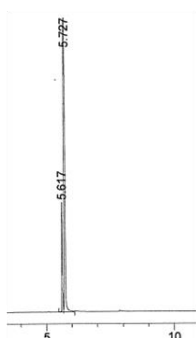
150°C



4	8.217	VV	0.0392	145.40382	58.05697	0.11271
5	8.628	VV	0.0351	641.38696	276.23810	0.49715

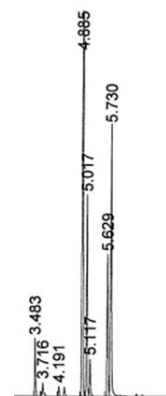


60 °C

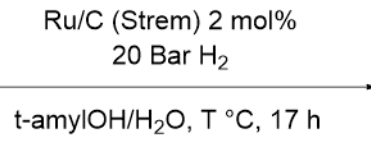
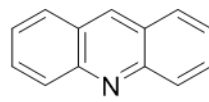


4	5.617	PV	0.0331	314.76846	158.67690	0.23441
5	5.727	VV	0.0327	2151.49121	1015.33002	1.60220

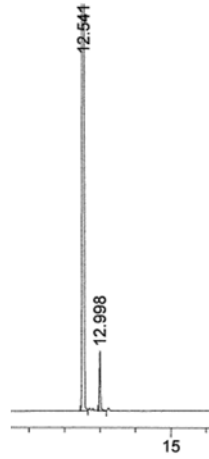
150 °C



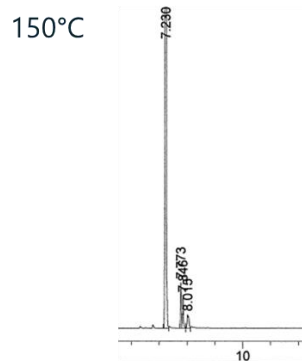
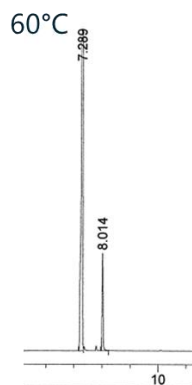
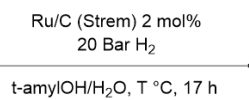
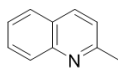
5	3.716	VV	T	0.0297	29.13133	14.32343	0.02165
6	4.191	VV	T	0.0264	16.13279	10.21810	0.01199
7	4.885	VV	T	0.0307	1313.77344	676.58167	0.97643
8	5.017	VV	T	0.0328	438.41943	224.24109	0.32585
9	5.117	VV	T	0.0350	88.33891	41.15372	0.06566
10	5.629	PV	T	0.0310	309.20084	156.99487	0.22981
11	5.730	VV	T	0.0353	653.30646	301.63412	0.48556



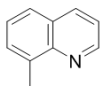
150°C



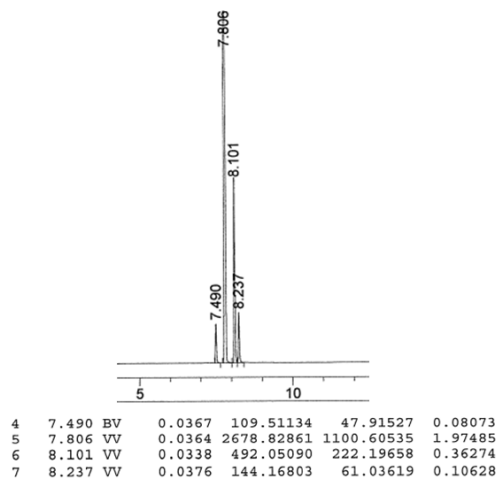
4	12.541	PV	0.0428	4174.60498	1579.50891	3.14346
5	12.998	VV	0.0357	140.33699	63.78743	0.10567



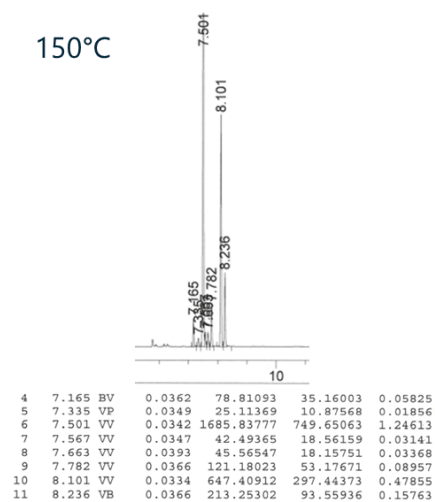
4	7.289	VV	0.0410	2999.84961	1129.65393	2.19688	4	7.230	VV	0.0392	2656.90332	1061.08301	1.99397
5	8.014	VV	0.0353	303.45160	129.58307	0.22223	5	7.773	BV	0.0336	133.24829	60.75514	0.10000
							6	7.846	VV	0.0361	103.89760	43.16279	0.07797
							7	8.015	VV	0.0604	79.95881	17.81334	0.06001

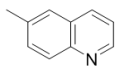


Ru/C (Strem) 2 mol%
20 Bar H₂
t-amylOH/H₂O, T °C, 17 h



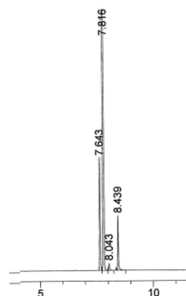
150°C



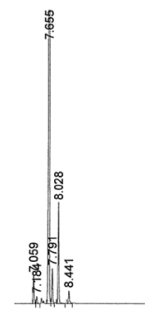


Ru/C (Strem) 2 mol%
20 Bar H₂
t-amylOH/H₂O, T °C, 17 h

60°C



150°C



4	7.643	BV	0.0363	417.20816	185.18349	0.30839	5	7.059	BV	0.0339	89.89054	40.50256	0.06827
5	7.816	VV	0.0378	2462.90820	1033.79749	1.82051	6	7.184	VV	0.0402	25.95689	10.01822	0.01971
6	8.043	VB	0.0413	30.59869	11.40992	0.02262	7	7.655	VV	0.0355	2455.81055	1041.18616	1.86515
7	8.439	BB	0.0373	224.73834	89.46207	0.16612	8	7.791	VV	0.0368	115.54636	50.38494	0.08776
							9	8.028	VV	0.0370	338.61597	146.12021	0.25717
							10	8.441	VV	0.0412	51.03959	17.93989	0.03876

Part II: Mild, selective and practical diastereoselective hydrogenation of pyridines and arenes.

I/Introduction

In the previous chapter, we described a diastereoselective hydrogenation of quinoline and related heteroarenes using a commercially available Ru/C catalyst. Based on that work, we also investigated the diastereoselective hydrogenation of pyridines and arenes.

Notably, the stereoselective hydrogenation of arenes/heteroarenes is a less explored area.¹⁵¹ One of the most interesting industrial examples is the selective hydrogenation of thymol to menthol¹⁵² (Figure 5, a). After vanillin, it is the most used aroma chemical in industry, and it is the main constituent of the essential oil of peppermint.¹⁵³ Furthermore, stereoselective hydrogenations of heterocycles are of interest in the pharmaceutical industry. Indeed, more than 60% of small molecule drugs are containing a heterocyclic ring.¹⁵⁴ For example, 2,6-dimethylpyridine is an attractive chiral secondary amine building block¹⁵⁵ and its selective hydrogenation is utilized as a key step in the syntheses of bioactive compounds (Figure 5, b).

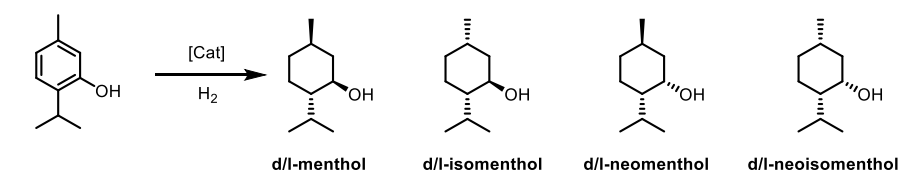


Figure 5: (a) Thymol hydrogenation to menthol

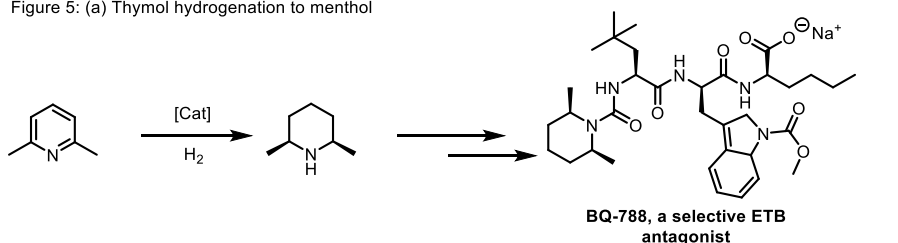


Figure 5: (B) Pirmenol multi-step reaction

One of the first stereoselective hydrogenations of aromatic N-heterocyclic compounds were carried out by Tungler and co-workers.¹⁵⁶ They hydrogenated pyridine and pyrrole derivatives using noble metals (Pd, Rh, Ru and Pt) combined with (S)-proline methylester as a chiral auxiliary. The diastereoselectivity obtained for the hydrogenation of picolinic and nicotinic acids modified by the addition of the chiral auxiliary was relatively high. However, the group of Pinel could not reproduce these results and the authors reported a diastereoselectivity less than 30%.¹⁵⁷ Later on, Douja and *al*¹⁵⁸ described the diastereoselective hydrogenation of methyl-2-nicotinic acid with several optically pure auxiliaries in the presence of supported

¹⁵¹ W.-B. Wang, S.-M. Lu, P. Y. Yang, X. W. Han, Y. G. Zhou, *J. Am. Chem. Soc.*, **2003**, *125*, 10536–10537.

¹⁵² A. Tungler, T. Máthé, Z. Bende, J. Petro, *Applied Catalysis*, **1985**, *19*, 365-374.

¹⁵³ J. Dudas, J. Hanika, *Chem. Eng. Res. Des.*, **2009**, *87*, 83–90.

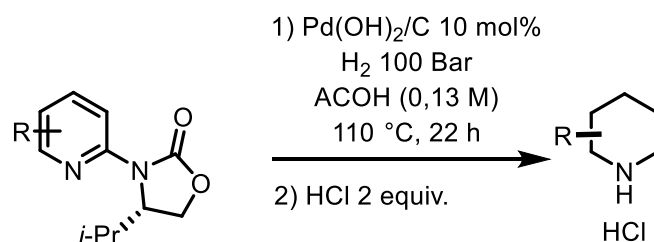
¹⁵⁴ E. Vitaku, D. T. Smith, J. T. Njardarson, *J. Med. Chem.*, **2014**, *57*, 10257-10274.

¹⁵⁵ J. Einhorn, C. Ratajczak, F. Durif, A. Averbuch, M. T., Pierre, J. L., *Tetrahedron Letters*, **1998**, *39*, 2565-2568.

¹⁵⁶ L. Hegedus, V. Hada, A. Tungler, T. Mathe, L. Szepesy, *Appl. Catal.*, **2000**, *201*, 1, 107-114.

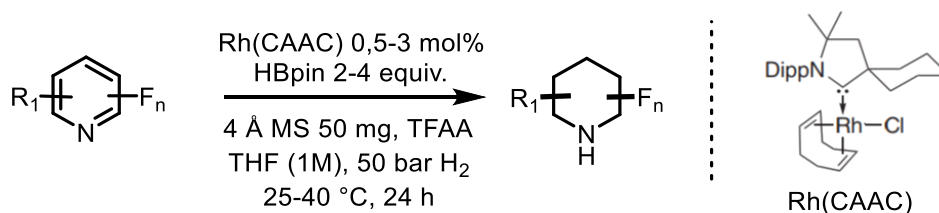
¹⁵⁷ N. Douja, M. Besson, P. Gallezot, C. Pinel, *J. Mol. Catal. A: Chem.*, **2002**, *186*, 145-151.

metal catalysts. After screening several reaction parameters, they obtained up to 35% diastereoselective excess, when (R)-pantolactone was used as a chiral auxiliary (50 atm H₂, room temperature). A year later, Pinel and co-workers¹⁵⁸ studied the diastereoselective hydrogenation of a nicotinic acid derivative with a supported metal catalyst. However, only low diastereoselectivity (11-27% d.e.) was achieved. Soon after, using oxazolidinone as a chiral auxiliary, Glorius and colleagues¹⁵⁹ reported a highly effective diastereoselective hydrogenation of N-(2-pyridyl)-oxazolidinones using Pd(OH)₂/C as a catalyst. With this catalytic system, under a hydrogen pressure of 100 atm, a series of single- or multi-controlled pyridines were hydrogenated (Scheme 8).



Scheme 8: Enantioselective synthesis of piperidines by the diastereoselective hydrogenation of pyridines using the Evans auxiliary.

More recently, the Glorius group¹⁶⁰ developed an elegant strategy for accessing partially fluorinated piperidines with high cis-selectivity using a rhodium catalyst (Scheme 9).



Scheme 9: Fluoro-arene hydrogenation by Rh(CAAC).

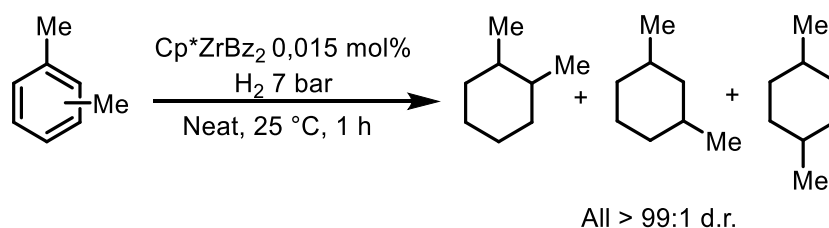
Compared to heteroarenes, the asymmetric hydrogenation of arenes is even more difficult due to the strong aromaticity and low coordination capacity of these compounds. In 2016, the Marks' group¹⁶¹ developed a single-site Cp-Zr(H)Bz/ZrS allowing highly selective hydrogenation of arenes. The catalyst was capable to perform selective hydrogenation of different alkyl arene derivatives (Scheme 10).

¹⁵⁸ N. Douja, R. Malacea, M. Banciu, M. Besson, C. Pinel, *Tetrahedron Lett.*, **2003**, *44*, 37, 6991-6993.

¹⁵⁹ F. Glorius, N. Spielkamp, S. Holle, R. Goddard, C. W. Lehmann, *Angew. Chem. Int. Ed.*, **2004**, *43*, 2850-2852.

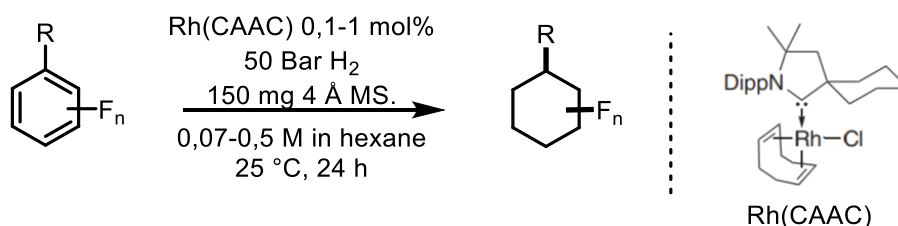
¹⁶⁰ Z. Nairoukh, M. Wollenburg, C. Schleppehorst, K. Bergander, F. Glorius, *Nature Chem.*, **2019**, *11*, 264-270.

¹⁶¹ M. M. Stalzer, C. P. Nicholas, A. Bhattacharyya, A. Motta, M. Delferro, T. J. Marks, *Angew. Chem. Int. Ed.*, **2016**, *55*, 5263-5267.



Scheme 10: Arene hydrogenation using a supported zirconium catalyst,

A year later, Wiesenfeldt and *al.*¹⁶² considered that multi-step processes could be avoided by designing a protocol for the catalytic hydrogenation of inexpensive and readily available fluoroarenes. Using a Rh-NHC catalyst with a specific (amino)carbene ligand, a range of fluoroarenes was transformed into the corresponding fluorinated saturated products. In addition to fluorobenzene, a number of mono- and polyfluoro-substituted benzenes have been reduced. Even hexafluorobenzene provided *cis*-hexafluorocyclohexane with a selectivity of 420:1 dr, although with a slightly reduced yield (34%). This approach represents a major synthetic advancement, as a previous pathway to obtain this product from glucose required 12 steps (Scheme 11).



Scheme 11: hydrogenation of fluorinated arene

In 2018, Chirik and co-worker,¹⁶³ developed a method for the hydrogenation of arenes catalyzed by a bis-(neosilyl)-molybdenum complex. Unfortunately, hydrogenations with heteroarene substrates failed due to catalyst deactivation.

II/Results and discussion

The catalytic materials were prepared adapting the protocol reported for other catalysts of this class.¹⁶⁴ After the *in-situ* generation of a chelate between $\text{RuCl}_3 \cdot x\text{H}_2\text{O}$ (or non-noble metals) and 1,10-phenanthroline, cellulose, chitin or chitosan, if necessary a corresponding metal oxide was also added, the heterogeneous mixture was stirred in ethanol for 24 h. Afterwards, the solvent was removed and the obtained solids were pyrolyzed at 800 °C (temperature ramp 25 °C·min⁻¹) under Ar atmosphere for 2 h. The resulting materials possess a ruthenium content of around 2,5 %wt. Applying this protocol, a small library of 16 materials was prepared. Their catalytic activity was then evaluated using 2,6 dimethylpyridine **1** as model substrate. The results of the catalytic screening are depicted in Table 8

¹⁶² M. P. Wiesenfeldt, Z. Nairoukh, W. Li, F. Glorius, *Science*, **2017**, 357, 908–912.

¹⁶³ M. V. Joannou, M. J. Bezdek, P. J. Chirik, *ACS Catal.*, **2018**, 8, 5276-5285

¹⁶⁴ R. V. Jagadeesh, T. Stemmler, A.-E. Surkus, M. Bauer, M.-M. Pohl, J. Radnik, K. Junge, H. Junge, A. Bruckner, M. Beller, *Nat. Protocols*, **2015**, 10, 916-926.

Table 8: Catalysts screening for diastereoselective hydrogenation of 2,6-dimethylpyridine^a

Entry	Catalyst	Conversion ^b (%)	Yield ^b (%)	d.r. ^c (%)
1	Ru/Phen(½)@TiO ₂ -800	100	92	96
2	Ru/C 5 wt%	100	82	96
3	Ru@Chitosan-800	0	0	0
4	Ru@Chitin-800	80	73	97
5	Ru/Phen(½)@C-800	100	88	98
6	Ru/Phen(1/10)@C-800	82	79	97
7	Ru/Phen(½)@SiO ₂ -800	100	62	97
8	Ru/Phen(½)@Al ₂ O ₃ -800	100	54	97
9	Co/Phen(½)@C-800	0	0	0
10	Cu/Phen(½)@C-800	0	0	0
11	Ni/Phen@SiO ₂ -800	0	0	0
12	Ni/Phen@C-800	0	0	0
13	Ni/Phen@TiO ₂ -600	0	0	0
14	Ni@Cellulose acetate-1000	0	0	0
15	Co@Cellulose acetate-1000	0	0	0
16	Cu@Cellulose acetate-1000	0	0	0

Reaction conditions: ^a2,6-dimethylpyridine (53.6 mg, 0.5 mmol), catalyst (20 mg), H₂O (2 mL), H₂ (30 bar), 80 °C, 17h. ^bConversion and yield determined by GC using hexadecane as internal standard. ^cd.r. determined by GC.

It is immediately noticeable that materials based on non-noble metals such as cobalt, nickel, copper showed no conversion (Table 8, entries 9-16). In contrast, using ruthenium as metal precursor gave better results. Interestingly, the ruthenium/chitosan material was inactive (Table 8, entry 3), while changing the support to chitin offered a good conversion of 80% (Table 8, entry 4). To improve the conversion, we added phenanthroline as a ligand and we investigated the ratio of phenanthroline compared to the metal precursors in the presence of carbon as the support. We observed a conversion of 82% with a 1:10 ratio (metal/phenanthroline) (Table 8, entry 6). Increasing the metal concentration to 1:2 (table 8, entry 5) permitted a full conversion. Different supports have been tested, too. Using TiO₂, SiO₂ and γ -Al₂O₃ (Table 8, entries 1,7, and 8), quantitative conversion could be achieved with a diastereoselective ratio of around 96% to cis-dimethylpiperidine. Finally, a commercially available heterogeneous ruthenium on carbon system has been tried, which showed full conversion of **1** with a good selectivity to the

corresponding cis product (Table 8, entry 2). The reaction conditions used so far did not allow us to select an optimal catalyst. Therefore, we performed additional tests at lower temperature (Table 9).

Table 9: Diastereoselective hydrogenation of 2,6-dimethylpyridine: Temperature screening^a.

Entry	Catalyst	T (°C)	Conversion ^b (%)	Yield ^b (%)	d.r. ^c (%)
1	Ru/Phen(1/2)@TiO ₂ -800		100	92	97
2	Ru/C 5 wt%		100	93	96
3	Ru/Phen(1/2)@C-800	60	100	89	97
4	Ru/Phen(1/2)@SiO ₂ -800		100	95	97
5	Ru/Phen(1/2)@Al ₂ O ₃ -800		100	92	96
6	Ru/Phen(1/2)@TiO ₂ -800		100	90	97
7	Ru/C 5 wt%		100	93	97
8	Ru/Phen(1/2)@C-800	40	100	92	97
9	Ru/Phen(1/2)@SiO ₂ -800		100	92	96
10	Ru/Phen(1/2)@Al ₂ O ₃ -800		100	88	97
11	Ru/Phen(1/2)@TiO ₂ -800		100	91	97
12	Ru/C 5 wt%		97	87	95
13	Ru/Phen(1/2)@C-800	25	0	0	0
14	Ru/Phen(1/2)@SiO ₂ -800		80	72	98
15	Ru/Phen(1/2)@Al ₂ O ₃ -800		100	91	97

Reaction conditions: ^a2,6-dimethylpyridine (53.6 mg, 0.5 mmol), catalyst (20 mg), H₂O (2 mL), H₂ (30 bar), T °C, 17 h. ^bConversion and yield determined by GC using hexadecane as internal standard. ^cd.r. determined by GC.

Here, five heterogeneous ruthenium catalysts were evaluated at different temperatures. All the catalysts were able to perform the diastereoselective hydrogenation of 2,6-dimethylpiperidine at 60 and 40 °C with a selectivity comprised between 96-97% (Table 9, entries 1-10). Notably, the Ru/Phen(1/2)@C-800 was inefficient at room temperature (Table 9, entry 13) and the Ru/Phen(1/2)@SiO₂-800 was less reactive leading only 80% conversion. Finally, three catalysts Ru/Phen(1/2)@TiO₂-800, Ru/C, and Ru/Phen(1/2)@Al₂O₃-800 were capable to perform the

reaction at room temperature with a conversion >95% and a selectivity comprised between 95% and 97%.

Table 10: Diastereoselective hydrogenation of 2,6-dimethylpyridine: Variation of hydrogen pressure^a.

Entry	Catalyst	P (Bar)	Conversion ^a (%)	Yield ^b (%)	d.R (Cis) ^c (%)
1	Ru/Phen(½)@TiO ₂ -800		100	91	97
2	Ru/C	30	97	87	95
3	Ru/Phen(½)@Al ₂ O ₃ -800		100	91	97
4	Ru/Phen(½)@TiO ₂ -800		100	90	97
5	Ru/C	20	100	87	97
6	Ru/Phen(½)@Al ₂ O ₃ -800		100	93	96
7	Ru/Phen(½)@TiO ₂ -800		100	87	97
8	Ru/C	10	100	87	97
9	Ru/Phen(½)@Al ₂ O ₃ -800		100	97	97

Reaction conditions: ^a2,6-dimethylpyridine (53.6 mg, 0.5 mmol), catalyst (20 mg), H₂O (2 mL), H₂ (P bar), 25 °C, 17 h. ^bConversion and yield determined by GC using hexadecane as internal standard. ^cd.r. determined by GC.

As depicted in Table 10, the pressure was not a limiting factor. Indeed, all the catalysts were tested at 30, 20 and 10 bar (Table 10, entries 1 to 9), and showed complete conversion of **1** to **2** with a high selectivity (97%).

The previous results were obtained using 20 mg of catalyst, which is equivalent to 1 mol% of catalyst. In case of ruthenium on carbon, which is commercially available with a higher concentration of ruthenium, this corresponds to 2 mol% catalyst. Reducing the amount of catalyst, Ru/Phen(½)@Al₂O₃-800 resulted in a minor conversion of **1** (37%) (Table 11, entry 6). Reducing the catalyst amount further on showed Ru/Phen(½)@TiO₂-800 as the most active catalyst (Table 11, entry 7). This system was then studied regarding solvent effects (Table 12).

Table 11: Diastereoselective hydrogenation of 2,6-dimethylpyridine: Optimization of the catalyst loading^a

Entry	Catalyst	Catalyst Loading (mg)	Conversion ^b (%)	Yield ^b (%)	d.r. (Cis) ^c (%)
1	Ru/Phen(1/2)@TiO ₂ 800		100	87	97
2	Ru/C	20	100	87	97
3	Ru/Phen(1/2)@Al ₂ O ₃ -800		100	97	97
4	Ru/Phen(1/2)@TiO ₂ -800		100	92	98
5	Ru/C	10	100	91	97
6	Ru/Phen(1/2)@Al ₂ O ₃ -800		33	23	97
7	Ru/Phen(1/2)@TiO ₂ -800		60	53	99
8	Ru/C	5	49	39	98
9	Ru/Phen(1/2)@Al ₂ O ₃ -800		24	17	98

Reaction conditions: ^a2,6-dimethylpyridine (53.6 mg, 0.5 mmol), catalyst (X mg), H₂O (2 mL), H₂ (10 bar), 25 °C, 17h. ^bConversion and yield determined by GC using hexadecane as internal standard. ^cd.r. determined by GC.

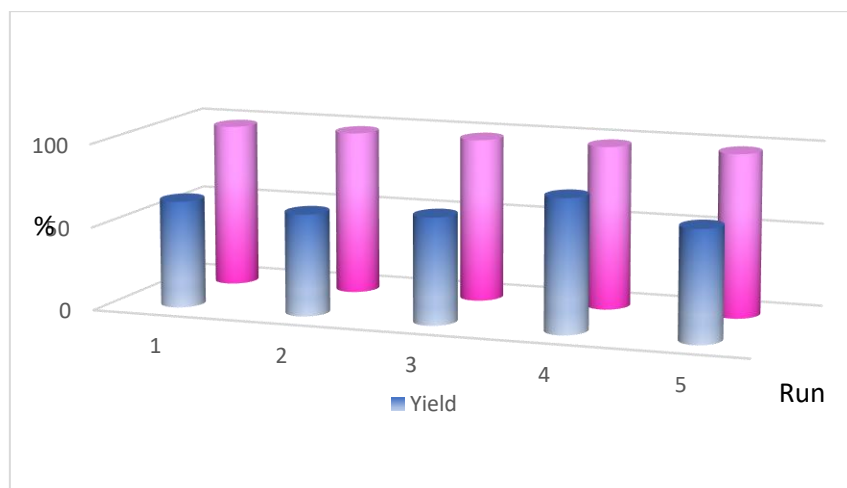
As shown in Table 12, different solvents have been tested for the diastereoselective hydrogenation of 2,6 dimethylpyridine. Notably, the reaction cannot take place without solvent. Performing the model reaction in both polar solvents such as THF and *i*-PrOH (Table 12, entries 2 and 3), as well as the non-polar solvent toluene (Table 12, entry 4) showed no conversion. In contrast, a combination of water/*i*-PrOH allowed for significant hydrogenation activity (Table 12, entry 5). Best results were observed with 0,5 mol% of Ru/phen(1/2)@TiO₂-800 in a mixture H₂O/*i*-PrOH under 10 bars of hydrogen at room temperature.

Table 12: Diastereoselective hydrogenation of 2,6-dimethylpyridine: Solvent screening^a

Entry	Catalyst loading (Mol%)	Solvent	Conversion ^b (%)	Yield ^b (%)	d.r. (Cis) ^c (%)
1	0,5	Neat	<5	<5	<5
2		THF	<5	<5	<5
3		<i>i</i> -PrOH	<5	<5	<5
4		Toluene	<5	<5	<5
5	0,25	H ₂ O	100	98	98
6		H ₂ O	100	89	98
7		THF/ H ₂ O	60	50	98
8		<i>i</i> -PrOH/ H ₂ O	38	33	98

Reaction conditions: ^a2,6-dimethylpyridine (53.6 mg, 0.5 mmol), catalyst (x mol%), solvent (2 mL), H₂ (10 bar), 25 °C, 17h. ^bConversion and yield determined by GC using hexadecane as internal standard. ^cd.r. determined by GC.

Eventually, the hydrogenation of 2,6-dimethylpyridine was chosen to assess the reusability of our novel Ru/Phen(1/2)@TiO₂-800 catalyst (Figure 6). After each cycle, the catalyst was filtered, washed several times with ethanol, dried under vacuum, and was used directly without any further reactivation. The recycled catalyst has been used for five times and no significant loss in activity and selectivity was observed.

**Figure 6:** 2,6-dimethylpyridine hydrogenation: recycling Ru/Phen(1/2)@TiO₂-800

With the optimized catalyst and conditions in hand, the scope and limitations of the described protocol were explored (Table 13).

Table 14: Diastereoselective hydrogenation of pyridines: Scope and limitations^a

Entry	Substrate	T (°C)	Product	Conversion (%)	Yield(%) ^b (Cis+Trans)	d.r. ^c (%)
1		80		>99	85	89
2		80		-	-	-
3		40		>99	94	93
4		60		>99	93	89
5		80		>99	98	88
6		60		>99	88	99
7		40		>99	-	93
8		80		-	-	-
9		60		>99	-	-

^a Reaction conditions: substrate (0.5 mmol), Ru:Phen(1:2)@TiO₂-800 (10 mg), H₂O (1 mL), *i*-PrOH (1 mL), H₂ (10 bar), 17 h. ^bIsolated yields. ^cd.r. determined by GC.

We started our investigation with different dimethylpyridines, which are substituted in different positions. Indeed, 2,5 dimethylpyridine was hydrogenated to the 2,5 dimethylpiperidine (Table 13, Entry 1) with a high yield (85%) and selectivity to the cis compound (89%) at 80°C, while

for the 2,6 dimethylpyridine the catalysis successfully works at room temperature. Surprisingly, the hydrogenation of 3,5-dimethylpyridine could not be achieved even at 80°C (Table 13, entry 2). A tri-substituted pyridine such as 2,4,6-trimethylpyridine has been hydrogenated to the corresponding cis-product with a high yield and diastereoselective ratio, respectively 94% and 93% (Table 13, entry 3). Hydrogenation of 2,6-tert-butylpyridine is also possible at 60°C with a yield of 93% and a selectivity of 89% (Table 13, entry 4). In addition to pyridines, 2,3-dimethylpyrazine can be selectively hydrogenated to the corresponding 2,3-dimethylpiperazine with 98% yield and 88% selectivity for the cis-compound (Table 13, entry 5). Then, challenging substrates with reducible groups were tested. In the case of ester (Table 13, entry 6) and amide substituents (Table 13, entry 7), the reaction proceeded with a high chemoselectivity. Finally, also a halide containing pyridine was tested. Here, we observed total conversion of the starting material. Unfortunately, the product formed was the dehalogenated compound (Table 13, entry 9).

In the previous chapter, we demonstrated that Ru/C allowed the complete hydrogenation of quinoline. Therefore, we also tested arene compounds in this catalytic reaction. We started with different xylenes derivatives, more specifically meta-, para-, and ortho-xylene (Table 14, entries 1-3). Those three compounds could be hydrogenated at room temperature, but we observed different selectivity. Ortho-xylene was the most selective one with a diastereomeric ratio of 94% for the cis compound. Meta- and para-xylene were less selective leading to 86% and 76%, respectively of the cis-compound. Due to the volatility of dimethylcyclohexanes, isolation was not possible and a GC yield of the cis compounds is given. Increasing the steric bulkiness in the para-position (Table 14, entry 4) gave 76% yield and a 73:27 d.r. The hydrogenation of phenols bearing aliphatic substituents (Table 14, entries 5-6) provided the corresponding cis-cyclohexanols in high yields. Moreover, hydrogenation of the para-cresol was easier than for the ortho-cresol, where the reaction temperature was 40 and 80°C, respectively. In addition, 4-tert-butylcyclohexanol (Table 14, Entry 7) was obtained in quantitative yield and 99:1 d.r. As an example, for the reduction of tri-substituted arenes, the hydrogenation of thymol (2-isopropyl-5-methylphenol) was investigated, which is industrially important for the synthesis of menthol isomers. At 150 °C, full conversion of thymol was observed using our novel base metal catalyst yielding 88% of menthol isomers. Here, (±)-neoisomenthol is the major product with 88% d.r. The chemoselectivity of the catalyst was investigated using either functionalized reagents or mixtures of reagents. Indeed, the selective hydrogenation of quinoline derivatives in the presence of an ester group or amide was demonstrated (Table 14, entries 9-12). In the case of methyl salicylate (Table 14, entry 11) methylcyclohexane carboxylate was observed as by-product. The formation of this product may be due to the water elimination that would form methyl 1-cyclohexene-1-carboxylate and by hydrogenation of the double bond the methylcyclohexane carboxylate.

Table 14: Scope and limitation for arene hydrogenations^a

Entry	Substrate	T (°C)	Product	Conversion (%)	Yield(%) ^b (Cis+Trans)	d.r. ^c (%)
1*		25		>99	75	86
2*		25		>99	57	76
3*		25		>99	82	94
4		25		>99	76	73
5		40		>99	98	>99
6		80		>99	75	70
7		80		>99	99	99
8		60		>99	88	81
9		60		>99	89	>99
10		40		>99	82	98
11		80		>99	79/21	99
12		80		>99	78	78

^aReaction conditions: substrate (0.5 mmol), Ru:Phen(1:2)@TiO₂-800 (10 mg), H₂O (1 mL), *i*-PrOH (1 mL), H₂ (10 bar), 17 h. * GC yield hexadecane as ISTD. ^bIsolated yields. ^cd.r. determined by GC.

III/ Conclusion

In conclusion, we have developed a heterogeneous ruthenium-based catalyst capable of performing diastereoselective hydrogenation of di- and trisubstituted pyridines and arenes under mild conditions with very good selectivity for cis compounds. This catalytic protocol can be applied for compounds which are of interest for industry. Thus, the hydrogenation of thymol produces (\pm)-neo-isomenthol and the reaction of 2,6 dimethylpiperidine leads to an important building block in pharmacy.

IV/Experimental Data

All the manipulations were conducted under air using standard glassware. RuCl_3 was purchased from Sigma Aldrich. Chitin from shrimp shells was purchased from Sigma Aldrich. Chitosan from shrimp shells with low viscosity was purchased from Sigma Aldrich. Cellulose microcrystalline was purchased from Alfa Aesar. Aluminum oxide γ -phase (nanopowder, > 99% trace metals basis) was purchased from Alfa Aesar. Titanium oxide (nanopowder, 21 nm primary particle size (TEM), $\geq 99.5\%$ trace metals basis) and fumed silica (SiO_2 , Aerosil OX-50) were purchased from Evonik Industries. Other chemicals and solvents were purchased from Sigma Aldrich, Alfa Aesar, Tokyo Chemical Industry, Acros Organics and used without any further purifications.

All hydrogenation experiments were carried out in 300 mL autoclave (PARR Instrument Company) in 8-mL glass vials.

GC Conversion and yields were determined by GC-FID, HP6890 with FID detector, column HP530 m x 250 mm x 0.25 μm . Analysis of the gas sample in the dehydrogenation process was performed using GC HP Plot Q (FID – hydrocarbons, Carboxen / TCD - permanent gases), Ar - carrier gas. The GC was externally calibrated using certified gas mixtures from commercial suppliers (Linde and Air Liquide).

Preparation of the Ru-Phen(1:2)@TiO₂ catalyst

A 100 mL round bottomed flask was charged with RuCl_3 (61.6 mg, 0.30 mmol), 1,10-phenanthroline monohydrate (108.2 mg, 0.55 mmol) and absolute ethanol (40 mL). After stirring at room temperature for 30 min, TiO_2 anatase (830.2 mg) was added to the reaction mixture via a funnel, and the resulting heterogeneous mixture was stirred at room temperature overnight. The solvent was removed *in vacuo* and dried under high vacuum for 4 hours. The sample was ground to a fine powder which was transferred to a ceramic crucible and placed in an oven. The furnace was heated to 800 °C at a rate of 25 °C/min and held at 800 °C for 2 hours under argon atmosphere. After the heating was switched off, the oven was allowed to reach room temperature, giving the Ru-Phen(1:2)@TiO₂ as a black powder. Note that during the whole process, argon was constantly passed through the oven.

General procedure for hydrogenations

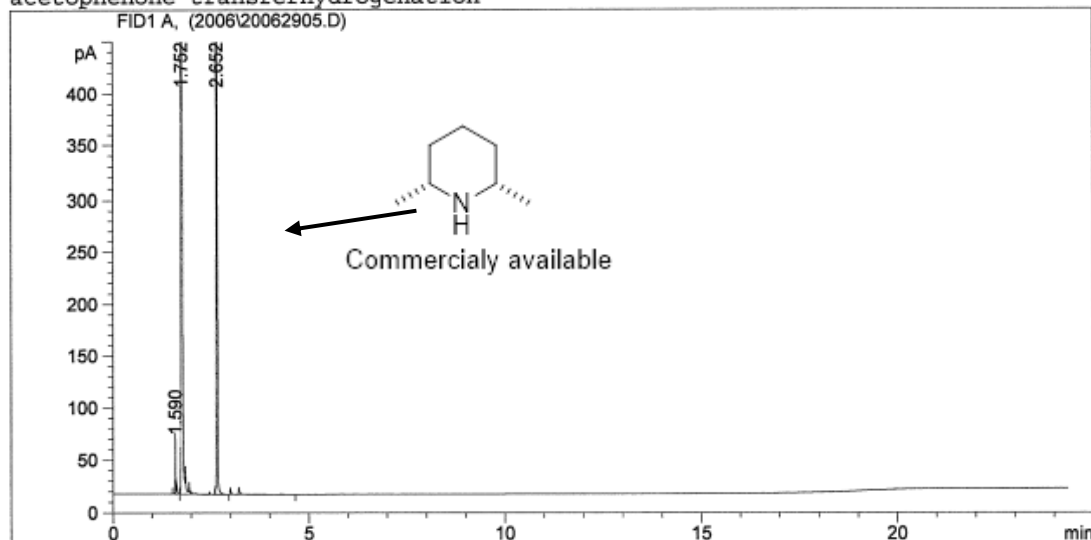
An 4 mL glass vial equipped with a Teflon coated oval magnetic stirring bar and a plastic screwcap was charged with a substrate (0.5 mmol, 1.0 equiv.), the Ru:Phen(1:2)@TiO₂-800 catalyst, and 2 mL of the appropriate solvent (or solvent mixture). The silicone septum was punctured with a syringe needle and the vial was placed in an aluminium plate, which was then transferred into the 300 mL autoclave. Once sealed, the autoclave was placed into an aluminium block and purged two times with hydrogen (at around 20 bar). Then, it was pressurised with H₂ and heated up to the required temperature under thorough stirring (700 rpm). After 16 hours, the autoclave was removed from the aluminium block and cooled to room temperature in a water bath. The remaining hydrogen was discharged, and the vials containing reaction products were removed from the autoclave. An internal standard (30 mg of *n*-hexadecane) was added to the crude reaction mixture, followed by the addition ethyl acetate to fill the 4 mL vial. The resulting mixture was intensively stirred for 30 s, and then, the solid catalyst was separated by filtration over a celite pad (~2 cm) and the liquid phase was subjected to GC analysis.

GC Data

```

=====
Injection Date   : 6/29/2020 3:13:15 PM           Seq. Line :    5
Sample Name     : cis 2-6piperidin                Location  : Vial 1
Acq. Operator   : 2.025                          Inj       :    1
Acq. Instrument : GC Lab 2.025                    Inj Volume: 1 µl
Acq. Method     : C:\HPCHEM\1\METHODS\ACETODF.M
Last changed    : 11/26/2019 4:32:26 PM by 2.025
Analysis Method : C:\HPCHEM\1\METHODS\ACETODF.M
Last changed    : 6/29/2020 4:09:35 PM by 2.025
                  (modified after loading)
  
```

acetophenone transferhydrogenation



Area Percent Report

```

=====
Sorted By       :      Signal
Multiplier      :      1.0000
Dilution       :      1.0000
Use Multiplier & Dilution Factor with ISTDs
  
```

Signal 1: FID1 A,

Peak #	RetTime [min]	Type	Width [min]	Area [pA*s]	Height [pA]	Area %
1	1.590	BV	0.0184	55.01823	51.60807	0.04251
2	1.752	VB S	0.0177	1.26399e5	1.25912e5	97.67346
3	2.652	VV T	0.0211	2955.75684	2276.73975	2.28402

Totals : 1.29410e5 1.28240e5

Results obtained with enhanced integrator!

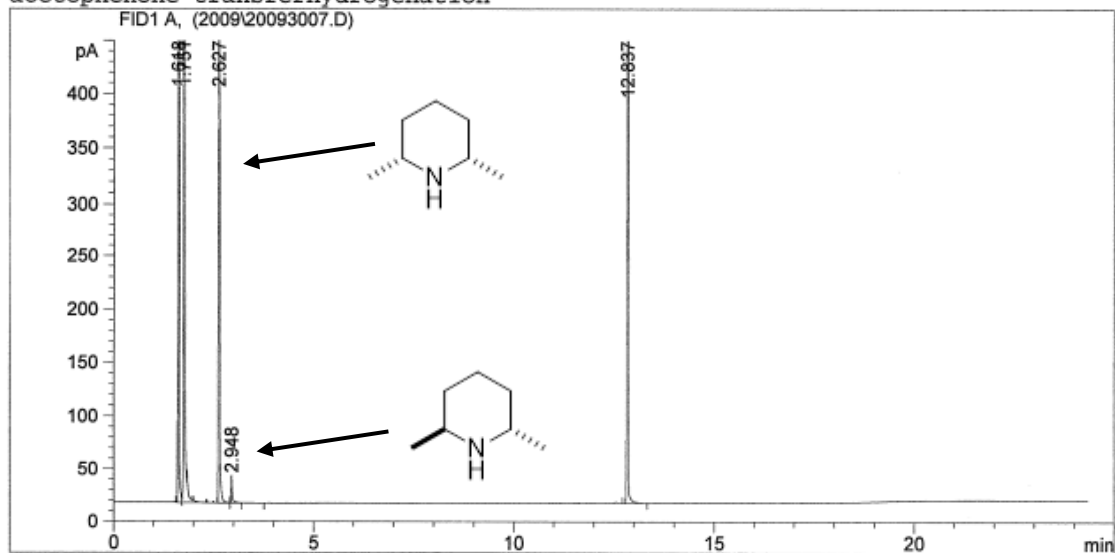
*** End of Report ***

```

=====
Injection Date   : 9/26/2020 10:13:02 AM           Seq. Line :    7
Sample Name     : JH-1747                          Location  : Vial 6
Acq. Operator   : 2.025                            Inj       :    1
Acq. Instrument : GC Lab 2.025                      Inj Volume: 1 µl
Acq. Method     : C:\HPCHEM\1\METHODS\ACETODF.M
Last changed    : 11/26/2019 4:32:26 PM by 2.025
Analysis Method : C:\HPCHEM\1\METHODS\ACETODF.M
Last changed    : 8/31/2020 11:57:07 AM by 2.025
                  (modified after loading)

```

acetophenone transferhydrogenation



=====
Area Percent Report
=====

```

Sorted By           :      Signal
Multiplier          :      1.0000
Dilution            :      1.0000
Use Multiplier & Dilution Factor with ISTDs

```

Signal 1: FID1 A,

Peak #	RetTime [min]	Type	Width [min]	Area [pA*s]	Height [pA]	Area %
1	1.618	BV S	0.0217	1.70913e4	2.05126e4	14.49345
2	1.751	VB S	0.0146	9.76460e4	1.11319e5	82.80398
3	2.627	VV T	0.0229	1851.57349	1280.53784	1.57014
4	2.948	VV T	0.0311	51.46262	23.91644	0.04364
5	12.837	VB	0.0345	1283.95715	611.54700	1.08880

Totals : 1.17924e5 1.33748e5

Results obtained with enhanced integrator!

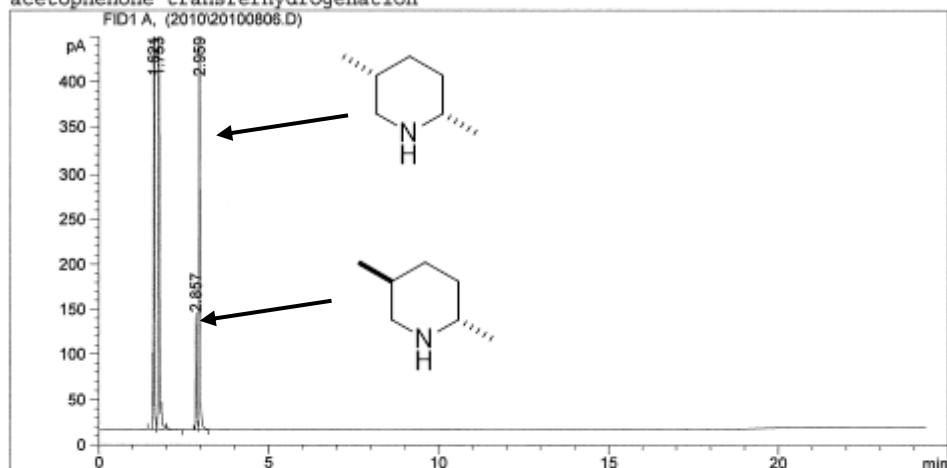
=====
*** End of Report ***

```

=====
Injection Date : 10/4/2020 9:58:36 AM      Seq. Line : 6
Sample Name    : JH-1821                    Location  : Vial 5
Acq. Operator  : 2.025                      Inj      : 1
Acq. Instrument : GC Lab 2.025              Inj Volume : 1 µl
Acq. Method    : C:\HPCHEM\1\METHODS\ACETODF.M
Last changed   : 11/26/2019 4:32:26 PM by 2.025
Analysis Method : C:\HPCHEM\1\METHODS\ACETODF.M
Last changed   : 8/31/2020 11:57:07 AM by 2.025
                (modified after loading)

```

acetophenone transferhydrogenation



=====
Area Percent Report
=====

```

Sorted By      : Signal
Multiplier     : 1.0000
Dilution      : 1.0000
Use Multiplier & Dilution Factor with ISTDs

```

Signal 1: FID1 A,

Peak #	RetTime [min]	Type	Width [min]	Area [pA*s]	Height [pA]	Area %
1	1.621	BV S	0.0172	1.15933e4	1.02429e4	9.42772
2	1.753	VB S	0.0166	1.10207e5	1.10581e5	89.62085
3	2.857	VV	0.0253	207.08939	125.42107	0.16841
4	2.959	VV	0.0281	962.89215	558.68451	0.78303

Totals : 1.22971e5 1.21508e5

Results obtained with enhanced integrator!

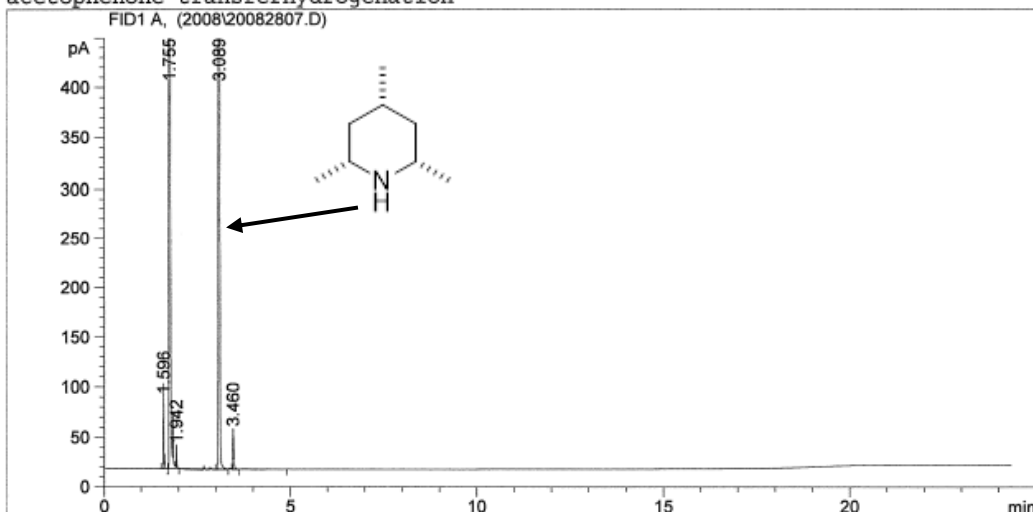
=====
*** End of Report ***

```

=====
Injection Date   : 8/24/2020 11:27:29 AM      Seq. Line :    7
Sample Name     : JH-1621                    Location  : Vial 6
Acq. Operator  : 2.025                       Inj       :    1
Acq. Instrument : GC Lab 2.025                Inj Volume: 1 µl
Acq. Method    : C:\HPCHEM\1\METHODS\ACETODF.M
Last changed   : 11/26/2019 4:32:26 PM by 2.025
Analysis Method : C:\HPCHEM\1\METHODS\ACETODF.M
Last changed   : 7/16/2020 10:52:36 AM by 2.025
                  (modified after loading)

```

acetophenone transferhydrogenation



=====
Area Percent Report
=====

```

Sorted By      :      Signal
Multiplier    :      1.0000
Dilution      :      1.0000
Use Multiplier & Dilution Factor with ISTDs

```

Signal 1: FID1 A,

Peak #	RetTime [min]	Type	Width [min]	Area [pA*s]	Height [pA]	Area %
1	1.596	BV	0.0156	69.09981	69.76647	0.05378
2	1.755	VB S	0.0149	1.23894e5	1.32977e5	96.42382
3	1.942	BV T	0.0161	20.44602	19.66970	0.01591
4	3.089	PV T	0.0241	4433.62988	2851.16577	3.45058
5	3.460	VV T	0.0299	71.83572	38.35253	0.05591

Totals : 1.28489e5 1.35956e5

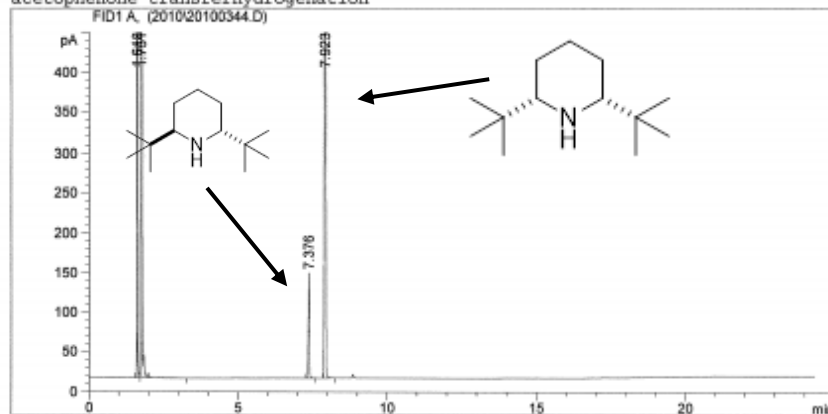
Results obtained with enhanced integrator!

=====
*** End of Report ***

```

-----
Injection Date : 9/30/2020 10:49:35 AM      Seq. Line : 4
Sample Name    : JH-1788                    Location  : Vial 3
Acq. Operator  : 2.025                      Inj      : 1
Acq. Instrument : GC Lab 2.025              Inj Volume : 1 µl
Acq. Method    : C:\HPCHEM\1\METHODS\ACETODF.M
Last changed   : 11/26/2019 4:32:26 PM by 2.025
Analysis Method : C:\HPCHEM\1\METHODS\ACETODF.M
Last changed   : 8/31/2020 11:57:07 AM by 2.025
                (modified after loading)
  
```

acetophenone transferhydrogenation



Area Percent Report

```

-----
Sorted By      : Signal
Multiplier    : 1.0000
Dilution      : 1.0000
Use Multiplier & Dilution Factor with ISTDs
  
```

Signal 1: FID1 A,

Peak #	RetTime [min]	Type	Width [min]	Area [pA*s]	Height [pA]	Area %
1	1.618	BV S	0.0212	1.13749e4	1.43961e4	9.30941
2	1.751	VB S	0.0149	1.07923e5	1.21010e5	88.32644
3	7.376	PB	0.0371	307.07718	132.37297	0.25132
4	7.923	BB	0.0402	2581.60083	998.73163	2.11283

Totals : 1.22187e5 1.36538e5

Results obtained with enhanced integrator!

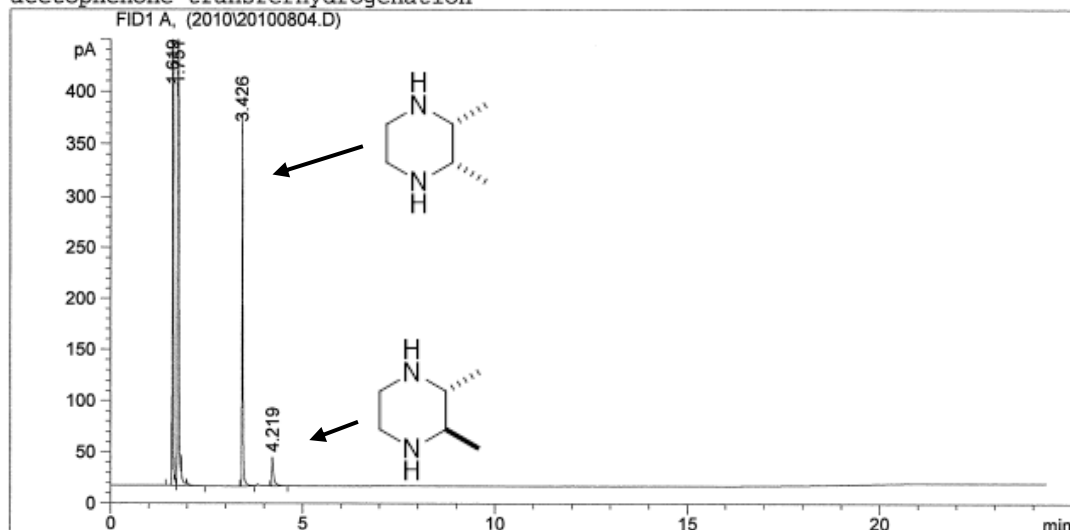
*** End of Report ***

```

=====
Injection Date   : 10/4/2020 8:59:17 AM           Seq. Line :    4
Sample Name     : JH-1819                       Location  : Vial 3
Acq. Operator   : 2.025                         Inj       :    1
Acq. Instrument : GC Lab 2.025                  Inj Volume: 1 µl
Acq. Method     : C:\HPCHEM\1\METHODS\ACETODF.M
Last changed    : 11/26/2019 4:32:26 PM by 2.025
Analysis Method : C:\HPCHEM\1\METHODS\ACETODF.M
Last changed    : 8/31/2020 11:57:07 AM by 2.025
                  (modified after loading)

```

acetophenone transferhydrogenation



=====
Area Percent Report
=====

```

Sorted By      :      Signal
Multiplier     :      1.0000
Dilution       :      1.0000
Use Multiplier & Dilution Factor with ISTDs

```

Signal 1: FID1 A,

Peak #	RetTime [min]	Type	Width [min]	Area [pA*s]	Height [pA]	Area %
1	1.619	BV S	0.0210	1.02491e4	1.33568e4	8.69868
2	1.751	VB S	0.0166	1.06886e5	1.17101e5	90.71736
3	3.426	BV	0.0279	595.60693	349.63690	0.50551
4	4.219	VB	0.0464	92.43570	28.11249	0.07845

Totals : 1.17823e5 1.30836e5

Results obtained with enhanced integrator!

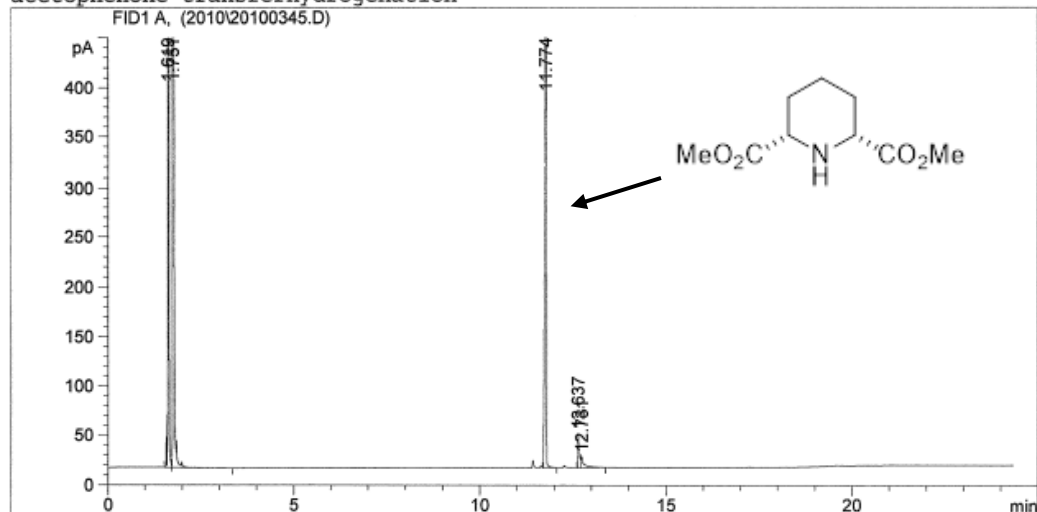
=====
*** End of Report ***

```

=====
Injection Date : 9/30/2020 11:19:13 AM      Seq. Line : 5
Sample Name    : JH-1789                    Location  : Vial 4
Acq. Operator  : 2.025                      Inj      : 1
Acq. Instrument : GC Lab 2.025              Inj Volume : 1 µl
Acq. Method    : C:\HPCHEM\1\METHODS\ACETODF.M
Last changed   : 11/26/2019 4:32:26 PM by 2.025
Analysis Method : C:\HPCHEM\1\METHODS\ACETODF.M
Last changed   : 8/31/2020 11:57:07 AM by 2.025
                (modified after loading)

```

acetophenone transferhydrogenation



=====
Area Percent Report
=====

```

Sorted By      :      Signal
Multiplier     :      1.0000
Dilution      :      1.0000
Use Multiplier & Dilution Factor with ISTDs

```

Signal 1: FID1 A,

Peak #	RetTime [min]	Type	Width [min]	Area [pA*s]	Height [pA]	Area %
1	1.619	BV S	0.0218	1.80214e4	2.14401e4	15.69779
2	1.751	VB S	0.0161	9.50729e4	1.09756e5	82.81477
3	11.774	VB	0.0420	1547.73254	563.97797	1.34818
4	12.637	VV	0.0370	90.62809	34.08140	0.07894
5	12.731	VB	0.0834	69.25517	10.71366	0.06033

Totals : 1.14802e5 1.31805e5

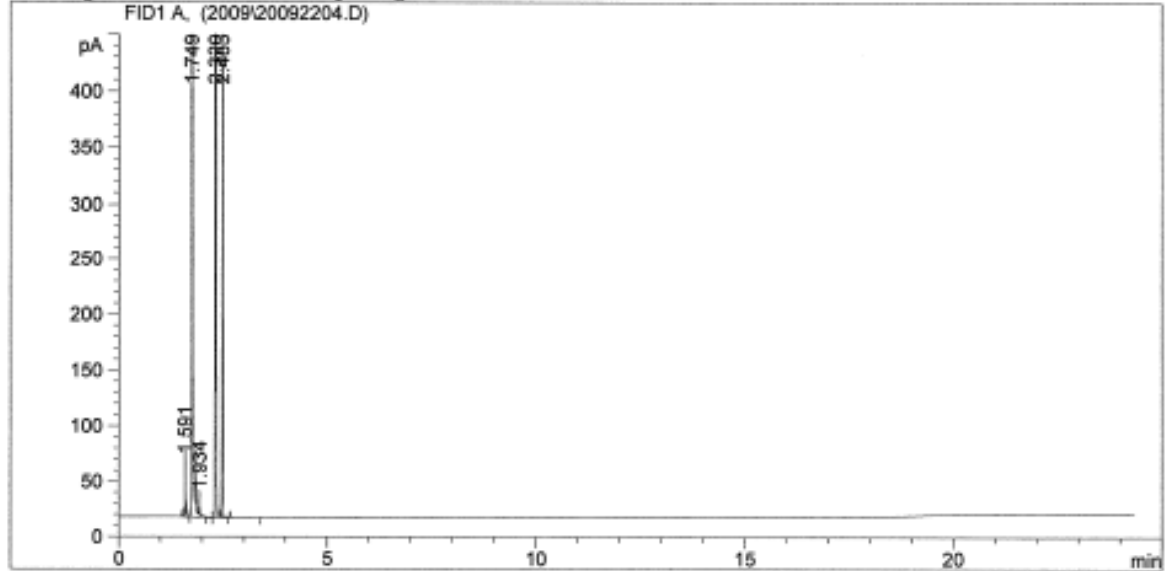
Results obtained with enhanced integrator!

=====
*** End of Report ***

```

=====
Injection Date   : 9/18/2020 8:53:39 AM      Seq. Line   :    4
Sample Name     : JH-1684                   Location    : Vial 3
Acq. Operator   : 2.025                     Inj         :    1
Acq. Instrument : GC Lab 2.025              Inj Volume  : 1 µl
Acq. Method     : C:\HPCHEM\1\METHODS\ACETODF.M
Last changed    : 11/26/2019 4:32:26 PM by 2.025
Analysis Method : C:\HPCHEM\1\METHODS\ACETODF.M
Last changed    : 8/31/2020 11:57:07 AM by 2.025
                  (modified after loading)
  
```

acetophenone transferhydrogenation



=====
Area Percent Report
=====

```

Sorted By       :      Signal
Multiplier      :      1.0000
Dilution        :      1.0000
Use Multiplier & Dilution Factor with ISTDs
  
```

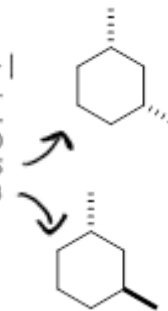
Signal 1: FID1 A,

Peak #	RetTime [min]	Type	Width [min]	Area [pA*s]	Height [pA]	Area %
1	1.591	BV	0.0264	55.42424	52.05882	0.04151
2	1.749	VP S	0.0168	1.29767e5	1.40413e5	97.18591
3	1.934	BV T	0.0140	15.22369	17.82849	0.01140
4	2.320	VB S	0.0166	3168.33813	2925.35522	2.37286
5	2.483	BV T	0.0193	518.50946	454.47427	0.38833

Totals : 1.33524e5 1.43862e5

Results obtained with enhanced integrator!

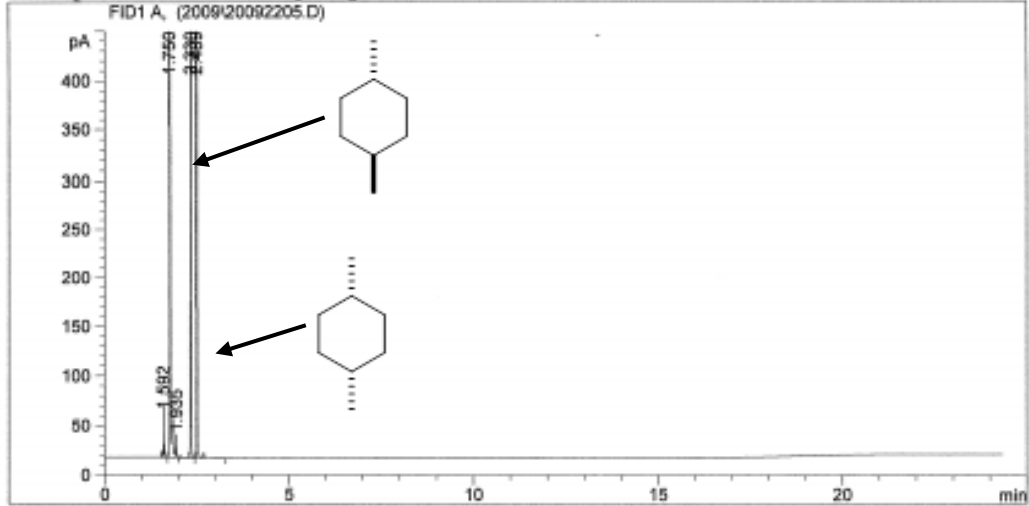
=====
*** End of Report ***



```

=====
Injection Date : 9/18/2020 9:23:12 AM      Seq. Line : 5
Sample Name    : JH-1685                    Location  : Vial 4
Acq. Operator : 2.025                       Inj      : 1
Acq. Instrument : GC Lab 2.025              Inj Volume : 1 µl
Acq. Method    : C:\HPCHEM\1\METHODS\ACETODF.M
Last changed   : 11/26/2019 4:32:26 PM by 2.025
Analysis Method : C:\HPCHEM\1\METHODS\ACETODF.M
Last changed   : 8/31/2020 11:57:07 AM by 2.025
                  (modified after loading)
    
```

acetophenone transferhydrogenation



Area Percent Report

```

Sorted By      : Signal
Multiplier     : 1.0000
Dilution      : 1.0000
Use Multiplier & Dilution Factor with ISTDs
    
```

Signal 1: FID1 A,

Peak #	RetTime [min]	Type	Width [min]	Area [pA*s]	Height [pA]	Area %
1	1.592	BV	0.0278	51.68422	43.67772	0.03899
2	1.750	VV S	0.0155	1.26869e5	1.36421e5	95.71655
3	1.935	BV T	0.0185	19.95356	18.66006	0.01505
4	2.330	FV T	0.0188	1329.06775	1211.62903	1.00272
5	2.489	VB S	0.0195	4276.83350	3698.54810	3.22668

Totals : 1.32546e5 1.41394e5

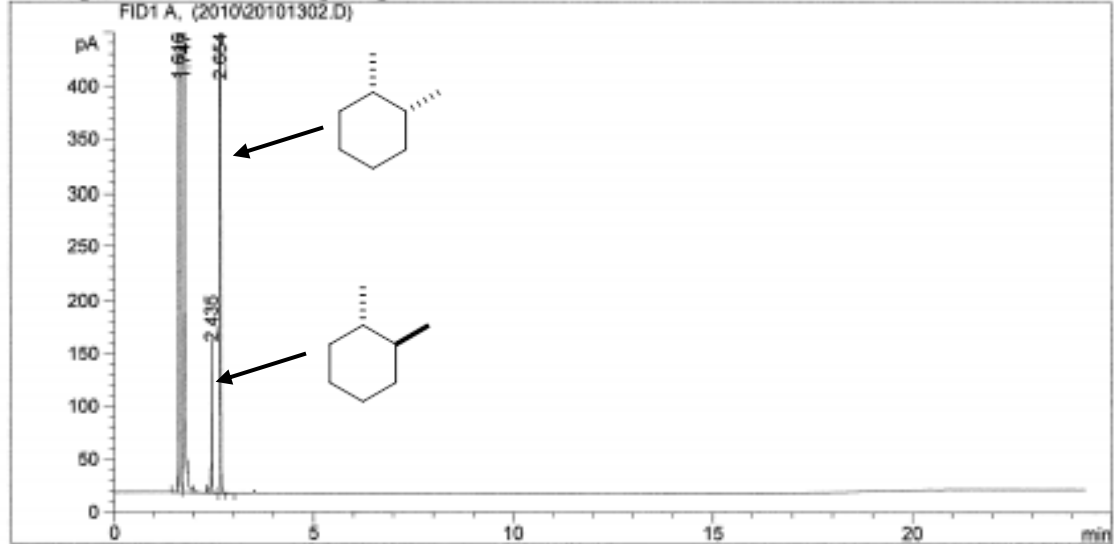
Results obtained with enhanced integrator!

*** End of Report ***

```

=====
Injection Date : 10/9/2020 8:19:44 AM          Seq. Line : 2
Sample Name    : JH-1827                      Location  : Vial 1
Acq. Operator : 2.025                         Inj      : 1
Acq. Instrument : GC Lab 2.025                Inj Volume : 1 µl
Acq. Method   : C:\HPCHEM\1\METHODS\ACETODF.M
Last changed  : 11/26/2019 4:32:26 PM by 2.025
Analysis Method : C:\HPCHEM\1\METHODS\ACETODF.M
Last changed  : 8/31/2020 11:57:07 AM by 2.025
                (modified after loading)
    
```

acetophenone transferhydrogenation



Area Percent Report

```

=====
Sorted By      : Signal
Multiplier    : 1.0000
Dilution      : 1.0000
Use Multiplier & Dilution Factor with ISTDs
    
```

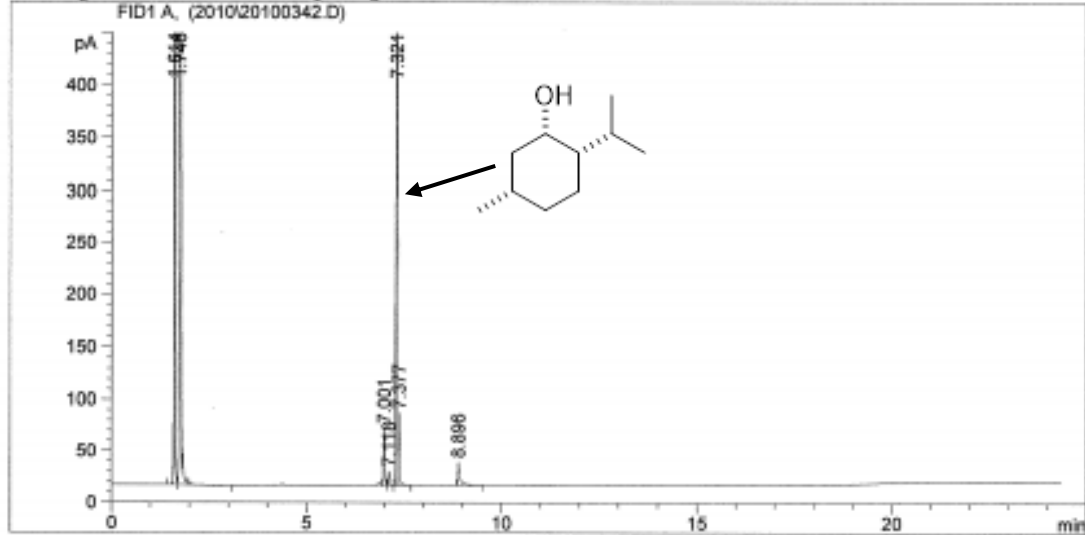
Signal 1: FID1 A,

Peak #	RetTime [min]	Type	Width [min]	Area [pA*s]	Height [pA]	Area %
1	1.616	BV S	0.0170	1.57195e4	1.66438e4	12.87838
2	1.747	VB S	0.0150	1.03942e5	1.09967e5	85.15561
3	2.435	PV T	0.0203	170.25447	138.83720	0.13948
4	2.654	VV T	0.0211	2229.48560	1718.13379	1.82653

```

-----
Injection Date   : 9/30/2020 9:50:22 AM           Seq. Line :    2
Sample Name     : JH-1786                         Location  : Vial 1
Acq. Operator  : 2.025                            Inj       :    1
Acq. Instrument : GC Lab 2.025                    Inj Volume: 1 µl
Acq. Method    : C:\HPCHEM\1\METHODS\ACETODP.M
Last changed   : 11/26/2019 4:32:26 PM by 2.025
Analysis Method: C:\HPCHEM\1\METHODS\ACETODP.M
Last changed   : 8/31/2020 11:57:07 AM by 2.025
                (modified after loading)
  
```

acetophenone transferhydrogenation



 Area Percent Report

```

Sorted By      :      Signal
Multiplier    :      1.0000
Dilution      :      1.0000
Use Multiplier & Dilution Factor with ISTDs
  
```

Signal 1: FID1 A,

Peak #	RetTime [min]	Type	Width [min]	Area [pA*s]	Height [pA]	Area %
1	1.614	BV S	0.0166	1.16173e4	1.07806e4	9.19376
2	1.746	VB S	0.0165	1.12763e5	1.14055e5	89.23890
3	7.001	VV	0.0356	130.59734	55.12947	0.10335
4	7.118	VV	0.0389	33.40866	13.47223	0.02644
5	7.321	VV	0.0348	1580.62585	687.07068	1.25089
6	7.377	VV	0.0328	147.36258	69.35233	0.11662
7	8.896	PB	0.0561	88.50480	21.46785	0.07004

Totals : 1.26360e5 1.25682e5

Results obtained with enhanced integrator!

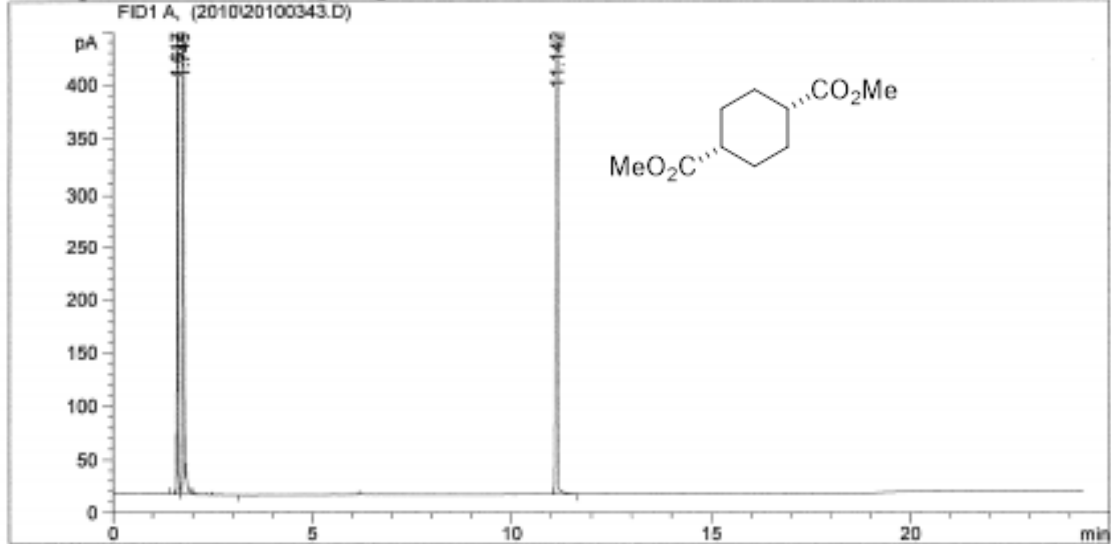
 *** End of Report ***

```

-----
Injection Date : 9/30/2020 10:19:58 AM      Seq. Line : 3
Sample Name    : JH-1787                    Location  : Vial 2
Acq. Operator  : 2.025                      Inj      : 1
Acq. Instrument : GC Lab 2.025              Inj Volume : 1 µl
Acq. Method    : C:\HPCHEM\1\METHODS\ACETODF.M
Last changed   : 11/26/2019 4:32:26 PM by 2.025
Analysis Method : C:\HPCHEM\1\METHODS\ACETODF.M
Last changed   : 8/31/2020 11:57:07 AM by 2.025
                (modified after loading)

```

acetophenone transferhydrogenation



Area Percent Report

```

Sorted By      : Signal
Multiplier     : 1.0000
Dilution       : 1.0000
Use Multiplier & Dilution Factor with ISTDs

```

Signal 1: FID1 A,

Peak #	RetTime [min]	Type	Width [min]	Area [pA*s]	Height [pA]	Area %
1	1.617	BV S	0.0160	1.49415e4	1.75060e4	12.28508
2	1.749	VB S	0.0163	1.04403e5	1.18089e5	85.84086
3	11.142	BB	0.0462	2279.30884	777.50616	1.87407

Totals : 1.21624e5 1.36373e5

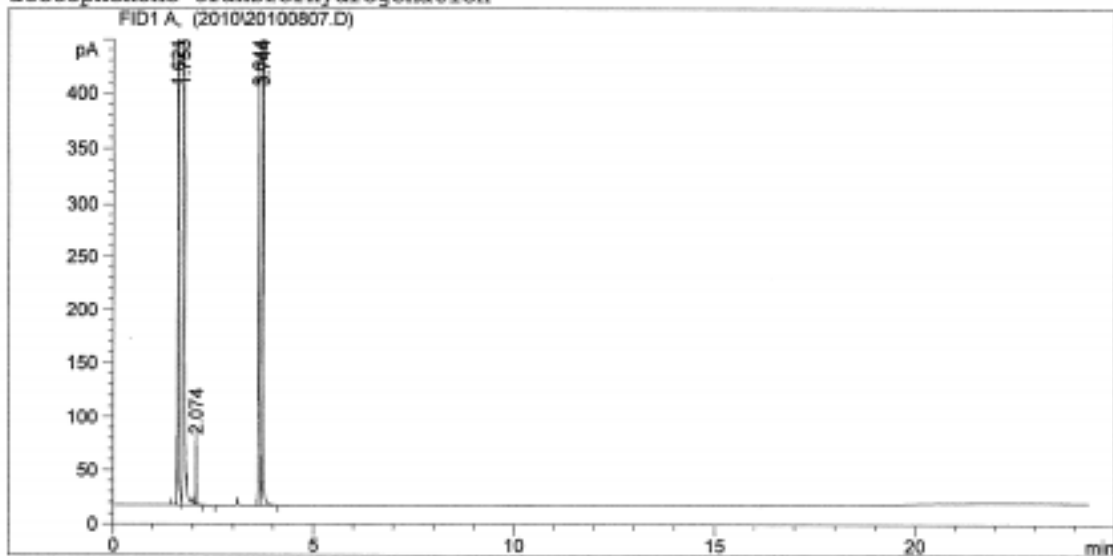
Results obtained with enhanced integrator!

*** End of Report ***

```

=====
Injection Date   : 10/4/2020 10:28:12 AM      Seq. Line :    7
Sample Name     : JH-1822                    Location  : Vial 6
Acq. Operator   : 2.025                      Inj       :    1
Acq. Instrument : GC Lab 2.025               Inj Volume: 1 µl
Acq. Method     : C:\HPCHEM\1\METHODS\ACETODF.M
Last changed    : 11/26/2019 4:32:26 PM by 2.025
Analysis Method : C:\HPCHEM\1\METHODS\ACETODF.M
Last changed    : 8/31/2020 11:57:07 AM by 2.025
                  (modified after loading)
  
```

acetophenone transferhydrogenation



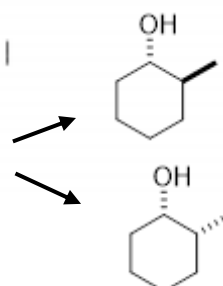
=====
Area Percent Report
=====

```

Sorted By      :      Signal
Multiplier     :      1.0000
Dilution       :      1.0000
Use Multiplier & Dilution Factor with ISTDs
  
```

Signal 1: FID1 A,

Peak #	RetTime [min]	Type	Width [min]	Area [pA*s]	Height [pA]	Area %
1	1.621	BV S	0.0175	1.57359e4	1.35763e4	13.08623
2	1.753	VB S	0.0161	1.02073e5	1.05892e5	84.88560
3	2.074	VB T	0.0161	62.36086	59.89599	0.05186
4	3.644	PV	0.0296	742.03790	400.00726	0.61709
5	3.744	VB	0.0274	1634.42041	889.44635	1.35921

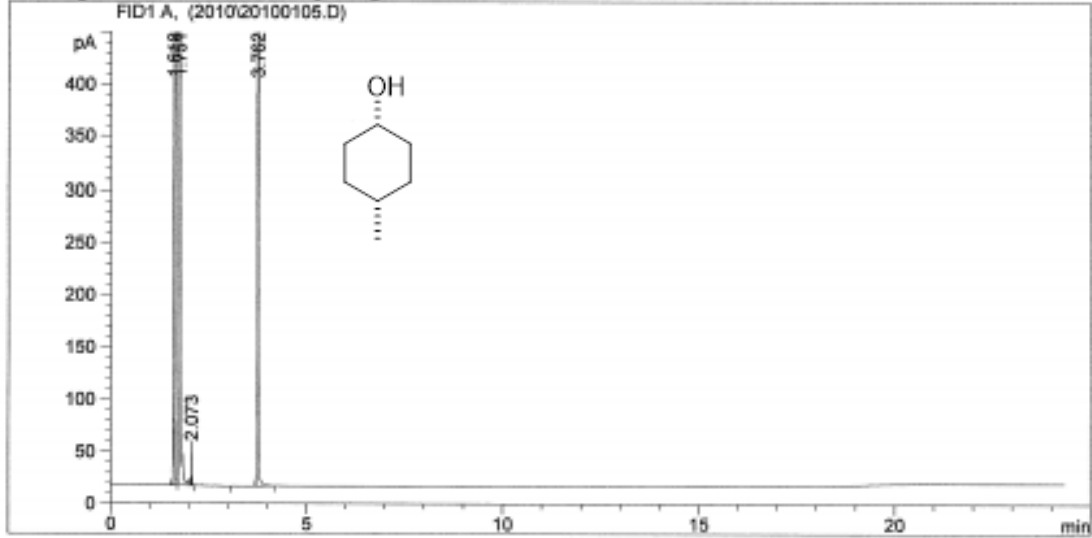


```

=====
Injection Date   : 9/27/2020 9:15:00 AM           Seq. Line :    5
Sample Name     : JH-1752                        Location  : Vial 4
Acq. Operator   : 2.025                          Inj       :    1
Acq. Instrument : GC Lab 2.025                   Inj Volume: 1 µl
Acq. Method     : C:\HPCHEM\1\METHODS\ACBTODF.M
Last changed    : 11/26/2019 4:32:26 PM by 2.025
Analysis Method : C:\HPCHEM\1\METHODS\ACBTODF.M
Last changed    : 8/31/2020 11:57:07 AM by 2.025
                  (modified after loading)

```

acetophenone transferhydrogenation



=====
Area Percent Report
=====

```

Sorted By      :      Signal
Multiplier     :      1.0000
Dilution       :      1.0000
Use Multiplier & Dilution Factor with ISTDs

```

Signal 1: FID1 A,

Peak #	RetTime [min]	Type	Width [min]	Area [pA*s]	Height [pA]	Area %
1	1.618	BV S	0.0218	1.36465e4	1.61968e4	11.30971
2	1.751	VB S	0.0152	1.05169e5	1.15653e5	87.16023
3	2.073	VB T	0.0168	37.59240	37.29895	0.03116
4	3.762	VB	0.0297	1808.60583	973.05389	1.49890

Totals : 1.20662e5 1.32860e5

Results obtained with enhanced integrator!

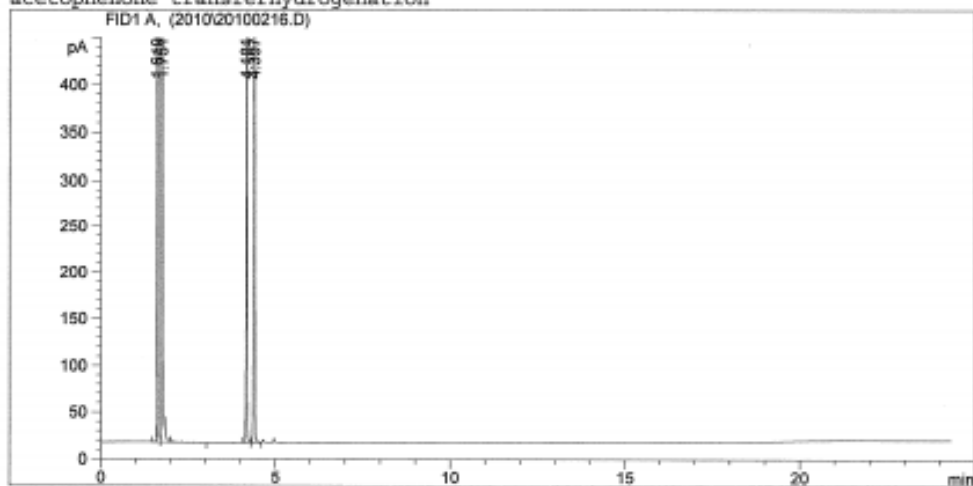
=====
*** End of Report ***

```

=====
Injection Date : 9/28/2020 2:49:22 PM      Seq. Line : 16
Sample Name    : JH-1761                   Location  : Vial 5
Acq. Operator  : 2.025                     Inj      : 1
Acq. Instrument : GC Lab 2.025             Inj Volume : 1 µl
Acq. Method    : C:\HPCHEM\1\METHODS\ACETODF.M
Last changed   : 11/26/2019 4:32:26 PM by 2.025
Analysis Method : C:\HPCHEM\1\METHODS\ACETODF.M
Last changed   : 8/31/2020 11:57:07 AM by 2.025
                (modified after loading)

```

acetophenone transferhydrogenation



=====
Area Percent Report
=====

```

Sorted By      :      Signal
Multiplier     :      1.0000
Dilution       :      1.0000
Use Multiplier & Dilution Factor with ISTDs

```

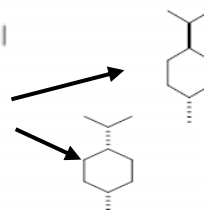
Signal 1: FID1 A,

Peak #	RetTime [min]	Type	Width [min]	Area [pA*s]	Height [pA]	Area %
1	1.619	BV S	0.0213	1.87048e4	2.34876e4	16.22677
2	1.751	VB S	0.0160	9.34127e4	1.08942e5	81.03703
3	4.181	BV	0.0298	846.13733	453.63834	0.73404
4	4.397	VV	0.0304	2307.92432	1199.37781	2.00216

Totals : 1.15272e5 1.34083e5

Results obtained with enhanced integrator!

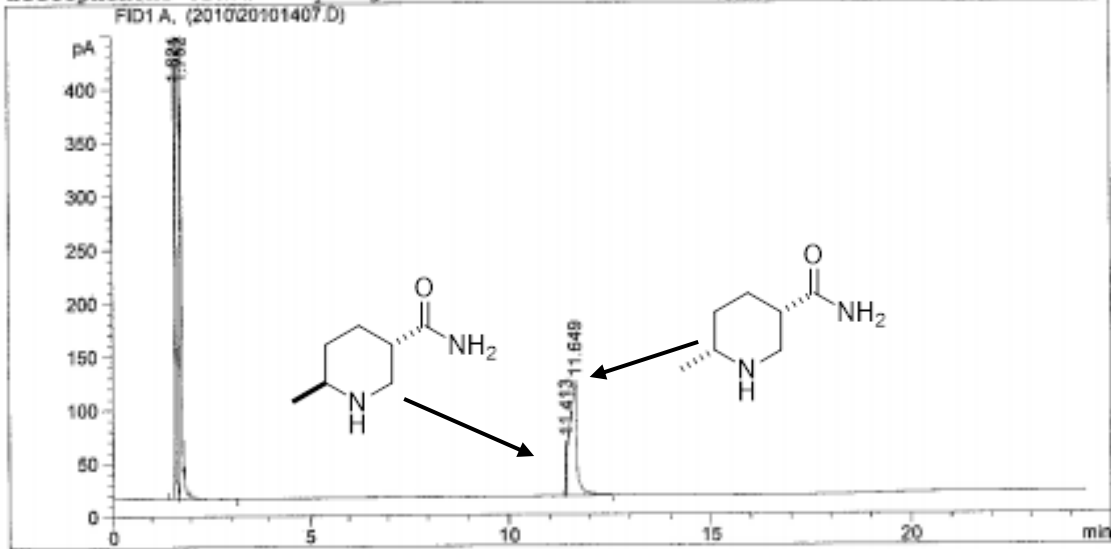
=====
*** End of Report ***



```

-----
Injection Date   : 10/10/2020 10:53:20 AM      Seq. Line :    7
Sample Name     : JH-1842                      Location  : Vial 6
Acq. Operator   : 2.025                       Inj       :    1
Acq. Instrument : GC Lab 2.025                 Inj Volume: 1 µl
Acq. Method     : C:\HPCHEM\1\METHODS\ACETODF.M
Last changed    : 11/26/2019 4:32:26 PM by 2.025
Analysis Method : C:\HPCHEM\1\METHODS\ACETODF.M
Last changed    : 8/31/2020 11:57:07 AM by 2.025
                  (modified after loading)
    
```

acetophenone transferhydrogenation



Area Percent Report

```

-----
Sorted By       :      Signal
Multiplier      :      1.0000
Dilution        :      1.0000
Use Multiplier & Dilution Factor with ISTDs
    
```

Signal 1: FID1 A,

Peak #	RetTime [min]	Type	Width [min]	Area [pA*s]	Height [pA]	Area %
1	1.621	BV S	0.0172	1.68441e4	1.48339e4	14.57898
2	1.752	VB S	0.0157	9.71784e4	1.03437e5	84.11049
3	11.413	VV	0.0314	103.56152	51.60732	0.08964
4	11.649	VB	0.1735	1410.57458	105.84410	1.22089

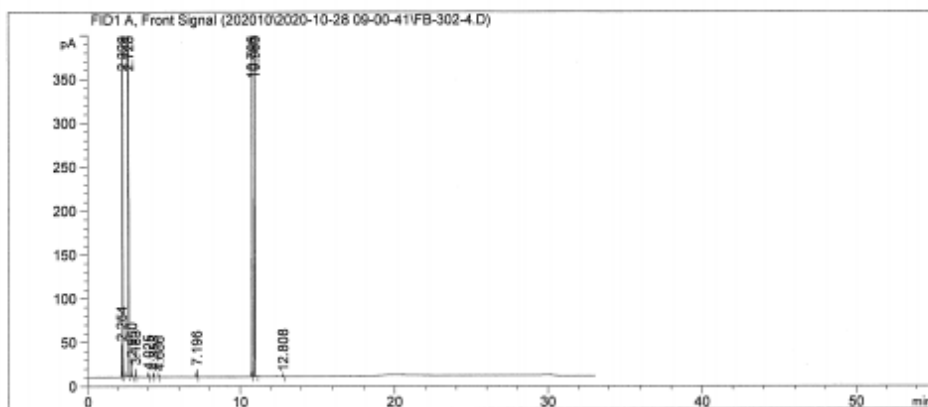
Totals : 1.15537e5 1.18428e5

Results obtained with enhanced integrator!

*** End of Report ***

Inj Volume : 1 µl

Acq. Method : C:\CHEM32\1\DATA\202010\2020-10-28 09-00-41\STANDARDMTHNEW.M
 Last changed : 6/25/2020 1:31:14 PM by Lab 2.112
 Analysis Method : C:\CHEM32\1\METHODS\STANDARDMTHNEW.M
 Last changed : 6/25/2020 1:31:14 PM by Lab 2.112
 Method Info : HP5 (30x0.25x0.25): 50/8-120/0/15-200/0/25-300/10/50-310/5
 ramped flow: 1/29/1-2; 2601320d; Split 100/1



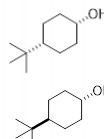
=====
 Area Percent Report
 =====

Sorted By : Signal
 Multiplier : 1.0000
 Dilution : 1.0000
 Use Multiplier & Dilution Factor with ISTDs

Signal 1: FID1 A, Front Signal

Peak #	RetTime [min]	Type	Width [min]	Area [pA*s]	Height [pA]	Area %
1	2.254	BV	0.0210	48.33932	36.67108	0.06661
2	2.328	VB S	0.0228	1.22959e4	9171.15918	16.94439
3	2.728	BB S	0.0377	5.80230e4	2.80486e4	79.95904
4	2.950	BB	0.0149	18.00957	17.90711	0.02482
5	3.183	BB	0.0164	9.83066	9.25410	0.01355
6	4.025	BB	0.0272	7.33302	3.96686	0.01011
7	4.358	BB	0.0235	5.03555	3.43916	0.00694
8	4.686	BB	0.0242	3.90231	2.56023	0.00538
9	7.196	BB	0.0315	17.16701	8.50631	0.02366
10	10.796	BB	0.0310	1078.66724	547.71686	1.48647
11	10.963	BB	0.0298	1055.62805	543.75122	1.45472
12	12.808	BB	0.0300	3.14367	1.61006	0.00433

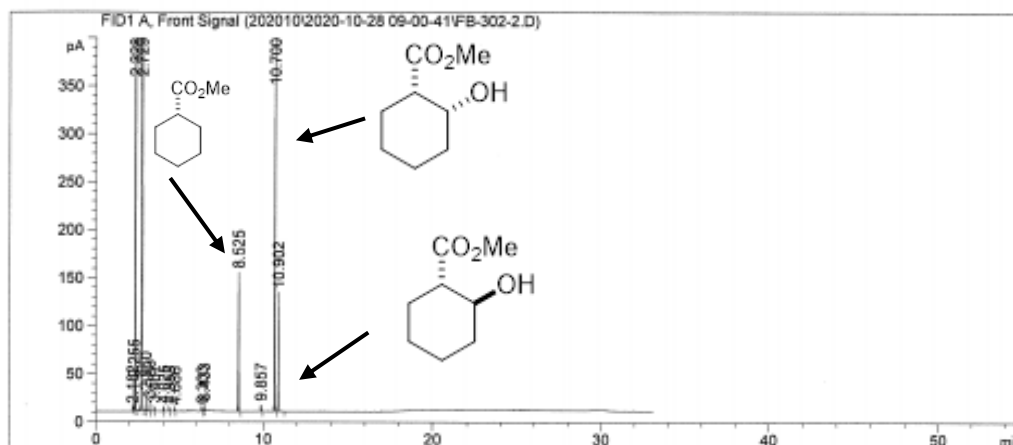
Totals : 7.25659e4 3.83951e4



```

=====
Acq. Operator   : Lab 2.112                      Seq. Line :    5
Acq. Instrument : GC Lab.133                    Location  : Vial 112
Injection Date  : 10/28/2020 12:09:27 PM        Inj       :    1
                                                Inj Volume: 1 µl
Acq. Method    : C:\CHEM32\1\DATA\202010\2020-10-28 09-00-41\STANDARDMTHNEW.M
Last changed   : 6/25/2020 1:31:14 PM by Lab 2.112
Analysis Method : C:\CHEM32\1\METHODS\STANDARDMTHNEW.M
Last changed   : 6/25/2020 1:31:14 PM by Lab 2.112
Method Info    : HP5 (30x0.25x0.25): 50/8-120/0/15-200/0/25-300/10/50-310/5
                ramped flow: 1/29/1-2; 2601320d; Split 100/1
=====

```



=====
Area Percent Report
=====

```

Sorted By      :      Signal
Multiplier     :      1.0000
Dilution      :      1.0000
Use Multiplier & Dilution Factor with ISTDs

```

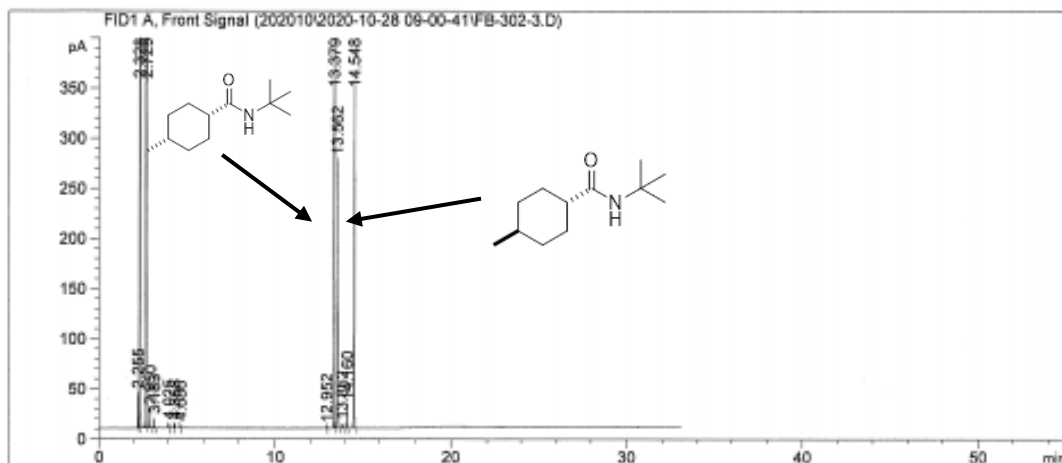
Signal 1: FID1 A, Front Signal

Peak #	RetTime [min]	Type	Width [min]	Area [pA*s]	Height [pA]	Area %
1	2.182	BB	0.0134	1.60084	1.99587	0.00224
2	2.255	BB	0.0199	35.78410	29.28092	0.05002
3	2.328	BB S	0.0226	1.20176e4	9103.11426	16.79971
4	2.729	BB S	0.0377	5.80192e4	2.80583e4	81.10642
5	2.950	BB	0.0137	16.14541	17.85486	0.02257
6	3.183	BB	0.0164	9.86035	9.30946	0.01378
7	3.467	BB	0.0186	4.71503	3.98543	0.00659
8	4.025	BB	0.0259	6.98088	3.85605	0.00976
9	4.358	BB	0.0232	4.91141	3.40992	0.00687
10	4.686	BB	0.0233	3.82488	2.52084	0.00535
11	6.303	BB	0.0282	5.88640	3.26649	0.00823
12	6.433	BB	0.0283	10.24480	5.65849	0.01432
13	8.525	BB	0.0309	284.34357	144.56508	0.39749
14	9.857	BB	0.0313	12.96850	6.26507	0.01813
15	10.700	BB	0.0314	884.20428	440.76797	1.23605
16	10.902	BB	0.0276	216.36839	123.68176	0.30247

```

=====
Acq. Operator   : Lab 2.112                      Seq. Line :    6
Acq. Instrument : GC Lab.133                     Location  : Vial 113
Injection Date  : 10/28/2020 12:49:31 PM        Inj       :    1
                                           Inj Volume: 1 µl
Acq. Method    : C:\CHEM32\1\DATA\202010\2020-10-28 09-00-41\STANDARDMTHNEW.M
Last changed   : 6/25/2020 1:31:14 PM by Lab 2.112
Analysis Method: C:\CHEM32\1\METHODS\STANDARDMTHNEW.M
Last changed   : 6/25/2020 1:31:14 PM by Lab 2.112
Method Info    : HP5 (30x0.25x0.25): 50/8-120/0/15-200/0/25-300/10/50-310/5
                  ramped flow: 1/29/1-2; 260i320d; Split 100/1
=====

```



```

=====
                          Area Percent Report
=====

```

```

Sorted By      :      Signal
Multiplier     :      1.0000
Dilution      :      1.0000
Use Multiplier & Dilution Factor with ISTDs

```

Signal 1: FID1 A, Front Signal

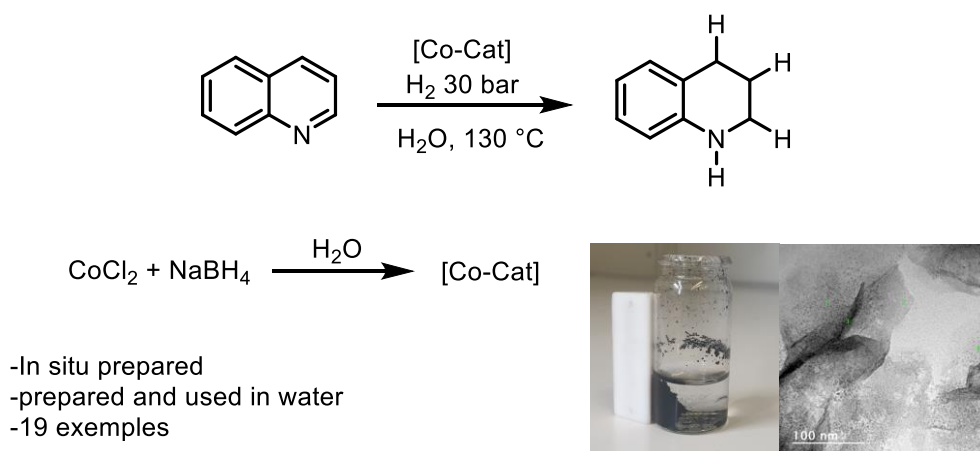
Peak #	RetTime [min]	Type	Width [min]	Area [pA*s]	Height [pA]	Area %
1	2.255	BB	0.0198	41.51150	34.14604	0.05724
2	2.328	BB S	0.0216	1.17139e4	8965.89746	16.15100
3	2.729	BB S	0.0378	5.81430e4	2.80585e4	80.16700
4	2.950	BB	0.0152	18.78766	18.27438	0.02590
5	3.183	BB	0.0162	9.88185	9.42479	0.01363
6	4.025	BB	0.0276	8.08025	4.28226	0.01114
7	4.358	BB	0.0234	6.50642	4.46289	0.00897
8	4.686	BB	0.0241	4.34820	2.85956	0.00600
9	12.952	BB	0.0303	2.86908	1.39971	0.00396
10	13.379	BB	0.0312	1541.43604	750.55096	2.12532
11	13.562	BB	0.0266	446.65369	268.02188	0.61584
12	13.852	BB	0.0310	8.83657	4.32429	0.01218
13	14.160	BB	0.0255	38.84357	23.71401	0.05356
14	14.548	BB	0.0247	542.70306	346.76047	0.74827

General Conclusion

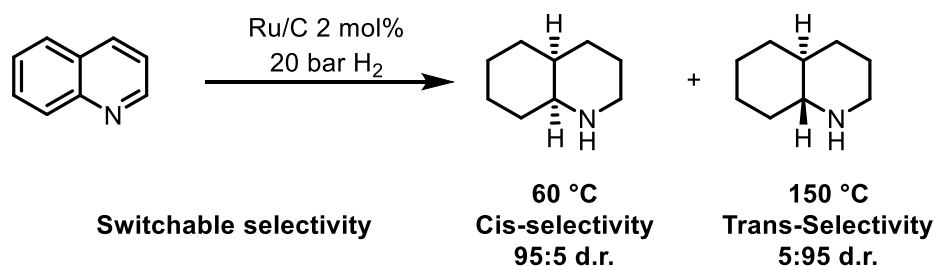
During this thesis we have tackled a number of challenging transformations ranging from the transformation of biosourced compounds to the selective hydrogenation of *N*-Heterocycles and arenes performed by heterogeneous catalysts.

In the first chapter, we synthesized and characterized eight different cobalt complexes for redox-neutral lignin cleavage. Unfortunately, we were not able to perform the reaction. Some results were obtained but we noticed that the catalyst was not involved in the reaction and that the base allowed the lignin to be cleaved.

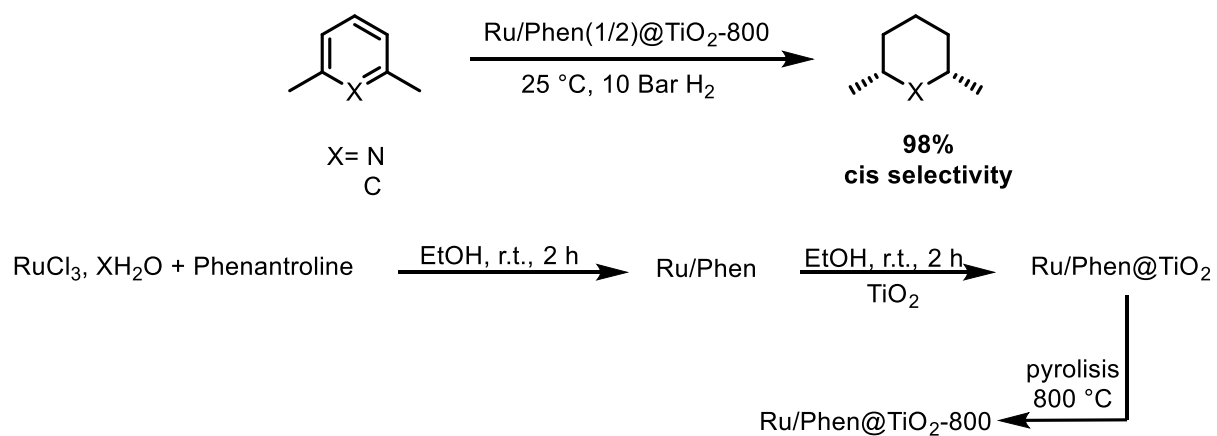
In the second chapter we turned our attention to other reactions that could be promoted by those catalysts. In particular, we performed with success the hydrogenation of quinoline into 1,2,3,4-tetrahydroquinoline. Initial tests with the cobalt pincer complexes showed the formation of black residue after the reaction and we quickly demonstrated the formation of cobalt particles. In situ generated particles including nanoparticles were prepared in a simple and straightforward manner from CoCl_2 and NaBH_4 and were found very efficient for the hydrogenation of a number of quinoline derivatives in water.



In a third part, we have developed a catalytic system based on commercially available Ru/C that allows the diastereoselective synthesis of decahydroquinoline from quinoline. Depending on the temperature of the catalytic system, we are able to obtain different diastereomers, the kinetic compound being favored at low temperature while the thermodynamic compound was obtained at higher temperature.



Finally, we have developed a new heterogeneous ruthenium-based catalyst capable of performing stereoselective hydrogenation of pyridine derivatives and aromatic derivatives under mild conditions. Indeed, this catalyst is able to promote the hydrogenation of a number of *N*-heterocycles and arenes at room temperature and 10 bar of hydrogen.



Titre : Catalyseurs moléculaires et nanostructurés pour la transformation de la lignine et de *N*-hétérocycles

Mots clés : Catalyse, Lignines, *N*-hétérocycles, Cobalt, Ruthénium.

Résumé : Le travail de recherche concerne l'utilisation de catalyseur à base de métaux de transition, spécifiquement le cobalt et le ruthénium pour la transformation de substrats de types lignines et *N*-hétérocycles. Un certain nombre de catalyseurs de cobalt supportés par des ligands « pince » bi-fonctionnels ont été synthétisés et caractérisés dans le but d'effectuer la coupure de la lignine. Les résultats obtenus n'étant pas satisfaisant, nous nous sommes tournés vers l'hydrogénation de composés *N*-hétérocycliques et plus particulièrement de la quinoléine. Nous avons dans un premier temps converti la quinoléine en 1,2,3,4-tétrahydroquinoléine par la formation *in situ* de particules de cobalt. Dans un second temps, nous avons effectué l'hydrogénation diastéréosélective de la quinoléine en décahydroquinoléine en utilisant un catalyseur de ruthénium commercial, le ruthénium sur charbon. Suivant la température utilisée nous sommes capables de choisir la sélectivité entre le produit *cis*-décahydroquinoléine et le produit *trans*-décahydroquinoléine. Enfin, nous avons développé un catalyseur hétérogène de ruthénium capable d'effectuer l'hydrogénation stéréosélective de pyridines et de groupements aromatiques dans des conditions douces.

Title : Molecular and Nanostructured Catalysts for Lignin and *N*-heterocycle Transformation

Keywords: Catalysis, Lignin, *N*-heterocycles, Cobalt, Ruthenium.

Abstract: Research work involves the use of catalysts based on transition metals, specifically cobalt and ruthenium for the transformation of lignin and *N*-heterocycle substrates. A number of cobalt catalysts supported by bi-functional "pincer" ligands have been synthesized and characterized for redox-Neutral lignin cleavage. The results obtained were not satisfactory and we turned our attention to the hydrogenation of *N*-heterocycle compounds and in particular quinoline. We converted quinoline into 1,2,3,4-tetrahydroquinolein by the *in situ* formation of cobalt particles. In a second step, we performed the hydrogenation of quinoline into decahydroquinoline using a commercially available ruthenium catalyst, ruthenium on charcoal. Depending on the temperature used, we are able to switch the selectivity toward the *cis*-decahydroquinoline or the *trans*-decahydroquinoline products. Finally, we have developed a heterogeneous ruthenium catalyst capable of performing stereoselective hydrogenation of pyridines and arenes under mild conditions.

Résumé :

Catalyseurs moléculaires et nanostructurés pour la transformation de la lignine et de *N*-hétérocycles

**Thèse présentée et soutenue à Rennes, Le 26 Janvier 2021 par
Hervochoch Julien**

Composition du Jury :

Examineurs : Karine Philippot Directrice de Recherche, LCC, Toulouse (France)

Axel Jacobi Von Wangelin Professeur, Université de Hambourg (Allemagne)

Alain Roucoux Professeur, Ecole Nationale Supérieure de Chimie de Rennes

Christophe Darcel Professeur, Université Rennes 1

Dir. de thèse : Cedric Fischmeister Ingénieur de Recherche, Université Rennes 1

Dir. de thèse : Matthias Beller Professeur, Leibniz-Institute für Katalysis, Rostock (Allemagne)

Le projet de thèse s'inscrit dans le développement durable. Le développement durable est la notion qui définit le besoin de transition et de changement dont a besoin notre planète et ses habitants pour vivre dans un monde plus équitable, en bonne santé et en respectant l'environnement¹. Il consiste en Le développement durable est un mode d'organisation de la société pour répondre le plus efficacement possible aux besoins du présent sans compromettre la capacité des générations futures de répondre aux leurs. Aujourd'hui, cette transition vers un modèle plus durable est nécessaire pour vivre dans un monde plus équitable et préserver notre planète et ses ressources naturelles. Le développement durable suppose un mode d'organisation basé sur 3 piliers essentiels :

- **La qualité environnementale** des activités humaines pour limiter les impacts environnementaux, préserver les écosystèmes et les ressources naturelles à long terme.
- **L'équité sociale** pour garantir à tous les membres de la société un accès aux ressources et services de base (éducation, santé, alimentation, logement...) pour satisfaire les besoins de l'humanité, réduire les inégalités et maintenir la cohésion sociale
- **L'efficacité économique** en diminuant l'extrême pauvreté et en garantissant l'emploi du plus grand nombre dans une activité économique dignement rémunérée. L'économie durable est une gestion saine des activités humaines sans préjudices pour l'Homme ou pour l'environnement.

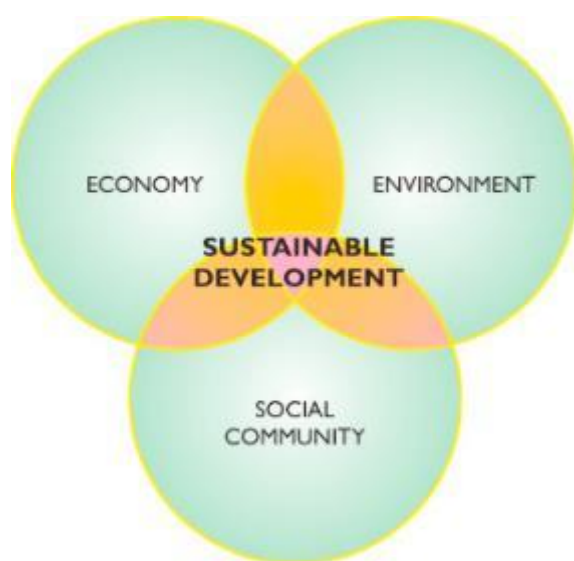


Figure 1: Pilier du développement durable.

La chimie et les chimistes peuvent avoir un impact dans le développement durable avec la chimie durable. La chimie durable est un concept scientifique qui vise à améliorer l'efficacité avec laquelle les ressources naturelles sont utilisées pour répondre aux besoins humains produits et services chimiques. La chimie durable englobe la conception, fabrication et utilisation de matériel efficace, sûr et le développement de produits et de procédés chimiques respectueux de l'environnement. La chimie durable est également un processus qui stimule

¹ Sylvain Antoniotti, Chimie verte – Chimie durable, Paris, Ellipses, 2013, 190 p.

l'innovation dans tous secteurs pour concevoir et découvrir de nouveaux produits chimiques et de procédés de production qui amélioreront les performances tout en atteignant les objectifs de protection et d'amélioration santé humaine et environnement. Pour cela, en 1998, Warner et Anastas² propose 12 principes qui sont maintenant appelé les 12 principes de la chimie verte, qui se décompose comme suit: utilisation de catalyseurs aussi sélectifs que possible; éviter le gaspillage; maximiser l'incorporation de tous les matériaux dans le produit final (économie d'atomes); production efficace; des produits peu ou non toxiques pour l'homme et l'environnement; réduire les accidents; réduire la dépense énergétique (température ordinaire et pression ordinaire); utiliser des matières premières renouvelables plutôt que celles qui s'épuisent; analyse en temps réel; éviter les modifications d'espèces; rendre les substances auxiliaires inutiles ou inoffensives pour la dégradation; produire des composés qui se dégradent après opération en dérivés inoffensifs pour l'environnement.



Les 12 principes de la chimie verte (Paul T. Anastas et John C. Warner, Green Chemistry: Theory and Practice, Oxford University Press, New York, 1998)

Figure 2: Les 12 principes de la chimie verte.

L'utilisation de ressources renouvelable est un point important et est très étudié dans l'optique de remplacer le pétrole. Le pétrole est une ressource qui n'est pas renouvelable à l'infini et les méthodes de transformations actuelles du pétrole ne sont pas bonne pour l'environnement, notamment par la production de dioxyde de carbone, qui est un gaz à effet de serre, responsable en partie du réchauffement climatique. Pour cela, quatre différentes générations de biomasse ont été développées. La première génération utilisant des produits alimentaires tels que la canne à sucre et le maïs, la deuxième génération utilisant des déchets issus de l'agriculture ou des procédés du bois, la troisième génération introduisant les algues et microalgues et enfin la quatrième génération utilisant des cultures génétiquement modifiées ou microalgues. L'une des applications de transformation de biomasse les plus connues et la synthèse de bioéthanol, utilisé comme bio-carburant. A l'heure actuelle, nous sommes capables de préparer du bioéthanol à partir des deux premières générations de biomasses. Lors de cette thèse, nous nous sommes particulièrement intéressés à la biomasse lignocellulosique, une biomasse de deuxième génération. Elle provient des déchets de l'agriculture et de bois. Elle consiste en trois composés majeurs³.

² P. T. Anastas, J. C. Warner, Green Chemistry, Theory and Practice, Oxford University Press, 1998

³ S. Laurichesse, L. Avérous, Progress in Polymer Science, 2014, 39, 1266-1290.

- La Cellulose
- L'hémicellulose
- La lignine

La lignine est biopolymères avec une teneur élevée en groupements aromatiques. Ce qui, par fragmentation, en fait un candidat idéal pour la synthèse de composé aromatique renouvelable. Il existe différentes façons de procéder à la fragmentation de la lignine. Nous avons choisi de procéder par transfert d'hydrogène. La réaction procède en deux étapes (Schéma 1). Dans un premier temps, le groupement hydroxyle va être déshydrogéné pour former la cétone correspondante et dans un second temps, l'hydrogène formé et réutiliser pour couper la liaison C-O présente dans la molécule⁴.

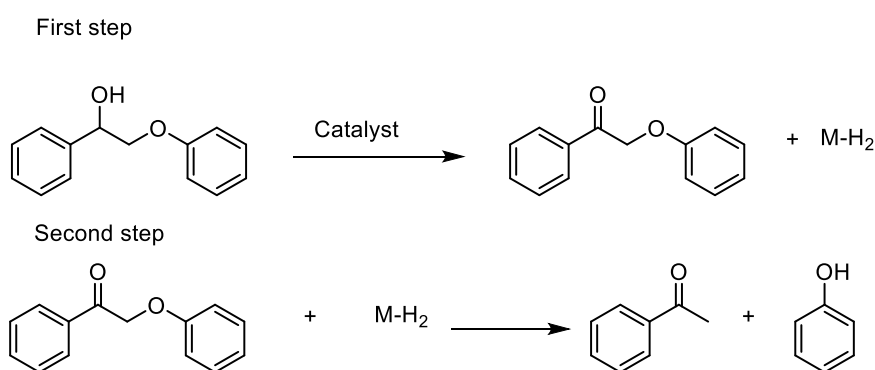


Schéma 1 : Fragmentation de la lignine par transfert d'hydrogène.

Pour cela, nous avons pour objectif d'utiliser des catalyseurs de cobalt supporté par des ligand bifonctionnels de type « Pince ». Ils sont notamment connus pour être actifs en hydrogénation et déshydrogénation⁵. Nous avons commencé notre investigation par la synthèse de catalyseur de cobalt supporté par différents ligands de type « PNP ». Les catalyseurs de Cobalts (II) étant paramagnétique, il est difficile de les caractériser par RMN. C'est pour cela que nous les avons analysés par diffractions des rayons X. Nous pouvons observer une particularité avec **Co-1**, où nous n'observons pas de coordinations entre l'azote de la pyridine et le centre métallique (Schéma 2).

⁴ M. Nichols, L. M. Bishop, R. G. Bergman, J. A. Ellman, J. Am. Chem. Soc., 2010, 132, 12554–12555.

⁵ Zhang, G. Leitus, Y. Ben-David, D. Milstein, Angew. Chem. Int. Ed., 2006, 45, 1113-1115.

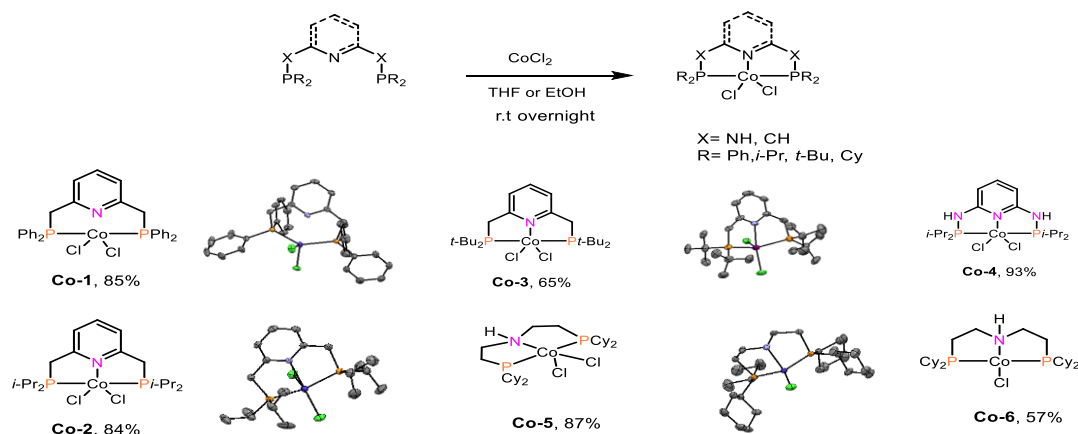


Schéma 2: Catalyseurs de cobalt supportés par ligand PNP.

La synthèse de ligand contenant des phosphines sont connus pour être relativement difficile à synthétiser, chère et sensible à l'air. C'est pour cela que nous également synthétiser des complexes de cobalt supportés par des ligands sans phosphine. Notamment deux complexes de types « NNN » et un « CNC » (Schéma 3).

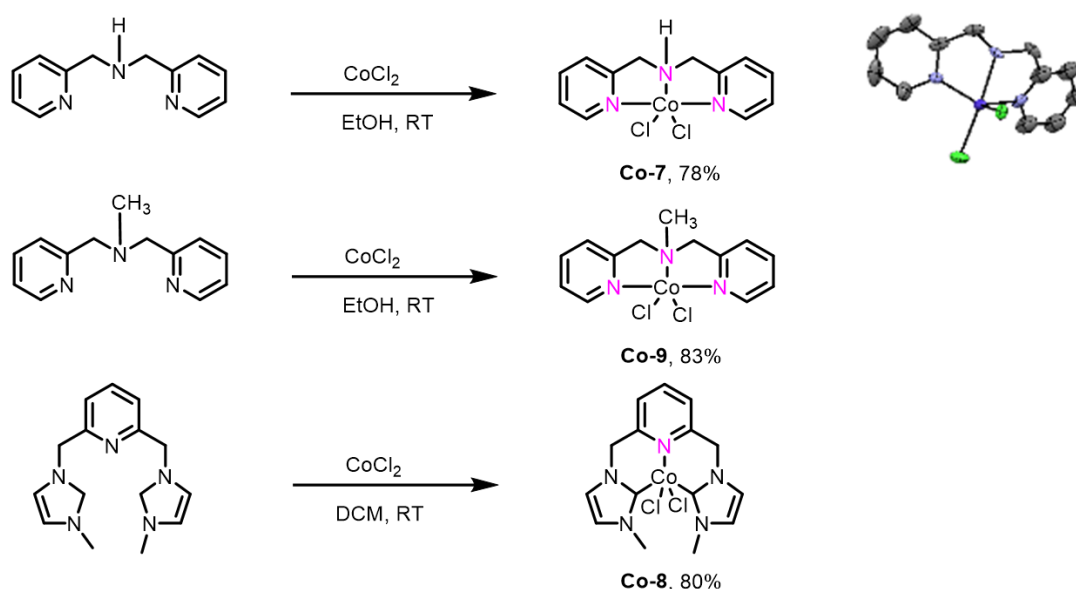
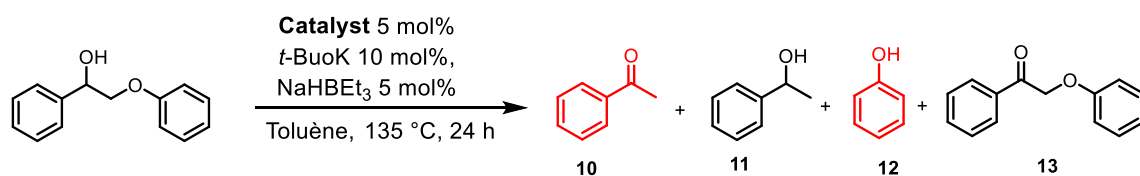


Schéma 3: Complexes de Cobalt sans ligand phosphine.

Tous les catalyseurs préparés et décrits ci-dessus ont été évalués dans les conditions décrites par Milstein pour l'amination réductive de l'alcool. Le modèle de lignine a ainsi été soumis à 5 mol% de catalyseur en présence de t-butoxyde de potassium et de triéthyle sodium borohydrure de sodium à 135 °C dans du toluène. Malheureusement après de nombreuses tentatives d'optimisations, nous n'avons pas été en mesure d'obtenir plus de 20% de conversion.

Tableau 1: Résultats catalytiques de la dépolymérisation de la lignine.



Entrée	Catalyseur	Conversion (%) ^a
1	Co-1	<20
2	Co-2	<20
3	Co-3	<20
4	Co-4	<20
5	Co-5	<20
6	Co-6	<20
7	Co-7	<20
8	Co-8	<20
9	Co-9	<20

Conditions : [Co] (0.023 mmol ; 5%) ; modèle de lignine (0,100 g ; 0,47 mmol) 115°C, 2 mL solvant a) GC, sans calibration.

Cependant, avec ces complexes en main, nous avons cherché une autre application dans le domaine de la chimie durable et nous nous sommes dirigés vers l'hydrogénation des N-hétérocycles comme une route pour le stockage chimique de l'hydrogène qui est un sujet d'intérêt actuel.

Les réactions de réduction et plus particulièrement les hydrogénations sont omniprésentes dans la synthèse organique et jouent un rôle majeur dans le cadre des processus industriels de synthèse chimique en vrac et fine. Cette situation persistera probablement en raison des préoccupations et des demandes croissantes d'approvisionnement durable en produits chimiques issus de la biomasse⁶ ainsi que de nouveaux vecteurs énergétiques basés sur le stockage chimique de l'hydrogène.⁷ Les N-hétérocycles sont des éléments constitutifs importants des molécules bioactives naturelles et synthétiques, parmi lesquelles la 1,2,3,4-tétrahydroquinoléine est particulièrement précieuse avec de nombreuses applications dans les médicaments et les produits agrochimiques.⁸ Récemment, ces molécules ont également été envisagées comme des réservoirs d'hydrogène.⁹ A l'on l'observe habituellement avec des composés aromatiques, l'hydrogénation catalytique des dérivés de la quinoléine est une réaction difficile en raison de la désactivation potentielle du catalyseur due à la coordination des réactifs de quinoléine et des dérivés de la tétrahydroquinoléine.

Divers catalyseurs homogènes¹⁰ ont été rapportés pour l'hydrogénation des quinoléines tandis que les catalyseurs à base d'iridium présentaient les meilleures performances et chimiosélectivités. Cependant, le coût de ces catalyseurs, la présence parfois nécessaire d'additifs et la non-recyclabilité des catalyseurs homogènes ont encouragé le développement de catalyseurs moins coûteux à base de fer,¹¹ manganèse,¹² et de cobalt.¹³ Malgré leur intérêt économique, ces catalyseurs doivent encore être améliorés car ils

⁶ P. N. R. Vennestrom, C. M. Osmundsen, C. H. Christensen and E. Taarning, *Angew. Chem. Int. Ed.*, 2011, 50, 10502

⁷ R. H. Crabtree, *Energy Environ. Sci.*, 2008, 1, 134.

⁸ V. Sridharan, P. A. Suryavanshi and J. Carlos Menendez, *Chem. Rev.*, 2011, 111, 7157.

⁹ D. Teichmann, W. Arlt, P. Wasserscheid and R. Freymann, *Energy Environ. Sci.*, 2011, 4, 2767.

¹⁰ R. A. Sanchez-Delgado and E. Gonzalez, *Polyhedron*, 1989.

¹¹ S. Chakraborty, W. B. Brennessel and W. D. Jones, *J. Am. Chem. Soc.*, 2014, 136, 8564.

¹² V. Papa, Y. Cao, A. Spannenberg, K. Junge, M. Beller, *Nature. Catal.* 2020, 10.1038/s41929-019-0404-6.

¹³ R. Xu, S. Chakraborty, H. Yuan and W. D. Jones, *ACS Catal.*, 2015, 5, 6350.

présentent en général un rendement inférieur à celui des catalyseurs à base de métaux nobles et ils nécessitent souvent des ligands coûteux tels que les ligands de pince. Au cours des dernières décennies, de nombreux catalyseurs hétérogènes à base de métaux nobles ont également été signalés pour l'hydrogénation des dérivés de la quinoléine.¹⁴ Bien qu'ils présentent généralement une réactivité élevée, ces catalyseurs souffrent d'une faible chimiosélectivité, ce qui entrave la portée du produit accessible. De rares exemples d'hydrogénation chimiosélective de la quinoléine utilisent des nanoparticules Rh, Au et Ru prises en charge. En ce qui concerne les catalyseurs homogènes, la recherche de catalyseurs hétérogènes à moindre coût est un sujet de grande importance en catalyse.

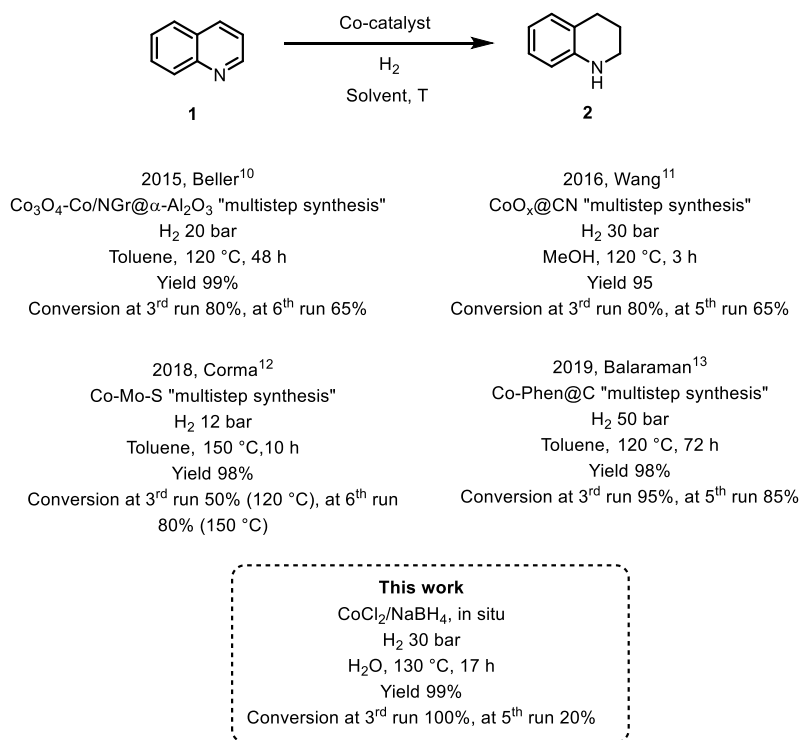


Schéma 4: Hydrogénation Quinoléine par le Cobalt

En 2015, certains d'entre nous ont signalé l'hydrogénation sélective d'hétéroarènes à l'aide de nanoparticules d'oxyde de cobalt/cobalt modifiées par des couches de graphène dopées à l'azote sur de l'alumine.¹⁵ Ces catalyseurs ont efficacement hydrogéné un certain nombre de dérivés de quinoléine en 60-72 h, dans le toluène à 120 °C et 20-30 bar de pression d'hydrogène. Un an plus tard, Wang a révélé du cobalt encapsulé dans des couches de graphène dopées au N pour l'hydrogénation des quinoléines en 3-15 h, dans du méthanol à 120 °C sous 30 bars de pression d'hydrogène.¹⁶ Plus récemment, Corma a signalé des sulfures de cobalt-molybdène nanocouches pour l'hydrogénation sélective des quinoléines.¹⁷ Ce catalyseur fonctionnant à 120 °C et 12 bar de pression d'hydrogène présentait une chimiosélectivité impressionnante car il n'hydrogénerait pas d'oléfines, fonctions de cétone, nitrile, ester et amide des dérivés de la quinoléine. Cependant, ce catalyseur était modérément recyclable car la conversion et les rendements ont chuté de 50% en une troisième série. Très récemment en 2019, Balaraman a signalé un catalyseur Co-Phen@C pour la réduction des quinoléines fonctionnant à 120 °C et 50 bars de pression d'hydrogène.¹⁸ Outre le cobalt, un exemple de catalyseur de fer hétérogène a été

¹⁴ N. Hashimoto, Y. Takahashi, T. Hara, S. Shimazu, T. Mitsudome, T. Mizugaki, K. Jitsukawa and K. Kaneda, *Chem. Lett.*, 2010.

¹⁵ F. Chen, A.-E. Surkus, L. He, M.-M. Pohl, J. Radnik, C. Topf, K. Junge and M. Beller, *J. Am. Chem. Soc.*, 2015, 137, 11718.

¹⁶ Z. Wei, Y. Chen, J. Wang, D. Su, M. Tang, S. Mao and Y. Wang, *ACS Catal.*, 2016, 6, 5816.

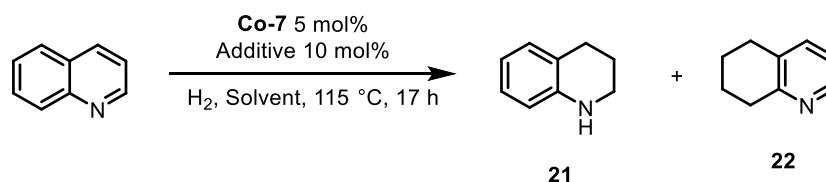
¹⁷ Sorribes, L. Liu, A. Doménech-Carbó and A. Corma, *ACS Catal.*, 2018, 8, 4545.

¹⁸ G. Jaiswal, M. Subaramanian, M. K. Sahoo and E. Balaraman, *ChemCatChem*, 2019, 11, 2449.

rapporté en 2018.¹⁹ (Schéma 4) Ici, un catalyseur à base de fer modifié au carbone dopé au N a effectué l'hydrogénation d'un certain nombre de dérivés de quinoléine à 130-150 °C sous 40-50 bar de pression d'hydrogène dans un mélange de solvant MeOH/H₂O. Les fractions nitrile, ester et amide n'ont pas été hydrogénées par ce catalyseur, qui a été recyclé 6 fois sans perte d'efficacité catalytique. Quelle que soit la nature du métal (noble/non noble), la plupart des catalyseurs hétérogènes connus pour cette transformation nécessitent une synthèse en plusieurs étapes ou leur mise à l'échelle est difficile. Ainsi, la préparation de catalyseurs généraux et sélectifs de manière simple est stimulante pour les chercheurs universitaires et industriels. À cet égard, les nanoparticules métalliques ont suscité un intérêt particulier ces dernières années. Par exemple, les nanoparticules nues d'oxyde d'iridium, facilement préparées à partir de trichlorure d'iridium et d'hydroxyde de sodium, se sont révélées être des catalyseurs efficaces pour l'hydrogénation de plusieurs dérivés de quinoléine dans des conditions douces (température ambiante, 1 bar (ballon H₂) à 60 bar.²⁰ De même, Jacobi von Wangelin a signalé des nanoparticules de cobalt « quasi nues » stabilisées par des substrats oléfiniques efficaces pour C = C, Hydrogénations de liaison C=O et C=N dans THF.²¹ Pour préparer les nanoparticules de cobalt de manière simple et pratique dans des milieux réactionnels aqueux, la réduction des sels de cobalt avec du borohydrure de sodium a attiré notre attention. Fait intéressant, l'activation du borohydrure de sodium est catalysée par de nombreux métaux de transition dont le cobalt a attiré le plus l'attention en raison de son coût inférieur. En fait, il est bien établi que l'hydrolyse de NaBH₄ en présence de sel de Co(II) conduit à diverses espèces de cobalt²², y compris des nanoparticules.²³ Inspirés par ces résultats, nous avons développé une nouvelle hydrogénation catalysée au cobalt de la quinoléine et des dérivés de la quinoléine dans des milieux aqueux. . Ici, nous rapportons la synthèse et l'application du système de catalyseur optimal, qui est facilement préparé à partir de précurseurs peu coûteux sans aucun additif ni espèce stabilisatrice.

Nous avons commencé l'optimisation de la réaction en utilisant le catalyseur **Co-7**. En effet, il est le plus simple à synthétiser ainsi que le moins chère. Dans un premier temps nous avons utilisé 5 mol% de **Co-7**, 10 mol% de borohydrure de sodium dans de l'eau et sous 30 bars de pression.

Tableau 2: Optimisation de l'hydrogénation de quinoléine.



Entry	Catalyst	Additive	Pressure H ₂ (Bar)	Solvent	21 (%)	22 (%)	Conversion (%) ^a
1	Co-7	NaBH ₄	20	Toluene	0	0	0
2	Co-7	NaBH ₄	30	Toluene	0	0	0
3	Co-7	NaBH ₄	20	Isopropanol	10	0	10
4	Co-7	NaBH ₄	30	Isopropanol	90	10	100
5	CoCl₂	NaBH ₄	30	Isopropanol	90	10	100
6	-	NaBH ₄	30	Isopropanol	0	0	0
5	CoCl₂	NaBH ₄	30	Eau	100	0	100

Conditions : [Co] (0,038 mmol ; 5%) ; quinoléine (0,100 g ; 0,77 mmol) 115°C, 1 mL solvant a) RMN

¹⁹ B. Sahoo, C. Kreyenschulte, G. Agostini, H. Lund, S. Bachmann, M. Scalone, K. Junge and M. Beller, Chem. Sci., 2018, 9, 8134.

²⁰ Y.-G. Ji, K. Wei, T. Liu, L. Wu and W.-H. Zhang, Adv. Synth. Catal., 2017, 359, 933.

²¹ S. Sandl, F. Schwarzhuber, S. Pöllath, J. Zweck and A. Jacobi von Wangelin, Chem. Eur. J., 2018, 24, 3403

²² U. B. Demerci and P. Miele, Phys. Chem. Chem. Phys., 2010, 12, 14651.

²³ G. N. Glavee, K. J. Klabunde, C. M. Sorensen and G. C. Hadjipanayis, Langmuir, 1993.

Nous obtenons une excellente conversion en utilisant de l'isopropanol comme solvant (Entrée 3) mais une faible sélectivité avec l'obtention d'un produit secondaire. Nous observons également la formation de particules noir après la réaction. C'est pour cela qu'avons effectué un réaction test avec le précurseur de cobalt CoCl_2 (Entrée 5) et nous obtenons les mêmes résultats qu'avec le complexe de cobalt **Co-7**. Nous pouvons conclure que l'utilisation d'un ligand n'est pas nécessaire pour effectuer la réaction d'hydrogénation de la quinoléine et nous avons probablement la formation de particules de cobalts. Enfin nous obtenons une excellente conversion et sélectivité en effectuant la réaction dans l'eau (Entrée 7).

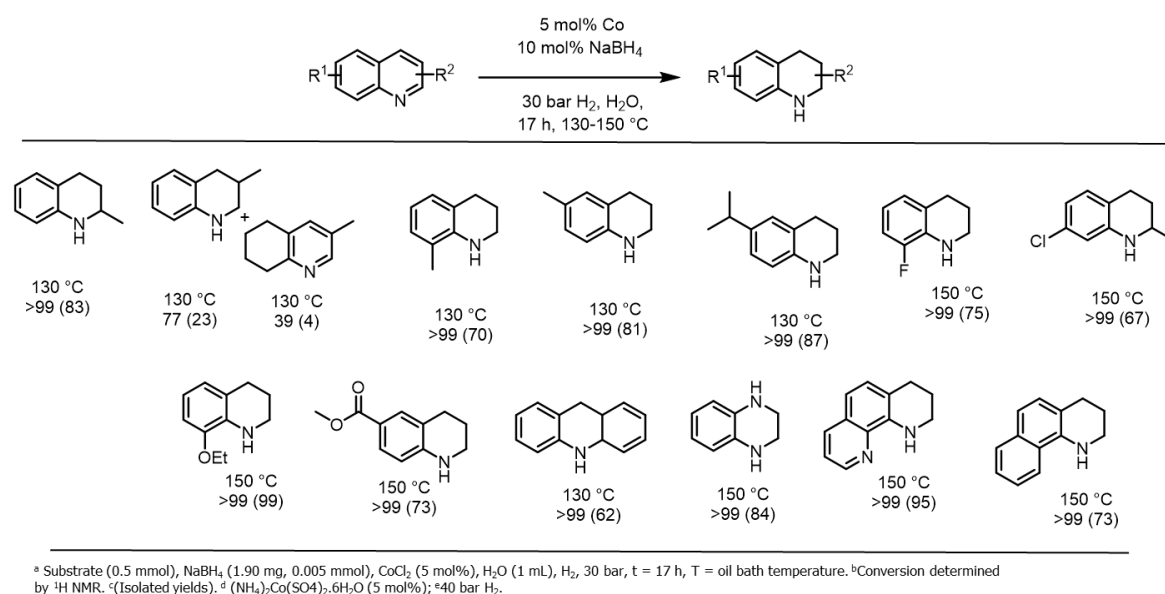


Figure 3: Scope hydrogénation quinoléine

Nous avons finalement testé les conditions réactionnelles optimiser précédemment sur différents dérivés de la quinoléine (Figure 3). Nous observons une bonne conversion pour les méthyl-quinoléines, les quinoléines contenant des groupements éthers, esters, halogènes.

En conclusion, nous avons préparé des nanoparticules de cobalt catalytiquement actives par hydrolyse de NaBH_4 en présence de sels de Co(II) . Le catalyseur se compose initialement d'un mélange de nanoparticules de cobalt et de nanofeuilles contenant du cobalt et évolue vers de plus grandes particules de Co lors de la réutilisation. L'activité et la chimiosélectivité de ce catalyseur sont comparables à d'autres catalyseurs hétérogènes bien définis constitués uniquement de cobalt.²² Notamment, ce catalyseur est facilement préparé à partir de précurseurs de cobalt peu coûteux et facilement accessible aux chimistes de synthèse. En outre, la préparation du catalyseur ne nécessite aucun additif et, contrairement à de nombreux catalyseurs hétérogènes, elle est préparée et utilisée dans l'eau, ce qui rend le processus global pratique et plus respectueux de l'environnement.

Dans le chapitre précédent, nous avons décrit des études pour l'hydrogénation de la quinoléine. Comme indiqué ci-dessus, de nombreux travaux ont été réalisés sur ce sujet en appliquant des catalyseurs homogènes ou hétérogènes à base de métaux nobles et non nobles. Par rapport à l'hydrogénation partielle, l'hydrogénation complète de la quinoline en décahydroquinoléine (DHQ) est une réaction plus difficile. Le décahydro-squelette est largement utilisé dans la synthèse de produits chimiques²⁴ et de

²⁴ G. Perot, *Catalysis Today*, 1991, 10, 4, 447-472.

produits pharmaceutiques. En général, cette hydrogénation s'effectue en deux étapes²⁵ (schéma 1). Pour une voie possible, on discute d'abord de l'hydrogénation de la quinoline en 1,2,3,4-THQ, suivie de la réduction en DHQ. Dans une seconde voie, on produit de préférence du 5,6,7,8-THQ, qui est ensuite hydrogéné en DHQ.

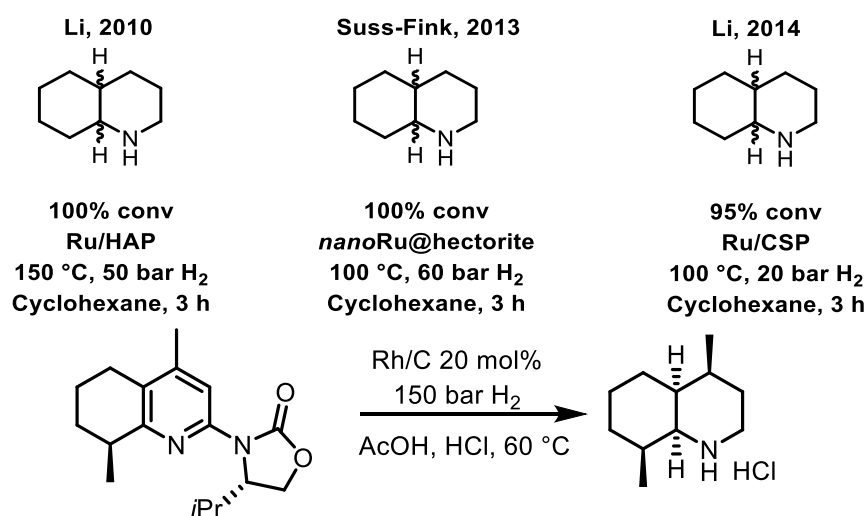


Schéma 5 : Hydrogénation de quinoléine en décahydroquinoléine.

En 2010, Li et ses collègues,²⁶ ont terminé l'hydrogénation de la quinoléine en DHQ à l'aide d'un système de catalyseur Ru/HAP. La réaction a été réalisée à 150 °C, 50 bars d'hydrogène, avec du cyclohexane comme solvant en 3 h. Le résultat de l'hydrogénation a été attribué à l'existence de groupes hydroxyles à la surface. Plus tard, Süss-Fink,²⁷ a rapporté un catalyseur nano-Ru@hectorite fournissant une méthode douce et efficace pour l'hydrogénation catalytique de la quinoléine avec une sélectivité commutable entre py-THQ (>99%) dans l'eau et DHQ (>99%) dans le cyclohexane. Le produit plus difficile DHQ a été obtenu à 100 °C, 60 bars d'hydrogène et 3 h. Un an plus tard, Li²⁸ a proposé une hydrogénation hautement active et sélective de la quinoléine en décahydroquinoléine dans l'eau dans des conditions douces en utilisant des nanoparticules de ruthénium soutenues sur des sphères de carbone dérivées du glucose (Figure 6). Ces résultats sont attribués à la liaison hydrogène entre les groupes quinoléine et hydroxyle du support ainsi qu'à l'interaction π - π d'empilement entre la quinoléine et le système aromatique du support carbone. En 2010, Glorius²⁸ a décrit l'hydrogénation stéréosélective des quinoléines substituées par des auxiliaires. Ils ont élégamment dévoilé la première stratégie pour la formation stéréosélective de 5,6,7,8-tétrahydro- et décahydroquinoléines chirales avec des stéréocentres nouvellement formés dans l'anneau cyclohexane. (Schéma 5)

Après optimisation de la réaction, le catalyseur commercial ruthénium sur charbon Ru/C est le plus actif avec l'hydrogénation totale de la quinoléine à 60 °C, 20 bars d'hydrogène, dans un mélange H₂O/t-amylOH pendant 17 h. L'un des intérêts de la décahydroquinoléine est de posséder deux carbones asymétrique qui donne une diastéréosélectivité à la molécule Cis ou Trans. Lors de l'optimisation de la réaction, nous nous sommes rendu compte de la possibilité de changer la sélectivité suivant la température. En effet, à 60 °C nous avons un ratio diastéréosélectif de 95% pour le composé Cis et à

²⁵ M. Campanati, S. Franceschini, O. Piccolo, A. Vaccari, *Catalysis of Organic Reactions*, 2005, 101-110.

²⁶ Y. P. Sun, H. Y. Fu, D. L. Zhang, R. X. Li, H. Chen, X. J. Li, *Catal. Commun.*, 2010, 12, 188-192.

²⁷ B. Sun, F. A. Khan, A. Vallat, G. Süss-Fink, *Appl. Catal. A*, 2013, 467, 310-314

²⁸ M. Heitbaum, R. Fröchlich, F. Glorius, *Adv. Synth.*, 2010, 352, 357-362

150 °C un ratio de 96% pour le composé Trans. Enfin, nous avons procédé à un scope de la réaction aux deux températures avec douze dérivés de la quinoléine capable d'être hydrogéné par cette méthode.

Pour conclure, nous avons effectué l'hydrogénation diastéréosélective commutable de la quinoléine à la décahydroquinoléine avec un catalyseur Ru/C disponible dans le commerce. La formation de cis-décahydroquinoléine a été possible dans des conditions relativement douces (60 °C), tandis que dans des conditions plus difficiles, la sélectivité a changé, conduisant à la trans-décahydroquinoléine. Au moment de la rédaction de ce manuscrit, la caractérisation des catalyseurs est en cours.

Dans le chapitre précédent, nous avons décrit une hydrogénation diastéréosélective de la quinoléine et des hétéroarènes apparentées à l'aide d'un catalyseur Ru/C disponible dans le commerce. Sur la base de ces travaux, nous avons également étudié l'hydrogénation diastéréosélective des pyridines et des arènes.

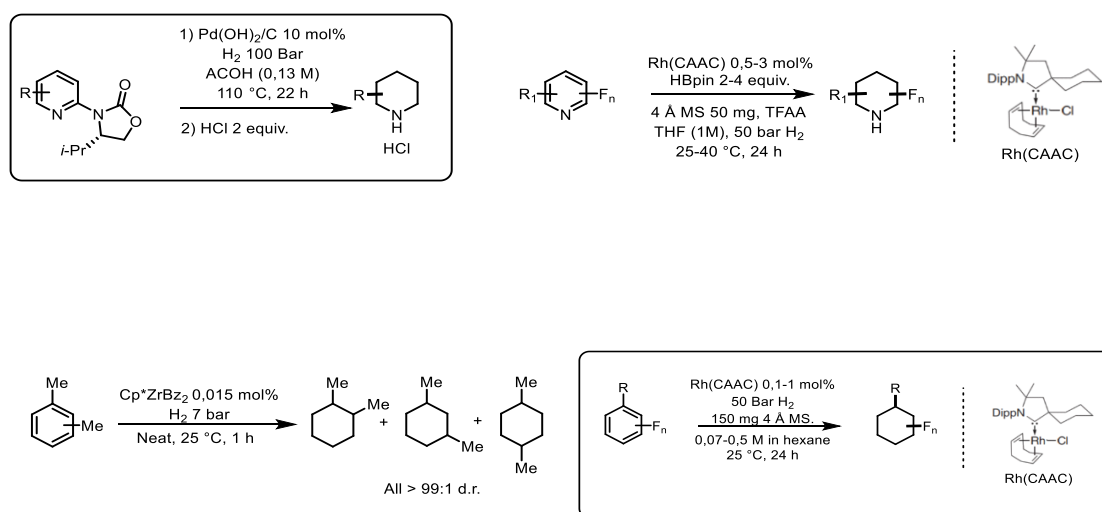


Schéma 6: Hydrogénation diastéréosélective de pyridines et d'arènes

en utilisant l'oxazolidinone comme auxiliaire chiral, Glorius et ses collègues²⁹ ont rapporté une hydrogénation diastéréosélective très efficace des N-(2-pyridyl)-oxazolidinones en utilisant Pd(OH)₂/C comme catalyseur. Avec ce système catalytique, sous une pression d'hydrogène de 100 atm, une série de pyridines à contrôle unique ou multiple ont été hydrogénées (schéma 6).

Plus récemment, le groupe Glorius³⁰ a développé une stratégie élégante pour accéder aux piperidines partiellement fluorées à haute sélectivité cis à l'aide d'un catalyseur au rhodium (schéma 6).

Par rapport aux hétéroarènes, l'hydrogénation asymétrique des arènes est encore plus difficile en raison de la forte aromaticité et de la faible capacité de coordination de ces composés. En 2016, le groupe de Marks³¹ a développé un Cp-Zr(H)Bz/ZrS à site unique permettant une hydrogénation hautement sélective des arènes. Le catalyseur était capable d'effectuer une hydrogénation sélective de différents dérivés d'alkyl arène (schéma 6).

Un an plus tard, Wiesenfeldt et al,³² ont considéré que les processus en plusieurs étapes pouvaient être évités en concevant un protocole pour l'hydrogénation catalytique de fluoroarènes peu coûteux et facilement disponibles. À l'aide d'un catalyseur Rh-NHC avec un ligand (amino)carbène spécifique,

²⁹ F. Glorius, N. Spielkamp, S. Holle, R. Goddard, C. W. Lehmann, *Angew. Chem. Int. Ed.*, 2004, 43, 2850-2852.

³⁰ Z. Nairoukh, M. Wollenburg, C. Schleppehorst, K. Bergander, F. Glorius. *Nature Chem.*, 2019, 11, 264–270.

³¹ M. M. Stalzer, C. P. Nicholas, A. Bhattacharyya, A. Motta, M. Delferro, T. J. Marks, *Angew. Chem. Int. Ed.*, 2016, 55, 5263-5267.

³² M. P. Wiesenfeldt, Z. Nairoukh, W. Li, F. Glorius, *Science*, 2017, 357, 908–912.

une gamme de fluoroarènes a été transformée en produits saturés fluorés correspondants. En plus du fluorobenzène, un certain nombre de benzènes mono- et polyfluoro-substitués ont été réduits. Même l'hexafluorobenzène a fourni du cis-hexafluorocyclohexane avec une sélectivité de 420:1 dr, bien qu'avec un rendement légèrement réduit (34%). Cette approche représente une avancée synthétique majeure, car une voie préalable pour obtenir ce produit à partir du glucose nécessitait 12 étapes.

Nous avons commencé notre travail de recherche par la synthèse de catalyseur par une méthode connue au laboratoire. Nous avons synthétisé 16 catalyseurs différents et après optimisation le meilleur catalyseur est Ru/Phen(1/2)@TiO₂-800, il est en effet capable d'hydrogéner la 2,6 lutidine, à 25 °C, 10 bars d'hydrogène, dans un mélange eau/Isopropanol, pendant 17 h, avec 100% de conversion et 99% de sélectivité pour le composé cis-2,6 diméthylpipéridine. Notre système catalytique est également efficace pour 6 dérivés de la pyridine et 12 arènes. Le catalyseur peut également être recyclé au moins 5 fois sans perte de réactivité.

En conclusion, nous avons développé un catalyseur hétérogène à base de ruthénium capable d'effectuer une hydrogénation diastéréosélective de pyridines et d'arènes di- et trisubstituées dans des conditions douces avec une très bonne sélectivité pour les composés cis. Ce protocole catalytique peut être appliqué aux composés qui présentent un intérêt pour l'industrie. Ainsi, l'hydrogénation du thymol produit du (±)-néo-isomenthol et la réaction de la 2,6 diméthylpipéridine conduit à un élément constitutif important en pharmacie.

Au cours de cette thèse, nous avons abordé un certain nombre de transformations difficiles allant de la transformation de composés biosourcés à l'hydrogénation sélective de N-hétérocycles et d'arènes effectuée par des catalyseurs hétérogènes. Dans le premier chapitre, nous avons synthétisé et caractérisé huit complexes de cobalt différents pour un clivage de lignine neutre en redox. Malheureusement, nous n'avons pas été en mesure d'effectuer la réaction. Certains résultats ont été obtenus mais nous avons remarqué que le catalyseur n'était pas impliqué dans la réaction et que la base permettait de cliver la lignine. Dans le deuxième chapitre, nous avons porté notre attention sur d'autres réactions qui pourraient être encouragées par ces catalyseurs. En particulier, nous avons réalisé avec succès l'hydrogénation de la quinoléine en 1,2,3,4-tétrahydroquinoléine. Les premiers tests avec les complexes de pinces au cobalt ont montré la formation de résidus noirs après la réaction et nous avons rapidement démontré la formation de particules de cobalt. Les particules générées in situ, y compris les nanoparticules, ont été préparées de manière simple à partir de CoCl₂ et de NaBH₄ et se sont avérées très efficaces pour l'hydrogénation d'un certain nombre de dérivés de la quinoléine dans l'eau.

Dans une troisième partie, nous avons développé un système catalytique basé sur le Ru/C disponible dans le commerce qui permet la synthèse diastéréosélective de la décahydroquinoléine à partir de la quinoléine. En fonction de la température du système catalytique, nous sommes en mesure d'obtenir différents diastéréoisomères, le composé cinétique étant favorisé à basse température tandis que le composé thermodynamique a été obtenu à température plus élevée.

Enfin, nous avons développé un nouveau catalyseur hétérogène à base de ruthénium capable d'effectuer une hydrogénation stéréosélective de dérivés de pyridine et de dérivés aromatiques dans des conditions douces. En effet, ce catalyseur est capable de favoriser l'hydrogénation d'un certain nombre de N-hétérocycles et d'arènes à température ambiante et de 10 bars d'hydrogène.